Transcriptomic analyses of the responses of corals to environmental stress

PhD Thesis submitted by

Catalina Aguilar Hurtado

in May 2016

For the degree of Doctor of Philosophy
College of Public Health, Medical and Veterinary Sciences
James Cook University

Acknowledgements

Firstly, I would like to thanks my supervisors Prof David Miller and Dr David Bourne for their continuous support during this PhD study, for their patience and motivation throughout these years. To David M for allowing me to join his lab and make that first journey to Australia, and to David B for giving me the opportunity to work at AIMS and access first-class facilities that were important for completing this thesis.

I would also like to thank my previous supervisors: Prof Juan Armando Sanchez and Prof James D. Reimer for encouraging me to pursue marine molecular research, and to have given me the opportunity to explore the Caribbean and Pacific reefs.

A sincere thank to my labmates in particular to Mei-Feng Lin, Aurelie Moya, Susanne Sprangala, Ben Mason and Bruno Lapeyre for the stimulating discussions and help during my experiments.

Special thanks to my friends in Townsville: Sam Noonan, Kelsy Miller, Daisie Ogawa, Julian Facundo Rinaudo, Andres Ramirez Yaksic, Raul Pøsse and Brett Blandford for their support and friendship.

Finally, to my family, for their unconditional support through this whole process. Without them I would not be where I am today.

Statement of contribution of others

Research funding:

- ARC Centre of Excellence for Coral Reef Studies (ARC COE)
- AIMS@JCU
- James Cook University (JCU)
- Australian Institute of Marine Science (AIMS)

Supervision:

- Professor David J. Miller, JCU
- Dr David G. Bourne, AIMS

Experimental set-up and instrumentation:

- Dr Chia-Miin Chua (JCU) (Chapter 2)
- Dr Andrew Negri (AIMS) (Chapter 3)
- Dr Cherie A. Motti (AIMS) (Chapter 4)
- Dr Jean-Baptiste Raina (UTS) (Chapter 3 and 4)
- Dr Victor Beltran (AIMS) (Chapter 3 and 4)
- National Sea Simulator staff (AIMS) (Chapter 3 and 4)

Laboratory analyses

- Dr David C. Hayward (ANU) (Chapter 3 and 4)
- Dr Bruno Lapeyre (Laboratoire d'excellence CORAIL) (Chapter 3 and 4)

Bioinformatics assistance:

- Dr Sylvain Fôret (ANU)

Editorial assistance:

- Prof David J. Miller and Dr David G. Bourne (whole thesis)
- Dr Aurelie Moya (Chapter 2)
- Dr Jean-Baptiste Raina (Chapter 3 and 4)
- Dr Cherie A. Motti (Chapter 4)

Abstract

Coral reefs are the oceans' most diverse and productive ecosystems. However, reef ecosystems are also one of the most endangered habitats on Earth, due to their fragility and exposure to both abiotic and biotic stressors. Understanding the impacts that environmental stressors have on the coral cellular mechanisms is integral for determining the coral health status. It also has important implications for persistence of coral reefs under rapidly changing climatic conditions. In this PhD study, I implemented a transcriptomic approach to investigate the response of the coral *A. millepora* to biotic and abiotic challenges in an attempt to better understand the molecular mechanisms underlying specific and general coral stress responses.

In Chapter 2, I focus on the coral response to lipopolysaccharidae (LPS) challenge in order to better understand innate immunity in corals. By using differential gene expression analysis and comparative genomics, I provide evidence that the coral response to LPS challenge resembles that of vertebrates. In addition, the effect of pre-exposure to high pCO_2 conditions on the response to LPS challenge was investigated where, as in vertebrates and *Drosophila*, hypercapnia impaired the innate immune response. The results obtained support the hypothesis that coral immunity is likely to be compromised by near-future ocean acidification conditions and that cumulative stressors may predispose corals to increased disease.

In Chapter 3, I investigate the molecular mechanisms underlying the coral response to hypo-osmotic stress, again through application of transcriptomic approaches. Previous studies on corals and other marine invertebrates have enabled identification of a group of genes that respond to a wide range of stressors, whereas distinct sets of genes respond to specific stressors. Results described in this chapter illustrate that common responses to environmental stressors in *Acropora* sp. include up-regulation of genes involved in

macromolecular and oxidative damage, while up-regulation of genes involved in amino acid metabolism and transport represent specific responses to salinity stress. These results provide important insights into how corals respond at the molecular level to low salinity events, which are predicted to increase under future climate scenarios due to increased frequency of intense rainfall events.

In Chapter 4, I examine the production of dimethylsulphoniopropionate (DMSP) by corals under salinity stress, in order to better understand the biosynthetic pathway and the role this compound in the coral. The concentration of DMSP increased in the coral under hypo-saline conditions, contradicting the assumption that DMSP functions as an osmolyte in corals, as is the case in higher plants and algae. Results described in this chapter suggest that DMSP production primarily serves as an overflow mechanism for removal of excess methionine arising from catabolism of betaines, although DMSP may also serve as a scavenger of ROS. The transcriptomic analyses also enabled identification of candidate genes for roles in DMSP biosynthesis. When DMSP was produced in response to hyposaline stress, coral homologues of each of the four enzymes classes implicated in DMSP biosynthesis (aminotransferase, reductase, methyltransferase, and decarboxylase) were up-regulated, linking specific genes to production of this compound from methionine in corals.

In Chapter 5, the published data and that described in all of the previous thesis chapters are used in attempt to establish the general mechanisms used by corals to respond to environmental stress. The transcriptomic data generated here provide novel insights into conserved and specific molecular mechanisms used by corals under stress, and advances our understanding of how corals are likely to respond to the challenges of a changing marine ecosystem.

Table of Contents

List of Tables

Chapter 2

Chapter 3

Chapter 4

Chapter 5

List of Figures

Chapter 1

Chapter 2

Chapter 3

Chapter 4

Chapter 5

Chapter 1: General introduction

The response of corals to environmental stress

1.1. The importance of coral reefs and their current decline

Coral reefs are biologically diverse ecosystems. Despite only constituting approximately 0.1% of the ocean's surface area, coral reefs provide habitat for nearly one quarter of all marine species (Hoegh-Guldberg 1999; Moberg & Folke 1999; Plaisance *et al.* 2011). Coral reefs are also of great economical importance, supporting fisheries and providing income to local communities through tourism based activities. For example, the Great Barrier Reef (GBR) off the east coast of Australia and the world's largest coral reef ecosystem, was estimated to contribute $5.7 billion to the Australian economy in 2012 (Economics 2013). Many coastal communities in developing countries rely on coral reefs for their primary source of protein, thereby making them central to the livelihood of millions of people globally (Moberg & Folke 1999). Coral reefs also provide a variety of other ecosystems goods and services including coastal protection, sediment production, and biotic services as habitat for a wide range of fish species and marine invertebrates (Harborne *et al.* 2006).

Globally, coral reefs are in decline, however, driven by environmental and anthropogenic factors, including coastal pollution, over-fishing, tourism, and climate change (Gardner *et al.* 2003; Hughes 1994; Pandolfi *et al.* 2003). Evidence for this decline can be most clearly seen in the Caribbean, where up to 80% of coral cover has been lost over three decades, attributed to several factors including coral bleaching, diseases, overfishing, and the collapse of the sea urchin, *Diadema antillarum* population. In many regions a phase shift from coral to macroalgal dominance has occurred on the reefs and persisted for 25 years (Figure 1.1) (Gardner *et al.* 2003). Recent assessments of the GBR show that a 50% decline in coral cover has occurred over the period from 1985 to 2012, largely attributable to three main factors - coral predation by crown-of-thorns starfish (COTS), cyclones and coral bleaching (De'ath *et al.* 2012). Anthropogenic factors contributing to the degradation of the GBR include water quality parameters, particularly elevated loads of nutrients, sediments, and pesticides from coastal run-off (Great Barrier Reef Marine Park 2014). Globally, these threats are

expanding with an estimated 30% of reefs threatened by coastal development, and 12% by marine pollution (Fabricius 2005).

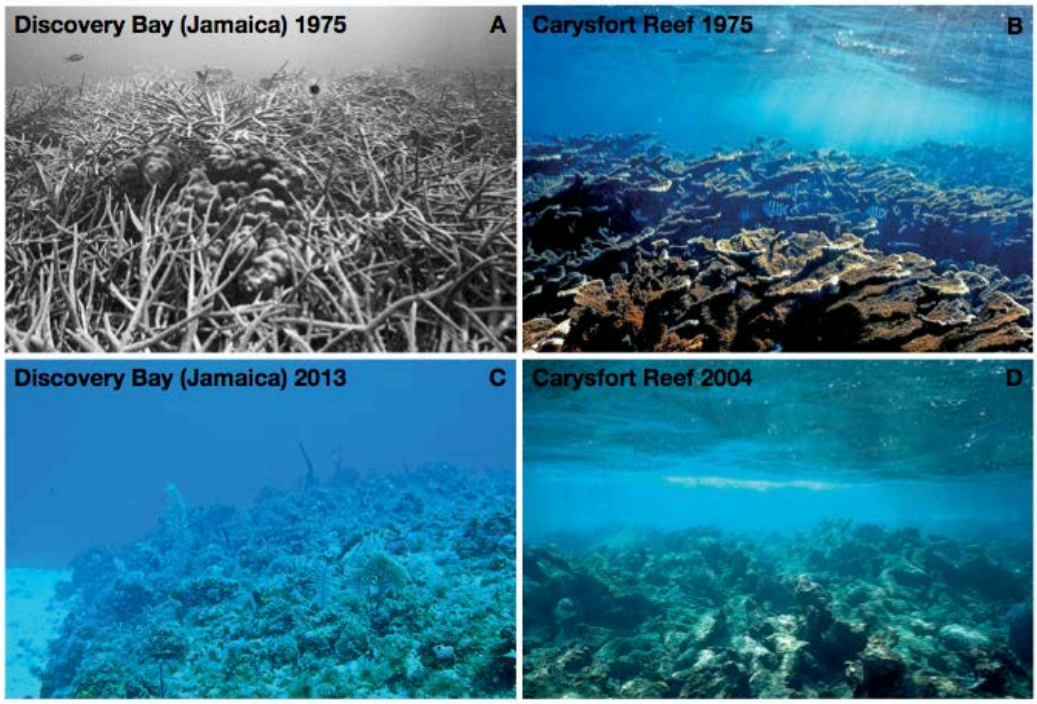

Figure 1.1 Phase shifts of Caribbean reefs from coral to macroalgal dominance in A) 1975 and C) 2013 Discovery Bay, Jamaica. B) 1975 and D) 2004 Carysfort Reef within the Florida Keys National Sanctuary. Figure taken from Jackson *et al*. (2014; Figure 2).

While localised disturbances have significantly impacted coral reefs, climate change effects, including increasing global temperatures and ocean acidification, are projected to have cumulative impacts on reef ecosystems, causing shifts in species distribution and further declines in coral cover. Global projections by the Intergovernmental Panel on Climate Change (IPCC 2013) predict that sea surface temperatures will increase over the next century by 1°C to more than 3°C depending on the emission scenarios. While the ocean pH is predicted to decrease by a further 0.2-0.4 units from the present value (Figure 1.2) (IPCC 2013, Chapter 12). Some studies imply that these two factors could contribute to major declines in calcification in coral reefs, where data from the GBR show that between 1990 and 2005 there was an 11% decline in coral calcification (De'ath *et al.* 2009; Orr *et al.* 2005).

Short-term laboratory experiments also provide evidence of direct impacts of high pCO_2 conditions on a wide range of marine calcifying organisms, though further research is needed to understand the long-term effects and population level impacts (Doney *et al.* 2009).

Changes in surface salinity that are linked to evaporation and precipitation over oceans have also been affected by climate change (IPCC 2013, Chapter 3). Projected global trajectories imply that as a result of climate shifts, wet regions are becoming wetter and dry regions are becoming drier (Durack *et al.* 2012). Over 50 years of data collected from the tropical western Pacific regions has demonstrated that sea surface salinity (SSS) has declined by 0.1 to 0.3 in regions with high precipitation (Cravatte *et al.* 2009). On the GBR, SSS is on average 35 practical salinity units (PSU), but varies depending on proximity to river mouths and fluctuates during heavy rainfall events (Great Barrier Reef Marine Park 2014). Freshwater plumes extend along 2300 km of the Queensland coast line and impact heavily the adjoining coral reef environments during the wet season (December to April; Figure 1.3) (Devlin & Brodie 2005). These plumes can cause bleaching and mortality of corals in addition to carrying heavy sediment loads, nutrients and pesticides onto the reef. For example, in the Harvey Bay region, repeated intensive flooding during the summers of 2010 to 2013 resulted in approximately a ~56% decline in coral cover. These flooding events were correlated with salinity decreases, increases of suspended solids and increase of total nitrogen and phosphorus, all likely contributing to the coral decline (Butler *et al.* 2015).

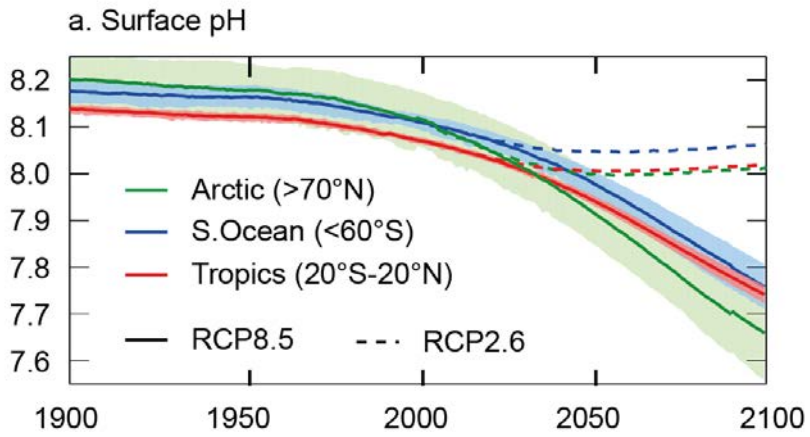

Figure 1.2 Projected ocean surface pH under the RCP8.5 and RCP2.6 scenarios (filled and dashed lines respectively). Surface pH in the Arctic (green), tropical (red) and Southern Oceans (blue). Figure from the IPCC 2013 (Chapter 6; Figure 6.28).

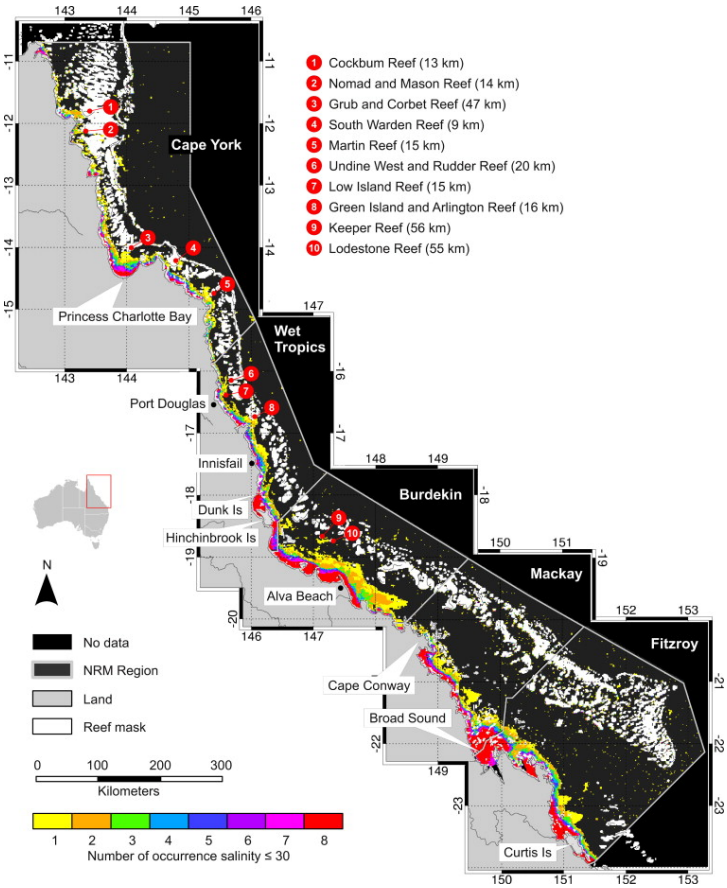

Figure 1.3 The extent of seasonal freshwater plumes during the 2003 and 2010 wet seasons, based on a salinity threshold of S ≤ 30. Figure from Schroeder *et al.* (2012; Figure 9).

1.2. The coral innate immune system

There is clear evidence that environmental and anthropogenic stressors impact coral health, however many of the underlying mechanisms that corals rely on to cope with these stressors remain largely unknown. In all animals, the innate immune system is essential for defence against biotic and abiotic challenges, but is poorly understood in corals. The innate immune system is fundamental for the interaction of multicellular organisms with the environment, and the elements of this system are shared throughout the metazoan lineage. Corals have clear counterparts of many of the key components of the vertebrate immune system (Miller *et al.* 2007) and, although their functions are unknown, some functional data are available for *Hydra* another representative cnidarian. Work on *Hydra* has established that some immune sensing pathways arose prior to the cnidarian-bilaterian divergence; for example, although *Hydra* lacks a canonical Toll-like receptor (TLR), TIR containing proteins (HyTRR-1 and HyTRR-2) are present, and mediate innate immunity via an NF-kb pathway (Figure 1.4), confirming that bacterial recognition via TLRs is an ancestral function (Augustin *et al.* 2010). The activation of the *Hydra* immune response via TLRs leads to the production of antimicrobial peptides (AMPs, Hydramacin-1), host-specific molecules used as defence mechanisms (Bosch *et al.* 2009).

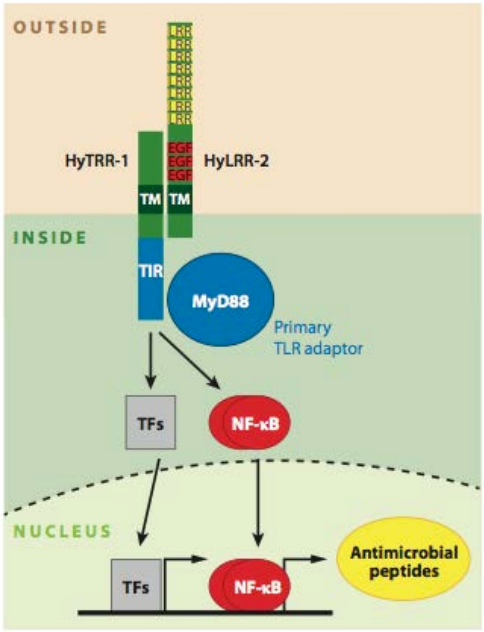

Figure 1.4 TLR signalling pathway in *Hydra*. The TIR containing protein (HyTRR1) interacts with HyLRR-2, a protein that contains a leucine-rich repeats (LRR) domain, leading to activation of NF-kB and thus the production of antimicrobial peptides. Figure from Bosch (2013; Figure 5).

Although cnidarians are often assumed to be simple organisms, genome sequencing has revealed the presence of a highly complex and vertebrate-like immune repertoire (Miller et al.,2007). Surveys of the *A. digitifera* and *A. millepora* genomes revealed the presence of the key pathogen-recognition receptors (PRR) families of vertebrates: the (extracellular) TLRs, tumor-necrosis factor receptors (TNFR), and the (cytosolic) Nod-like receptors (NLRs) as well as many components of the corresponding down-stream signalling cascades (Figure 1.5A) (Miller *et al.* 2007; Shinzato *et al.* 2011). Moreover, the cnidarian repertoires of candidate immune receptors are large by comparison with those of other animals; for example, the A*. digitifera* genome encodes 496 NACHT domain proteins and 40 TNFR family members (Figure 1.5B) (Hamada *et al.* 2012; Quistad SD *et al.* 2014). In vertebrates, these PRRs recognise pathogen-associated molecular patterns (PAMPs) such as lipopolysaccharides (LPS) and muramyl dipeptide (MDP), inducing a pro-inflammatory and apoptotic response by the innate immune signalling pathway (Akira *et al.* 2006). Transcriptomic analyses of the response of *Acropora millepora* to MDP (muramyl dieptide)

revealed interesting similarities with vertebrate immunity, including acute up-regulation of several members of the GiMAP family of regulatory proteins (Weiss *et al.* 2013). These data demonstrate that we are starting to understand the mechanisms that corals rely upon when exposed to immunogens, but the detailed mechanisms remain largely unknown.

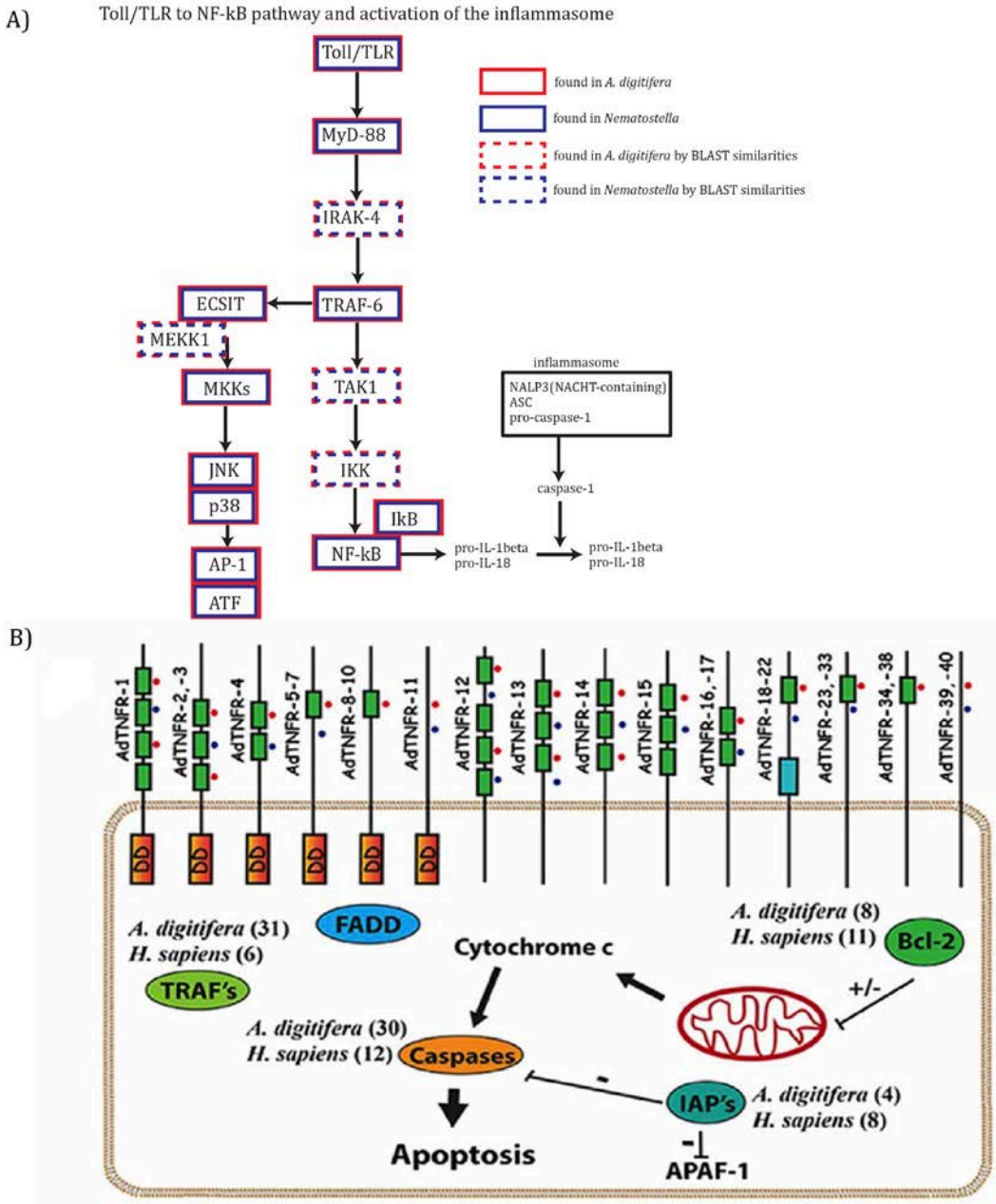

Figure 1.5 Components of the *A. digitifera* innate immune repertoire. A) TLR signalling pathway components identified in *Nematostella* and *A. digitifera*. Red and blue boxes indicate genes found in the *A. digitifera* and *Nematostella* genomes respectively. B) TNFR repertoire of *A. digitifera* indicating the protein domains and members of the death receptor pathway with the numbers of proteins of each type in *A. digitifera* and *H. sapiens.* Figures from Shinzato *et al.* (2011; Figure 13) and Quistad *et al.* (2014; Figure 1).

The complement system is a second arm of the innate immune response, and again homologs of several key components have been found in cnidarians but little is known about their roles. As with the TLRs, in both vertebrates and invertebrates, lectin members of the complement system recognize PAMPs, leading to activation of a phagocytic response to eliminate pathogens (Fujita *et al.* 2004). Homologues of some of the key components of the vertebrate system have been characterized in the sea anemone, *Nematostella vectensis*: the complement component 3 (C3), factor B (Bf), and the mannan-binding protein associated serine protease (MASP) (Kimura *et al.* 2009). The *Acropora millepora* C3 (C3-Am) has the canonical complement C3 domain structure (shown in Figure 1.6) (Miller *et al*. 2007), and was up-regulated in response to injury (Kvennefors *et al.* 2010) and under challenge with *Alteromonas* sp. (Brown *et al.* 2013). These studies are consistent with an important role for C3-Am in the coral innate immune response.

Moreover, the *Acropora millepora*, mannose-binding lectin (MBL), Millectin has been implicated in pathogen recognition (Kvennefors *et al.* 2010). A number of other lectins (PdC-lectin, Concanavalin, P-selectin) were up-regulated after exposure of the coral *Pocillopora damicornis* to the pathogen *Vibrio coralliilyticus* (Vidal-Dupiol *et al.* 2011). Other proteins implicated in coral immunity include phenoloxidase (PO) and a number of fluorescent proteins (FPs), these proteins showed higher concentrations in unhealthy than in healthy corals (Palmer *et al.* 2010; Palmer *et al.* 2008).

Figure 1.6 Protein domains present in vertebrate complement component C3, and the presence (+)/absence (-) of these in the corresponding proteins from *Hydra, Nematostella* and *Acropora*. Figure taken from Miller *et al.* (2007; Figure 5).

1.3. Environmental stressors and coral health

As in other organisms, coral health and disease can be understood as the interaction between the environment, causative agents (e.g. virus, bacteria, fungi), and host susceptibility (Figure 1.7) (Rosenberg *et al.* 2008). This interaction is evident in studies that suggest that elevated temperatures can compromise host immunity and increase pathogen virulence, making corals more susceptible to disease (Harvell *et al.* 2009). Consistent with the idea of additive or synergistic effects of stressors, Cervino *et al*. (2004) reported that elevated water temperature increased progression of yellow blotch/band disease (YBD) lesions on the Caribbean coral *Montastrea*. Vidal-dupiol *et al*. (2014) demonstrated down-regulation of innate immune system components (including TIR, NF-kB, P38, AP1 genes) during the response of *Pocillopora domicornis* to bacterial challenge under thermal stress, suggesting immune suppression.

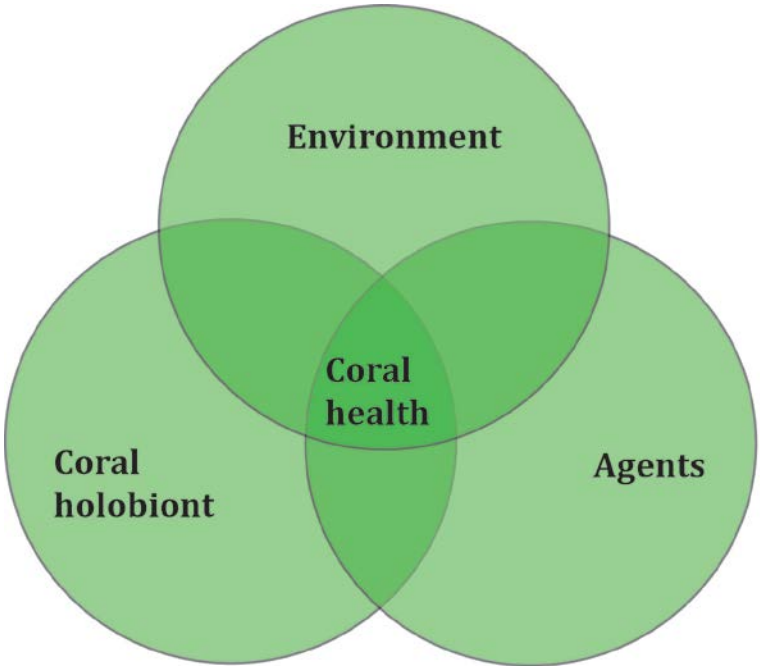

Figure 1.7 Coral health is result of the interaction between the environment, the causative agents and the coral holobiont (as described in Rosenberg *et al.* 2008).

Whilst some studies have focused on the effects that temperature has on coral health and immune responses (Pinzón *et al.* 2015; Ricaurte *et al.* 2016), little attention has been paid to the impact that ocean acidification (OA) could have on the coral innate immune system despite OA being considered a major threat to coral reefs over the next century. Clear evidence that elevated pCO_2 can impair immune responses comes from both mammals and *Drosophila*, where exposure to elevated pCO_2 conditions suppresses the production of key immune proteins and increases bacterial pathogen virulence, making these organisms more prone to disease (Cummins *et al.* 2010; Helenius *et al.* 2009; Taylor & Cummins 2011). Relatively few studies have addressed the effects of elevated pCO_2 on immunity in marine organisms. Activation of the stress signalling molecule (p38 MAP-kinase) was significantly inhibited in the echinoderm *Asterias rubens,* after six months of elevated pCO_2 (Hernroth *et al.* 2011). Likewise, increased infection by the bacterium *Vibrio tubiashii* was observed in blue mussels (*Mytilus edulis)* after four months exposure to high pCO_2 conditions (Asplund *et al.* 2014). After nine days of exposure, primary polyps of *A. millepora* responded to 750 ppm pCO_2 by increased transcription of genes encoding specific heat shock (HSPs) and anti-apoptotic Bcl-2 proteins (Moya *et al*. 2015 and 2016), but the impacts of this treatment on immunity are unknown.

1.4. Coral responses to salinity changes

1.4.1. Corals and osmoregulation

Freshwater intrusions onto the GBR have major impacts on near-shore reefs by decreasing water quality, impacting the health of corals and other marine organisms (Fabricius *et al.* 2005). Although there are current efforts to improve water quality to mitigate the impacts on the GBR (Great Barrier Reef Marine Park 2014), the effects of low salinity due to heavy rainfall will require global efforts to minimize climate change impacts on the water cycle. The consequences of low salinity events on corals are only now being revealed; for example, data from the Keppel Islands (GBR) indicated that 15 days of exposure to hypo-saline conditions (28 PSU) after heavy rainfall events, is the limit for survival of

Acropora sp. (Berkelmans *et al.* 2012). In the case of the coral *Stylophora pistillata,* exposure to hypo-saline conditions leads to swelling of cells, loss of *Symbiodinium,* and tissue necrosis (Downs *et al.* 2009). Other studies suggest that the response to low salinity may differ between species; for example, in contrast to *Acropora* and *Pocillopora*, species of *Porites* did not bleach during a low salinity event on a Gulf of Thailand reef (Nakano *et al.* 2009).

To understand the coral response to changes in salinity, it is necessary to investigate the regulatory mechanisms involved. Although there have been few studies on cnidarian osmoregulation, as in other marine invertebrates, corals respond to osmotic changes by adjusting the concentration of inorganic or organic molecules such as: K^+, Cl^-, free amino acids (FAA), glycine betaine, trimethylamine-N-oxide (TMAO) and proline betaine (Hochachka & Somero 2002). Changes in levels of these compounds under osmotic stress differ substantially between species (Pierce 1982). For example, FAA concentrations increased in the coral *Acropora aspera* under hyposaline conditions, whereas they decreased in the anemone *Anthopleura aureoradiata* (Cowlin 2012), suggesting taxon-specific responses. Overall, we have a very limited understanding of the molecules and processes used by corals to cope with changes in salinity, and the cellular mechanisms that are leading to bleaching and mortality after low salinity events are unknown.

1.4.2. DMSP production in corals

Sulphur is an essential element whose global biogeochemical cycle links the terrestrial, atmosphere and ocean systems (Andreae 1990). The oceans are one of the largest reservoirs of sulphur, from which sulphur is naturally released as the organic compound dimethylsulphide (DMS). This volatile gas is the breakdown product of dimethylsulphoniopropionate (DMSP) and, after entering the atmosphere, can regulate local climate by inducing cloud formation (Ayers & Gras 1991; Sievert *et al.* 2007). DMSP is a key molecule in the marine sulphur cycle, and is particularly significant in reef ecosystems since

corals are amongst the largest DMSP producers in the marine environment. DMSP production by corals exceeds levels reported by the highly productive sea ice algae, thus corals are important contributors to the biogenic sulphur cycle (Broadbent & Jones 2004). Pathways of DMSP biosynthesis have been described for several groups of algae and a few higher plants (Caruana 2010) and, on this basis, the production of DMSP by corals was attributed until recently to their dinoflagellate symbionts (Broadbent *et al.* 2002). However, a recent study by Raina *et al*. (2013) demonstrated production of DMSP by aposymbiotic coral larvae and the presence of candidate genes for roles in its biosynthesis in *A. millepora*. DMSP has been associated with a wide range of functions in organisms that produce it, including as an osmolyte, a cryoprotectant, and in scavenging reactive oxygen species (ROS) (Kirst 1990; Nishiguchi & Somero 1992; Sunda *et al.* 2002). For example, DMSP production by the sea-ice diatom *Fragilariopsis cylindrus* increased by 85% under hypersaline conditions, in order to maintain osmotic balance (Lyon *et al.* 2011). The biological significance of DMSP production by corals is unknown, although previous studies have reported concentration increases with temperature stress (Raina *et al.* 2013), and roles in scavenging of ROS have been suggested (Deschaseaux *et al.* 2014).

Pathways of DMSP biosynthesis are not well documented, although it has been proposed that this trait has arisen independently at least three times - twice in higher plants and once in algae (Gage *et al.* 1997; Hanson *et al.* 1994; Kocsis *et al.* 1998). Information on DMSP biosynthesis pathways is scarce and patchy. The identification of key intermediates, such as dimethylsulphonio-2-hydroxybutyrate (DMSHB), is assumed to reflect the presence of a complete pathway for DMSP biosynthesis but, while some of the enzymes involved have been identified, others await confirmation (Stefels 2000). To date, corals are the only animals known to produce DMSP, therefore elucidation of the corresponding biosynthetic pathway is of fundamental interest (Raina *et al.* 2013).

1.5. Corals and transcriptomics

Transcriptomics is a powerful tool with which to investigate the molecular mechanisms that organisms rely upon to cope with external challenges (Lockwood *et al.* 2015). RNA sequencing (RNA-Seq) has provided new insights into the genetic and regulatory complexity of eukaryotes (Wang *et al.* 2009), and has proven to be particularly useful in the case of non-model "lower" animals, where it has revealed unexpected levels of complexity. For example, transcriptomics has revealed the diverse and vertebrate-like immune (Hemmrich *et al.* 2007) and apoptotic (Moya *et al*. 2016) repertoires of corals.

Whereas previous studies have used incomplete datasets, the work outlined in this thesis uses gene predictions based on a whole genome assembly for *Acropora millepora* as a reference for understanding several aspects of coral stress responses. Other studies have used candidate gene approaches – for example, in the investigation of coral responses to temperature stress (Leggat *et al.* 2011; Ogawa *et al.* 2013; Seveso *et al.* 2014) – or been based on non-comprehensive transcriptome assemblies (see, for example, DeSalvo *et al*. (Bay *et al.* 2009; 2010). Some previous work on *A. millepora* stress responses has been based on a near-complete transcriptome assembly (Moya *et al.* 2012; Moya *et al.* 2015; Weiss *et al.* 2013), but the work described here is the first to be based on a comprehensive set of gene predictions.

1.6. Study aims and objectives

The general aim of this study is to understand the response of corals to abiotic (environmental) and biotic (immunogen) challenges using transcriptomic approaches. Four specific topics were investigated: (i) the coral response to an immune challenge, (ii) how the immune response is affected by high pCO_2 conditions, (iii) the coral response to low salinity, and (iv) the impact of low salinity on DMSP metabolism by corals. Data from these four lines of investigation allow the following objectives to be addressed:

1. **To understand the coral response to immune (LPS) challenge (Chapter 2).** Corals have clear homologues of many components of the vertebrate immune system, although the roles of most of these are unknown. To establish similarities with the vertebrate immune response, I will analyses the transcriptomic response of the coral after challenge with the well-characterised immunogen, LPS.

2. **To understand the effects of high pCO_2 conditions on the coral response to LPS (Chapter 2)**. High pCO_2 is known to impair the immune response of higher organisms, making them more prone to disease. Despite the potential significance of this for the susceptibility of corals to disease, at present no data are available on the effects of changes in ocean pH on the immune responses of marine organisms. To establish whether hypercapnia supresses coral immune responses, I will compare the transcriptomic response of corals to LPS challenge under "normal" and high pCO_2 conditions.

3. **Investigate and determine the molecular mechanisms that underpin coral response to salinity stress (Chapter 3).** The molecular mechanisms underlying coral bleaching and mortality during flooding events in the GBR are unknown to date. To understand these events, I will investigate gene expression changes in corals under hypo-saline conditions using transcriptomic approaches. Comparison of these results with published data for other stressors should enable general stress responses to be distinguished from those that are specific to osmotic stress.

4. **Investigate DMSP production by corals under salinity stress (Chapter 4).** Despite corals been major sources of DMSP and contributors to the biogenic sulphur cycle, the function of this molecule in corals is still unknown. DMSP is known to function as an osmolyte in some species of algae and plants, leading to the suggestion that this may also be the case in corals, but this idea presently lacks empirical support. By using nuclear magnetic resonance (NMR) techniques to measure DMSP

concentrations in coral tissue, I will investigate how levels of this metabolite change in response to variation in salinity, allowing the hypothesis that DMSP serves as an osmolyte to be tested.

5. **Identify the specific genes involved in DMSP biosynthesis in coral adults and juveniles (Chapter 4).** Essential steps of the DMSP biosynthesis pathway has been described in two species of higher plants and one algae, but never investigated in the only known animal to produce DMSP, corals. To identify which of several candidate genes are involved in the biosynthesis of DMSP in corals, I will use differential gene expression analysis. This approach is based on the hypothesis that DMSP biosynthesis will be influenced by changes in salinity, and that candidate genes will up-regulated under conditions that lead to increase of DMSP production.

6. **Identify the core set of genes that respond to different environmental stressors in corals (Discussion Chapter 5).** Several transcriptomic studies have identified genes involved in the response of corals to elevated temperature, high pCO_2 and bacterial challenge, but there is no current consensus on genes that are involve as a general response to stress. The available trancriptomic data will be used in an attempt to establish which stress responses of coral are general and which are specific for particular stressors.

Chapter 2

Elevated *p*CO_2 suppresses the innate immune response of the coral *Acropora millepora* to LPS challenge

2.1. Introduction

Coral diseases pose a major and increasing threat to the persistence of tropical reefs, contributing, along with other impacts, such as thermal stress, overfishing, ocean acidification and eutrophication, to declines in reef ecosystems globally (Harvell *et al.* 1999). Anecdotal evidence suggests that diseases have a greater impact on corals that are already under stress (Harvell *et al.* 2007) but, while this is entirely plausible, until recently there has been little empirical support for this hypothesis.

One chronic stress that coral reefs face over the next century is ocean acidification, as increased levels of carbon dioxide in the atmosphere equilibrate with the oceans (Hoegh-Guldberg *et al.* 2007). According to the most recent IPCC report (Intergovernmental Panel on Climate Change) (2013), the current surface ocean pH of ~8.1 will decrease 0.2–0.4 units by the end of this century, which will have significant impacts on ocean chemistry. Near future pH conditions have been shown to significantly impact calcification and the net production of corals (Kleypas & Langdon 2006), and transcription of genes involved in many basic processes in coral juveniles (Moya *et al.* 2012). To date, few studies have addressed potential synergistic effects of low pH and pathogen challenge on corals, although high pCO_2 conditions are known to impair immune responses in terrestrial animals (Taylor & Cummins 2011). While corals have clear homologues of many components of the vertebrate immune repertoire (Miller *et al.* 2007; Shinzato *et al.* 2011), we have only a limited understanding of coral immunity (Weiss *et al.* 2013) and almost nothing is known about the influence of elevated pCO_2 on the coral immune response.

Emerging coral diseases have been studied intensively over the last twenty years though the specific underlying causative agents (both biotic and abiotic) have been elusive (Harvell *et al.* 2007). In a number of specific case studies, bacterial species from the genus *Vibrio* have been implicated as the causatives agents of coral disease (Bourne *et al.* 2009; Rosenberg *et al.* 2007). Although the physiological impacts of *Vibrio* sp. challenge on corals

have been described (Kushmaro *et al.* 2001; Rosenberg & Falkovitz 2004; Sussman *et al.* 2008), only recently have cellular aspects of the response been investigated. For example, Vidal-Dupiol *et al*. (2014) used transcriptomics to characterise the expression of candidate immune genes of the *Pocillopora damicornis* after challenge with the coral pathogen *Vibrio coralliilyticus*, and they found that three days post challenge a number of immune recognition and signalling pathways (TIR containing proteins, IKK, NF-kB, AP1 among other) were down-regulated. Interestingly, the virulence of *Vibrio coralliilyticus* is temperature-dependent (Ben-Haim *et al.* 2003), with higher seawater temperatures resulting in increased tissue lysis in the coral *P. damicornis* following bacterial challenge (Vidal-Dupiol *et al.* 2011). This observation is consistent with an additive or synergistic effect, where increased temperature not only changes the virulence patterns of the pathogen but may also compromise the host coral immune system.

Currently, coral immune responses are poorly understood, and most experiments have been based on the assumption that coral homologues of vertebrate genes function as in higher organisms (Miller *et al.* 2007). EST databases have in some cases provided candidate immune system components, including the mannose-binding lectin (MBL), Millectin and complement C3 (Kvennefors *et al.* 2008). Subsequently, Millectin, but not the complement factor C3-like protein (C3-Am), was shown to be significant up-regulated after challenge of *A. millepora* with either lipopolysaccharide or peptidoglycan (Kvennefors *et al.* 2010). Beside C3 itself, Bf and MASP (mannan-binding protein-associated serine protease) - other members of the complement component 3 (C3) system - have been characterised from a sister cnidarian, the starlet sea anemone, *Nematostella vectensis* (Kimura *et al.* 2009).

Comparative genomics has revealed that the immune repertoire of the coral *A. digitifera* is significantly more complex than that of the sea anemone, *N. vectensis* (Shinzato *et al.* 2011), and whole genome sequencing has made possible comprehensive surveys of the

immune and apoptotic genes present in corals, including NOD-like receptors (NLRs) (Hamada *et al.* 2012), tumor necrosis factors (TNFs) and their receptors (TNFRs) (Quistad SD *et al.* 2014), toll-like receptors (TLRs) (Poole & Weis 2014), and caspases and their multi-domain regulators (Moya *et al.* 2016). Collectively, these studies have revealed a major gene expansion of many immune gene families in the coral relative to the sea anemone. For example, *A. digitifera* had the highest number (total = 27) of toll/interleukin1 receptor (TIR)-domain containing proteins compared to other cnidarians (Poole & Weis 2014), and a higher number of NACHT (NAIP, CIITA, HET-E, and TP1) domain proteins (total = 496) than man (total = 27) (Shinzato *et al.* 2014). The complexity of these gene families has consequences for attempts to understand immune responses in corals, as in mammals these protein domains are involved in TLR and NLR signalling, as well as activation of NF-kB and MAPK signalling pathways, and lead to the expression of pro-inflammatory cytokines (Poole & Weis 2014). There is also evidence of functional conservation between coral and human immune systems – for example, the human cytokine TNF (HuTNFα) appears to activate a coral TNFR, but further experiments are needed to identify which specific coral TNFR binds is involved (Quistad SD *et al.* 2014).

To better understand the effect of cumulative stressors on the underlying immune response of corals, we undertook a transcriptomic analysis of the response of *Acropora millepora* to LPS (lipopolysacharidae) challenge, both under ambient pCO_2 conditions and after pre-exposure to high pCO_2 conditions. LPS is a pathogen-associated molecular pattern (PAMPs) found in the outer membrane of gram-negative bacteria, and elicits a strong and well-characterised immune response in mammals. LPS signalling in mammals activates extracellular TLR receptors (Takeda & Akira 2005). A previous study (Weiss *et al.* 2013) addressed the transcriptomic response of *A. millepora* to MDP (muramyl dipeptide), a PAMP derived from the cell walls of both gram-negative and gram positive bacteria that activates intracellular NLRs. Challenge with MDP led to increased expression of coral homologues of

mammalian GiMAP/IAN proteins, suggesting conservation of function between corals and mammals (Weiss *et al.* 2013). In the present study, LPS can essentially be regarded as a proxy for pathogen challenge. Exposure to LPS induced changes in the expression of specific coral TLRs, NLRs, TNF/TNFRs and components of the associated down-stream signalling systems. Pre-exposure of corals to elevated pCO_2 conditions impaired the responses of several of the LPS-regulated genes, implying that near-future ocean conditions may compromise coral health by impairing immune responses. This study documents for the first time this kind of response in a marine organism.

2.2. Material and methods

2.2.1. Aquarium experimental design

Five colonies of *Acropora millepora* were collected off the coast of Orpheus Island, Queensland, Australia (18°39'52. 43"S, 146°29'42.38"E) under GBRMPA permit #G12/34321.1 during April 2012 and transported to the Orpheus Island Research Station, where they were maintained at a 27 °C (±0.015) in a flow-through system with 10 µ filtered seawater (FSW). Each colony was divided in four fragments and allocated randomly on twelve replicate 50 l aquaria under ambient conditions (pH 8.09 ± 0.04, 508.7 ppm pCO_2) during a period of 8 days for acclimation. After the acclimation period six aquaria were exposed to high pCO_2 (pH 7.82 ± 0.11, 1072 ppm pCO_2, details below) and six kept at control conditions (508.7 ppm pCO_2) over a 14 day experimental period.

The high pCO_2 condition was achieved by injecting pCO_2 with a solenoid into a 500 l sump aquarium regulated with a pH-controller (Aqua Medic) and distributed to the 50 l aquaria. Temperature and pH were measured daily with portable pH and temperature meters (Milwaukee model: MW102) and calibrated daily with NBS buffers (pH 4 and 7, Labchem). Dissolved oxygen was measured with a 55 dissolved oxygen instrument (YSI 55), and monitored at 8 am daily with temperature, pH, and total alkalinity (TA). TA of seawater

(mmol/kgSW) was estimated using Gran titrations (888 Titrando, Metrohm, Switzerland) from a total of 47 water samples. Average seawater pCO_2 was calculated with these parameters in the program CO2SYS (Lewis & Wallace 1998) dissociation constants from (Mehrbach *et al.* 1973) as refitted by (Dickson & Millero 1987). Average pCO_2 was estimated to 508 and 1072 µmol during the 14 days of the experiment, with a summary of parameters shown in Table S2.1 (Supporting information).

2.2.2. Coral immune challenges

After the 14 days under control and high pCO_2 conditions, each colony was injected evenly with of two different substances: sterile phosphate buffered saline (3x PBS, n= 12 per colony) as a control, and a defined immunogen Ultrapure lipopolysaccharide (LPS InvivoGen, Catalog # tlrl-3pelps, San Diego, USA; n=12 per colony). PBS (3x) was used as the dilution buffer for the LPS immune-stimulant and diluted to a concentration of 0.03 mgr/ml. Each nubbin was injected on the axial polyp with 100 µl of either PBS of LPS using a 1 ml syringe fitted with a 27-gaude needle. One hour and six hours after exposure, 3 nubbins (~2 cm fragments) per colony per treatment were collected and snap-frozen in liquid nitrogen before being stored at -80 °C.

2.2.3. RNA extraction, high-throughput sequencing and data analysis

The three coral nubbins collected per colony were crushed together in liquid nitrogen and ~1g of the resulting powder homogenized for 15 min by vortexing in 3 mL of TRIzol Reagent (Invitrogen), followed by centrifugation at 4,000 g for 15 min. The supernatant was recovered with a 1 mL pipet leaving the coral tissue pellet. 4-Bromo-2-chlorophenol (150 µl) was added to the recovered supernatant according to the TRIzol manufacturer's specifications with a slight modification, 0.5 mL of 100% isopropanol was replaced with a mixture of 300 µl 100% isopropanol and 200 µl of high-salt buffer (0.8M Na citrate, 1.2 M NaCl) per 1.5 ml of TRIzol in the precipitation step. The RNA pellet was solubilized in ~50 µl

of RNAse-free water and stored at -80 °C. The quality and quantity of RNA preparations were determined using a Bioanalyzer (Agilent 2100 Bioanalyzer) using samples prepared following the Agilent RNA 6000 Nano Kit instructions (cat # 5067-1511).

A total of 40 RNAseq libraries were constructed using the TruSeq RNA Library Preparation Kit v2 (RS-122-2001) following the manufacturers recommended protocol and 100 bp single-end sequence data obtained using a HiSeq 2000 at the Biomolecular Resource Facility (John Curtin School of Medical Research, Australian National University). Reads were mapped onto the *Acropora millepora* genome (Foret el al., in preparation) using TopHat2 (Kim *et al.* 2013) to produce a count data gene expression matrix for subsequent analysis. Counts were generated using htseq-count (Anders *et al.* 2015).

Data was analysed in sSeq package (Yu *et al.* 2013) (R Core Team 2014) using a design formula for differential gene expression that tests for the effects LPS challenge, by using a paired design that takes colony and treatment as factors, and runs the negative binomial model with shrinkage approach of dispersion (nbTestSH). Log_2 fold changes (log_2FC) in gene expression levels were obtained in sSeq by comparing control (PBS) vs. LPS challenge of four different datasets: (i) control vs. LPS challenge at 1 h, (ii) control vs. LPS challenge at 1 h under pCO_2 exposure, (iii) control vs. LPS challenge at 6 h, and (iv) control vs. LPS challenge at 6 h under pCO_2 exposure. False discovery rate (FDR) adjusted *p* values for each gene, was controlled at 5% according to the methods of Benjamini and Hochberg (1995).

Statistically over-represented gene ontology (GO) categories were determined in BiNGO (Maere *et al.* 2005) in Cytoscape 3.1.1 (Smoot *et al.* 2011) by using the set of genes that were differentially up or down-regulated in each dataset (FDR < 0.01). These GO categories were used to identify specific immune related proteins and subsequent search for their gene family (TNF, PF00229.13; TNFR, PF00020.13; TIR, PF01582.15; TRAF,

PF02176.13; NACHT, PF05729.7; IRF, PF00605.12) in the *A. millepora* gene protein predictions. Moreover, sequences from immune related signalling pathways (NLRs , hsa04621; TLRs, hsa04620; NF-kappa B, hsa04064) were downloaded from the Kyoto Encyclopedia of Genes and Genomes (KEGG) and blasted against the *A. millepora* protein predictions. All the results are based on homology of the *A. millepora* protein predictions to a reference annotated proteins (*e*−val cut-off = 1e−4), and differentially expressed genes (FDR <0.05, $\log_2$FC ≥ 0.05) were used for subsequent analysis.

2.3. Results

Coral colonies did not show any symptoms of bleaching or disease during the acclimation or after the LPS challenge.

2.3.1. Differential gene expression analyses

Transcriptomic analysis revealed that, under control (pH 8.1) conditions, at 1 h after the LPS challenge 583 (2.2% of the total) *A. millepora* genes were differentially expressed (DEGs, FDR <0.01) relative to control (PBS) injection. At six hours after the LPS challenge, the number of DEGs increased to 2251 (8.5% of the total); 305 genes were differentially expressed at both time points, but 122 of these (i.e. 40%) were up-regulated at 1 h and down-regulated 6 h (Figure 2.1 and Figure S2.2, Supporting Information). Gene Ontology (GO) analysis of the up-regulated genes after 1 h of LPS challenge identified six over-represented categories (FDR <0.05), including response to chemical stimulus, central nervous system development and regulation of Wnt receptor signalling pathway. No over-represented categories could be identified in the set of down-regulated genes. After 6 h, over-represented categories were mostly in the down-regulated gene set, including the GO categories: amino acid metabolism, regulation of Wnt receptor signalling pathway, and extracellular matrix organization (Table S2.2 Supporting Information).

In order to better understand the effects of elevated pCO_2 on coral immunity, the next phase of analysis focused on specific components of the innate immune repertoire, including the toll-like and Nod-like receptor signalling pathways. These genes were annotated based on similarity with key components of the immune systems of higher animals, and changes in the expression of some of these coral genes under immune challenge have previously been described (Weiss *et al*. 2015).

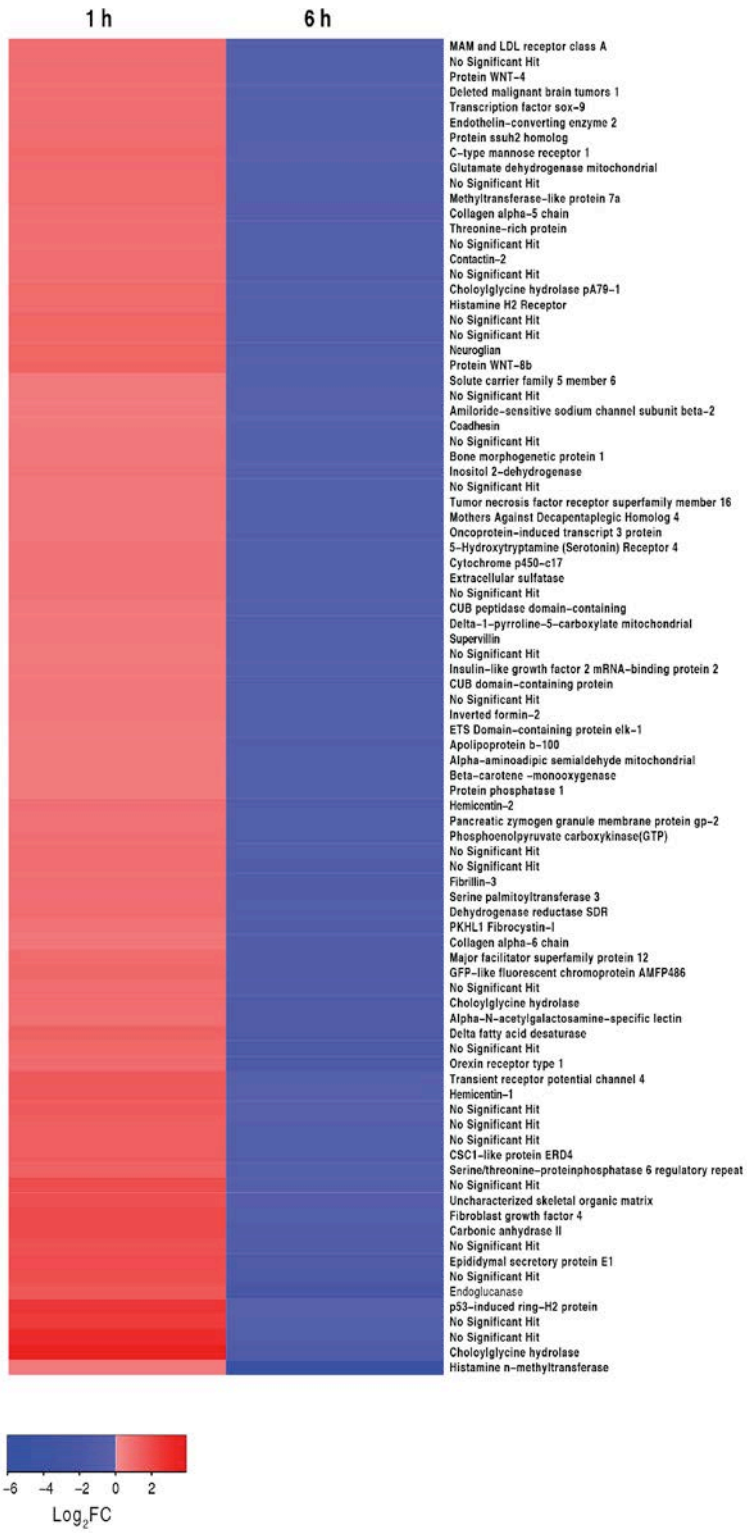

Figure 2.1 Heat map of the normalized expression (log_2FC) of genes differentially expressed (FDR <0.01, log_2FC >0.05) in response to LPS challenge after 1 and 6 h. Clustering of the genes was based on their expression pattern. Heat map is based on 88 shared genes that are up-regulated after 1 h and down-regulated after 6 h. The colour bar indicates log_2FC between control and LPS challenge, red representing up-regulation, blue down-regulation, and white no change. Refer to Table S2.3, Supporting information for values for each gene and complete list of the shared response genes.

2.3.2. Activation of innate immune pathways after LPS challenge

The complement system is involved in the detection and clearance of potential pathogens, and is a key component of the mammalian innate immune system (Delanghe *et al.* 2014). Coral homologues of only three components of the mammalian complement system have been identified, these being complement C3 (Miller *et al.* 2007) of which two paralogues are present in corals and in sea anemones (Kimura *et al.* 2009; Ocampo *et al.* 2015; Shinzato *et al.* 2011), factor B (Bf) where again, two paralogues are present in anthozoans (Kimura *et al.* 2009), and MASP (Ocampo *et al.* 2015). In the present case, three C3 predictions, likely corresponding to the two loci, were identified. One of the C3 genes was up-regulated after 1 h of LPS challenge (by 0.27 $\log_2$FC), whereas factor B and MASP expression were essentially unaltered. At the 6 h time point, expression of all three C3 genes was down-regulated (Table S2.4, Supporting information). Whereas expression of the lectin, Millectin was down-regulated at both the 1 and 6 h time points, a number of other C-type lectins, including the macrophage mannose receptor (MRC1; 1.2.20551.m1), were up-regulated after 1 h but down-regulated after 6 h (Table S4, Supporting Information).

Exposure to LPS also induced changes in the expression of components of other innate immune signalling pathways, including several toll-like receptors (TLRs), NF-kB, MAPK, and NOD-like receptors (NLRs; Figure 2.2, Table S2.2.5-8 Supporting Information). Three of the four interleukin-1 receptor-like (IL-1R-like) and two of the five TLRs identified in the *A. millepora* genome were up-regulated after 1 h of LPS challenge, although one TLR and the remaining IL-1R-like homologues were down-regulated (Table 2.1, Table S2.5, Supporting information). In vertebrates, TLRs and IL-1Rs interact with pathogen associated molecular patterns (PAMP) via extracellular domains, but also characteristically contain an intracellular toll/interleukin1 receptor (TIR) domain that is also present in several other proteins, including MyD88 (myeloid differentiation primary response 28 protein 88; (Poole & Weis 2014). Moreover, TLRs and IL-1Rs can bind to MyD88 to activate the NF-kB response

via the MyD88–dependant pathway (Akira & Takeda 2004). However in the current coral gene expression data, neither MyD88 nor NF-kB homologues were differentially expressed after LPS challenge. Alternatively, signalling via these receptors can follow a MyD88–independent pathway and activate interferon regulatory factors (IRF) downstream, where two homologues to these genes were differentially up-regulated and one down-regulated under LPS challenge (Figure 2.3, Table S2.8, Supporting information). Subsequently, two candidate tumor necrosis factor alpha (TNF–α) genes were up-regulated after 1 h and down-regulated after 6 h of challenge (1.2.13359.m1 and1.2.17029.m1) (Figure 2.3, Table S2.6, Supporting information).

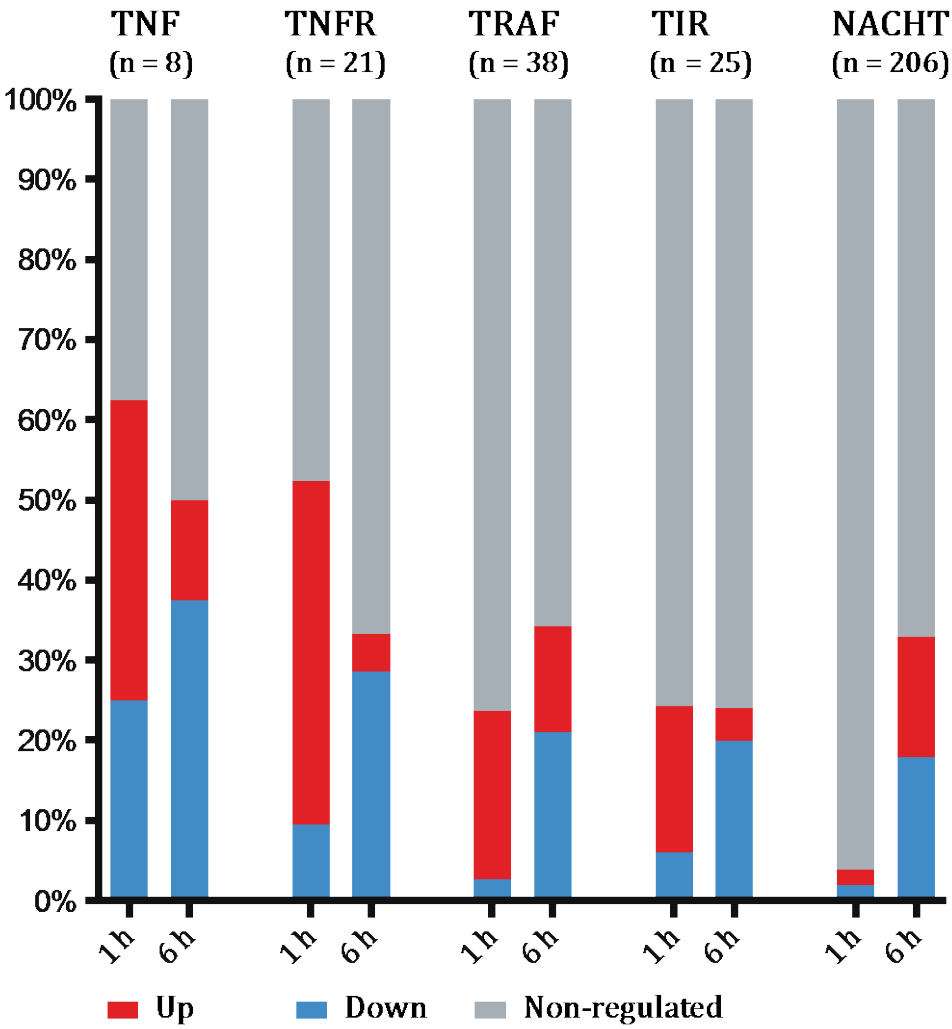

Figure 2.2 Percentages of each gene family differentially expressed under LPS challenge. The coloured sectors of the bars represent percentages of the total number of genes of each type differentially expressed after 1 and 6 h (FDR < 0.05): up (red), down (blue), or non-regulated

(grey). The total numbers of genes in each category are indicated in parentheses above the bars. TNF, tumor necrosis factor; TNFR, TNF receptor; TRAF, TNF receptor-associated factor; TIR, Toll/interleukin-1 receptor; NACHT, NAIP, CIITA, HET-E, and TP1.

Table 2.1 TIR-domain-containing proteins that were differentially expressed (FDR <0.05, $log_2FC > 0.05$) in response to LPS challenge after 1 and 6 h. Log_2FC colour indicates up (red) and down (blue) regulated genes.

								Log_2FC	
Genome ID	NCBI Domain	*A. digitifera* ID	*A. digitifera* Blast Hit	Blast Hit	Hit ID	Length	e-Value	1 h	6 h
1.2.22324.m1	IG|IG|IG|TIR	Ad_ILR2	aug_v2a.11844	HMCN2_Hemicentin-2	A2AJ76.1|HMCN2_MOUSE	524	3.40E-19	1.60	–
1.2.10735.m1	IG|IG|IG|TIR	Ad_ILR1	aug_v2a.20402	TLR2_Toll-like receptor 2	B2LT62.1|TLR2_CAPIB	586	4.40E-13	-0.12	–
1.2.22473.m1	IG|TIR	Ad_ILR2	aug_v2a.11844	TLR13_Toll-like receptor 13	Q6R5N8.1|TLR13_MOUSE	435	1.20E-15	0.37	–
1.2.2434.m1	IG|TIR	Ad_ILR6	aug_v2a.14217	TLR2_Toll-like receptor 2	Q689D1.1|TLR2_CANFA	334	4.00E-13	0.20	–
1.2.13179.m1	LRR|LRR|TIR	Ad_TLR1	aug_v2a.20813	TOLL_Protein toll	P08953.1|TOLL_DROME	1110	1.50E-64	0.39	–
1.2.13177.m1	LRR|TIR	Ad_TLR4	aug_v2a.14728	TOLL_Protein toll	P08953.1|TOLL_DROME	481	3.60E-52	0.34	–
1.2.13178.m1	LRR|LRR|TIR	Ad_TLR1	aug_v2a.20813	TOLL_Protein toll	P08953.1|TOLL_DROME	838	1.10E-59	–	-0.18
1.2.13180.m1	LRR|TIR	Ad_TLR1	aug_v2a.20813	TOLL_Protein toll	P08953.1|TOLL_DROME	851	1.80E-58	-0.44	–
1.2.5856.m1	TIR	Ad_TIR6	aug_v2a.05635	TLR2_Toll-like receptor 2	Q2PZH4.1|TLR2_BUBBU	404	2.60E-16	0.40	-0.20
1.2.16257.m1	TIR	Ad_TIR2_1	aug_v2a.23782	TLR6_Toll-like receptor 6	Q704V6.1|TLR6_BOVIN	245	2.10E-18	–	-0.05
1.2.2436.m1	TIR	Ad_ILR4	aug_v2a.16874	TLR6_Toll-like receptor 6	Q704V6.1|TLR6_BOVIN	185	2.20E-15	–	-0.34
1.2.5845.m1	TIR	Ad_unknown1	aug_v2a.13087	TLR2_Toll-like receptor 2	Q2V897.1|TLR2_BOSTR	445	6.10E-18	–	-0.15
1.2.849.m1	TIR2	Ad_TIR2_12	aug_v2a.16869	–		314	–	–	0.06

The observed transcriptional response of the TNF−α ligands was supported by the changes in expression of several TNF receptor (TNFR) superfamily members (Table 2.2); in mammals, TNFRs are involved in inflammation and apoptosis, and in molluscs and some other marine invertebrates (De Zoysa *et al.* 2009) are activated after LPS challenge. The *A. digitifera* immune repertoire includes 13 TNFSF members and 40 TNFRSF (Quistad SD *et al.* 2014), while in the *A. millepora* genome eight genes with the TNF domain (PF00229.13) and 22 genes with the TNFR domain (PF00020.13) have been identified. Ten of the 22 *A. millepora* TNFRSF homologues were differentially up-regulated after 1 h of LPS challenge, and eight of these were down-regulated after 6 h (Figure 2.2, Table 2.2). Moreover, TRAF homologues (TNFR-associated factor; PF02176.13), which play key roles in both TNFR and TLR signalling (Quistad SD *et al.* 2014), were differentially expressed during LPS challenge in the coral (Table 2.2). Nine of the 38 *A. millepora* TRAF genes (31in *A. digitifera*) were differentially regulated at 1 h after immune challenge (eight were up-regulated, one was

down-regulated). At 6 h, the number of differentially expressed TRAFs had increased to 13, but the majority of these (8) were down-regulated (Table 2.2, Table S2.7, Supporting information). One outcome of TNF/TNFR signalling is the triggering of apoptosis, in which the caspases and Bcl-2 proteins are the key implementers and regulators respectively. After 1 h of LPS challenge, two (likely pro-apoptotic) caspase-3/6 type genes (AmCaspase E and AmCaspase D, see Moya *et al*. 2015) were up-regulated, whereas at 6 h, one caspase 3/6 and 3 Bcl-2 (two anti-apoptotic genes and the pro-apoptotic Bax) were down-regulated (Figure 2.3, Table S2.9, Supporting information).

Table 2.2 TNF, TNFR and TRAF genes that were differentially expressed (FDR <0.05, log_2FC > 0.05) in response to LPS challenge after 1 and 6 h. Log_2FC colour indicates up (red) and down (blue) regulated genes.

							Log_2FC	
	Genome ID	NCBI Domain	Blast Hit	Hit ID	Length	e-Value	1 h	6 h
TNF	1.2.13359.m1	TNF	TNFa_Tumor necrosis factor	P16599.1|TNFA_RAT	231	1.60E-06	1.31	0.17
	1.2.17029.m1	TNF	TNFa_Tumor necrosis factor	P16599.1|TNFA_RAT	207	5.00E-06	1.06	–
	1.2.4528.m1	TNF	TNF10_Tumor necrosis factor ligand superfamily member 10	P50591.1|TNF10_HUMAN	174	5.90E-04	0.16	–
	1.2.607.m1	TNF	TNFb_Tumor necrosis factor ligand superfamily member 1	P26445.1|TNFB_PIG	135	9.40E-05	-0.28	-0.15
	1.2.17031.m1	TNF	TNF15_Tumor necrosis factor ligand superfamily member 15	Q5UBV8.2|TNF15_MOUSE	159	6.00E-05	–	-0.20
TNFR	1.2.15238.m1	TNFRSF|Death	TNFR1b_Tumor necrosis factor receptor superfamily member 1b	P20333.3|TNR1B_HUMAN	381	6.00E-04	0.66	0.19
	1.2.20632.m1	TNFRSF|Death	Netrin receptor UNC5C	Q761X5.1|UNC5C_RAT	931	4.00E-06	0.62	-0.18
	1.2.20630.m1	TNFRSF|Death	TNFR16_Tumor necrosis factor receptor superfamily member 16	P18519.1|TNR16_CHICK	580	7.40E-06	0.46	–
	1.2.20633.m1	TNFRSF	TNFR16_Tumor necrosis factor receptor superfamily member 16	P08138.1|TNR16_HUMAN	237	2.70E-05	0.67	–
	1.2.20631.m1	TNFRSF	TNFR16_Tumor necrosis factor receptor superfamily member 16	P08138.1|TNR16_HUMAN	253	4.00E-05	0.54	-0.24
	1.2.6590.m1	TNFRSF	TNFR16_Tumor necrosis factor receptor superfamily member 16	P18519.1|TNR16_CHICK	416	3.00E-02	0.46	–
	1.2.4347.m1	TNFRSF	TNFR16_Tumor necrosis factor receptor superfamily member 16	P18519.1|TNR16_CHICK	416	7.00E-03	0.39	–
	1.2.4349.m1	TNFRSF	TNFR16_Tumor necrosis factor receptor superfamily member 16	P18519.1|TNR16_CHICK	416	1.90E-01	0.27	-0.49
	1.2.6598.m1	TNFRSF	TNFR19_Tumor necrosis factor receptor superfamily member 19	Q9NS68.1|TNR19_HUMAN	391	2.70E-04	0.24	–
	1.2.10769.m1	TNFRSF	EDAR_Tumor necrosis factor receptor superfamily member EDAR	Q90VY2.1|EDAR_ORYLA	497	6.10E-05	0.09	-0.05
	1.2.17682.m1	TNFRSF	TNFR16_Tumor necrosis factor receptor superfamily member 16	P18519.1|TNR16_CHICK	416	7.80E-02	-0.29	–
	1.2.6595.m1	TNFRSF	TNFR19_Tumor necrosis factor receptor superfamily member 19	Q9JLL3.2|TNR19_MOUSE	416	3.20E-02	-0.41	–
	1.2.4350.m1	TNFRSF	TNFR14_Tumor necrosis factor receptor superfamily member 14;	Q92956.3|TNR14_HUMAN	283	4.00E-03	–	-0.08
	1.2.6597.m1	TNFRSF	TNFR19_Tumor necrosis factor receptor superfamily member 19	Q9NS68.1|TNR19_HUMAN	423	2.00E-03	–	-0.26
	1.2.11264.m1	TNFRSF	TNFR16_Tumor necrosis factor receptor superfamily member 16	P18519.1|TNR16_CHICK	489	1.20E-04	–	-0.40
TRAF	1.2.2898.m1	TRAF|MATH	TRAF6_TNF receptor-associated factor 6	Q3ZCC3.1|TRAF6_BOVIN	450	1.50E-63	1.02	–
	1.2.2891.m1	TRAF|MATH	TRAF6_TNF receptor-associated factor 6	B5DF45.1|TRAF6_RAT	362	1.40E-74	1.00	–
	1.2.2897.m1	RING|TRAF|MATH	TRAF6_TNF receptor-associated factor 6	B5DF45.1|TRAF6_RAT	498	2.30E-104	0.58	-0.08
	1.2.2881.m1	TRAF|MATH	TRAF6_TNF receptor-associated factor 6	Q3ZCC3.1|TRAF6_BOVIN	366	4.60E-59	0.56	-0.38
	1.2.2899.m1	RING|TRAF|MATH	TRAF6_TNF receptor-associated factor 6	Q3ZCC3.1|TRAF6_BOVIN	418	2.80E-81	0.42	–
	1.2.6455.m1	TRAF	TRAF6_TNF receptor-associated factor 6	Q3ZCC3.1|TRAF6_BOVIN	551	2.20E-13	0.08	-0.14
	1.2.2752.m1	RING|TRAF|MATH	TRAF3_TNF receptor-associated factor 3	Q13114.2|TRAF3_HUMAN	528	3.40E-103	0.09	–
	1.2.4647.m1	RING|TRAF|MATH	TRAF4_TNF receptor-associated factor 4	Q61382.2|TRAF4_MOUSE	456	6.80E-69	0.06	–
	1.2.10762.m1	RING|TRAF|MATH	TRAF3_TNF receptor-associated factor 3	Q60803.2|TRAF3_MOUSE	552	1.40E-94	-0.16	–
	1.2.16730.m1	RING|TRAF|MATH	TARF6b_TNF receptor-associated factor 6-b	Q6DJN2.1|TRF6B_XENLA	412	6.40E-53	–	0.15
	1.2.5451.m1	RING|TRAF|MATH	TRAF6_TNF receptor-associated factor 6	P70196.2|TRAF6_MOUSE	411	1.40E-39	–	0.14
	1.2.3972.m1	RING|TRAF|MATH	TRAF4_TNF receptor-associated factor 4	Q9BUZ4.1|TRAF4_HUMAN	363	1.90E-37	–	0.13
	1.2.2754.m1	RING|TRAF|MATH	TRAF3_TNF receptor-associated factor 3	Q13114.2|TRAF3_HUMAN	593	8.50E-99	–	0.12
	1.2.2892.m1	TRAF|MATH	TRAF6_TNF receptor-associated factor 6	Q3ZCC3.1|TRAF6_BOVIN	412	3.70E-68	–	0.09
	1.2.5426.m1	RING|TRAF|MATH	TRAF3_TNF receptor-associated factor 3	Q60803.2|TRAF3_MOUSE	556	4.10E-117	–	-0.37
	1.2.866.m1	ZF|TRAF|MATH	TRAF4_TNF receptor-associated factor 4	Q61382.2|TRAF4_MOUSE	500	1.10E-62	–	-0.14
	1.2.5457.m1	RING|TRAF|MATH	TRAF4_TNF receptor-associated factor 4	Q61382.2|TRAF4_MOUSE	422	4.20E-65	–	-0.10
	1.2.5463.m1	RING|TRAF|TRAF	TRAF6_TNF receptor-associated factor 6	B6CJY4.1|TRAF6_CERAT	416	6.60E-38	–	-0.09
	1.2.4735.m1	RING|TRAF	TRAF7_TNF receptor-associated factor 7	Q6Q0C0.1|TRAF7_HUMAN	316	3.20E-31	–	-0.06

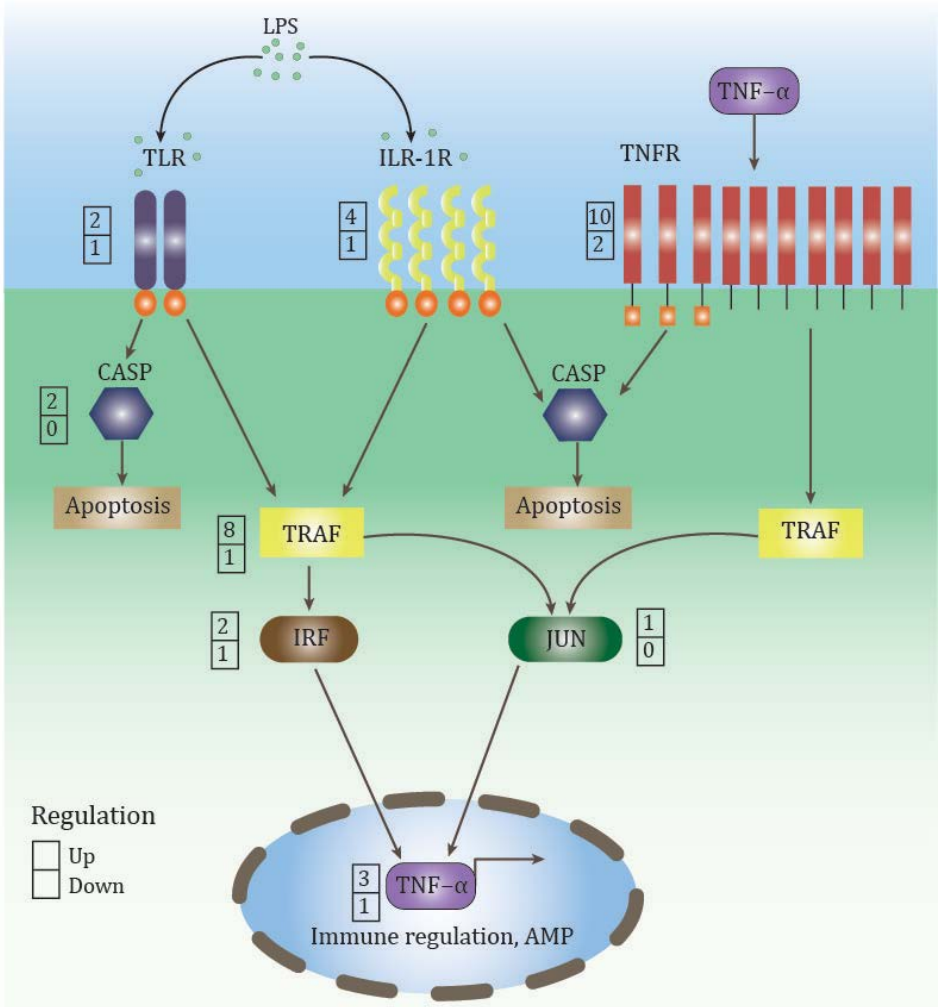

Figure 2.3 Summary of the coral immune response after 1 h of LPS challenge under control conditions. The numbers indicate numbers of genes per category that were differentially (FDR < 0.05, $\log_2$FC > 0.05) up- or down-regulated (see Table S2.2-S7, Supporting information for more complete details). Figure adapted from KEGG pathway database (pathways 04620 and 04064).

2.3.3. The intracellular NLRs were regulated after prolonged (6 h) LPS challenge

At the 1 h time point, few changes were observed in expression of NLR/NACHT genes, whereas after 6 h of LPS challenge a total of 68 genes of this type were differentially expressed (Figure 2.2, Table S2.8, Supporting information). NLRs are a family of intracellular pattern recognition receptors (PRR) that play critical roles in the innate immune response in mammals - they activate the caspase -1, NF-kB and MAPK signalling pathways (Kanneganti *et al.* 2007; Yuen *et al.* 2014). These receptors are characterized by the presence of a NACHT domain; 461 genes of this type have been identified in the *A. digitifera* genome (Hamada *et al.*

2012), and the corresponding number of *A. millepora* is 205 (cut-off 1e-5, Pfam 05729.7). The *A. millepora* NACHT genes include a group of 42 genes that encode only a NACHT domain, 116 genes with a NACHT – leucine-rich repeats (LRR) structure, 12 with NACHT– WD40, and a group of 26 genes glycosyl_transferase 1 – NACHT domain (Table S2.8, Supporting information). As in the case of TLR signalling, in mammals, NLRs interact with TRAFs to activate NF-kB. However, in the case of *A. millepora,* fewer TRAFs were up-regulated at 6 h post-challenge (n = 5) compared to 1 h (n = 8; Table S2.7, Supporting information). Overall, 1 h after LPS challenge a number of TLR and TNFR-type cell surface receptors were up-regulated, although by 6 hours the receptor response had been down-regulated (Tables S2.5 and S2.6). By contrast, in the case of the NLRs, many more genes were differentially expressed after 6 h (33% of NLR genes identified) compared to the 1 h time point (4% of NLRs; Figure 2.2 and 2.3).

Choloylglycine hydrolases (CBAH, PF02275.14) are of particular interest because they may have roles in regulation of the microbial communities associated with corals (Miller, personal communication). A total of seven choloylglycine hydrolases were identified in the *A. millepora* genome, and one of these displayed the highest log_2FC of all of the annotated DEGs (1.2.7139.m1, 3.85 Log_2FC). Four of the seven CBCH genes were up-regulated at 1 h post LPS challenge, and five down-regulated after 6 h (Table S2.8, Supporting information).

2.3.4. Elevated pCO_2 suppresses the innate immune response of the coral to LPS challenge

In corals that had been pre-exposed to high pCO_2 conditions (pH 7.8), the expression of 51% (n = 371) of genes that were up-regulated at 1 h post-LPS challenge under control conditions (pH 8.1) was supressed (Figure S2.3, Supporting information). The differentially expressed genes described here as high pCO_2 conditions post LPS challenge, refers to the log_2FC of the LPS treatment relative to the control injection (PBS), both pre-exposed to high

pCO_2 levels. In corals that had been pre-exposed to high pCO_2 conditions, GO analysis of genes up-regulated at 1h post-immune challenge identified five over-represented categories (FDR <0.05), while down-regulated genes had 16 over-represented categories including regulation of transcription, central nervous system development, regulation of signalling pathway and negative regulation of apoptosis (Table S2.10, Supporting information). A group of genes (n = 20) were up-regulated 1 h after immune challenge under both control and high pCO_2 conditions, including three heat shock proteins (HSPs), two fibroblast growth factor receptors (FGFR), two metalloproteinases, and a green fluorescent protein (GFP, 2.85 Log_2FC) (Table S2.11, Supporting information). A second group of genes (n = 70), which included four TIR-domain containing proteins, six TNFRs and three TRAFs (Am_TRAF4, Am_TRAF24 Am_TRAF25), were up-regulated under control conditions but down-regulated under high pCO_2 conditions (Figure 2.4, Table S2.12, Supporting information). Moreover, the expression of two caspases (AmCaspase D and Am Caspase E), a Bcl-2 protein (AmBclWD), and five C-type lectins was also suppressed by high pCO_2 conditions, suggesting that a high pCO_2 environment impairs coral apoptotic responses (Table S2.11, Supporting information). Interestingly, high pCO_2 conditions strongly affected the responses of genes encoding NACHT domains; at 1 h post challenge, 33 NACHT genes were down-regulated and 14 genes up-regulated under pCO_2 treatment, compared to four genes up and four down-regulated after 1 h under control conditions (Table S2.8, Supporting information). Also significant was the relative suppression of the CBAH homologue with the highest expression value, while two other CBAH genes were unaffected by the high pCO_2 treatment.

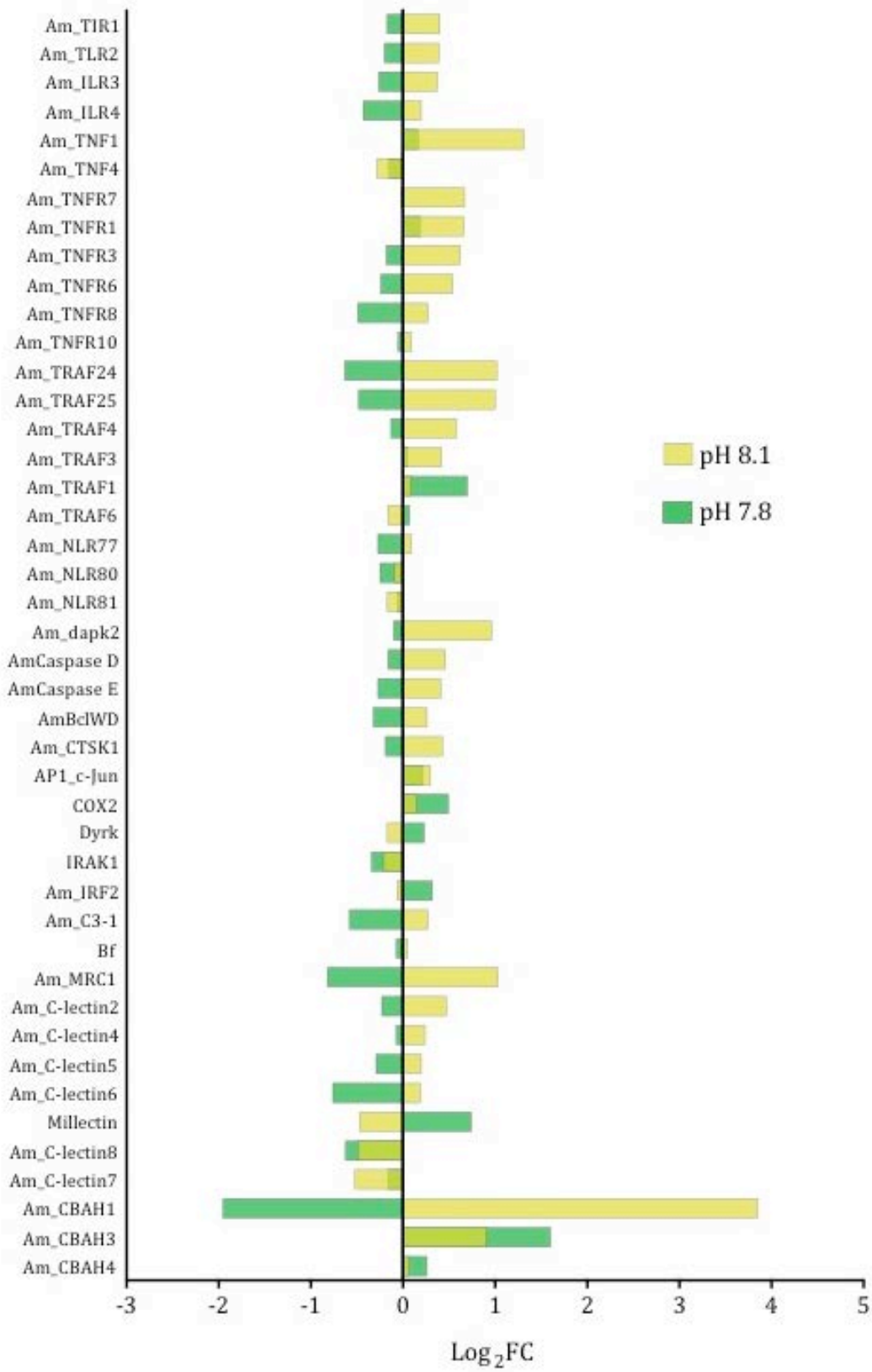

Figure 2.4 Immune and stress-response genes responding differentially under control and high pCO_2 conditions at 1 h post LPS challenge. Bars show the $\log_2$FC of the differentially expressed genes (FDR < 0.05, $\log_2$FC > 0.05) for LPS under control (yellow), and LPS under high pCO_2 conditions (green). Original data are summarised as Tables S2.4-S11 (Supporting information).

2.4. Discussion

The immune system of the coral *A millepora* is poorly understood. Similar to higher animals, LPS induced the expression of immune related genes in the coral. This immune response included changes in the expression of coral genes belonging to families that are known to be LPS-induced in mammals, including the TLRs and IL-1Rs (Takeda & Akira 2005), as well as downstream components of the corresponding signalling pathways (Figure 2.3). Likewise high pCO_2 conditions suppressed several of the up-regulated LPS-induced genes (Figure 2.4), suggesting that elevated pCO_2 may compromise coral immunity. This hypothesis is consistent with the idea that stressed corals are more susceptible to disease (Harvell *et al.* 1999).

2.4.1. LPS activates Toll-like, TNF and NOD-like receptors

TLRs are well characterised pattern recognition receptors (PRR) that control host defence against pathogens and immune disorders in mammals (Takeda & Akira 2005). In the current study, two TLRs (Am_TLR2 and Am_TLR5) were significantly up-regulated (0.39 and 0.34 Log_2FC respectively). Previous investigations of the demosponge *Suberites domuncula* have described the increased expression of a specific TLR, and Ser/Thr/Tyr kinase domain (IRAK) and a caspase-like proteins in response to LPS challenge, suggestive of an immune response like those of higher metazoans (Wiens *et al.* 2007). In corals, the availability of the whole genome sequence allowed us to investigate changes in expression of the complete TLR and IL-1R gene repertoires (Table S2.5, Supporting information). Changes in expression of pathway components down-stream of these receptors (TRAF6 and IRF, Figure 2.3) provide further evidence for mammalian–like roles for these pathways in the early innate immune response of corals. NLRs are the second major class of metazoan PRRs – essentially they are the cytosolic counterparts of the TLRs. The *A. millepora* NLR repertoire is large and complex, and changes in the expression of members of this family in response to immune challenge were similarly complex (Figure 2.2). Since the functions of these genes are unknown,

interpretation of responses is by analogy with higher animals and essentially speculative at this point. Studies in *Hydra* have, however, revealed increased expression of specific NLRs in response to LPS challenge (Lange *et al.* 2011), potentially indicating conserved roles of these receptors in both cnidarians. However additional research is needed to better understand the significance and roles of the diverse NLR repertoire of corals.

LPS challenge also resulted in the up-regulation of specific coral TNFRs, members of a family of proteins that are involved in regulating cell death and inflammatory responses in mammals (Wiens & Glenney 2011). The activation of this system was also indicated by changes in the expression of the downstream pathway components JUN, TRAF and caspase (Figure 2.3, Table S2.9, Supporting information). TNFR activation has also previously been documented in *Hydra,* where JUN, TNFR and an associated TRAF were up-regulated from 1 to 4 h after injury (Wenger 2014). Although these are very different types of stressors, it is interesting to find that in both cnidarians these receptors and their down-stream members appear to function as components of a stress signalling system.

2.4.2. Comparative response between LPS and other immune challenges in corals

The use of transcriptomics allowed us to compare the responses of specific genes that are activated by both MDP (muramyl dipeptide) and LPS challenge in *A. millepora*, as the MDP response has previously been descried (Weiss *et al.* 2013). With both of these immunogens, choloylglycine hydrolase (CBH) pA79-1 was strongly up-regulated 1 h post immune-challenge (Table S2.3, Supporting information), which is consistent with a role for CBH in regulating the coral- associated microbial community. One significant difference between the responses to the two immunogens is that, whereas MDP induced strong up-regulation of several GiMAP/IAN family members (Weiss *et al.* 2013), in the present study, these genes were not differentially expressed after LPS challenge. NLRs, that are known to be activated by MDP in mammals (Girardin *et al.* 2003), were induced 6 h after LPS challenge, so it would be

interesting to examine the 6 h response of corals to MDP. Interestingly, in experiments where *Pocillopora damicornis* was challenged with *Vibrio coralliilyticus*, after 3 days of exposure, the expression of many immune related genes was suppressed (Vidal-Dupiol *et al.* 2014). In the case of both this *Vibrio* experiment and the LPS challenge reported here, the expression of complement system homologues (Bf and MBL Lectin) and of a phospholipase A2 gene increased. However, clear differences between these datasets with respect to the expression of homologous genes (for example, TIR3, TRAF6, AP1, and ATF were down-regulated in the *Vibrio* challenge paper, but up-regulated in the present study) were also observed.

2.4.3. High pCO_2 suppressed the coral LPS-induced innate immune response

High pCO_2 conditions appear to supress the LPS-induced immune response in corals, as the expression of several TLRs, TNFRs and NLRs and key pathway components was suppressed under high pCO_2 conditions relative to controls (Figure 2.4). This response is consistent with studies in mammalian cells and *Drosophila,* where NF-kB, TNF−α and interleukin (IL)-6 responses were impaired by hypercapnia, making these organisms more prone to disease (Cummins *et al.* 2014; Wang *et al.* 2010; West *et al.* 1997). Although in corals LPS did not activate expression of NF-kB, expression of several TNF−α homologues was up-regulated under control conditions and these responses were suppressed under high pCO_2 conditions (Table S2.6, Supporting information). High pCO_2 treatment also suppressed expression of complement component 3 (C3), Bf and several C-type lectins, suggesting that high pCO_2 conditions may comprehensively compromise the coral immune response. Such an effect may mean that corals become more sensitive to disease, as has been documented in *Drosophila* and for mammalian cells and (Cummins *et al.* 2014).

These results are consistent with anecdotal reports that stressed corals are more susceptible to disease (Harvell *et al.* 1999), and highlight the complex molecular mechanisms underlying coral responses to elevated pCO_2 (Cummins *et al.* 2010).

2.5. Conclusions

This work significantly extends the body of data available on the responses of corals to immune challenges. The experiment described here was, of necessity, relatively short-term and simple in design, and for these reasons may not accurately reflect how corals will respond to long-term changes in ocean acidification. Nevertheless, these data highlight some of the potential consequences of elevated pCO_2 that are not necessarily obvious. Juvenile corals appear to be capable of rapid acclimation to elevated pCO_2 (Moya *et al.* 2015), but the present work implies that they may be more susceptible to disease. In summary, this work has two major implications: (i) this is the first study to show that the expression of coral homologs of several key components of the vertebrate innate immune system are activated in response to an immune challenge,, (ii) ocean acidification may seriously compromise coral health, by suppressing normal innate immune responses that are essential for host defence.

2.6. Supporting information

Tables

Table S2.1 Summary of seawater parameters in control and high CO_2 treatment

	pH_{NBS}	Total alkalinity (µmol/kg)	Temperature (°C)	$\Omega_{aragonite}$	pCO_2 (µatm)
Control	8.09 ± 0.04	2227.3 ± 72.9	27.3 ± 0.1	2.94 ± 0.27	508.7 ± 55.3
High CO_2	7.82 ± 0.11	2203.8 ± 45.2	27.3 ± 0.1	1.74 ± 0.43	1072.1 ± 247.7

Table S2.2. GO terms of the differentially expressed genes after (A) 1 h and (B) 6 h post LPS challenge. FDR values were obtained from the Benjamini & Hochberg correction using BiNGO. Shaded terms (purple) are significantly over-represented (FDR < 0.05).

(A)

Up-regulated				Down-regulated			
GO Biological processes	**GO ID**	**Total genes**	**FDR**	**GO Biological processes**	**GO ID**	**Total genes**	**FDR**
regulation of Wnt receptor signaling pathway	30111	5	1.27E-03	bioluminescence	8218	2	2.48E-01
regulation of gene expression	10468	31	6.86E-03	thyroid hormone generation	6590	1	2.48E-01
enzyme linked receptor protein signaling pathway	7167	10	1.92E-02	immature T cell proliferation	33079	1	2.48E-01
central nervous system development	7417	12	2.63E-02	negative regulation of Wnt receptor signaling pathway	30178	3	2.48E-01
transmembrane receptor protein tyrosine kinase signaling pathway	7169	8	4.17E-02	membrane	16020	29	2.48E-01
response to chemical stimulus	42221	21	4.35E-02	T cell proliferation	42098	1	2.97E-01
response to stimulus	50896	37	5.08E-02	calcium channel activity	5262	2	2.97E-01
sensory organ development	7423	10	6.01E-02	calcium ion transport	6816	2	2.97E-01
response to inorganic substance	10035	6	6.05E-02	carbon dioxide transport	15670	1	2.97E-01
response to osmotic stress	6970	3	6.28E-02	carbonate dehydratase activity	4089	1	2.97E-01
nervous system development	7399	21	6.89E-02	stress-activated MAPK cascade	51403	1	2.97E-01
protein tyrosine kinase activity	4713	7	7.37E-02	hypotonic salinity response	42539	1	2.97E-01
generation of neurons	48699	15	8.04E-02	passive transmembrane transporter activity	22803	5	2.97E-01
PAMP dependent induction by symbiont of host innate immunity	52033	2	8.29E-02				
T cell activation	42110	3	1.01E-01				
oxidoreductase activity, acting on the CH-NH2 group of donors	16638	2	1.06E-01				
immune system process	2376	13	1.08E-01				
transcription regulator activity	30528	11	1.14E-01				
regulation of MAPKKK cascade	43408	5	1.14E-01				
ATP-binding cassette (ABC) transporter complex	43190	1	1.14E-01				
regulation of signaling pathway	35466	13	1.28E-01				
regulation of signaling process	23051	11	1.29E-01				
transmembrane receptor protein tyrosine kinase activity	4714	3	1.31E-01				
neuron cell-cell adhesion	7158	3	1.31E-01				
regulation of cellular process	50794	53	1.36E-01				
negative regulation of biosynthetic process	9890	10	1.36E-01				
cell communication	7154	11	1.44E-01				
signaling pathway	23033	22	1.49E-01				
regulation of nervous system development	51960	7	1.54E-01				
central nervous system segmentation	35283	1	1.54E-01				
phosphoenolpyruvate carboxykinase (GTP) activity	4613	1	1.54E-01				
glutamate catabolic process	6538	1	1.54E-01				
response to nitric oxide	71731	1	1.54E-01				
hydrogen peroxide catabolic process	42744	1	1.54E-01				
cellular response to abiotic stimulus	71214	3	1.54E-01				
transmembrane receptor protein kinase activity	19199	3	1.54E-01				
cell-cell adhesion	16337	4	1.60E-01				
regulation of response to stimulus	48583	9	1.61E-01				
system process	3008	12	1.61E-01				
cellular response to organic substance	71310	8	1.61E-01				
regulation of metal ion transport	10959	3	1.66E-01				
regulation of cell projection organization	31344	5	1.66E-01				
positive regulation of cellular biosynthetic process	31328	10	1.68E-01				
protein kinase activity	4672	12	1.69E-01				
negative regulation of signal transduction	9968	3	1.69E-01				
cell surface	9986	4	1.69E-01				
histone lysine methylation	34968	2	1.69E-01				
negative regulation of Ras GTPase activity	34261	1	1.69E-01				
endocrine system development	35270	3	1.76E-01				

(B)

Up-regulated				Down-regulated			
GO Biological processes	**GO ID**	**Total genes**	**FDR**	**GO Biological processes**	**GO ID**	**Total genes**	**FDR**
lipid metabolic process	6629	19	3.49E-02	cellular amino acid and derivative metabolic process	6519	35	4.43E-05
sphingomyelin metabolic process	6684	3	3.49E-02	bioluminescence	8218	9	1.04E-04
fatty acid metabolic process	6631	7	1.49E-01	L-serine biosynthetic process	6564	5	4.09E-04
bioluminescence	8218	3	2.70E-01	glycine metabolic process	6544	5	2.58E-03
alcohol biosynthetic process	46165	4	3.61E-01	IMP metabolic process	46040	5	9.44E-03
phospholipid metabolic process	6644	6	3.61E-01	hypotonic salinity response	42539	4	2.65E-02
G-protein coupled receptor protein signaling pathway	7186	10	3.61E-01	regulation of Wnt receptor signaling pathway	30111	15	2.85E-02
positive regulation of endothelial cell proliferation	1938	2	3.66E-01	extracellular matrix organization	30198	10	2.86E-02
cell surface receptor linked signaling pathway	7166	21	3.66E-01	sulfur metabolic process	6790	13	3.10E-02
transmembrane receptor activity	4888	13	4.51E-01	L-glutamate transmembrane transporter activity	5313	3	4.73E-02
cell death	8219	7	4.59E-01	oxygen and reactive oxygen species metabolic process	6800	4	7.03E-02
regulation of cGMP metabolic process	30823	1	4.59E-01	peroxidase activity	4601	4	1.10E-01
positive regulation of RNA metabolic process	51254	11	4.76E-01	response to tumor necrosis factor	34612	4	1.57E-01
enzyme linked receptor protein signaling pathway	7167	8	4.78E-01	response to transforming growth factor beta stimulus	71559	4	1.57E-01
apoptosis	6915	6	4.78E-01	cell development	48468	46	2.40E-01
carboxylic acid metabolic process	19752	11	4.78E-01	nervous system development	7399	61	2.78E-01
				lipid metabolic process	6629	12	2.82E-01
				sphingomyelin metabolic process	6684	2	2.82E-01
				cytokine-mediated signaling pathway	19221	4	2.82E-01
				apoptotic nuclear change	30262	4	2.86E-01
				sulfur amino acid metabolic process	96	4	3.62E-01
				phospholipid biosynthetic process	8654	8	3.62E-01
				regulation of cell migration	30334	13	3.62E-01
				response to chemical stimulus	42221	56	3.62E-01
				calcium-dependent phospholipid binding	5544	3	3.62E-01

Table S2.3 Differentially expressed genes (total = 88) (FDR <0.01, log_2FC >0.05) in response to LPS challenge after 1 and 6 h. Order as presented in the heat map Figure 2.1.

Genome ID	Protein ID	Log_2FC	
		1 h	6 h
1.2.7139.m1	Choloylglycine hydrolase	3.85	-1.03
1.2.22417.m1	No Significant Hit	2.97	-0.57
1.2.16616.m1	p53-induced ring-H2 protein	2.57	-0.08
1.2.1337.m1	No Significant Hit	2.43	-0.13
1.2.21686.m1	Fibroblast growth factor 4	1.97	-0.30
1.2.8860.m1	Carbonic anhydrase II	1.91	-0.62
1.2.6508.m1	Epididymal secretory protein E1	1.88	-1.14
1.2.1016.m1	No Significant Hit	1.82	-1.23
1.2.21266.m1	No Significant Hit	1.81	-0.19
1.2.21472.m1	Uncharacterized skeletal organic matrix	1.77	-0.29
1.2.6642.m1	No Significant Hit	1.74	-0.84
1.2.9411.m1	Endoglucanase	1.61	-1.95
1.2.1111.m1	Transient receptor potential channel 4	1.53	-0.11
1.2.9159.m1	Hemicentin-1	1.48	-0.08
1.2.8662.m1	No Significant Hit	1.44	-0.13
1.2.16367.m1	CSC1-like protein ERD4	1.38	-0.52
1.2.8656.m1	No Significant Hit	1.30	-0.30
1.2.12318.m1	No Significant Hit	1.30	-0.36
1.2.7877.m1	Serine/threonine-proteinphosphatase 6 regulatory repeat	1.26	-0.45
1.2.9227.m1	Delta fatty acid desaturase	1.18	-1.10
1.2.22670.m1	Neuroglian	1.17	-0.29
1.2.16253.m1	Protein WNT-8b	1.15	-0.11
1.2.23282.m1	No Significant Hit	1.14	-0.23
1.2.4159.m1	No Significant Hit	1.10	-0.21
1.2.20442.m1	No Significant Hit	1.09	-1.25
1.2.21562.m1	GFP-like fluorescent chromoprotein AMFP486	1.07	-0.82
1.2.16853.m1	Choloylglycine hydrolase pA79-1	1.03	-0.36
1.2.23285.m1	No Significant Hit	1.03	-0.20
1.2.20551.m1	C-type mannose receptor 1	1.03	-0.14
1.2.15849.m1	Methyltransferase-like protein 7a	1.01	-0.25
1.2.6956.m1	Major facilitator superfamily protein 12	1.00	-0.71
1.2.12363.m1	Glutamate dehydrogenase mitochondrial	0.98	-0.10
1.2.15012.m1	Orexin receptor type 1	0.97	-1.31
1.2.17261.m1	Dehydrogenase reductase SDR	0.96	-0.55
1.2.7303.m1	Histamine H2 Receptor	0.94	-0.36
1.2.10516.m1	Contactin-2	0.91	-0.31
1.2.13415.m1	Choloylglycine hydrolase	0.91	-1.01

1.2.20843.m1	No Significant Hit	0.91	-0.70
1.2.3332.m1	Protein ssuh2 homolog	0.90	-0.23
1.2.6958.m1	No Significant Hit	0.90	-0.87
1.2.14438.m1	Protein WNT-4	0.89	-0.16
1.2.20943.m1	Fibrillin-3	0.87	-0.66
1.2.14882.m1	MAM and LDL receptor class A	0.87	-0.16
1.2.8432.m1	Threonine-rich protein	0.86	-0.42
1.2.14.m1	No Significant Hit	0.86	-0.17
1.2.19174.m1	Deleted malignant brain tumors 1	0.86	-0.19
1.2.4223.m1	Collagen alpha-5 chain	0.86	-0.40
1.2.8651.m1	No Significant Hit	0.86	-0.29
1.2.7734.m1	Transcription factor sox-9	0.86	-0.21
1.2.14080.m1	Endothelin-converting enzyme 2	0.84	-0.20
1.2.20939.m1	No Significant Hit	0.84	-0.47
1.2.13251.m1	Phosphoenolpyruvate carboxykinase(GTP)	0.83	-0.54
1.2.15486.m1	Serine palmitoyltransferase 3	0.82	-0.61
1.2.6310.m1	No Significant Hit	0.82	-0.39
1.2.15008.m1	Alpha-N-acetylgalactosamine-specific lectin	0.81	-0.98
1.2.3152.m1	Hemicentin-2	0.81	-0.50
1.2.4311.m1	Pancreatic zymogen granule membrane protein gp-2	0.78	-0.51
1.2.15857.m1	Cytochrome p450-c17	0.77	-0.31
1.2.1472.m1	No Significant Hit	0.75	-0.41
1.2.23786.m1	Extracellular sulfatase	0.74	-0.37
1.2.8939.m1	Inositol 2-dehydrogenase	0.72	-0.08
1.2.14400.m1	PKHL1 Fibrocystin-l	0.70	-0.68
1.2.6172.m1	5-Hydroxytryptamine (Serotonin) Receptor 4	0.70	-0.25
1.2.6311.m1	No Significant Hit	0.69	-0.16
1.2.15765.m1	Oncoprotein-induced transcript 3 protein	0.68	-0.31
1.2.22505.m1	Mothers Against Decapentaplegic Homolog 4	0.68	-0.30
1.2.20633.m1	Tumor necrosis factor receptor superfamily member 16	0.67	-0.02
1.2.4382.m1	No Significant Hit	0.67	-0.10
1.2.15762.m1	Collagen alpha-6 chain	0.67	-0.82
1.2.12142.m1	Insulin-like growth factor 2 mRNA-binding protein 2	0.63	-0.43
1.2.16855.m1	No Significant Hit	0.63	-0.48

Table S2.4 *A. millepora* homologues to the complement system and C-lectins-domain proteins (PF00059.16). (A) BlastP search results are listed for each protein (total = 21). (B) Log_2FC values of significantly expressed genes (FDR <0.05, log2FC > 0.05) in response to LPS challenge relative to the control (PBS) after 1 and 6 h. For samples under control (pH 8.1) and high pCO_2 (pH 7.8) conditions. Log_2FC colour indicates up (red) and down (blue) regulated genes.

(A)

Protein type	Genome ID	*A. millepora* ID	Protein ID	Length	% ID	*e*-Value
Complement system						
C3	1.2.8186.m1	Am_C3-1	complement component C3 precursor [Nematostella vectensis]	655	33.44	3.00E-88
	1.2.2282.m1	Am_C3-2	complement component C3 precursor [Nematostella vectensis]	1758	41.47	0
	1.2.10886.m1	Am_C3-3	complement component C3 precursor [Nematostella vectensis]	1394	44.69	0
Bf	1.2.3633.m1	–	complement factor B precursor [Nematostella vectensis]	687	49.64	0
	1.2.2084.m1	–	complement factor B precursor [Nematostella vectensis]	671	32.49	8.00E-81
	1.2.2081.m1	–	complement factor B precursor [Nematostella vectensis]	625	36.32	1.00E-106
MASP	1.2.14429.m1	–	mannose-binding lectin associated serine protease precursor [Nematostella vectensis]	689	52.69	0
	1.2.12093.m1	–	mannose-binding lectin associated serine protease precursor [Nematostella vectensis]	276	35.87	5.00E-47
	1.2.2071.m1	–	mannose-binding lectin associated serine protease precursor [Nematostella vectensis]	268	35.07	6.00E-43
apextrin	1.2.20644.m1	Apextrin	apextrin [Acropora millepora]	805	99.50	0
Lectins	1.2.20551.m1	Am_MRC1	MRC1_human ame: full=macrophage mannose receptor 1	544	43.20	2.00E-16
	1.2.4223.m1	Am_C-lectin1	CO6A5_human ame: full=collagen alpha-5 chain	507	55.00	2.60E-21
	1.2.13586.m1	Am_C-lectin2	C209A_mouse ame: full=cd209 antigen-like protein A	154	56.00	7.80E-20
	1.2.16950.m1	Am_C-lectin3	CL17A_human ame: full=c-type lectin domain family member A	228	47.00	3.30E-06
	1.2.17036.m1	Am_C-lectin4	LADD_oncmy ame: full=ladderlectin	234	47.60	4.60E-18
	1.2.3603.m1	Am_C-lectin5	CLC4A_mouse ame: full=c-type lectin domain family 4 member A	273	47.00	4.60E-13
	1.2.12034.m1	Am_C-lectin6	FCER2_mouse ame: full=lymphocyte receptor	121	48.40	1.00E-11
	1.2.13360.m1	Am_C-lectin7	LADD_oncmy ame: full=ladderlectin	223	49.80	9.30E-14
	1.2.12155.m1	Am_C-lectin8	FCER2_mouse ame: full=lymphocyte receptor	121	48.20	3.30E-13
	1.2.22673.m1	Millectin	LECG_patpe ame: full=alpha-n-acetylgalactosamine-specific lectin	244	46.40	4.00E-12
	1.2.8560.m1	Am_C-lectin9	FCER2_mouse ame: full=lymphocyte receptor	150	43.40	2.10E-15
	1.2.21223.m1	Am_C-lectin10	PLCL_mytga ame: full=perlucin-like protein	176	45.20	3.00E-14

(B)

Genome ID	*A. millepora* ID	Control (pH 8.1)				High CO_2 (pH 7.8)			
		1 h		6 h		1 h		6 h	
		Log_2FC	FDR	Log_2FC	FDR	Log_2FC	FDR	Log_2FC	FDR
1.2.8186.m1	Am_C3-1	0.27	1.27E-02	-0.35	4.42E-02	-0.58	1.84E-03	-0.48	2.44E-03
1.2.2282.m1	Am_C3-2	–	–	-0.41	2.84E-02	–	–	–	–
1.2.10886.m1	Am_C3-3	–	–	-0.50	2.09E-02	–	–	-0.03	4.94E-02
1.2.3633.m1	–	–	–	–	–	0.79	9.46E-06	–	–
1.2.2084.m1	–	0.07	3.89E-02	–	–	–	–	–	–
1.2.2081.m1	–	0.05	4.58E-02	-0.27	2.01E-03	-0.07	3.90E-02	–	–
1.2.14429.m1	–	–	–	–	–	–	–	–	–
1.2.12093.m1	–	–	–	–	–	–	–	–	–
1.2.2071.m1	–	–	–	–	–	–	–	–	–
1.2.20644.m1	Apextrin	–	–	–	–	0.79	9.46E-06	-0.13	1.38E-06
1.2.20551.m1	Am_MRC1	1.03	4.13E-03	-0.14	1.28E-04	-0.82	3.55E-05	-0.77	1.16E-06
1.2.4223.m1	Am_C-lectin1	0.86	3.10E-03	-0.40	1.09E-03	–	–	-0.39	7.02E-14
1.2.13586.m1	Am_C-lectin2	0.47	1.11E-02	–	–	-0.23	2.39E-02	-0.31	3.84E-02
1.2.16950.m1	Am_C-lectin3	0.42	1.41E-02	–	–	–	–	–	–
1.2.17036.m1	Am_C-lectin4	0.24	1.69E-02	0.33	6.64E-11	-0.07	2.10E-03	-0.26	3.25E-06
1.2.3603.m1	Am_C-lectin5	0.20	2.06E-02	-0.05	7.42E-07	-0.29	7.48E-04	0.10	1.07E-03
1.2.12034.m1	Am_C-lectin6	0.19	2.21E-02	0.24	3.29E-07	-0.76	2.67E-02	-0.45	4.97E-05
1.2.13360.m1	Am_C-lectin7	-0.52	1.25E-02	-0.63	1.96E-06	-0.16	3.02E-03	0.10	5.86E-08
1.2.12155.m1	Am_C-lectin8	-0.49	2.52E-02	0.67	1.70E-05	-0.62	1.27E-05	-0.36	1.12E-02
1.2.22673.m1	Millectin	-0.47	1.75E-03	-1.12	4.53E-26	0.74	1.63E-07	0.36	2.37E-27
1.2.8560.m1	Am_C-lectin9	-0.25	6.08E-04	-1.13	1.38E-08	–	–	-0.11	2.68E-05
1.2.21223.m1	Am_C-lectin10	-0.22	1.39E-02	-0.45	1.78E-02	–	–	-0.20	2.38E-03

Table S2.5 TIR-domain-containing proteins (total = 37). (A) Results of the domain search (PF01582.15 with a 1e-4 cut-off) in the *A. millepora* genome and their *A. digitifera* homologues *(Poole & Weis 2014)*. NCBI domain and BlastP search results are listed for each protein. (B) Log_2FC values of significantly expressed genes (FDR <0.05, log2FC > 0.05) in response to LPS challenge relative to the control (PBS) after 1 and 6 h. For samples under control (pH 8.1) and high pCO_2 (pH 7.8) conditions. Log_2FC colour indicates up (red) and down (blue) regulated genes.

(A)

Genome ID	*A. millepora* ID	NCBI domain	*A. digitifera* ID	*A. digitifera* Blast Hit	Best Blast Hit	Hit ID	Length	e-Value
1.2.12032.m1	Am_Myd881	DD|TIR	Ad_Myd881	aug_v2a.00120	MyD88a_xenla ame: full=myeloid differentiation primary response protein 88-a	Q9DF60.1|MYB8A_XENLA	261	1.70E-37
1.2.12031.m1	Am_Myd882	DD|TIR	Ad_Myd882	aug_v2a.01135	MyD88a_xenla ame: full=myeloid differentiation primary response protein 88-a	Q5XJ85.2|MYD88_DANR	373	4.20E-28
1.2.10735.m1	Am_ILR1	IG|IG|IG|TIR	Ad_ILR1	aug_v2a.20402	TLR2_capib ame: full=toll-like receptor 2	B2LT62.1|TLR2_CAPIB	586	4.40E-13
1.2.22324.m1	Am_ILR2	IG|IG|IG|TIR	Ad_ILR2	aug_v2a.11844	HMCN2_mouse ame: full=hemicentin-2	A2AJ76.1|HMCN2_MOUSE	524	3.40E-19
1.2.22473.m1	Am_ILR3	IG|TIR	Ad_ILR2	aug_v2a.11844	TLR13_mouse ame: full=toll-like receptor 13	Q6R5N8.1|TLR13_MOUSE	435	1.20E-15
1.2.2434.m1	Am_ILR4	IG|TIR	Ad_ILR6	aug_v2a.14217	TLR2_canfa ame: full=toll-like receptor 2	Q689D1.1|TLR2_CANFA	334	4.00E-13
1.2.13178.m1	Am_TLR1	LRR|LRR|TIR	Ad_TLR1	aug_v2a.20813	TOLL_drome ame: full=protein toll	P08953.1|TOLL_DROME	838	1.10E-59
1.2.13179.m1	Am_TLR2	LRR|LRR|TIR	Ad_TLR1	aug_v2a.20813	TOLL_drome ame: full=protein toll	P08953.1|TOLL_DROME	1110	1.50E-64
1.2.13181.m1	Am_TLR3	LRR|LRR|TIR	Ad_TLR1	aug_v2a.20813	TOLL_drome ame: full=protein toll	P08953.1|TOLL_DROME	1481	1.70E-63
1.2.13180.m1	Am_TLR4	LRR|TIR	Ad_TLR1	aug_v2a.20813	TOLL_drome ame: full=protein toll	P08953.1|TOLL_DROME	851	1.80E-58
1.2.13177.m1	Am_TLR5	LRR|TIR	Ad_TLR4	aug_v2a.14728	TOLL_drome ame: full=protein toll	P08953.1|TOLL_DROME	481	3.60E-52
1.2.5856.m1	Am_TIR1	TIR	Ad_TIR6	aug_v2a.05635	TLR2_bubbu ame: full=toll-like receptor 2	Q2PZH4.1|TLR2_BUBBU	404	2.60E-16
1.2.16257.m1	Am_TIR2	TIR	Ad_TIR2_1	aug_v2a.23782	TLR6_bovin ame: full=toll-like receptor 6	Q704V6.1|TLR6_BOVIN	245	2.10E-18
1.2.2436.m1	Am_TIR3	TIR	Ad_ILR4	aug_v2a.16874	TLR6_bovin ame: full=toll-like receptor 6	Q704V6.1|TLR6_BOVIN	185	2.20E-15
1.2.5845.m1	Am_TIR4	TIR	Ad_unknown1	aug_v2a.13087	TLR2_bostr ame: full=toll-like receptor 2	Q2VB97.1|TLR2_BOSTR	445	6.10E-18
1.2.1935.m1	Am_TIR5	TIR	Ad_TIR13	aug_v2a.02686	TLR6_human ame: full=toll-like receptor 6	Q9Y2C9.2|TLR6_HUMAN	174	5.80E-19
1.2.4752.m1	Am_TIR6	TIR	Ad_ILR7	aug_v2a.19280	TLR4_pig ame: full=toll-like receptor 4	Q68Y56.1|TLR4_PIG	147	1.60E-16
1.2.849.m1	Am_TIR7	TIR2	Ad_TIR2_12	aug_v2a.16869	0	0	0	0
1.2.5844.m1	Am_TIR8	TIR2	Ad_TIR3	aug_v2a.10450	TLR1_human ame: full=toll-like receptor	Q15399.3|TLR1_HUMAN	403	2.90E-12
1.2.7189.m1	Am_TIR9	TIR2	Ad_ILR3	aug_v2a.23366	TLR6_bovin ame: full=toll-like receptor 6	Q15399.3|TLR1_HUMAN	206	1.90E-10
1.2.12302.m1	Am_TIR10	TIR2	Ad_ILR5	aug_v2a.08563	TLR2_capib ame: full=toll-like receptor 2	B2LT62.1|TLR2_CAPIB	147	6.70E-13
1.2.5843.m1	Am_TIR11	TIR2	Ad_TIR1	aug_v2a.09825	TLR13_mouse ame: full=toll-like receptor 13	Q6R5N8.1|TLR13_MOUSE	406	3.30E-10
1.2.5842.m1	Am_TIR12	TIR2	Ad_TIR7	aug_v2a.10451	TLR6_bovin ame: full=toll-like receptor 6	Q704V6.1|TLR6_BOVIN	332	7.10E-12
1.2.2023.m1	Am_TIR13	TIR2	0	aug_v2a.08379	0	0	0	0
1.2.21921.m1	Am_TIR14	TIR2	Ad_TIR2_1	aug_v2a.23782	0	0	0	0
1.2.21920.m1	Am_TIR15	ARM|TIR2	Ad_TIR2_2	aug_v2a.07172	ADLO2_arath ame: full=protein arabidillo 2	Q9M224.1|ADLO2_ARATH	414	3.70E-04
1.2.4599.m1	Am_TIR16	ARM|TIR2	Ad_TIR2_3	aug_v2a.07723	ADLO1_arath ame: full=protein arabidillo 1	O22161.1|ADLO1_ARATH	680	6.70E-06
1.2.6982.m1	Am_TIR17	ARM|TIR2	Ad_TIR2_2	aug_v2a.23782	GDS1_bovin ame: full=RAP1 GTPase-gdp dissociation stimulator 1	Q04173.1|GDS1_BOVIN	624	5.40E-04
1.2.20158.m1	Am_TIR18	ARM|TIR2	Nv_TIR2_5	aug_v2a.11251	ADLO2_arath ame: full=protein arabidillo 2	Q9M224.1|ADLO2_ARATH	689	1.50E-05
1.2.24704.m1	Am_TIR19	ARM|TIR2	Ad_TIR2_1	aug_v2a.23782	0	0	0	0
1.2.2167.m1	Am_TIR20	ARM|TIR2	0	aug_v2a.14442	0	0	0	0
1.2.1547.m1	Am_TIR21	ARM|TIR2	Ad_TIR2_2	aug_v2a.07172	0	0	0	0
1.2.21925.m1	Am_TIR22	ARM|TIR2	Ad_TIR2_1	aug_v2a.23782	0	0	0	0
1.2.17046.m1	Am_TIR23	ARM|TIR2	Ad_TIR2_7	aug_v2a.22195	0	0	0	0
1.2.21546.m1	Am_TIR24	TIR2|TIR2|TIR2	Nv_TIR2_2	aug_v2a.03936	0	0	0	0
1.2.25362.m1	Am_TIR25	PkC|ROC|TIR2	Nv_TIR2_1	aug_v2a.18447	PATS1_dicdi ame: full=probable serine threonine-protein kinase pats1	Q5SE58.1|PATS1_DICDI	1313	8.90E-19
1.2.25360.m1	Am_TIR26	ROC|TIR2	Nv_TIR2_1	aug_v2a.18448	PATS1_dicdi ame: full=probable serine threonine-protein kinase pats1	Q5SE58.1|PATS1_DICDI	1586	8.60E-17
1.2.3056.m1	Am_TIR27	SAM|TIR2	Nv_TIR2_3	Nemve1|223246	0	0	0	0

(B)

Genome ID	*A. millepora* ID	Control (pH 8.1)				High CO_2 (pH 7.8)			
		1 h		6 h		1 h		6 h	
		Log_2FC	FDR	Log_2FC	FDR	Log_2FC	FDR	Log_2FC	FDR
1.2.12032.m1	Am_Myd881	–	–	–	–	–	–	0.17	3.47E-02
1.2.12031.m1	Am_Myd882	–	–	–	–	–	–	–	–
1.2.10735.m1	Am_ILR1	-0.12	4.10E-02	–	–	–	–	–	–
1.2.22324.m1	Am_ILR2	1.60	2.39E-03	–	–	–	–	-0.69	4.91E-02
1.2.22473.m1	Am_ILR3	0.37	2.90E-02	–	–	-0.26	2.03E-02	–	–
1.2.2434.m1	Am_ILR4	0.20	7.06E-03	–	–	-0.43	5.42E-03	-0.09	1.28E-02
1.2.13178.m1	Am_TLR1	–	–	-0.18	3.05E-02	–	–	-0.33	2.02E-02
1.2.13179.m1	Am_TLR2	0.39	2.15E-02	–	–	-0.20	2.84E-02	-0.28	5.73E-03
1.2.13181.m1	Am_TLR3	–	–	–	–	–	–	0.43	2.56E-03
1.2.13180.m1	Am_TLR4	-0.44	3.64E-02	–	–	–	–	–	–
1.2.13177.m1	Am_TLR5	0.34	4.40E-02	–	–	–	–	-0.85	1.78E-04
1.2.5856.m1	Am_TIR1	0.40	1.91E-02	-0.20	8.62E-04	-0.17	5.20E-03	-0.44	8.42E-04
1.2.16257.m1	Am_TIR2	–	–	-0.05	3.12E-03	-0.41	2.56E-02	-0.33	7.15E-05
1.2.2436.m1	Am_TIR3	–	–	-0.34	1.13E-02	-0.18	1.49E-02	-0.51	2.27E-03
1.2.5845.m1	Am_TIR4	–	–	-0.15	3.71E-02	–	–	–	–
1.2.1935.m1	Am_TIR5	–	–	–	–	-0.37	6.20E-04	-0.24	2.37E-02
1.2.4752.m1	Am_TIR6	–	–	–	–	–	–	–	–
1.2.849.m1	Am_TIR7	–	–	0.06	7.04E-03	0.09	3.97E-02	–	–
1.2.5844.m1	Am_TIR8	–	–	–	–	–	–	-0.14	4.28E-02
1.2.7189.m1	Am_TIR9	–	–	–	–	-0.05	3.89E-02	–	–
1.2.12302.m1	Am_TIR10	–	–	–	–	–	–	-0.63	3.03E-03
1.2.5843.m1	Am_TIR11	–	–	–	–	–	–	-0.21	4.87E-02
1.2.5842.m1	Am_TIR12	–	–	–	–	–	–	–	–
1.2.2023.m1	Am_TIR13	–	–	–	–	–	–	–	–
1.2.21921.m1	Am_TIR14	–	–	–	–	–	–	–	–
1.2.21920.m1	Am_TIR15	0.16	1.69E-02	0.19	7.60E-03	-0.61	1.48E-02	–	–
1.2.4599.m1	Am_TIR16	–	–	0.27	1.96E-02	-0.70	2.19E-02	-0.09	6.03E-03
1.2.6982.m1	Am_TIR17	-0.23	2.65E-02	–	–	–	–	–	–
1.2.20158.m1	Am_TIR18	-0.22	2.80E-02	–	–	-0.45	1.45E-09	-0.71	2.78E-03
1.2.24704.m1	Am_TIR19	-0.20	3.40E-02	–	–	–	–	–	–
1.2.2167.m1	Am_TIR20	–	–	–	–	0.15	2.35E-02	–	–
1.2.1547.m1	Am_TIR21	–	–	–	–	–	–	–	–
1.2.21925.m1	Am_TIR22	–	–	–	–	–	–	–	–
1.2.17046.m1	Am_TIR23	–	–	–	–	–	–	–	–
1.2.21546.m1	Am_TIR24	–	–	–	–	–	–	0.12	2.45E-02
1.2.25362.m1	Am_TIR25	0.33	4.04E-02	–	–	-0.09	4.80E-02	–	–
1.2.25360.m1	Am_TIR26	–	–	–	–	–	–	–	–
1.2.3056.m1	Am_TIR27	–	–	–	–	-0.35	2.19E-03	-0.10	3.55E-02

Table S2.6 TNF and TNFR-domain containing proteins (total = 36). (A) Results of the domain search in the *A. millepora* genome (PF00229.13 and PF00020.13 with a 1e-4 cut-off). NCBI domain and BlastP search results are listed for each protein. (B) Log_2FC values of significantly expressed genes (FDR <0.05, log2FC > 0.05) in response to LPS challenge relative to the control (PBS) after 1 and 6 h. For samples under control (pH 8.1) and high pCO_2 (pH 7.8) conditions. Log_2FC colour indicates up (red) and down (blue) regulated genes.

(A)

Genome ID	*A. millepora* ID	NCBI domain	Blast Hit	Hit ID	Length	e.Value	% ID
1.2.13359.m1	Am_TNF1	TNF	TNFa_Tumor necrosis factor	gi|135938|sp|P16599.1|TNFA_RAT	231	1.60E-06	39.8
1.2.17029.m1	Am_TNF2	TNF	TNFa_Tumor necrosis factor	gi|135938|sp|P16599.1|TNFA_RAT	207	5.00E-06	40.6
1.2.4528.m1	Am_TNF3	TNF	TNF10_Tumor necrosis factor ligand superfamily member 10	gi|1730015|sp|P50591.1|TNF10_HUMAN	174	5.90E-04	50
1.2.607.m1	Am_TNF4	TNF	TNFb_Tumor necrosis factor ligand superfamily member 1	gi|135942|sp|P26445.1|TNFB_PIG	135	9.40E-05	46.8
1.2.17031.m1	Am_TNF5	TNF	TNF15_Tumor necrosis factor ligand superfamily member 15	gi|189036103|sp|Q5UBV8.2|TNF15_MOUSE	159	6.00E-05	39
1.2.604.m1	Am_TNF6	Col| TNF	TNFb_Tumor necrosis factor ligand superfamily member 1	gi|135942|sp|P26445.1|TNFB_PIG	300	2.50E-06	47.2
1.2.2376.m1	Am_TNF7	Col | Col | TNF	TNF10_Tumor necrosis factor ligand superfamily member 10	gi|1730016|sp|P50592.1|TNF10_MOUSE	347	4.00E-15	49
1.2.602.m1	Am_TNF8	Col | TNF | Co | TNF	TNF12_Tumor necrosis factor ligand superfamily member 12	gi|21362987|sp|O43508.1|TNF12_HUMAN	583	2.70E-05	44.2
1.2.15238.m1	Am_TNFR1	TNFRSF|Death	TNFR1b_Tumor necrosis factor receptor superfamily member 1b	gi|21264534|sp|P20333.3|TNR1B_HUMAN	381	6.00E-04	54
1.2.20630.m1	Am_TNFR2	TNFRSF|Death	TNFR16_Tumor necrosis factor receptor superfamily member 16	gi|128155|sp|P18519.1|TNR16_CHICK	580	7.40E-06	46.33
1.2.20632.m1	Am_TNFR3	TNFRSF|Death	UNC5C_Full=Netrin receptor	sp|Q76185.1|UNC5C_RAT	931	4.00E-06	–
1.2.23959.m1	Am_TNFR4	TNFRSF|Death	TNFR11b_Tumor necrosis factor receptor superfamily member 11b	gi|298351871|sp|A5D7R1.1|TR11B_BOVIN	418	1.20E-17	49.6
1.2.18305.m1	Am_TNFR5	TNFRSF|Death	TNR1a_Tumor necrosis factor receptor superfamily member 1a	gi|135959|sp|P19438.1|TNR1A_HUMAN	408	4.10E-17	51.6
1.2.20631.m1	Am_TNFR6	TNFRSF	TNFR16_Tumor necrosis factor receptor superfamily member 16	gi|128156|sp|P08138.1|TNR16_HUMAN	253	4.00E-05	44
1.2.20633.m1	Am_TNFR7	TNFRSF	TNFR16_Tumor necrosis factor receptor superfamily member 16	gi|128156|sp|P08138.1|TNR16_HUMAN	237	2.70E-05	43.8
1.2.4349.m1	Am_TNFR8	TNFRSF	TNFR16_Tumor necrosis factor receptor superfamily member 16	sp|P18519.1|TNR16_CHICK	416	1.90E-01	–
1.2.4347.m1	Am_TNFR9	TNFRSF	TNFR16_Tumor necrosis factor receptor superfamily member 16	sp|P18519.1|TNR16_CHICK	416	7.00E-03	–
1.2.10769.m1	Am_TNFR10	TNFRSF	EDAR_Tumor necrosis factor receptor superfamily member EDAR	gi|21263557|sp|Q90VY2.1|EDAR_ORYLA	497	6.10E-05	44
1.2.6591.m1	Am_TNFR11	TNFRSF	TNFR19_Tumor necrosis factor receptor superfamily member 19	gi|21264102|sp|Q9NS68.1|TNR19_HUMAN	391	2.70E-04	42
1.2.6590.m1	Am_TNFR12	TNFRSF	TNFR16_Tumor necrosis factor receptor superfamily member 16	sp|P18519.1|TNR16_CHICK	416	3.00E-02	–
1.2.17682.m1	Am_TNFR13	TNFRSF	TNFR16_Tumor necrosis factor receptor superfamily member 16	sp|P18519.1|TNR16_CHICK	416	7.80E-02	–
1.2.6595.m1	Am_TNFR14	TNFRSF	TNFR19_Tumor necrosis factor receptor superfamily member 19	sp|Q9JLL3.2|TNR19_MOUSE	416	3.20E-02	–
1.2.6597.m1	Am_TNFR15	TNFRSF	TNFR19_Tumor necrosis factor receptor superfamily member 19	sp|Q9NS68.1|TNR19_HUMAN	423	2.00E-03	–
1.2.4350.m1	Am_TNFR16	TNFRSF	TNFR14_Tumor necrosis factor receptor superfamily member 14	sp|Q92956.3|TNR14_HUMAN	283	4.00E-03	–
1.2.11264.m1	Am_TNFR17	TNFRSF	TNFR16_Tumor necrosis factor receptor superfamily member 16	gi|128155|sp|P18519.1|TNR16_CHICK	489	1.20E-04	37
1.2.6591.m1	Am_TNFR18	TNFRSF	TNFR19_Tumor necrosis factor receptor superfamily member 19	sp|Q9NS68.1|TNR19_HUMAN	423	2.00E-04	–
1.2.6592.m1	Am_TNFR19	TNFRSF	UL144_TNF alpha-like receptor ul144	gi|363805602|sp|F5HAM0.1|UL144_HCMVM	521	2.20E-05	49.67
1.2.6593.m1	Am_TNFR20	TNFRSF	UL144_TNF alpha-like receptor ul144	sp|Q68396.1|UL144_HCMVO	176	1.00E-05	–
1.2.4338.m1	Am_TNFR21	TNFRSF	TNFR16_Tumor necrosis factor receptor superfamily member 16	gi|128155|sp|P18519.1|TNR16_CHICK	305	7.00E-06	45.8
1.2.11261.m1	Am_TNFR22	TNFRSF|Zu5	TNFR16_Tumor necrosis factor receptor superfamily member 16	gi|128155|sp|P18519.1|TNR16_CHICK	795	1.40E-08	43.5
1.2.13438.m1	Am_TNFR23	TNFRSF|Zu5|Death	unc5b_xenla ame: full=netrin receptor unc5b	gi|54036590|sp|Q8JGT4.1|UNC5B_XENLA	969	1.10E-07	47.8
1.2.13439.m1	Am_TNFR24	TNFRSF|Zu5|Death	unc5b_xenla ame: full=netrin receptor unc5b	gi|54036590|sp|Q8JGT4.1|UNC5B_XENLA	823	8.60E-09	53.2
1.2.6589.m1	Am_TNFR25	TNFRSF|Zu5|Death	unc5c_chick ame: full=netrin receptor unc5c	gi|54036585|sp|Q7TZZ5.1|UNC5C_CHICK	799	3.70E-08	44.4
1.2.13437.m1	Am_TNFR26	TNFRSF|Zu5|Death	zo1_canfa ame: full=tight junction protein zo-1	gi|62901480|sp|O97758.1|ZO1_CANFA	995	6.10E-09	52.2
1.2.24806.m1	Am_TNFR27	TNFRSF|Zu5	zo1_canfa ame: full=tight junction protein zo-1	gi|62901480|sp|O97758.1|ZO1_CANFA	501	3.60E-07	51.6
1.2.17684.m1	Am_TNFR28	TNFRSF|I_set	malt1_human ame: full=malt lymphoma-associated translocation	gi|20455075|sp|Q9UDY8.1|MALT1_HUMAN	581	1.70E-06	50

(B)

Genome ID	*A. millepora* ID	Control (pH 8.1)				High CO_2 (pH 7.8)			
		1 h		6 h		1 h		6 h	
		Log_2FC	FDR	Log_2FC	FDR	Log_2FC	FDR	Log_2FC	FDR
1.2.13359.m1	Am_TNF1	1.31	3.40E-04	-1.25	7.82E-06	0.17	4.32E-04	-0.29	1.49E-04
1.2.17029.m1	Am_TNF2	1.06	7.50E-04	-1.04	1.00E-05	–	–	-0.24	6.98E-03
1.2.4528.m1	Am_TNF3	0.16	4.38E-02	-0.20	3.62E-02	–	–	-0.46	2.32E-04
1.2.607.m1	Am_TNF4	-0.28	1.03E-03	0.14	1.64E-02	-0.15	2.25E-02	0.32	1.21E-03
1.2.17031.m1	Am_TNF5	–	–	–	–	-0.20	1.73E-02	-0.38	1.91E-04
1.2.604.m1	Am_TNF6	–	–	–	–	–	–	0.13	8.61E-02
1.2.2376.m1	Am_TNF7	–	–	–	–	-0.41	3.63E-02	–	–
1.2.602.m1	Am_TNF8	-0.14	2.41E-02	–	–	–	–	0.16	6.67E-02
1.2.15238.m1	Am_TNFR1	0.66	1.43E-02	-0.12	9.45E-03	0.19	1.99E-02	–	–
1.2.20630.m1	Am_TNFR2	0.46	1.46E-02	–	–	–	–	–	–
1.2.20632.m1	Am_TNFR3	0.62	2.50E-03	-0.27	1.89E-06	-0.18	2.58E-02	-0.25	1.22E-02
1.2.23959.m1	Am_TNFR4	–	–	–	–	–	–	–	–
1.2.18805.m1	Am_TNFR5	–	–	–	–	–	–	–	–
1.2.20631.m1	Am_TNFR6	0.54	6.56E-03	-0.48	5.64E-05	-0.24	1.51E-02	-0.38	4.70E-03
1.2.20633.m1	Am_TNFR7	0.67	8.05E-03	-0.39	4.16E-05	-0.02	7.91E-03	–	–
1.2.4349.m1	Am_TNFR8	0.27	1.48E-02	-0.49	1.61E-06	-0.49	2.26E-02	-0.71	3.90E-04
1.2.4347.m1	Am_TNFR9	0.39	2.27E-02	-0.27	1.58E-03	–	–	–	–
1.2.10769.m1	Am_TNFR10	0.09	1.90E-02	0.69	4.93E-04	-0.05	9.34E-03	-0.61	9.79E-03
1.2.6598.m1	Am_TNFR11	0.24	2.81E-02	-0.44	3.71E-07	–	–	–	–
1.2.6590.m1	Am_TNFR12	0.46	3.94E-02	-0.13	2.79E-02	–	–	–	–
1.2.17682.m1	Am_TNFR13	-0.29	4.53E-02	0.38	2.71E-02			-0.09	7.03E-02
1.2.6595.m1	Am_TNFR14	-0.41	4.94E-02	–	–	–	–	-0.37	4.84E-02
1.2.6597.m1	Am_TNFR15	–	–	0.27	7.87E-07	-0.26	4.83E-02	-0.50	5.08E-03
1.2.4350.m1	Am_TNFR16	–	–	0.08	4.41E-06	-0.08	5.71E-03	–	–
1.2.11264.m1	Am_TNFR17	–	–	–	–	-0.40	3.63E-02	–	–
1.2.6591.m1	Am_TNFR18	–	–	–	–	–	–	–	–
1.2.6592.m1	Am_TNFR19	–	–	–	–	–	–	–	–
1.2.6593.m1	Am_TNFR20	–	–	–	–	–	–	–	–
1.2.4338.m1	Am_TNFR21	–	–	–	–	–	–	0.68	3.13E-05
1.2.11261.m1	Am_TNFR22	–	–	–	–	–	–	–	–
1.2.13438.m1	Am_TNFR23	0.06	1.14E-02	–	–	–	–	-0.51	8.46E-05
1.2.13439.m1	Am_TNFR24	-0.29	1.16E-02	0.45	1.69E-02	0.25	1.53E-02	0.38	1.04E-02
1.2.6589.m1	Am_TNFR25	-0.17	3.08E-02	–	–	–	–	-0.08	1.95E-02
1.2.13437.m1	Am_TNFR26	–	–	–	–	–	–	0.25	1.41E-03
1.2.24806.m1	Am_TNFR27	-0.58	3.67E-02	0.48	9.87E-03	0.33	4.05E-02	0.29	3.52E-02
1.2.17684.m1	Am_TNFR28	–	–	–	–	–	–	0.34	3.01E-03

Table S2.7 TRAF-domain containing proteins (total = 38) (A) Results of the domain search in the *A. millepora* genome (PF02176.13 with a 1e-4 cut-off). NCBI domain and BlastP search results are listed for each protein. (B) Log_2FC values of significantly expressed genes (FDR <0.05, log2FC > 0.05) in response to LPS challenge relative to the control (PBS) after 1 and 6 h. For samples under control (pH 8.1) and high pCO_2 (pH 7.8) conditions. Log_2FC colour indicates up (red) and down (blue) regulated genes.

(A)

Genome ID	*A. millepora* ID	NCBI Domain	Blast Hit	Hit ID	Length	e.Value
1.2.2752.m1	Am_TRAF1	RING|TRAF|MATH	TRAF3_human ame: full=tnf receptor-associated factor 3	Q13114.2|TRAF3_HUMAN	528	3.40E-103
1.2.2754.m1	Am_TRAF2	RING|TRAF|MATH	TRAF3_human ame: full=tnf receptor-associated factor 3	Q13114.2|TRAF3_HUMAN	593	8.50E-99
1.2.2899.m1	Am_TRAF3	RING|TRAF|MATH	TRAF6_bovin ame: full=tnf receptor-associated factor 6	Q3ZCC3.1|TRAF6_BOVIN	418	2.80E-81
1.2.2897.m1	Am_TRAF4	RING|TRAF|MATH	TRAF6_rat ame: full=tnf receptor-associated factor 6	B5DF45.1|TRAF6_RAT	498	2.30E-104
1.24647.m1	Am_TRAF5	RING|TRAF|MATH	TRAF4_mouse ame: full=tnf receptor-associated factor 4	Q61382.2|TRAF4_MOUSE	456	6.80E-69
1.210762.m1	Am_TRAF6	RING|TRAF|MATH	TRAF3_mouse ame: full=tnf receptor-associated factor 3	Q60803.2|TRAF3_MOUSE	552	1.40E-94
1.23972.m1	Am_TRAF7	RING|TRAF|MATH	TRAF4_human ame: full=tnf receptor-associated factor 4	Q9BUZ4.1|TRAF4_HUMAN	363	1.90E-37
1.216730.m1	Am_TRAF8	RING|TRAF|MATH	TRAF6b_xenla ame: full=tnf receptor-associated factor 6-b	Q6DJN2.1|TRF6B_XENLA	412	6.40E-53
1.25426.m1	Am_TRAF9	RING|TRAF|MATH	TRAF3_mouse ame: full=tnf receptor-associated factor 3	Q60803.2|TRAF3_MOUSE	556	4.10E-117
1.25451.m1	Am_TRAF10	RING|TRAF|MATH	TRAF6_mouse ame: full=tnf receptor-associated factor 6	P70196.2|TRAF6_MOUSE	411	1.40E-39
1.25452.m1	Am_TRAF11	RING|TRAF|MATH	TRAF6_rat ame: full=tnf receptor-associated factor 6	B5DF45.1|TRAF6_RAT	442	7.50E-65
1.25457.m1	Am_TRAF12	RING|TRAF|MATH	TRAF4_mouse ame: full=tnf receptor-associated factor 4	Q61382.2|TRAF4_MOUSE	422	4.20E-65
1.25463.m1	Am_TRAF13	RING|TRAF|TRAF	TRAF6_cerat ame: full=tnf receptor-associated factor 6	B6CJY4.1|TRAF6_CERAT	416	6.60E-38
1.23871.m1	Am_TRAF14	RING|TRAF|MATH	TRAF3_mouse ame: full=tnf receptor-associated factor 3	Q60803.2|TRAF3_MOUSE	559	8.70E-119
1.22896.m1	Am_TRAF15	RING|TRAF|MATH	TRAF6_rat ame: full=tnf receptor-associated factor 6	B5DF45.1|TRAF6_RAT	532	3.80E-109
1.22871.m1	Am_TRAF16	RING|TRAF|MATH	TRAF6_rat ame: full=tnf receptor-associated factor 6	B5DF45.1|TRAF6_RAT	508	3.00E-102
1.213059.m1	Am_TRAF17	RING|TRAF|MATH	TRAF6_human ame: full=tnf receptor-associated factor 6	Q9Y4K3.1|TRAF6_HUMAN	435	2.70E-59
1.26450.m1	Am_TRAF18	RING|TRAF|Mei5	TRAF6b_xenla ame: full=tnf receptor-associated factor 6-	Q6DJN2.1|TRF6B_XENLA	616	1.40E-27
1.26856.m1	Am_TRAF19	RING|TRAF|WD40	TRAF7_human ame: full=tnf receptor-associated factor 7	Q6Q0C0.1|TRAF7_HUMAN	640	0.00E+00
1.24735.m1	Am_TRAF20	RING|TRAF	TRAF7_human ame: full=tnf receptor-associated factor 7	Q6Q0C0.1|TRAF7_HUMAN	316	3.20E-31
1.24181.m1	Am_TRAF21	RING|TRAF	TRAF5_human ame: full=tnf receptor-associated factor 5	O00463.2|TRAF5_HUMAN	175	1.30E-10
1.215982.m1	Am_TRAF22	RING|TRAF	TRAF5_mouse ame: full=tnf receptor-associated factor 5	P70191.1|TRAF5_MOUSE	203	5.60E-10
1.22881.m1	Am_TRAF23	TRAF|MATH	TRAF6_bovin ame: full=tnf receptor-associated factor 6	Q3ZCC3.1|TRAF6_BOVIN	366	4.60E-59
1.22898.m1	Am_TRAF24	TRAF|MATH	TRAF6_bovin ame: full=tnf receptor-associated factor 6	Q3ZCC3.1|TRAF6_BOVIN	450	1.50E-63
1.22891.m1	Am_TRAF25	TRAF|MATH	TRAF6_rat ame: full=tnf receptor-associated factor 6	B5DF45.1|TRAF6_RAT	362	1.40E-74
1.22892.m1	Am_TRAF26	TRAF|MATH	TRAF6_bovin ame: full=tnf receptor-associated factor 6	Q3ZCC3.1|TRAF6_BOVIN	412	3.70E-68
1.2866.m1	Am_TRAF27	Zf|TRAF|MATH	TRAF4_mouse ame: full=tnf receptor-associated factor 4	Q61382.2|TRAF4_MOUSE	500	1.10E-62
1.220050.m1	Am_TRAF28	TRAF|MATH	TRAF1_mouse ame: full=tnf receptor-associated factor 1	P39428.2|TRAF1_MOUSE	421	2.00E-46
1.27866.m1	Am_TRAF29	TRAF|MATH	TRAF5_mouse ame: full=tnf receptor-associated factor 5	P70191.1|TRAF5_MOUSE	453	1.30E-35
1.2863.m1	Am_TRAF30	TRAF|MATH	TRAF4_human ame: full=tnf receptor-associated factor 4	Q9BUZ4.1|TRAF4_HUMAN	517	1.70E-86
1.23975.m1	Am_TRAF31	TRAF|MATH	TRAF4_human ame: full=tnf receptor-associated factor 4	Q9BUZ4.1|TRAF4_HUMAN	291	1.30E-46
1.21943.m1	Am_TRAF32	TRAF|TRAF|MATH	TRAF3_mouse ame: full=tnf receptor-associated factor 3	Q60803.2|TRAF3_MOUSE	568	1.00E-103
1.21949.m1	Am_TRAF33	TRAF|TRAF|MATH	TRAF3_human ame: full=tnf receptor-associated factor 3	Q13114.2|TRAF3_HUMAN	569	6.10E-105
1.26455.m1	Am_TRAF34	TRAF	TRAF6_bovin ame: full=tnf receptor-associated factor 6	Q3ZCC3.1|TRAF6_BOVIN	551	2.20E-13
1.225278.m1	Am_TRAF35	TRAF	TRAF5_mouse ame: full=tnf receptor-associated factor 5	P70191.1|TRAF5_MOUSE	346	1.50E-14
1.23224.m1	Am_TRAF36	TRAF	TRAF4_mouse ame: full=tnf receptor-associated factor 4	Q61382.2|TRAF4_MOUSE	272	3.10E-14
1.25418.m1	Am_TRAF37	TRAF|Filj|MATH	TRAF3_mouse ame: full=tnf receptor-associated factor 3	Q60803.2|TRAF3_MOUSE	468	1.30E-80
1.23886.m1	Am_TRAF38	Csm|RING|TRAF|MATH	TRAF4_mouse ame: full=tnf receptor-associated factor 4	Q61382.2|TRAF4_MOUSE	812	4.60E-46

(B)

Genome ID	*A. millepora* ID	Control (pH 8.1)				High CO_2 (pH 7.8)			
		1 h		6 h		1 h		6 h	
		Log_2FC	FDR	Log_2FC	FDR	Log_2FC	FDR	Log_2FC	FDR
1.2.2752.m1	Am_TRAF1	0.09	1.16E-02	–	–	0.70	1.97E-04	-0.51	1.17E-03
1.2.2754.m1	Am_TRAF2	–	–	0.12	1.09E-03	0.19	1.37E-02	–	–
1.2.2899.m1	Am_TRAF3	0.42	2.01E-02	–	–	0.05	8.67E-03	–	–
1.2.2897.m1	Am_TRAF4	0.58	2.37E-02	-0.08	2.70E-02	-0.13	1.19E-02	-0.25	1.16E-02
1.2.4647.m1	Am_TRAF5	0.06	4.88E-02	–	–	–	–	–	–
1.2.10762.m1	Am_TRAF6	-0.16	7.79E-03	–	–	0.07	9.88E-03	–	–
1.2.3972.m1	Am_TRAF7	–	–	0.13	7.61E-03	0.10	3.00E-02	0.19	9.18E-03
1.2.16730.m1	Am_TRAF8	–	–	0.15	3.37E-02	-0.95	2.66E-02	–	–
1.2.5426.m1	Am_TRAF9	–	–	-0.37	1.21E-04	0.60	2.05E-10	-0.33	9.38E-03
1.2.5451.m1	Am_TRAF10	–	–	0.14	3.04E-02	-0.20	2.20E-02	–	–
1.2.5452.m1	Am_TRAF11	–	–	–	–	–	–	–	–
1.2.5457.m1	Am_TRAF12	–	–	-0.10	1.41E-02	0.16	2.74E-02	–	–
1.2.5463.m1	Am_TRAF13	–	–	-0.09	2.87E-02	–	–	–	–
1.2.3871.m1	Am_TRAF14	–	–	–	–	–	–	–	–
1.2.2896.m1	Am_TRAF15	–	–	–	–	–	–	–	–
1.2.2871.m1	Am_TRAF16	–	–	–	–	–	–	–	–
1.2.13059.m1	Am_TRAF17	–	–	–	–	–	–	–	–
1.2.6450.m1	Am_TRAF18	–	–	–	–	0.24	4.05E-02	–	–
1.2.6856.m1	Am_TRAF19	–	–	–	–	–	–	–	–
1.2.4735.m1	Am_TRAF20	–	–	-0.06	3.67E-02	–	–	–	–
1.2.4181.m1	Am_TRAF21	–	–	–	–	0.38	4.82E-02	–	–
1.2.15982.m1	Am_TRAF22	–	–	–	–	–	–	–	–
1.2.2881.m1	Am_TRAF23	0.56	1.67E-02	-0.38	3.18E-02	–	–	0.27	1.08E-02
1.2.2898.m1	Am_TRAF24	1.02	2.70E-03	–	–	-0.63	4.99E-05	0.43	1.15E-03
1.2.2891.m1	Am_TRAF25	1.00	3.01E-03	–	–	-0.48	2.74E-06	–	–
1.2.2892.m1	Am_TRAF26	–	–	0.09	1.44E-02	-0.12	1.52E-02	0.27	8.90E-03
1.2.866.m1	Am_TRAF27	–	–	-0.14	3.30E-02	-0.10	2.85E-02	–	–
1.2.20050.m1	Am_TRAF28	–	–	–	–	-0.21	1.10E-02	–	–
1.2.7866.m1	Am_TRAF29	–	–	–	–	-0.25	6.00E-03	–	–
1.2.863.m1	Am_TRAF30	–	–	–	–	–	–	–	–
1.2.3975.m1	Am_TRAF31	–	–	–	–	–	–	–	–
1.2.1943.m1	Am_TRAF32	–	–	–	–	–	–	–	–
1.2.1949.m1	Am_TRAF33	–	–	–	–	–	–	–	–
1.2.6455.m1	Am_TRAF34	0.08	4.27E-02	-0.14	3.43E-02	–	–	0.44	1.20E-03
1.2.25278.m1	Am_TRAF35	–	–	–	–	0.94	2.50E-02	–	–
1.2.3224.m1	Am_TRAF36	–	–	–	–	–	–	–	–
1.2.5418.m1	Am_TRAF37	–	–	–	–	–	–	–	–
1.2.3886.m1	Am_TRAF38	–	–	–	–	–	–	–	–

Table S2.8 NACHT-domain containing proteins (total = 206). (A) Results of the domain search in the *A. millepora* genome (PF05729.7 with a 1e-4 cut-off). NCBI domain and BlastP search results are listed for each protein. (B) Log_2FC values of significantly expressed genes (FDR <0.05, log2FC > 0.05) in response to LPS challenge relative to the control (PBS) after 1 and 6 h. For samples under control (pH 8.1) and high pCO_2 (pH 7.8) conditions. Log_2FC colour indicates up (red) and down (blue) regulated genes.

(A)

Genome ID	*A. millepora* ID	NCBI Domain	Blast Hit	Length	e.Value	% ID
1.2.26019.m1	Am_NLR1	Glycos_transf_1|NACHT	nlrc4_xentr ame: full=nlr family card domain-containing protein 4	787	4.80E-07	46.20
1.2.5900.m1	Am_NLR2	Glycos_transf_1|NACHT	msha_acic1 ame: full=d-inositol 3-phosphate glycosyltransferase	1618	6.10E-11	47.40
1.2.5883.m1	Am_NLR3	Glycos_transf_1|NACHT	nlrc4_xentr ame: full=nlr family card domain-containing protein 4	1727	5.10E-07	43.60
1.2.5906.m1	Am_NLR4	Glycos_transf_1|NACHT	msha_acic1 ame: full=d-inositol 3-phosphate glycosyltransferase	1667	2.90E-08	46.60
1.2.19850.m1	Am_NLR5	Glycos_transf_1|NACHT	nlrc4_xentr ame: full=nlr family card domain-containing protein 4	1131	3.10E-09	42.00
1.2.25480.m1	Am_NLR6	Glycos_transf_1|NACHT	nlrc4_xentr ame: full=nlr family card domain-containing protein 4	1485	4.00E-10	41.80
1.2.25481.m1	Am_NLR7	Glycos_transf_1|NACHT	nlrc4_xentr ame: full=nlr family card domain-containing protein 4	1018	2.80E-04	41.00
1.2.25484.m1	Am_NLR8	Glycos_transf_1|NACHT	nlrc4_xentr ame: full=nlr family card domain-containing protein 4	1477	1.10E-07	42.20
1.2.5889.m1	Am_NLR9	Glycos_transf_1|NACHT	nalp2_human ame: full=lrr and pyd domains-containing protein 2	803	1.60E-07	43.40
1.2.15887.m1	Am_NLR10	Glycos_transf_1|NACHT|LRRs	nlrc3_mouse ame: full=protein nlrc3	1548	7.70E-49	55.40
1.2.23033.m1	Am_NLR11	Glycos_transf_1|NACHT|LRRs	nlrc3_human ame: full=protein nlrc3 ame: full=card15-like protein	1509	5.80E-36	54.00
1.2.23034.m1	Am_NLR12	Glycos_transf_1|NACHT|LRRs	nlrc3_mouse ame: full=protein nlrc3	1266	2.50E-54	52.40
1.2.3761.m1	Am_NLR13	Glycos_transf_1|NACHT|LRR	nlrc3_human ame: full=protein nlrc3 ame: full=card15-like protein	1065	6.30E-22	40.40
1.2.9939.m1	Am_NLR14	Glycos_transf_1|NACHT|LRR	nlrc3_human ame: full=protein nlrc3 ame: full=card15-like protein	1250	4.30E-61	53.20
1.2.19702.m1	Am_NLR15	Glycos_transf_1|NACHT|LRRs	nlrc3_mouse ame: full=protein nlrc3	1481	3.30E-44	54.60
1.2.24451.m1	Am_NLR16	Glycos_transf_1|NACHT|LRRs	nlrc3_human ame: full=protein nlrc3 ame: full=card15-like protein	1243	2.70E-48	57.60
1.2.4814.m1	Am_NLR17	Glycos_transf_1|NACHT|LRRs	nlrc3_human ame: full=protein nlrc3 ame: full=card15-like protein	1466	1.90E-54	49.60
1.2.23717.m1	Am_NLR18	Glycos_transf_1|NACHT|LRRs	nlrc3_human ame: full=protein nlrc3 ame: full=card15-like protein	1324	5.70E-69	56.40
1.2.15454.m1	Am_NLR19	Glycos_transf_1|NACHT|LRRs	nlrc3_human ame: full=protein nlrc3 ame: full=card15-like protein	1511	7.80E-66	50.00
1.2.9916.m1	Am_NLR20	Glycos_transf_1|NACHT|LRR	nlrc3_human ame: full=protein nlrc3 ame: full=card15-like protein	1385	2.50E-44	52.20
1.2.23996.m1	Am_NLR21	Glycos_transf_1|NACHT|LRR	nlrc3_mouse ame: full=protein nlrc3	1300	5.90E-40	47.40
1.2.20866.m1	Am_NLR22	Glycos_transf_1|NACHT|LRR	lr74a_human ame: full=leucine-rich repeat-containing protein 74a	1099	2.50E-16	52.40
1.2.1531.m1	Am_NLR23	Glycos_transf_1|NACHT|LRRs	nlrc3_mouse ame: full=protein nlrc3	1200	5.40E-22	47.00
1.2.19821.m1	Am_NLR24	Glycos_transf_1|NACHT|LRRs	nlrc3_human ame: full=protein nlrc3 ame: full=card15-like protein	1343	3.50E-55	56.60
1.2.23781.m1	Am_NLR25	Glycos_transf_1|NACHT|LRRs	nlrc3_human ame: full=protein nlrc3 ame: full=card15-like protein	1289	1.30E-41	56.80
1.2.23782.m1	Am_NLR26	Glycos_transf_1|NACHT|LRRs	nlrc3_mouse ame: full=protein nlrc3	1331	2.30E-43	52.60
1.2.4220.m1	Am_NLR27	incomplete-NACHT	nod2_mouse ame: full=nucleotide-binding oligomerization domain-containing protein 2	478	3.20E-08	51.00
1.2.18769.m1	Am_NLR28	incomplete-NACHT	dtip3_mouse ame: full=e3 ubiquitin-protein ligase dtip3	314	7.20E-09	49.50
1.2.5888.m1	Am_NLR29	incomplete-NACHT	nlrc4_xentr ame: full=nlr family card domain-containing protein 4	219	4.80E-04	55.00
1.2.15942.m1	Am_NLR30	incomplete-NACHT	nlrc5_ictpu ame: full=protein nlrc5	191	2.90E-04	48.00
1.2.16740.m1	Am_NLR31	incomplete-NACHT|	mtan_despa ame: full=5'-methylthioadenosine/s-adenosylhomocysteine nucleosidase	507	5.00E-05	46.00
1.2.4218.m1	Am_NLR32	incomplete-NACHT|LRRs	nod1_mouse ame: full=nucleotide-binding oligomerization domain-containing protein 1	554	2.50E-17	42.40
1.2.6137.m1	Am_NLR33	incomplete-NACHT|LRRs	nlrc3_human ame: full=protein nlrc3 ame: full=card15-like protein	643	4.60E-09	42.00
1.2.9759.m1	Am_NLR34	NACHT	nod2_mouse ame: full=nucleotide-binding oligomerization domain-containing protein 2	341	2.80E-10	46.40
1.2.19297.m1	Am_NLR35	NACHT	nlrc4_xentr ame: full=nlr family card domain-containing protein 4	541	2.40E-17	42.00
1.2.24253.m1	Am_NLR36	NACHT	nlrc5_ictpu ame: full=protein nlrc5	645	1.10E-25	44.20
1.2.13860.m1	Am_NLR37	NACHT	nlrc5_ictpu ame: full=protein nlrc5	332	1.00E-09	43.00
1.2.19126.m1	Am_NLR38	NACHT	nlrc4_xentr ame: full=nlr family card domain-containing protein 4	555	2.20E-18	43.40
1.2.9130.m1	Am_NLR39	NACHT	dtip3_human ame: full=e3 ubiquitin-protein ligase dtip3	527	8.60E-16	52.50
1.2.5896.m1	Am_NLR40	NACHT	nal10_mouse ame: full=lrr and pyd domains-containing protein 10	1296	1.10E-07	43.40
1.2.18491.m1	Am_NLR41	NACHT	nod2_mouse ame: full=nucleotide-binding oligomerization domain-containing protein 2	542	7.10E-21	43.40
1.2.15251.m1	Am_NLR42	NACHT	nlrc4_xentr ame: full=nlr family card domain-containing protein 4	464	4.20E-15	43.80
1.2.5897.m1	Am_NLR43	NACHT	nlrc4_mouse ame: full=nlr family card domain-containing protein 4	1259	4.70E-13	43.00
1.2.25683.m1	Am_NLR44	NACHT	nlrc5_ictpu ame: full=protein nlrc5	1102	1.50E-09	43.20
1.2.10017.m1	Am_NLR45	NACHT	dtip3_human ame: full=e3 ubiquitin-protein ligase dtip3	758	7.70E-15	50.00
1.2.5895.m1	Am_NLR46	NACHT	nlrc5_ictpu ame: full=protein nlrc5	740	1.90E-06	42.60
1.2.13880.m1	Am_NLR47	NACHT	nlrc5_ictpu ame: full=protein nlrc5	761	1.10E-12	44.00
1.2.22640.m1	Am_NLR48	NACHT	nlrc5_ictpu ame: full=protein nlrc5	402	7.70E-04	49.00
1.2.9743.m1	Am_NLR49	NACHT	nod1_mouse ame: full=nucleotide-binding oligomerization domain-containing protein 1	573	7.30E-25	42.80
1.2.7526.m1	Am_NLR50	NACHT	nlrc4_xentr ame: full=nlr family card domain-containing protein 4	482	1.60E-11	40.80
1.2.2411.m1	Am_NLR51	NACHT	nlrc4_xentr ame: full=nlr family card domain-containing protein 4	899	7.60E-16	40.80

1.2.15816.m1	Am_NLR52	NACHT	nalp5_bovin ame: full= lrr and pyd domains-containing protein 5	157	3.20E-08	47.20
1.2.25488.m1	Am_NLR53	NACHT	nlrc4_xentr ame: full=nlr family card domain-containing protein 4	1156	1.20E-05	46.00
1.2.24834.m1	Am_NLR54	NACHT	nlrc4_xentr ame: full=nlr family card domain-containing protein 4	455	1.00E-10	42.20
1.2.13873.m1	Am_NLR55	NACHT	nlrc5_ictpu ame: full=protein nlrc5	1139	6.60E-13	43.20
1.2.5902.m1	Am_NLR56	NACHT	nlrc4_xentr ame: full=nlr family card domain-containing protein 4	1222	7.10E-08	41.00
1.2.17935.m1	Am_NLR57	NACHT	nal10_human ame: full= lrr and pyd domains-containing protein 10	338	1.10E-05	42.40
1.2.19570.m1	Am_NLR58	NACHT	nlrc5_ictpu ame: full=protein nlrc5	559	2.40E-11	44.40
1.2.14194.m1	Am_NLR59	NACHT	nlrc4_xentr ame: full=nlr family card domain-containing protein 4	419	5.80E-22	43.20
1.2.26008.m1	Am_NLR60	NACHT	nlrc5_ictpu ame: full=protein nlrc5	1134	8.60E-14	42.80
1.2.5907.m1	Am_NLR61	NACHT	nalp2_human ame: full= lrr and pyd domains-containing protein 2	1251	7.10E-07	40.40
1.2.13875.m1	Am_NLR62	NACHT	nlrc5_ictpu ame: full=protein nlrc5	1496	2.10E-15	43.40
1.2.18956.m1	Am_NLR63	NACHT	nlrc4_xentr ame: full=nlr family card domain-containing protein 4	734	8.10E-23	42.20
1.2.25684.m1	Am_NLR64	NACHT	nlrc5_ictpu ame: full=protein nlrc5	1318	2.70E-14	41.60
1.2.18074.m1	Am_NLR65	NACHT	nlrc4_mouse ame: full=nlr family card domain-containing protein 4	1156	2.60E-13	43.80
1.2.18656.m1	Am_NLR66	NACHT	nlrc5_ictpu ame: full=protein nlrc5	1395	2.30E-07	41.60
1.2.19942.m1	Am_NLR67	NACHT	nlrc5_ictpu ame: full=protein nlrc5	1289	3.20E-13	42.80
1.2.18363.m1	Am_NLR68	NACHT	nlrc4_xentr ame: full=nlr family card domain-containing protein 4	456	7.20E-20	43.00
1.2.14831.m1	Am_NLR69	NACHT	nlrc4_xentr ame: full=nlr family card domain-containing protein 4	731	1.50E-15	43.40
1.2.16739.m1	Am_NLR70	NACHT	nlrc5_ictpu ame: full=protein nlrc5	1160	1.90E-15	42.20
1.2.19569.m1	Am_NLR71	NACHT	nlrc5_ictpu ame: full=protein nlrc5	1203	1.80E-17	43.00
1.2.25971.m1	Am_NLR72	NACHT	nlrc4_xentr ame: full=nlr family card domain-containing protein 4	532	6.00E-13	40.80
1.2.1368.m1	Am_NLR73	NACHT	nlrc4_xentr ame: full=nlr family card domain-containing protein 4	1243	1.60E-06	42.00
1.2.24286.m1	Am_NLR74	NACHT	nlrc5_ictpu ame: full=protein nlrc5	404	2.30E-10	41.00
1.2.18370.m1	Am_NLR75	NACHT	nod2_mouse ame: full=nucleotide-binding oligomerization domain-containing protein 2 ame: full=caspase recruitment domain-containing protein 15	449	2.00E-20	42.80
1.2.16522.m1	Am_NLR76	NACHT	nlrc4_xentr ame: full=nlr family card domain-containing protein 4	521	8.50E-18	41.60
1.2.18796.m1	Am_NLR77	NACHT|LRRs	nod1_human ame: full=nucleotide-binding oligomerization domain-containing protein 1	1038	5.50E-39	40.60
1.2.20864.m1	Am_NLR78	NACHT|LRRs	nlrc3_human ame: full=protein nlrc3	835	7.40E-43	53.60
1.2.11040.m1	Am_NLR79	NACHT|LRRs	nlrc3_mouse ame: full=protein nlrc3	820	3.10E-30	51.80
1.2.18997.m1	Am_NLR80	NACHT|LRRs	nlrc3_mouse ame: full=protein nlrc3	716	1.30E-33	55.60
1.2.18795.m1	Am_NLR81	NACHT|LRRs	nod1_mouse ame: full=nucleotide-binding oligomerization domain-containing protein 1	1057	3.80E-37	40.60
1.2.24320.m1	Am_NLR82	NACHT|LRRs	nal14_human ame: full= lrr and pyd domains-containing protein 14	1216	1.10E-53	42.20
1.2.20938.m1	Am_NLR83	NACHT|LRRs	nlrc3_mouse ame: full=protein nlrc3	867	1.00E-36	59.00
1.2.22378.m1	Am_NLR84	NACHT|LRRs	nlrc3_mouse ame: full=protein nlrc3	982	2.30E-59	40.40
1.2.18794.m1	Am_NLR85	NACHT|LRRs	nalp3_mouse ame: full= lrr and pyd domains-containing protein 3	1059	1.70E-34	40.20
1.2.16092.m1	Am_NLR86	NACHT|LRRs	nod2_mouse ame: full=nucleotide-binding oligomerization domain-containing protein 2	988	6.00E-32	42.60
1.2.19740.m1	Am_NLR87	NACHT|LRRs	nlrc3_human ame: full=protein nlrc3	933	5.70E-50	55.00
1.2.12473.m1	Am_NLR88	NACHT|LRRs	nlrc3_human ame: full=protein nlrc3	914	3.00E-51	58.40
1.2.26460.m1	Am_NLR89	NACHT|LRRs	nlrc3_human ame: full=protein nlrc3	1082	2.00E-24	39.00
1.2.22230.m1	Am_NLR90	NACHT|LRRs	nal12_human ame: full= lrr and pyd domains-containing protein 12	1086	1.20E-41	41.20
1.2.9751.m1	Am_NLR91	NACHT|LRRs	nod2_mouse ame: full=nucleotide-binding oligomerization domain-containing protein 2	712	1.00E-33	41.20
1.2.6154.m1	Am_NLR92	NACHT|LRRs	nal12_mouse ame: full= lrr and pyd domains-containing protein 12	1262	2.20E-57	40.80
1.2.17969.m1	Am_NLR93	NACHT|LRRs	nod1_mouse ame: full=nucleotide-binding oligomerization domain-containing protein 1	1024	4.80E-40	41.00
1.2.6155.m1	Am_NLR94	NACHT|LRRs	nlrc3_human ame: full=protein nlrc3	1174	5.20E-39	40.20
1.2.22373.m1	Am_NLR95	NACHT|LRRs	nlrc3_human ame: full=protein nlrc3	874	1.30E-50	54.20
1.2.6132.m1	Am_NLR96	NACHT|LRRs	nod2_mouse ame: full=nucleotide-binding oligomerization domain-containing protein 2	902	5.30E-32	41.60
1.2.15102.m1	Am_NLR97	NACHT|LRRs	nod2_mouse ame: full=nucleotide-binding oligomerization domain-containing protein 2	1053	6.70E-36	39.60
1.2.19719.m1	Am_NLR98	NACHT|LRRs	nalp3_bovin ame: full= lrr and pyd domains-containing protein 3	1147	6.40E-37	39.40
1.2.13398.m1	Am_NLR99	NACHT|LRRs	nalp3_mouse ame: full= lrr and pyd domains-containing protein 3	1068	1.30E-31	40.60
1.2.22377.m1	Am_NLR100	NACHT|LRRs	nlrc3_human ame: full=protein nlrc3	1060	3.90E-63	56.60
1.2.18648.m1	Am_NLR101	NACHT|LRRs	nlrc3_human ame: full=protein nlrc3	753	5.00E-30	41.00

1.2.22379.m1	Am_NLR102	NACHT|LRRs	nlrc3_human ame: full=protein nlrc3	769	1.80E-36	56.60
1.2.17580.m1	Am_NLR103	NACHT|LRRs	nlrc3_human ame: full=protein nlrc3	1507	1.80E-11	44.80
1.2.16964.m1	Am_NLR104	NACHT|LRR	nlrc3_mouse ame: full=protein nlrc3	884	1.40E-42	49.00
1.2.18364.m1	Am_NLR105	NACHT|LRR	nlrc3_mouse ame: full=protein nlrc3	778	1.90E-47	51.40
1.2.19603.m1	Am_NLR106	NACHT|LRRs	nlrc3_human ame: full=protein nlrc3	978	2.90E-36	43.20
1.2.17576.m1	Am_NLR107	NACHT|LRR	nlrc3_human ame: full=protein nlrc3	1013	1.20E-35	46.80
1.2.6164.m1	Am_NLR108	NACHT|LRRs	nal12_mouse ame: full= lrr and pyd domains-containing protein 12	1228	1.80E-53	40.60
1.2.4467.m1	Am_NLR109	NACHT|LRRs	nod2_mouse ame: full=nucleotide-binding oligomerization domain-containing protein 2	734	2.60E-28	41.40
1.2.6152.m1	Am_NLR110	NACHT|LRRs	nal12_mouse ame: full= lrr and pyd domains-containing protein 12	1266	7.30E-44	40.60
1.2.4470.m1	Am_NLR111	NACHT|LRRs	nal12_human ame: full= lrr and pyd domains-containing protein 12	841	7.40E-34	40.00
1.2.9750.m1	Am_NLR112	NACHT|LRRs	nod2_mouse ame: full=nucleotide-binding oligomerization domain-containing protein 2	792	2.40E-31	42.60
1.2.26065.m1	Am_NLR113	NACHT|LRRs	nal12_mouse ame: full= lrr and pyd domains-containing protein 12	1080	1.90E-40	41.00
1.2.17971.m1	Am_NLR114	NACHT|LRRs	nal12_human ame: full= lrr and pyd domains-containing protein 12	1150	3.30E-48	41.40
1.2.22224.m1	Am_NLR115	NACHT|LRRs	nal12_human ame: full= lrr and pyd domains-containing protein 12	1124	2.10E-45	41.00
1.2.16104.m1	Am_NLR116	NACHT|LRRs	nod1_human ame: full=nucleotide-binding oligomerization domain-containing protein 1	951	2.70E-27	44.40
1.2.24463.m1	Am_NLR117	NACHT|LRRs	nlrc3_human ame: full=protein nlrc3 ame: full=card15-like protein	1410	3.00E-76	53.40
1.2.24495.m1	Am_NLR118	NACHT|LRRs	nod2_mouse ame: full=nucleotide-binding oligomerization domain-containing protein 2	777	5.20E-40	40.80
1.2.19473.m1	Am_NLR119	NACHT|LRRs	nlrc3_mouse ame: full=protein nlrc3	731	1.60E-35	43.20
1.2.17970.m1	Am_NLR120	NACHT|LRRs	nal12_mouse ame: full= lrr and pyd domains-containing protein 12	1195	4.70E-48	41.20
1.2.17966.m1	Am_NLR121	NACHT|LRRs	nal12_mouse ame: full= lrr and pyd domains-containing protein 12	1222	5.40E-36	42.40
1.2.24494.m1	Am_NLR122	NACHT|LRRs	nod2_mouse ame: full=nucleotide-binding oligomerization domain-containing protein 2	1043	1.10E-41	40.40
1.2.13403.m1	Am_NLR123	NACHT|LRRs	nod2_mouse ame: full=nucleotide-binding oligomerization domain-containing protein 2	932	6.10E-34	41.80
1.2.17239.m1	Am_NLR124	NACHT|LRRs	nod1_human ame: full=nucleotide-binding oligomerization domain-containing protein 1	854	1.50E-38	41.80
1.2.23718.m1	Am_NLR125	NACHT|LRRs	nlrc3_human ame: full=protein nlrc3 ame: full=card15-like protein	914	6.60E-33	56.80
1.2.17756.m1	Am_NLR126	NACHT|LRRs	nlrc3_human ame: full=protein nlrc3 ame: full=card15-like protein	996	1.70E-64	55.40
1.2.19308.m1	Am_NLR127	NACHT|LRRs	nlrc3_human ame: full=protein nlrc3 ame: full=card15-like protein	736	4.80E-26	61.00
1.2.4875.m1	Am_NLR128	NACHT|LRRs	nlrc3_mouse ame: full=protein nlrc3	1068	6.30E-68	46.60
1.2.4870.m1	Am_NLR129	NACHT|LRRs	nlrc3_human ame: full=protein nlrc3	1069	3.90E-73	45.00
1.2.4464.m1	Am_NLR130	NACHT|LRRs	nal12_mouse ame: full= lrr and pyd domains-containing protein 12	1014	9.10E-33	40.80
1.2.15100.m1	Am_NLR131	NACHT|LRRs	nod2_mouse ame: full=nucleotide-binding oligomerization domain-containing protein 2	1014	7.80E-46	40.80
1.2.24493.m1	Am_NLR132	NACHT|LRRs	nod1_human ame: full=nucleotide-binding oligomerization domain-containing protein 1	1085	1.70E-37	41.00
1.2.14307.m1	Am_NLR133	NACHT|LRRs	nod2_mouse ame: full=nucleotide-binding oligomerization domain-containing protein 2	1112	1.60E-43	40.40
1.2.17757.m1	Am_NLR134	NACHT|LRRs	nlrc3_human ame: full=protein nlrc3 ame: full=card15-like protein	750	8.50E-38	56.60
1.2.26034.m1	Am_NLR135	NACHT|LRRs	nlrc3_mouse ame: full=protein nlrc3	692	2.10E-29	53.00
1.2.24858.m1	Am_NLR136	NACHT|LRRs	nod2_mouse ame: full=nucleotide-binding oligomerization domain-containing protein 2	1099	1.10E-39	41.80
1.2.9752.m1	Am_NLR137	NACHT|LRRs	nod1_mouse ame: full=nucleotide-binding oligomerization domain-containing protein 1	1009	3.30E-30	41.20
1.2.16210.m1	Am_NLR138	NACHT|LRRs	nlrc3_mouse ame: full=protein nlrc3	867	3.80E-33	47.00
1.2.6131.m1	Am_NLR139	NACHT|LRRs	nod2_mouse ame: full=nucleotide-binding oligomerization domain-containing protein 2	1158	2.00E-28	40.60
1.2.19602.m1	Am_NLR140	NACHT|LRRs	nlrc3_human ame: full=protein nlrc3 ame: full=card15-like protein	901	3.00E-84	46.40
1.2.17893.m1	Am_NLR141	NACHT|LRRs	nlrc3_human ame: full=protein nlrc3 ame: full=card15-like protein	887	1.10E-71	57.20
1.2.7886.m1	Am_NLR142	NACHT|LRRs	nod2_mouse ame: full=nucleotide-binding oligomerization domain-containing protein 2	1084	1.40E-28	41.80
1.2.25905.m1	Am_NLR143	NACHT|LRRs	nod2_mouse ame: full=nucleotide-binding oligomerization domain-containing protein 2	748	6.50E-41	45.00
1.2.22817.m1	Am_NLR144	NACHT|LRRs	nod2_mouse ame: full=nucleotide-binding oligomerization domain-containing protein 2	752	1.30E-14	41.80
1.2.3762.m1	Am_NLR145	NACHT|LRRs	nlrc3_mouse ame: full=protein nlrc3	1028	9.80E-71	50.00
1.2.19820.m1	Am_NLR146	NACHT|LRRs	nlrc3_human ame: full=protein nlrc3	919	3.60E-48	51.20
1.2.13020.m1	Am_NLR147	NACHT|LRRs	nlrc3_human ame: full=protein nlrc3	744	2.30E-29	53.60
1.2.17749.m1	Am_NLR148	NACHT|LRRs	nlrc3_mouse ame: full=protein nlrc3	737	5.10E-49	59.20
1.2.26517.m1	Am_NLR149	NACHT|LRRs	nlrc3_human ame: full=protein nlrc3	586	1.20E-20	57.00
1.2.15882.m1	Am_NLR150	NACHT|LRRs	nlrc3_mouse ame: full=protein nlrc3	794	2.10E-33	53.00
1.2.26187.m1	Am_NLR151	NACHT|LRRs	nlrc3_human ame: full=protein nlrc3	1016	1.20E-78	57.40

1.2.4873.m1	Am_NLR152	NACHT|LRRs	nlrc3_human ame: full=protein nlrc3	746	9.20E-26	56.80
1.2.17577.m1	Am_NLR153	NACHT|LRRs	nlrc3_mouse ame: full=protein nlrc3	888	4.80E-37	45.00
1.2.24063.m1	Am_NLR154	NACHT|LRRs	nlrc3_human ame: full=protein nlrc3	735	1.00E-22	48.40
1.2.25680.m1	Am_NLR155	NACHT|LRRs	nlrc5_ictpu ame: full=protein nlrc5	1332	8.70E-16	44.20
1.2.18367.m1	Am_NLR156	NACHT|LRRs	nlrc3_human ame: full=protein nlrc3	719	2.30E-23	50.20
1.2.22381.m1	Am_NLR157	NACHT|LRRs	nlrc3_human ame: full=protein nlrc3	699	5.80E-49	51.00
1.2.24261.m1	Am_NLR158	NACHT|LRRs	nod2_mouse ame: full=nucleotide-binding oligomerization domain-containing protein 2	669	7.30E-36	40.80
1.2.19311.m1	Am_NLR159	NACHT|LRRs	nlrc5_ictpu ame: full=protein nlrc5	695	1.20E-13	43.20
1.2.4466.m1	Am_NLR160	NACHT|LRRs	nod2_mouse ame: full=nucleotide-binding oligomerization domain-containing protein 2	969	9.30E-32	40.20
1.2.23780.m1	Am_NLR161	NACHT|LRRs	nlrc3_human ame: full=protein nlrc3 ame: full=card15-like protein	959	2.30E-33	55.20
1.2.20620.m1	Am_NLR162	NACHT|LRRs	cog7_human ame: full=conserved oligomeric golgi complex subunit 7	1763	4.20E-141	55.00
1.2.17572.m1	Am_NLR163	NACHT|LRRs	nlrc3_mouse ame: full=protein nlrc3	1267	2.00E-38	45.00
1.2.13402.m1	Am_NLR164	NACHT|LRRs	nalp3_human ame: full= lrr and pyd domains-containing protein 3	1173	5.90E-32	40.20
1.2.6156.m1	Am_NLR165	NACHT|LRRs	nod2_mouse ame: full=nucleotide-binding oligomerization domain-containing protein 2	1023	1.80E-27	42.00
1.2.4868.m1	Am_NLR166	NACHT|LRRs	nlrc3_human ame: full=protein nlrc3	1043	9.70E-80	48.00
1.2.24947.m1	Am_NLR167	NACHT|LRRs	nod2_mouse ame: full=nucleotide-binding oligomerization domain-containing protein 2	1074	4.50E-35	42.60
1.2.24403.m1	Am_NLR168	NACHT|LRRs	nlrc3_human ame: full=protein nlrc3 ame: full=card15-like protein	987	1.50E-37	52.20
1.2.17472.m1	Am_NLR169	NACHT|LRRs	nlrc3_mouse ame: full=protein nlrc3	975	9.80E-37	52.00
1.2.18792.m1	Am_NLR170	NACHT|LRRs	nalt12_mouse ame: full= lrr and pyd domains-containing protein 12	1174	2.20E-54	41.40
1.2.24636.m1	Am_NLR171	NACHT|LRRs	nlrc5_human ame: full=protein nlrc5	980	2.00E-23	47.20
1.2.19240.m1	Am_NLR172	NACHT|LRRs	nlrc3_human ame: full=protein nlrc3	720	8.40E-30	54.60
1.2.24321.m1	Am_NLR173	NACHT|LRRs	nod1_mouse ame: full=nucleotide-binding oligomerization domain-containing protein 1	1016	3.10E-29	42.40
1.2.4431.m1	Am_NLR174	NACHT|LRRs	nalp4_human ame: full= lrr and pyd domains-containing protein 4	927	7.20E-17	43.00
1.2.14595.m1	Am_NLR175	NACHT|LRRs	nlrc3_human ame: full=protein nlrc3 ame: full=card15-like protein	1042	2.60E-63	57.60
1.2.15447.m1	Am_NLR176	NACHT|LRRs	nlrc3_human ame: full=protein nlrc3 ame: full=card15-like protein	795	1.10E-30	42.60
1.2.22629.m1	Am_NLR177	NACHT|LRRs	nlrc3_human ame: full=protein nlrc3 ame: full=card15-like protein	673	7.00E-11	52.00
1.2.24496.m1	Am_NLR178	NACHT|LRRs	nod2_mouse ame: full=nucleotide-binding oligomerization domain-containing protein 2	937	2.30E-29	48.20
1.2.14610.m1	Am_NLR179	NACHT|LRRs	nlrc3_human ame: full=protein nlrc3 ame: full=card15-like protein	805	4.90E-46	53.40
1.2.22825.m1	Am_NLR180	NACHT|LRRs	nlrc3_human ame: full=protein nlrc3 ame: full=card15-like protein	913	1.20E-42	49.80
1.2.24718.m1	Am_NLR181	NACHT|LRRs	nlrc3_mouse ame: full=protein nlrc3	738	1.70E-28	49.00
1.2.15133.m1	Am_NLR182	NACHT|LRRs	nlrc4_xentr ame: full=nlr family card domain-containing protein 4	794	1.40E-22	43.80
1.2.1644.m1	Am_NLR183	NACHT|LRRs	nlrc3_mouse ame: full=protein nlrc3	1133	5.80E-41	41.20
1.2.4577.m1	Am_NLR184	NACHT|LRRs	nlrc3_mouse ame: full=protein nlrc3	642	2.10E-21	59.60
1.2.17495.m1	Am_NLR185	NACHT|LRRs	nlrc3_human ame: full=protein nlrc3	798	8.30E-54	58.60
1.2.9646.m1	Am_NLR186	NACHT|LRRs	nlrc3_mouse ame: full=protein nlrc3	761	7.90E-16	50.60
1.2.15075.m1	Am_NLR187	NACHT|LRRs	nlrc3_mouse ame: full=protein nlrc3	756	9.80E-48	41.80
1.2.5252.m1	Am_NLR188	NACHT|LRRs	nlrc3_mouse ame: full=protein nlrc3	713	8.00E-32	44.80
1.2.22635.m1	Am_NLR189	NACHT|LRRs	nlrc3_human ame: full=protein nlrc3	874	2.00E-50	45.60
1.2.19842.m1	Am_NLR190	NACHT|LRRs	nlrc3_human ame: full=protein nlrc3	830	3.10E-30	49.20
1.2.17320.m1	Am_NLR191	NACHT|LRRs	nlrc3_human ame: full=protein nlrc3	1075	6.10E-35	47.80
1.2.20049.m1	Am_NLR192	NACHT|LRRs	nlrc3_mouse ame: full=protein nlrc3	922	4.80E-16	53.40
1.2.1404.m1	Am_NLR193	NACHT|TPR	nphp3_human ame: full=nephrocystin-3	981	0.00E+00	60.00
1.2.12322.m1	Am_NLR194	NACHT|WD40	nwd1_human ame: full=nacht domain- and wd repeat-containing protein 1	1565	5.30E-112	46.20
1.2.9136.m1	Am_NLR195	NACHT|WD40	dzip3_human ame: full=e3 ubiquitin-protein ligase dzip3	1498	6.20E-17	52.00
1.2.23031.m1	Am_NLR196	NACHT|WD40	nlrc3_human ame: full=protein nlrc3	1230	2.20E-40	49.60
1.2.17490.m1	Am_NLR197	NACHT|WD40	nwd1_mouse ame: full=nacht domain- and wd repeat-containing protein 1	1838	2.90E-94	47.60
1.2.9119.m1	Am_NLR198	NACHT|WD40	dzip3_human ame: full=e3 ubiquitin-protein ligase dzip3	1474	1.20E-13	42.60
1.2.16539.m1	Am_NLR199	NACHT|WD40	dzip3_mouse ame: full=e3 ubiquitin-protein ligase dzip3	1635	1.10E-13	44.60
1.2.9133.m1	Am_NLR200	NACHT|WD40	dzip3_human ame: full=e3 ubiquitin-protein ligase dzip3	1445	1.00E-17	45.00
1.2.9079.m1	Am_NLR201	NACHT|WD40	dzip3_human ame: full=e3 ubiquitin-protein ligase dzip3	1465	6.90E-14	45.25
1.2.9139.m1	Am_NLR202	NACHT|WD40	dzip3_human ame: full=e3 ubiquitin-protein ligase dzip3	1475	1.70E-14	51.50
1.2.9126.m1	Am_NLR203	NACHT|WD40	dzip3_human ame: full=e3 ubiquitin-protein ligase dzip3	1430	6.80E-13	45.00
1.2.16351.m1	Am_NLR204	NACHT|WD40	nwd1_mouse ame: full=nacht domain- and wd repeat-containing protein 1	1758	1.50E-106	47.80
1.2.17525.m1	Am_NLR205	NACHT|WD40	dzip3_human ame: full=e3 ubiquitin-protein ligase dzip3	1497	5.80E-13	48.67
1.2.9138.m1	Am_NLR206	NACHT|WD40	dzip3_human ame: full=e3 ubiquitin-protein ligase dzip3	1472	8.10E-12	45.20

(B)

Genome ID	*A. millepora* ID	Control (pH 8.1)				High CO_2 (pH 7.8)			
		1 h		6 h		1 h		6 h	
		Log_2FC	FDR	Log_2FC	FDR	Log_2FC	FDR	Log_2FC	FDR
1.2.26019.m1	Am_NLR1	–	–	-0.16	2.35E-02	–	–	-0.07	4.01E-02
1.2.5900.m1	Am_NLR2	–	–	-0.14	2.46E-02	–	–	–	–
1.2.5883.m1	Am_NLR3	–	–	–	–	0.10	1.35E-02	0.18	1.81E-02
1.2.5906.m1	Am_NLR4	–	–	–	–	0.32	3.08E-02	0.18	2.48E-02
1.2.19850.m1	Am_NLR5	–	–	–	–	0.20	4.91E-02	–	–
1.2.25484.m1	Am_NLR8	–	–	–	–	–	–	0.15	3.97E-02
1.2.15887.m1	Am_NLR10	–	–	0.06	4.74E-02	–	–	-0.23	3.91E-02
1.2.23033.m1	Am_NLR11	–	–	–	–	-0.06	2.80E-02	–	–
1.2.23034.m1	Am_NLR12	–	–	0.31	3.37E-02	–	–	0.37	2.85E-02
1.2.3761.m1	Am_NLR13	–	–	-0.32	2.55E-02	–	–	–	–
1.2.9939.m1	Am_NLR14	–	–	-0.27	4.86E-02	–	–	–	–
1.2.19702.m1	Am_NLR15	–	–	-0.59	7.48E-04	–	–	–	–
1.2.24451.m1	Am_NLR16	–	–	-0.47	2.04E-02	0.05	3.73E-02	–	–
1.2.4814.m1	Am_NLR17	–	–	–	–	-0.18	1.98E-03	–	–
1.2.23717.m1	Am_NLR18	–	–	–	–	–	–	0.06	2.49E-02
1.2.15454.m1	Am_NLR19	–	–	–	–	–	–	0.25	2.72E-02
1.2.4220.m1	Am_NLR27	–	–	-0.20	1.18E-03	-0.37	4.83E-02	0.20	4.45E-02
1.2.18769.m1	Am_NLR28	–	–	0.05	4.35E-02	–	–	–	–
1.2.16740.m1	Am_NLR31	–	–	-0.11	3.57E-02	–	–	0.17	3.36E-02
1.2.4218.m1	Am_NLR32	–	–	-0.11	1.09E-02	–	–		
1.2.6137.m1	Am_NLR33	–	–	0.64	3.41E-04	–	–	0.36	4.37E-02
1.2.9759.m1	Am_NLR34	–	–	0.05	3.71E-02	–	–	-0.32	2.19E-02
1.2.19297.m1	Am_NLR35	–	–	0.46	4.50E-02	–	–	-0.20	4.16E-02
1.2.24253.m1	Am_NLR36	–	–	0.13	1.59E-02	-0.08	1.18E-02	–	–
1.2.13860.m1	Am_NLR37	–	–	0.09	1.69E-02	–	–	–	–
1.2.19126.m1	Am_NLR38	–	–	0.08	1.57E-02	–	–	–	–
1.2.9130.m1	Am_NLR39	–	–	0.53	8.99E-03	–	–	0.67	2.30E-02
1.2.5896.m1	Am_NLR40	–	–	-0.21	4.51E-02	–	–	–	–
1.2.18491.m1	Am_NLR41	0.59	2.08E-02	-0.22	2.45E-02	–	–	0.25	8.05E-03
1.2.15251.m1	Am_NLR42	–	–	-0.42	2.35E-02	–	–	–	–
1.2.5897.m1	Am_NLR43	–	–	-0.38	1.78E-02	–	–	–	–
1.2.25683.m1	Am_NLR44	–	–	-0.07	2.47E-02	–	–	–	–
1.2.10017.m1	Am_NLR45	–	–	-0.25	3.33E-02	-0.15	2.50E-02	–	–
1.2.5895.m1	Am_NLR46	–	–	–	–	-0.20	3.94E-02	–	–
1.2.13880.m1	Am_NLR47	–	–	–	–	-0.12	3.58E-02	–	–
1.2.22640.m1	Am_NLR48	–	–	–	–	0.11	2.09E-02	–	–
1.2.9743.m1	Am_NLR49	–	–	–	–	0.25	2.28E-02	–	–
1.2.7526.m1	Am_NLR50	–	–	–	–	0.40	1.07E-02	–	–
1.2.2411.m1	Am_NLR51	–	–	–	–	–	–	0.25	4.14E-02
1.2.15816.m1	Am_NLR52	–	–	–	–	–	–	0.17	3.18E-02
1.2.20864.m1	Am_NLR78	0.32	3.19E-02	–	–	–	–	0.08	2.11E-02
1.2.11040.m1	Am_NLR79	0.41	4.14E-02	–	–	–	–	–	–
1.2.18997.m1	Am_NLR80	-0.09	2.60E-02	–	–	-0.25	4.01E-02	–	–
1.2.18795.m1	Am_NLR81	-0.17	2.22E-02	0.11	1.39E-02	-0.06	8.89E-03	–	–
1.2.24320.m1	Am_NLR82	–	–	0.07	1.19E-02	-0.07	1.52E-02	–	–
1.2.20938.m1	Am_NLR83	–	–	0.08	6.79E-03	–	–	–	–
1.2.22378.m1	Am_NLR84	–	–	0.10	2.09E-02	–	–	-0.07	2.21E-02
1.2.18794.m1	Am_NLR85	–	–	0.19	3.09E-02	-0.26	3.82E-02	–	–
1.2.16092.m1	Am_NLR86	–	–	0.19	3.72E-02	0.08	2.49E-03	–	–
1.2.19740.m1	Am_NLR87	–	–	0.12	4.78E-02	0.12	4.68E-02	–	–
1.2.12473.m1	Am_NLR88	–	–	0.16	4.37E-02	–	–	–	–

1.2.26460.m1	Am_NLR89	–	–	0.08	4.71E-02	-0.20	4.76E-02	0.22	2.11E-02
1.2.22230.m1	Am_NLR90	–	–	0.08	1.87E-02	–	–	0.11	3.74E-04
1.2.9751.m1	Am_NLR91	–	–	0.18	2.91E-02	–	–	0.23	3.50E-02
1.2.6154.m1	Am_NLR92	–	–	0.14	3.04E-02	–	–	–	–
1.2.17969.m1	Am_NLR93	–	–	0.05	4.11E-02	–	–	0.24	1.37E-02
1.2.6155.m1	Am_NLR94	–	–	0.13	1.54E-02	-0.07	3.29E-02	0.34	2.84E-03
1.2.22373.m1	Am_NLR95	–	–	0.28	2.63E-02	–	–	–	–
1.2.6132.m1	Am_NLR96	-0.40	2.32E-02	0.11	5.84E-03	–	–	–	–
1.2.15102.m1	Am_NLR97	–	–	0.18	4.75E-02	-0.09	1.28E-03	–	–
1.2.19719.m1	Am_NLR98	–	–	1.00	3.28E-03	-0.38	2.23E-02	–	–
1.2.13398.m1	Am_NLR99	–	–	0.09	2.83E-02	–	–	–	–
1.2.22377.m1	Am_NLR100	–	–	0.33	1.41E-02	–	–	–	–
1.2.18648.m1	Am_NLR101	–	–	-0.14	1.35E-02	–	–	–	–
1.2.22379.m1	Am_NLR102	–	–	-0.26	4.87E-02	–	–	–	–
1.2.17580.m1	Am_NLR103	–	–	-0.16	3.31E-02	–	–	–	–
1.2.16964.m1	Am_NLR104	–	–	-0.29	3.28E-02	–	–	–	–
1.2.18364.m1	Am_NLR105	–	–	-0.27	1.47E-02	–	–	–	–
1.2.19603.m1	Am_NLR106	–	–	-0.22	4.41E-02	–	–	–	–
1.2.17576.m1	Am_NLR107	–	–	-0.34	4.51E-02	–	–	–	–
1.2.6164.m1	Am_NLR108	–	–	-0.14	3.70E-02	-0.17	1.40E-02	0.08	2.44E-02
1.2.4467.m1	Am_NLR109	–	–	-0.06	2.02E-02	–	–	0.09	2.63E-02
1.2.6152.m1	Am_NLR110	–	–	-0.07	4.90E-02	–	–	0.10	4.92E-02
1.2.4470.m1	Am_NLR111	–	–	-0.12	6.76E-03	-0.05	2.52E-02	0.11	2.83E-02
1.2.9750.m1	Am_NLR112	–	–	-0.07	2.15E-02	–	–	0.14	4.61E-02
1.2.26065.m1	Am_NLR113	–	–	-0.05	1.46E-02	–	–	0.15	1.29E-02
1.2.17971.m1	Am_NLR114	–	–	-0.07	1.56E-02	–	–	0.15	2.69E-02
1.2.22224.m1	Am_NLR115	–	–	-0.12	2.88E-04	–	–	0.22	1.51E-03
1.2.16104.m1	Am_NLR116	–	–	–	–	-0.16	2.35E-02	0.18	2.38E-02
1.2.24463.m1	Am_NLR117	–	–	–	–	-0.05	1.57E-02	0.25	1.61E-02
1.2.24495.m1	Am_NLR118	–	–	–	–	-0.14	4.02E-02	0.27	1.07E-02
1.2.19473.m1	Am_NLR119	–	–	–	–	–	–	0.16	4.84E-02
1.2.17970.m1	Am_NLR120	–	–	–	–	–	–	0.18	2.47E-02
1.2.17966.m1	Am_NLR121	–	–	–	–	–	–	0.20	1.77E-02
1.2.24494.m1	Am_NLR122	–	–	–	–	–	–	0.22	3.35E-02
1.2.13403.m1	Am_NLR123	–	–	–	–	–	–	0.30	1.72E-02
1.2.17239.m1	Am_NLR124	–	–	–	–	–	–	0.30	7.13E-04
1.2.23718.m1	Am_NLR125	–	–	–	–	–	–	-0.06	4.84E-02
1.2.17756.m1	Am_NLR126	–	–	-0.25	3.28E-02	-0.05	4.04E-02	–	–
1.2.19308.m1	Am_NLR127	–	–	–	–	-0.06	2.66E-02	–	–
1.2.4875.m1	Am_NLR128	–	–	–	–	-0.43	1.46E-02	–	–
1.2.4870.m1	Am_NLR129	–	–	–	–	-0.44	4.89E-02	–	–
1.2.4464.m1	Am_NLR130	–	–	–	–	-0.34	4.40E-02	–	–
1.2.15100.m1	Am_NLR131	–	–	–	–	-0.33	3.75E-02	–	–
1.2.24493.m1	Am_NLR132	–	–	–	–	-0.35	3.15E-04	–	–
1.2.14307.m1	Am_NLR133	–	–	–	–	-0.11	5.76E-03	–	–
1.2.17757.m1	Am_NLR134	–	–	–	–	-0.24	4.71E-02	–	–
1.2.26034.m1	Am_NLR135	–	–	–	–	0.19	3.02E-02	–	–
1.2.24858.m1	Am_NLR136	–	–	–	–	0.22	1.66E-02	–	–
1.2.9752.m1	Am_NLR137	–	–	–	–	0.31	1.37E-02	–	–
1.2.16210.m1	Am_NLR138	–	–	–	–	0.15	3.02E-02	–	–
1.2.6131.m1	Am_NLR139	–	–	-0.47	1.20E-03	0.43	1.67E-02	–	–
1.2.19602.m1	Am_NLR140	–	–	–	–	0.14	4.28E-02	–	–
1.2.1404.m1	Am_NLR193	–	–	–	–	-0.22	4.18E-02	–	–
1.2.12322.m1	Am_NLR194	-0.34	4.35E-02	–	–	–	–	–	–
1.2.9136.m1	Am_NLR195	–	–	0.14	2.87E-03	–	–	0.48	8.13E-03
1.2.23031.m1	Am_NLR196	–	–	-0.20	4.78E-04	–	–	–	–
1.2.17490.m1	Am_NLR197	–	–	-0.17	3.04E-04	-0.69	3.82E-04	0.40	2.28E-02
1.2.9119.m1	Am_NLR198	–	–	-0.29	1.59E-02	–	–	–	–
1.2.16539.m1	Am_NLR199	–	–	-0.05	5.50E-03	–	–	–	–
1.2.9133.m1	Am_NLR200	–	–	-0.15	1.83E-02	–	–	–	–
1.2.9079.m1	Am_NLR201	–	–	–	–	-0.17	1.72E-02	-0.12	3.34E-02

Table S2.9 Significantly expressed genes under LPS challenge, including members of the NF-kB and MAPK signalling pathway (total = 46). (A) BlastP search results are listed for each protein. Including *A. millepora* genome homologues to caspases and Bcl2 members annotated in the *A. millepora* transcriptome (Moya *et al.* 2015). (B) Log_2FC values of significantly expressed genes (FDR <0.05, log2FC > 0.05) in response to LPS challenge relative to the control (PBS) after 1 and 6 h. For samples under control (pH 8.1) and high pCO_2 (pH 7.8) conditions. Log_2FC colour indicates up (red) and down (blue) regulated genes.

(A)

Function	Genome ID	*A. millepora* ID	Blast Hit	Length	e.Value	% ID
Cholylglycine hydrolase	1.2.7139.m1	Am_CBAH1	Penicillin acylase; gi|129549|sp|P12256.1|PAC_LYSSH	327	1.61E-45	31.19
	1.2.16853.m1*	Am_CBAH2	Uncharacterized protein YxeI; gi|254763363|sp|P54948.2|YXEI_BACS	316	1.51E-38	29.84
	1.2.13415.m1	Am_CBAH3	Choloylglycine hydrolase; gi|1705662|sp|P54965.3|CBH_CLOPE	321	7.90E-38	31.77
	1.2.13416.m1	Am_CBAH4	Choloylglycine hydrolase; gi|1705662|sp|P54965.3|CBH_CLOPE	322	1.18E-42	34.16
	1.2.16857.m1	Am_CBAH5	Penicillin acylase; gi|129549|sp|P12256.1|PAC_LYSSH	230	2.36E-31	33.48
	1.2.4576.m1	Am_CBAH6	Acid ceramidase; gi|239977071|sp|A5A6P2.1|ASAH1_PANTR	367	5.20E-142	51.77
	1.2.7128.m1	Am_CBAH7	Choloylglycine hydrolase; gi|1705662|sp|P54965.3|CBH_CLOPE	322	8.45E-42	31.05
Cathepsins	1.2.5972.m1	Am_CTSK1	hsa:1513_PKND_cathepsin_K	332	6.00E-101	52.71
	1.2.6471.m1	Am_CTSK2	hsa:1513_PKND_cathepsin_K	332	7.00E-111	50
	1.2.6472.m1	Am_CTSK3	hsa:1513_PKND_cathepsin_K	308	1.00E-104	50.97
IRAK	1.2.8695.m1	IRAK	hsa:3654_IRAK1_pelle_interleukin-1_receptor-associated_kinase_1	235	2.00E-18	31.91
IRF	1.2.25424.m1	Am_IRF1	hsa:3665_IRF7_interferon_regulatory_factor_7	111	4.00E-12	37.84
	1.2.25425.m1	Am_IRF2	hsa:3661_IRF3_interferon_regulatory_factor_3	115	4.00E-16	34.78
	1.2.9013.m1	Am_IRF3	hsa:3663_IRF5_interferon_regulatory_factor_5	109	8.00E-22	42.2
	1.2.22788.m1	Am_IRF4	hsa:3663_IRF5_interferon_regulatory_factor_5	111	1.00E-22	37.84
	1.2.22790.m1	Am_IRF5	hsa:3663_IRF5_interferon_regulatory_factor_5	163	3.00E-20	30.06
	1.2.12173.m1	Am_IRF6	hsa:3665_IRF7_interferon_regulatory_factor_7	103	2.00E-12	33.98
JUN	1.2.21516.m1	Am_JUN1	hsa:3725_JUN_AP1_c-Jun_jun_proto-oncogene	349	5.00E-45	36.1
	1.2.17406.m1	Am_JUN2	hsa:3725_JUN_AP1_c-Jun_jun_proto-oncogene	108	3.00E-32	58.33
NF-kB	1.2.3977.m1	Am_Nf-kb	hsa:4790_NFKB1_p50_nuclear_factor_of_kappa_light_polypeptide_gene_enhancer_in_B-cells_1	913	0	42.28
Caspases	1.2.8454.m1	Am_Caspase E	hsa:841_CASP8__caspase_8_apoptosis-related_cysteine_peptidase	272	1.00E-44	37.13
	1.2.779.m1	Am_Caspase D	Cluster004864p	349	0	99.43
	1.2.12876.m1	Am_Caspase A	Cluster010971	307	0	97.72
Bcl2	1.2.11925.m1	Am_BokB	Cluster002778p	200	2.00E-103	82.5
	1.2.6211.m1	Am_BclWD	hsa:596_BCL2_B-cell_CLL/lymphoma_2	121	5.00E-25	36.36
	1.2.7664.m1	Am_Mcl1-like	hsa:596_BCL2_PP1R50_B-cell_CLL/lymphoma_2	188	7.00E-19	27.66
	1.2.8813.m1	Am_BclWB	hsa:596_BCL2_B-cell_CLL/lymphoma_2	119	1.00E-22	38.66
	1.2.26503.m1	Am_BclWC	hsa:597_BCL2A1_BCL2-related_protein_A1	132	2.00E-09	29.55
	1.2.7767.m1	Am_BclWD	Cluster011480	63	6.00E-38	98.41
	1.2.7024.m1	Am_Bax	hsa:597_BCL2A1_BCL2-related_protein_A1	83	7.00E-11	39.76
	1.2.14607.m1	Am_BclRAMBO	Cluster015074	347	0	99.71
	1.2.2124.m1	Am_BokC	Cluster011056	240	4.00E-179	98.75
Inhibitor NFkB	1.2.11031.m1	Am_IKBKB	hsa:3551_IKBKB__inhibitor_of_kappa_light_polypeptide_gene_enhancer_in_B-cells_kinase_beta	621	6.00E-132	39.45
RIG-I	1.2.2079.m1	Am_RIG1	hsa:23586_RIG-I_DEAD_(Asp-Glu-Ala-Asp)_box_polypeptide_58	364	2.00E-59	37.36
	1.2.16130.m1	Am_RIG2	hsa:23586_RIG-I_DEAD_(Asp-Glu-Ala-Asp)_box_polypeptide_58	723	1.00E-125	34.99
COX	1.2.11189.m1	Am_COX1	hsa:5743_COX-2prostaglandin-endoperoxide_synthase_2	127	6.00E-16	35.43
	1.2.3032.m1	Am_COX2	hsa:5743_COX-2prostaglandin-endoperoxide_synthase_2	328	1.00E-14	24.7
	1.2.14349.m1	Am_COX3	hsa:5743_COX-2prostaglandin-endoperoxide_synthase_2	454	2.00E-21	26.43
PIAS	1.2.11953.m1	Am_PIAS	hsa:51588_PIAS4_protein_inhibitor_of_activated_STAT_4	497	5.00E-115	41.05
PLAU	1.2.1698.m1	Am_PLAU1	hsa:5328_PLAU_plasminogen_activator_urokinase	252	2.00E-38	35.32
	1.2.1699.m1	Am_PLAU2	hsa:5328_PLAU_plasminogen_activator_urokinase	279	3.00E-44	35.13
C-FOS	1.2.3957.m1	Am_C-FOS1	hsa:2353_FOS_murine_osteosarcoma_viral_oncogene_homolog	64	3.00E-07	42.19
	1.2.13975.m1	Am_C-FOS2	hsa:2353_FOS_murine_osteosarcoma_viral_oncogene_homolog	111	3.00E-07	30.63
Death kinase	1.2.21388.m1	Am_dapk1	dapk3_human_ame:_full=death-associated_protein_kinase_3	331	2.80E-44	54.00
	1.2.16753.m1	Am_dapk2	dapk3_human_ame:_full=death-associated_protein_kinase_3	320	3.50E-84	66.60
	1.2.14589.m1	Am_dyrk	dyrk2_ame:_full=dual_specificity_tyrosine-phosphorylation-regulated_kinase_2	525	4.00E-30	43.20

* Gene up-regulated under MDP challenge in *A. millepora* (Weiss *et al.* 2013)

(B)

Genome ID	*A. millepora* ID	Control (pH 8.1)				High CO_2 (pH 7.8)			
		1 h		6 h		1 h		6 h	
		Log_2FC	FDR	Log_2FC	FDR	Log_2FC	FDR	Log_2FC	FDR
1.2.7139.m1	Am_CBAH1	3.85	5.40E-06	-1.03	8.48E-15	-1.95	9.92E-12	-1.84	8.02E-17
1.2.16853.m1*	Am_CBAH2	1.03	6.34E-03	-0.36	2.08E-10	–	–	–	–
1.2.13415.m1	Am_CBAH3	0.91	8.19E-03	-1.01	3.93E-04	1.60	1.49E-07	0.55	1.46E-02
1.2.13416.m1	Am_CBAH4	0.07	3.92E-02	-0.91	1.27E-07	0.26	4.26E-03	0.27	1.98E-06
1.2.16857.m1	Am_CBAH5	–	–	-0.22	5.43E-02	–	–	-0.13	4.24E-03
1.2.4576.m1	Am_CBAH6	–	–	–	–	–	–	–	–
1.2.7128.m1	Am_CBAH7	–	–	–	–	–	–	–	–
1.2.5972.m1	Am_CTSK1	0.43	4.07E-02	–	–	-0.19	4.48E-02	–	–
1.2.6471.m1	Am_CTSK2	–	–	0.05	7.69E-03	–	–	–	–
1.2.6472.m1	Am_CTSK3	–	–	–	–	–	–	–	–
1.2.8695.m1	IRAK	-0.21	3.63E-02	–	–	-0.34	1.28E-02	–	–
1.2.25424.m1	Am_IRF1	–	–	-0.30	2.61E-02	0.34	1.72E-02	0.47	1.59E-04
1.2.25425.m1	Am_IRF2	-0.06	1.74E-02	0.34	3.11E-02	0.32	1.76E-02	0.18	4.58E-02
1.2.9013.m1	Am_IRF3	0.16	2.78E-02	–	–	–	–	–	–
1.2.22788.m1	Am_IRF4	0.05	1.82E-02	–	–	–	–	–	–
1.2.22790.m1	Am_IRF5	–	–	–	–	0.06	6.31E-05	0.64	2.20E-07
1.2.12173.m1	Am_IRF6	–	–	–	–	–	–	–	–
1.2.21516.m1	Am_JUN1	0.30	4.04E-02	–	–	0.22	1.50E-08	-0.71	1.43E-06
1.2.17406.m1	Am_JUN2	–	–	–	–	–	–	-0.55	1.69E-02
1.2.3977.m1	Am_Nf-kb	–	–	–	–	–	–	–	–
1.2.8454.m1	Am_Caspase E	0.41	1.54E-02	–	–	-0.27	2.09E-02	-0.50	3.53E-04
1.2.779.m1	Am_Caspase D	0.46	2.09E-02	–	–	-0.16	1.47E-07	-0.51	4.97E-04
1.2.12876.m1	Am_Caspase A	–	–	-0.09	4.09E-02	–	–	–	–
1.2.11925.m1	Am_BokB	–	–	–	–	0.11	3.74E-02	–	–
1.2.6211.m1	Am_BclWD	–	–	–	–	0.22	1.11E-06	-0.35	2.12E-02
1.2.7664.m1	Am_Mcl1-like	–	–	-0.19	4.75E-02	0.08	1.12E-03	-0.32	3.18E-02
1.2.8813.m1	Am_BclWB	–	–	–	–	–	–	-0.31	4.09E-02
1.2.26503.m1	Am_BclWC	–	–	–	–	–	–	–	–
1.2.7767.m1	Am_BclWD	0.263	1.45E-02	-0.271	5.17E-04	-0.32	6.01E-05	-0.604	2.66E-04
1.2.7024.m1	Am_Bax	–	–	-0.24	3.59E-02	–	–	–	–
1.2.14607.m1	Am_BclRAMBO	–	–	–	–	-0.276	3.23E-04	–	–
1.2.2124.m1	Am_BokC	–	–	–	–	–	–	–	–
1.2.11031.m1	Am_IKBKB	–	–	-0.09	4.52E-02	–	–	0.27	4.02E-04
1.2.2079.m1	Am_RIG1	-0.10	2.49E-02	-0.20	3.30E-02			0.40	3.00E-04
1.2.16130.m1	Am_RIG2	–	–	-0.13	4.60E-03	0.13	4.11E-02	0.26	2.22E-03
1.2.11189.m1	Am_COX1	–	–	–	–	-0.25	9.40E-02	-0.33	1.99E-02
1.2.3032.m1	Am_COX2	0.15	2.07E-02	-0.86	3.57E-06	0.49	6.18E-04	–	–
1.2.14349.m1	Am_COX3	–	–	-0.33	1.66E-02	-0.20	4.33E-02	–	–
1.2.11953.m1	Am_PIAS	0.26	4.13E-02	–	–	–	–	–	–
1.2.1698.m1	Am_PLAU1	–	–	–	–	-0.07	2.34E-02	0.21	4.27E-02
1.2.1699.m1	Am_PLAU2	–	–	-0.20	4.80E-03	–	–	–	–
1.2.3957.m1	Am_C-FOS1	–	–	0.23	4.90E-02	0.32	3.36E-03	–	–
1.2.13975.m1	Am_C-FOS2	–	–	–	–	-0.25	3.34E-02	–	–
1.2.21388.m1	Am_dapk1	-0.45	6.10E-03	0.10	3.75E-03	–	–	0.31	5.91E-05
1.2.16753.m1	Am_dapk2	0.96	2.99E-03	-0.06	1.09E-02	-0.10	1.58E-04	-0.44	6.61E-03
1.2.14589.m1	Am_dyrk	-0.17	4.14E-02	–	–	0.23	1.20E-03	–	–

Table S2.10 GO terms of the differentially expressed genes at 1 h post LPS challenge of *A. millepora* samples pre-exposed to high pCO_2 conditions. FDR values were obtained from the Benjamini & Hochberg correction using BiNGO. Shaded terms (purple) are significantly over-represented (FDR < 0.05).

Up-regulated				Down-regulated			
GO Biological processes	**GO ID**	**Total genes**	**FDR**	**GO Biological processes**	**GO ID**	**Total genes**	**FDR**
bioluminescence	8218	8	1.35E-05	regulation of macromolecule biosynthetic process	10556	77	1.28E-05
transcription regulator activity	30528	27	1.14E-03	regulation of transcription, DNA-dependent	6355	67	1.28E-05
transcription factor activity	3700	22	2.05E-03	sequence-specific DNA binding	43565	29	1.56E-05
hatching gland development	48785	3	4.09E-02	biological regulation	65007	189	1.66E-05
DNA binding	3677	33	4.59E-02	regulation of RNA metabolic process	51252	68	2.18E-05
superoxide-generating NADPH oxidase activity	16175	2	1.24E-01	regulation of nitrogen compound metabolic process	51171	79	5.25E-05
calcium-dependent phospholipase A2 activity	47498	2	2.19E-01	tissue development	9888	46	5.75E-05
regulation of transcription, DNA-dependent	6355	34	3.59E-01	central nervous system development	7417	29	6.32E-04
signaling	23052	52	3.78E-01	negative regulation of cellular process	48523	62	1.73E-03
apoptotic nuclear change	30262	3	3.78E-01	positive regulation of intracellular protein kinase cascade	10740	13	3.44E-03
signaling pathway	23033	38	3.78E-01	regulation of developmental process	50793	37	3.92E-03
lipid metabolic process	6629	16	3.78E-01	G-protein coupled receptor activity	4930	23	3.97E-03
G-protein coupled receptor protein signaling pathway	7186	11	3.78E-01	regulation of signaling pathway	35466	36	5.68E-03
cerebral cortex GABAergic interneuron development	21894	1	3.78E-01	response to chemical stimulus	42221	50	7.81E-03
regulation of macromolecule biosynthetic process	10556	37	3.99E-01	cell surface receptor linked signaling pathway	7166	44	8.08E-03
Wnt receptor signaling pathway	16055	5	4.18E-01	negative regulation of apoptosis	43066	17	9.64E-03
regulation of nitrogen compound metabolic process	51171	40	4.18E-01	signal transducer activity	4871	44	1.01E-02
cellular lipid metabolic process	44255	12	4.36E-01	response to stimulus	50896	87	5.56E-02
positive regulation of transcription from RNA polymerase II promoter	45944	10	4.40E-01	caspase regulator activity	43028	3	5.56E-02
response to stress	6950	32	4.47E-01	modulation by symbiont of host immune response	52553	3	6.55E-02
cell differentiation	30154	35	4.47E-01	response to interleukin-1	70555	4	7.25E-02
				regulation of MAPKKK cascade	43408	10	7.82E-02
				response to stress	6950	49	9.53E-02
				positive regulation of apoptosis	43065	9	1.04E-01
				regulation of protein kinase B signaling cascade	51896	4	1.07E-01
				response to abiotic stimulus	9628	16	1.24E-01
				positive regulation of immune system process	2684	11	1.25E-01
				caspase inhibitor activity	43027	2	1.42E-01
				G-protein coupled receptor protein signaling pathway	7186	15	1.71E-01
				regulation of immune response	50776	10	2.09E-01

Table S2.11 Differentially expressed genes (FDR <0.01, log2FC > 0.05) after 1 h post LPS challenge of samples under control and high pCO_2 conditions. Log_2FC colour indicates up (red) and down (blue) regulated genes.

Genome ID	Blast Hit	1h	
		Control (pH 8.1)	High CO_2 (pH 7.8)
1.2.884.m1	DAO_D-Amino-Acid Oxidase	3.65	-1.02
1.2.16616.m1	ZN363_p53-Induced Ring-H2 Protein	2.57	-0.26
1.2.6508.m1	NPC2_Niemann-Pick Disease Type C2	1.88	-0.62
1.2.9914.m1	AOSL_Arachidonate 8-Lipoxygenase	1.69	-0.90
1.2.25722.m1	NAS15_Zinc Metalloproteinase nas-15	1.64	-0.23
1.2.9411.m1	GUNE_Endoglucanase	1.61	-0.25
1.2.3857.m1	RIT1_GTP-Binding Protein RIT1	1.53	-0.35
1.2.1111.m1	TRPC4_Transient Receptor Potential Channel 4	1.53	-0.82
1.2.168.m1	OLM2a_Olfactomedin-Like Protein 2A	1.49	-1.60
1.2.6008.m1	ZN106_Zinc Finger Protein 106	1.27	-0.67
1.2.24581.m1	APRV1_Retroviral-Like Aspartic Protease 1	1.27	-0.17
1.2.19840.m1	CBX8_Chromobox Homolog 8	1.25	-1.05
1.2.16253.m1	WNT8b_Wingless-Type MMTV Integration Site Family, Member 8B	1.15	-0.36
1.2.999.m1	FGF10_Fibroblast Growth Factor 10	1.07	-1.00
1.2.16853.m1	PAC_Penicillin Acylase	1.03	-0.03
1.2.4364.m1	TLL1_Tolloid-Like 1	1.03	-0.42
1.2.2898.m1	TRAF6_TNF Receptor-Associated Factor 6	1.02	-0.63
1.2.2891.m1	TRAF7_TNF Receptor-Associated Factor 7	1.00	-0.48
1.2.12363.m1	GDH_Glutamate Dehydrogenase Mitochondrial	0.98	-0.31
1.2.16753.m1	DAPK3_Death-Associated Protein Kinase 3	0.96	-0.10
1.2.10516.m1	CNTN2_Contactin 2	0.91	-0.51
1.2.3332.m1	SSUH2_Ssuh2 Homolog	0.90	-0.57
1.2.14438.m1	WNT4_Wingless-Type MMTV Integration Site Family, Member 4	0.89	-0.90
1.2.22360.m1	GBPC_Cyclic GMP-binding protein C	0.88	-0.14
1.2.14882.m1	MALRD1_MAM and LDL Receptor Class A Domain Containing 1	0.87	-0.92
1.2.7734.m1	SOX9_SRY (Sex Determining Region Y)-Box9	0.86	-0.12
1.2.1332.m1	EGLN1_Hypoxia-Inducible Factor Prolyl Hydroxylase 2	0.85	-0.52
1.2.14080.m1	ECE2_Endothelin Converting Enzyme 2	0.84	-0.51
1.2.13251.m1	PCK2_Phosphoenolpyruvate Carboxykinase	0.83	-0.25
1.2.18947.m1	FGFR3_Fibroblast Growth Factor Receptor 3	0.82	-0.08
1.2.15486.m1	SPTC3_Serine Palmitoyltransferase 3	0.82	-0.35
1.2.25219.m1	NU5M_NADH Dehydrogenase Subunit 5	0.80	-1.10
1.2.6253.m1	NLK_Nemo-Like Kinase	0.79	-0.25
1.2.2501.m1	TRIM71_Tripartite Motif Containing, E3 Ubiquitin-Protein Ligase	0.79	-0.18
1.2.5368.m1	SPRY2_Sprouty Homolog 2	0.78	-0.20
1.2.4311.m1	GP2_Pancreatic Zymogen Granule Membrane Protein GP-2	0.78	-0.31
1.2.15857.m1	CRYP17_Cytochrome p450-c17	0.77	-0.11
1.2.299.m1	AR1_NADPH-Dependent Aldehyde Reductase	0.77	-0.27
1.2.10529.m1	DOT1L_Lysine n-Methyltransferase 4	0.74	-0.36
1.2.13654.m1	CALM_Calmodulin	0.73	-0.84
1.2.8976.m1	ZMYND19_Zinc Finger MYND Domain-Containing 19	0.73	-0.06
1.2.6172.m1	HTR4_5-Hydroxytryptamine (Serotonin) Receptor 4	0.70	-0.28
1.2.22505.m1	SMAD4_Mothers Against Decapentaplegic Homolog 4	0.68	-0.44
1.2.17251.m1	STRADA_STE20-Related Kinase Adapter Protein Alpha	0.68	-0.69
1.2.25218.m1	COX1_Cytochrome C Oxidase Subunit I	0.62	-1.48
1.2.3888.m1	MBNL3_Muscleblind-Like Protein 3	0.62	-0.12
1.2.12494.m1	ALDH4A1_Delta-1-Pyrroline-5-Carboxylate Mitochondrial	0.62	-0.25
1.2.16354.m1	INF2_Inverted Formin-2	0.60	-0.41
1.2.9806.m1	ELK1_ETS Domain-containing protein elk-1	0.57	-0.67
1.2.21239.m1	ADAMTS2_Procollagen I N-Proteinase	0.56	-0.33
1.2.4919.m1	MOXD2P_DBH-Like Monooxygenase Protein 2	0.54	-0.43
1.2.21427.m1	SLC6A13_Solute Carrier Family 6 (Neurotransmitter, GABA), Member 13	0.54	-0.28
1.2.6863.m1	PMM_Phosphomannomutase	0.54	-0.10
1.2.3832.m1	ETV6_Transcription Factor ETV6	0.53	-0.23
1.2.17027.m1	PTK7_Tyrosine-Protein Kinase-Like 7	0.53	-0.01
1.2.14641.m1	BCO1_Beta-Carotene Monooxygenase 1	0.52	-0.05
1.2.2028.m1	SCNN_Amiloride-Sensitive Sodium Channel Subunit Beta-2	0.50	-0.38
1.2.9195.m1	HRH2_Histamine H2 Receptor	0.49	-0.07
1.2.12594.m1	FOXL1_Forkhead Box Protein L1	0.46	-0.45

1.2.11672.m1	TLL1_Tolloid-Like Protein 1	0.43	-0.17
1.2.7885.m1	AGTX_Alanine—Glyoxylate Aminotransferase	0.39	-0.20
1.2.821.m1	TBX1_T-Box Transcription Factor TBX1	0.38	-0.10
1.2.12675.m1	ABCF2_ATP-Binding Cassette Sub-Family F Member 2	0.36	-0.24
1.2.11518.m1	AQP3_Aquaporin 3	0.35	-0.24
1.2.17245.m1	MRC1_Mannose Receptor, C Type 1	0.31	-0.37
1.2.21120.m1	CTRC_Chymotrypsin C	0.29	-0.73
1.2.25371.m1	PNLIPRP2_Pancreatic Lipase-Related Protein 2	0.24	-0.33
1.2.2434.m1	TLR2_Toll-Like Receptor 2	0.20	-0.43
1.2.545.m1	FZD8_Frizzled-8	0.14	-0.51
1.2.10850.m1	TACR1_Tachykinin Receptor 1	0.09	-1.48
1.2.6992.m1	CAT_Catalase	0.05	-0.28
1.2.20887.m1	CUBN_Cubilin	-0.06	0.66
1.2.25845.m1	PNPO_Pyridoxine 5-Phosphate Oxidase	-0.09	0.60
1.2.3216.m1	PLA2G4A_Cytosolic Phospholipase A2	-0.10	0.14
1.2.1794.m1	ADAM22_Metalloproteinase-Disintegrin ADAM22	-0.12	0.11
1.2.13663.m1	SLC2A8_Solute Carrier Family (Facilitated Glucose Transporter) Member 8	-0.13	1.53
1.2.10762.m1	TRAF3_TNF Receptor-Associated Factor 3	-0.16	0.07
1.2.12306.m1	ADGRD1_Adhesion G-Protein Coupled Receptor D1	-0.20	0.28
1.2.10230.m1	PSD3_Phosphatidylserine Decarboxylase Proenzyme 3	-0.21	0.10
1.2.8410.m1	FRZB_Secreted Frizzled-Related Protein 3	-0.23	0.57
1.2.14857.m1	TRIM71_Tripartite Motif Containing, E3 Ubiquitin-Orotein Ligase	-0.24	0.12
1.2.9606.m1	NOTUM_Palmitoleoyl-Protein Carboxylesterase NOTUM1A	-0.29	0.54
1.2.14234.m1	ADAM22_Metalloproteinase-Disintegrin ADAM22	-0.31	0.06
1.2.4226.m1	SMPD2_Shingomyelin Phospholipase 2	-0.32	0.03
1.2.17015.m1	ANPEP_Aminopeptidase A	-0.34	0.19
1.2.22673.m1	MRC2_Mannose Receptor, C Type 2	-0.47	0.74
1.2.22051.m1	KOZA_Homeobox Protein Koza	-0.51	0.44
1.2.5412.m1	ANX13_Annexin A13	-0.55	0.30
1.2.21557.m1	GFPL_GFP-Like Fluorescent Chromoprotein AMFP486	-0.57	0.04
1.2.9802.m1	ETS-Related Transcription Factor ELF-1	-0.58	0.29
1.2.16980.m1	CA_Carbonic Anhydrase	-0.58	0.29
1.2.9809.m1	ETS-Related Transcription Factor ELF-1	-1.01	0.10
1.2.22452.m1	Acyl-CoA Desaturase	-1.80	0.36
1.2.8189.m1	RIT1_GTP-Binding Protein RIT1	-0.18	-0.05
1.2.8560.m1	MRC2_Mannose Receptor, C Type 2	-0.25	-0.04
1.2.5952.m1	ADRB2_Beta-2 Adrenergic Receptor	-0.29	-0.11
1.2.26031.m1	TLR2_Toll-Like Receptor 2	-0.35	-0.12
1.2.22453.m1	SCD5_Stearoyl-CoA Desaturase 5	-1.92	-0.05
1.2.13093.m1	MMP7_Matrix Metalloproteinase-7	1.18	0.07
1.2.21562.m1	GFPL_GFP-Like Fluorescent Chromoprotein AMFP486	1.07	2.85
1.2.5134.m1	IPHN3_Latrophilin-3	1.07	0.02
1.2.8762.m1	NAS14_Zinc Metalloproteinase nNAS-14	1.00	0.31
1.2.15012.m1	OX1R_orexin receptor type 1	0.97	0.29
1.2.13415.m1	CBH_choloylglycine hydrolase	0.91	1.60
1.2.5767.m1	CAMK2A_Calcium/Calmodulin-Dependent Protein Kinase II Alpha	0.78	0.05
1.2.4072.m1	FHL2_skeletal muscle lim-protein 3	0.70	0.05
1.2.20514.m1	NPFF2_Neuropeptide FF Receptor 2	0.67	0.06
1.2.10514.m1	FGFR_Fibroblast Growth Factor Receptor	0.63	0.29
1.2.18951.m1	FGFR3_Fibroblast Growth Factor Receptor 3	0.60	0.15
1.2.11510.m1	HNMT_Histamine H-Methyltransferase	0.59	1.72
1.2.14044.m1	CYP17A1_Cytochrome P450 17A1	0.58	0.19
1.2.6574.m1	HSP12_Heat Shock Protein	0.57	0.64
1.2.3017.m1	ATTY_Tyrosine Aminotransferase	0.54	0.17
1.2.4075.m1	GP157_G-Protein Coupled Receptor 157	0.54	0.33
1.2.19257.m1	HSP68_Heat Shock Protein 68	0.39	0.82
1.2.6070.m1	HSP12_Heat Shock Protein	0.37	0.50
1.2.13081.m1	DEGS2_Sphingolipid Delta -Desaturase C4-Hydroxylase	0.12	0.12
1.2.21453.m1	CTHR1_Collagen Triple Helix Repeat-Containing 1	0.11	0.11
1.2.7210.m1	CYP3A4_Cytochrome p450 3A4	0.08	0.45

Figures

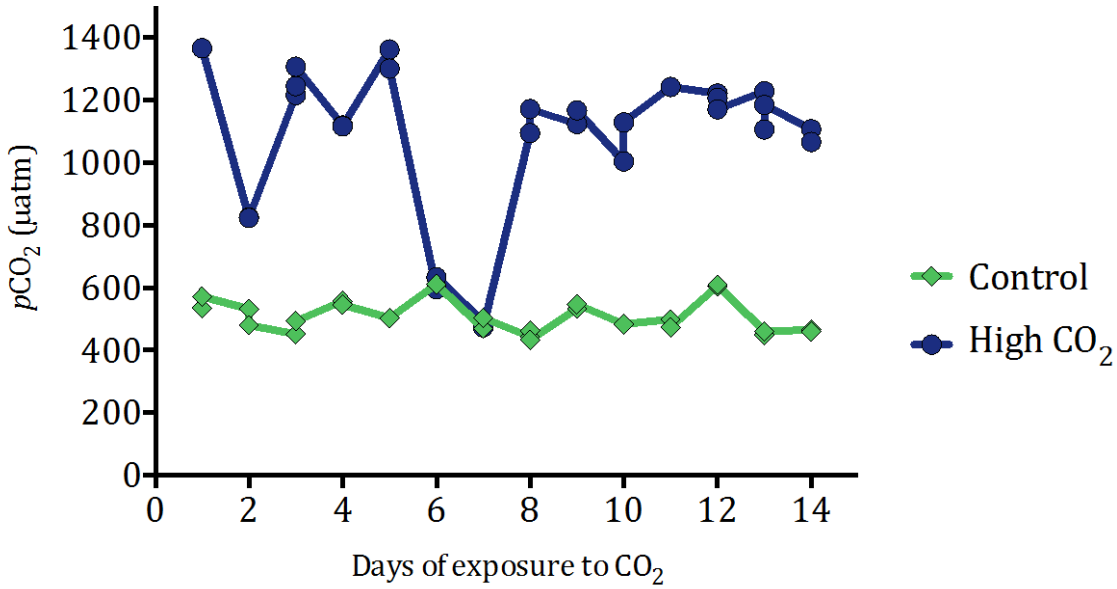

Figure S2.1. pCO_2 (µatm) values from control (green) and high pCO_2 (blue) conditions in the aquaria during the course of the experiment. Each point represents an individual measurement from the control (total measurements =27) and treatment (total measurements =28) aquaria.

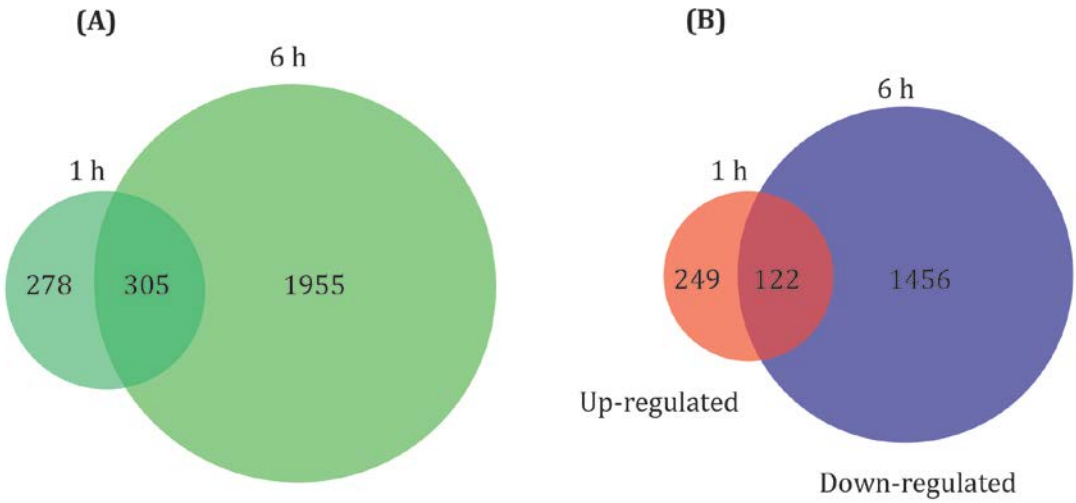

Figure S2.2 Venn diagrams of the of the differentially expressed genes (FDR <0.01) in response to LPS challenge after 1 and 6 h on the coral *A. millepora*. (A) Indicate the total number of differentially expressed genes per time point and subset of shared genes between them. (B) Show the total up (red) and down (blue)-regulated genes after 1 and 6 h respectively, including a subset of shared genes.

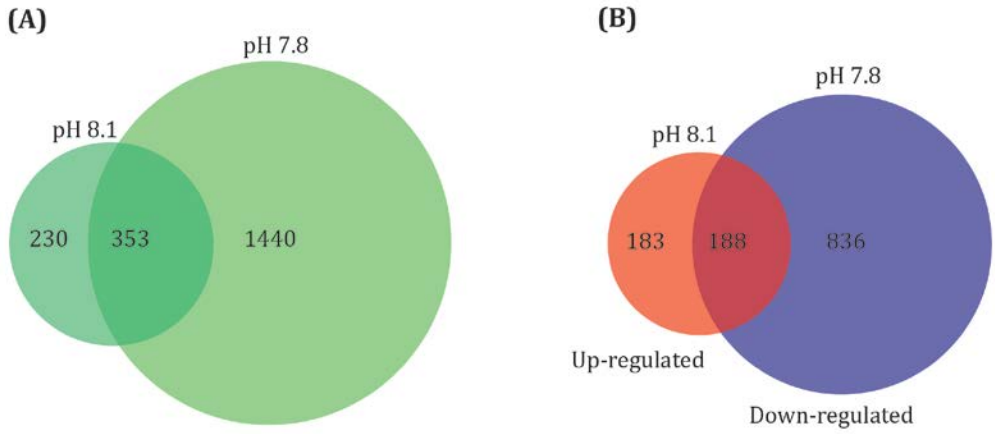

Figure S2.3 Venn diagrams of the differentially expressed genes (FDR <0.01) in response to LPS challenge after 1 h under control (pH 8.1) and high pCO_2 conditions (pH 7.8) on the coral *A. millepora*. (A) Indicates the total number of differentially expressed genes under control and treatment conditions and a subset of shared genes between them. (B) The total up (red) and down (blue)-regulated genes under control and high pCO_2 conditions respectively, including a subset of shared genes.

Chapter 3

Transcriptomic analysis reveals protein homeostasis breakdown in the coral *Acropora millepora* during hypo-saline stress

3.1. Introduction

Coral reefs are amongst the diverse and complex ecosystems and, as well as their biological significance, are of enormous social and economical importance (Moberg & Folke 1999). However, coral reefs are experiencing long-term decline on a global scale due to overfishing, pollution, and climate change (Bellwood *et al.* 2004; De'ath *et al.* 2012). Climate change is likely to be an increasingly significant cause of coral decline (Cantin *et al.* 2010). Climate change effects include not only thermal stress and ocean acidification, but also increases in the frequency and intensity of tropical storms and cyclones which would expose coral reefs to more extreme and sudden salinity variations (Baker *et al.* 2008; Durack *et al.* 2012; Xie *et al.* 2010). These conditions affect the Great Barrier Reef (GBR), where rain associated with tropical cyclones can lower the salinity of surface waters significantly (up to 7-10 PSU) (Van Woesik *et al.* 1995), with hypo-saline conditions sometimes prevailing for weeks (Devlin *et al.* 1998). Although the impacts of heavy rainfall can be correlated with coral decline on the GBR (Butler *et al.* 2015), the physiological effects of hypo-saline stress have not been thoroughly investigated. A few studies have described loss of *Symbiodinium* and coral mortality following hypo-saline stress events (Berkelmans *et al.* 2012; Downs *et al.* 2009; Kerswell & Jones 2003), but no data are available on the molecular response of corals during these events.

Like many other marine invertebrates, corals are considered to be osmoconformers – their internal environment is near isotonic with the external environment – but can tolerate a relatively narrow range of salinity (i.e. they are stenohaline). Our current understanding of osmoregulation processes in corals is largely derived from other marine invertebrates such as sea anemones and bivalves; in these organisms, small organic molecules and inorganic ions are used to prevent osmotic lysis (Deaton & Hoffman 1988; Pierce & Warren 2001). These molecules, known as osmolytes, include free amino acids (FAAs), FAA derivates (taurine, glycine betaine) and other methyl-ammonium compounds such as

dimethylsulfoniopropionate (DMSP) (Hochachka & Somero 2002; Pierce 1982). In many cases, organisms use a variety of osmolytes and related species may use quite different mechanisms. For example, the sea anemone *Metridium senile,* and the marine sponges *Halichondria okadai* and *H. japonica* exhibit a general decrease of their FAA content during hypo-osmotic stress, whereas FAA content appears to increase in the coral *Acropora aspera* under these conditions (Cowlin 2012; Deaton & Hoffman 1988; Shinagawa *et al.* 1992). Therefore, decreases in specific candidate osmolytes during reduced salinity events may occur.

Other physiological effects are to be expected in both corals and their symbionts when adult corals are forced to adjust to osmotic stress, including increased expression of genes involved in responses to oxidative stress and heat shock proteins. These categories of genes respond to other environmental stressors, such as temperature and CO_2 increase (Barshis *et al.* 2013; Moya *et al.* 2015), and are likely to be part of a general stress response system. Whereas the literature for corals is very limited, more comprehensive data are available on the molecular responses of other marine invertebrates to hypo-osmotic stress (Lockwood & Somero 2011; Tomanek & Zuzow 2010). In these organisms, responses include increases in proteolysis, increased levels of oxidative stress proteins, and changes in expression of membrane transporter proteins, although closely related species have sometimes been shown to respond differently (Lockwood *et al.* 2010).

In the present study, the transcriptomic response of the model coral *Acropora millepora* to hypo-saline conditions was investigated. Through the availability of a whole genome assembly and a comprehensive set of protein predictions for this organism, it is now possible to compare the response of the coral to those of other marine invertebrates, and to tease apart specific and general responses of the coral to different environmental stressors (Barshis *et al.* 2013; Lockwood & Somero 2011; Moya *et al.* 2015). It is also possible to

compare the response between aposymbiotic juveniles (devoid of any photosynthetic symbionts) and adults corals, in order to investigate the coral animal response to environmental stress without the influence of its photosynthetic partner (Davy *et al.* 2012). Here we exposed both adult colonies of *Acropora millepora* and juveniles, to hypo-saline conditions mimicking those experienced in extreme weather events (25 PSU for the adults and 28 PSU for the juveniles). This is the first study to comprehensively describe the molecular response of a coral to salinity stress, and identifies both specific and general components of the response of *A. millepora* to this environmental stress.

3.2. Materials and Methods

3.2.1. Coral salinity stress experiment

Five *Acropora millepora* colonies were collected from Orpheus Island, Queensland, Australia (18°39'52. 43"S, 146°29'42.38"E) in June 2013 and transferred to the Australian Institute of Marine Science's National Sea Simulator (SeaSim) facility where the colonies were acclimated for 14 days in outdoor aquaria at ~27 °C. Each colony was fragmented into 25 nubbins (~6 cm) that were then randomly distributed across three 50 l tanks. The tanks were linked to a computer controlled flow-through system supplying 0.04 µ filtered seawater (FSW) maintained at 25.7 °C (±0.6 °C) and an ambient salinity of 35 PSU. UV-filtered lights were mounted above each tank and nubbins were exposed to an intensity of 250 µE over a 12:12 h light/dark cycle (type of lights: 400W metal halide lamps, BLV). The nubbins were acclimated in this system for a further 19 days to allow recovery. At the beginning of the experiment the flow was stopped to ensure no water exchange and tanks were oxygenated via a pump (Tunze 6015). The nubbins were subsequently exposed to one of three salinity regimes for 24 h: ambient/control salinity of 35 PSU (n = 81) for the duration of the experiment, low salinity of 25 PSU (n = 68) or high salinity of 40 PSU (n = 71). The 25 PSU FSW was prepared by diluting 700 ml of 35 PSU FSW with 300 ml reverse-osmosis water while the 40 PSU FSW was prepared by adding 11 g of Red Sea Coral Pro Salt (Red Sea

Aquatics Ltd, Houston, TX) to 1 L of 35 PSU FSW. The temperature during the treatment period was maintained at 25.9±0.7°C. Salinity was monitored using a water quality meter (TPS 90FL, ThermoFisher). Coral nubbins (n = 2 per colony) were sampled at three time points for RNA analysis: prior to the salinity change, and after 1 and 24 h post the salinity change. Nubbins for RNA analysis were snap frozen in liquid nitrogen and stored at -80 °C.

3.2.2. Juvenile coral salinity stress experiment

For the experiment on coral juveniles, *Acropora millepora* colonies were collected from Trunk Reef, GBR, Australia (18°22'15.10"S/ 146°48'27.82"E) and transferred to the National Sea Simulator (SeaSim) facility prior to the predicted spawning event in November 2013. Colonies were individually placed in 70 l tanks with 0.2 □m of filtered s

After spawning, coral larvae were raised as described in Tebben *et al.* (2011) and Raina *et al.* (2013). At 13 days post-fertilization, larvae were collected using a 1 mm mesh net, washed three times in 0.2 µm FSW and then settled in (sterile) 6-well plates (8 plates per species, 40 larvae per well; each well filled with 40 ml of ambient salinity (35 PSU) 0.2-µm FSW) using a cue (5 µL) derived from crustose coralline algae (CCA; see Siboni (2014)). Throughout the incubation phase, the plates were maintained in the dark at 26.3 °C (±0.01) and the FSW was changed every second day. Four days post-settlement (T0), plates were separated into two groups: 16 plates were maintained at 35 PSU (control salinity) while the water in the remaining 16 plates was exchanged for 28 PSU sea water (salinity stress treatment). Samples were collected for RNA after 24 (T24), and 48 h (T48).

3.2.3. RNA extraction sequencing and gene expression analyses

Total RNA was extracted from the adult nubbins of 25 and 35 PSU treatments following the same methods described in Chapter 2 (section 2.2.3.). Coral juveniles were sampled by removing the water and adding 1.5 mL of RNA*later* (Ambion, cat# AM7021) simultaneously to each well and scraping the content with a sterile 200 µL plastic tip to

transfer the contents into a 2 mL tube and stored at -20 °C. Total RNA of the 24 juvenile samples was extracted using the RNAaqueous-Micro total RNA isolation kit (AM1931, AMBION). The quality and quantity of RNA preparations were determined using a Bioanalyzer (Agilent 2100 Bioanalyzer) using samples prepared following the Agilent RNA 6000 Nano Kit instructions (cat # 5067-1511).

RNAseq libraries (18 for the adults and 23 for the juveniles) were constructed using the NEB Next Ultra Directional RNA Library Prep Kit for Illumina (NEB, E7420S) following the manufacturers recommended protocol, and 100 bp paired-end sequence data obtained using a HiSeq 2000 at the Biomolecular Resource Facility (Australian National University). Reads were mapped onto the *Acropora millepora* genome (Fôret *et al*. in prep) using TopHat2 (Kim *et al.* 2013) to produce a count data gene expression matrix for subsequent analysis.

Data were analysed in DESeq2 package (Love *et al.* 2014) in R (R Core Team 2014) using a formula for differential gene expression that tests for the effects of salinity, and accounted for the colony type in the adult dataset. Log_2 fold changes (log_2FC) in gene expression levels were obtained in DESeq2 by comparing control vs. salinity treatment of six different comparisons: (i) control vs. treatment at 1 h in the adults, (ii) control vs. treatment at 24 h in the adults, (iii) control vs. treatment at 1 and 24 h in the adults (iv) control vs. treatment at 24 h in the juveniles, (v) control vs. treatment at 48 h in the juveniles, and (vi) control vs. treatment at 24 and 48 h in the juveniles. False discovery rate (FDR) adjusted *p* values were controlled at 5% for each gene according to the methods of Benjamini and Hochberg (Benjamini & Hochberg 1995).

Statistically over-represented gene ontology (GO) categories were determined in BiNGO (Maere *et al.* 2005) in Cytoscape 3.1.1 (Smoot *et al.* 2011) by using the set of genes

that were differentially up- or down-regulated in each dataset (FDR < 0.01). These GO categories were used to search specific pathways in the Kyoto Encyclopedia of Genes and Genomes (KEGG) by downloading pathway sequences (using *Homo sapiens* and *Nematostella vectensis* as references) and blasting these sequences against the *A. millepora* protein predictions. All the results are based on homology of the *A. millepora* protein predictions to a reference annotated proteins (e−val cut-off = 1e−4).

3.3. Results

3.3.1. Differential gene expression analyses

In adult coral samples, 5.5 - 10.2 million RNAseq reads were obtained for each treatment sampling time while 3.4 - 8.8 million reads were obtained for each juvenile coral sample. Principal component analysis (PCA) of the count matrix of the 26,622 *A. millepora* gene predictions revealed that in the case of adult corals, the colony (i.e. genotype) had a stronger effect on gene expression than did the salinity treatment, whereas in the case of juveniles, separation was determined primarily by treatment and time (Figure S3.1, Supporting information). After 1 h of salinity stress, 2,657 genes were differentially expressed (DEGs; FDR < 0.05) in the adults, increasing to 3,713 after 24 h of exposure (Figure S3.2, Supporting information). At that time, 3,462 genes were differentially expressed in the juveniles while sharing 38% of up-regulated genes (total number: 1707; FDR <0.05) and 31% of down-regulated genes (total number: 1755) with the adults (see Figure S3.3, Supporting information). This number decreased after 48 h of stress, with 1,485 genes differentially regulated in the juveniles (Figure S3.2, Supporting information).

GO analysis revealed that several categories were consistently down-regulated at 1 h and up-regulated at 24 h in the adults (Figure 3.1, Table S3.1, Supporting information): (i) a group of categories associated with protein homeostasis, including: endoplasmic reticulum (ER), ER lumen, proteasome complex, cell catabolism and oxidoreductase activity; and (ii) a

second group associated with amino acid (AA) and nitrogen metabolism (Table S3.1, Supporting information). Based on these results, specific pathways were annotated to analyse the coral transcriptomic response to hypo-saline stress.

Figure 3.1 Heat map of over-represented (FDR >0.05) GO terms for 109 genes that were differentially expressed between the various salinity treatments (25 PSU for the adults and 28 PSU for the juveniles) and the corresponding controls. Values represent $\log_2$FC relative to the control for genes that are up (red) or down-regulated (blue). For values and gene IDs refer to Table S3.1, Supporting information.

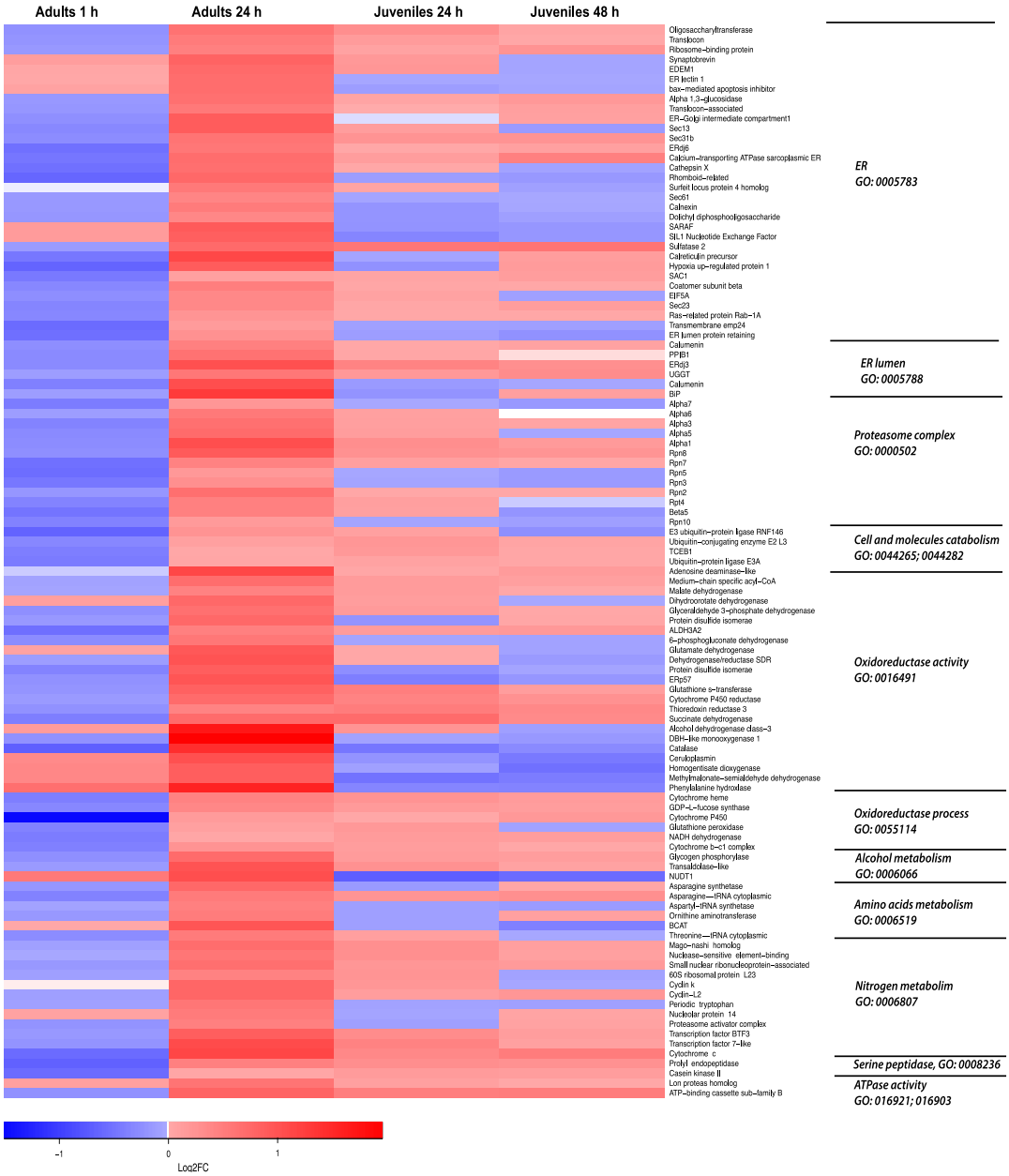

3.3.2. Proteolysis within the ER under hypo-saline conditions

Up-regulation of several genes involved in ER-associated degradation (ERAD, ko04141) and the ubiquitin-proteasome system (UPS) after 24 h of hypo-saline stress implied increased protein degradation activity. By contrast, many of the same genes were down-regulated under acute (1 h) salinity stress, suggesting protein homeostasis disruption (Figure 3.2; Table S3.2, Supporting information). The ER pathway involves several processes, including: protein folding and translocation into the ER lumen, degradation of misfolded proteins through the ERAD system and proteolysis through the UPS. Amongst the genes up-regulated after 24 h were coral homologues of components of the system responsible for translocation into the ER lumen; the oligosaccharyl transferase (OST) and SEC61protein transport systems. The expression of genes involved in protein glycosylation - glucosidase II (GlcII) increased by 0.66 $\log_2$FC, and UDP-glucose/glycoprotein glucosyltransferase (UGGT) increased by 0.59 $\log_2$FC after 24 h. Moreover, luminal chaperones and co-chaperones were also up-regulated at 24 h, including the HSP70 family member GRP70, also known as binding immunoglobulin protein (BiP; 1.2.4351.m1; 1.3 $\log_2$FC at 24 h), along with the BiP co-chaperones ERdj1, ERdj3 and ERdj6 (DnaJ Hsp40 family members; 1.2.7940.m1, 1.2.25530.m1, 1.2.21656.m1). Increased expression was also observed for members of the ERAD retrotranslocon complexes, including the endoplasmic reticulum lectin 1 (XTP3B , 1.2.21359.m1), heat shock protein 90kDa (GRP94, 1.2.15211.m1), translocating chain-associated membrane protein (TRAM, 1.2.11248.m1), and the translocon-associated protein (TRAP, 1.2.3165.m1), suggesting increased protein translocated from the ER to the cytosol (Araki & Nagata 2011). The enzyme involved in maintaining the ER oxidative state, disulfide-isomerase (PDI, EC:5.3.4.1), was differentially expressed from a $\log_2$FC of -0.36 at 1 h to a 0.87 $\log_2$FC after 24 h of stress (Table S3.2, Supporting information). Interestingly the coral homologues of the ER oxidoreductase 1 (ERO1), known to interact with PDI, were not differentially expressed during this experiment.

Higher levels of expression of components of the ubiquitin-proteasome system (UPS) provide further evidence of increased proteolysis after 24 h of stress. Members of the three enzyme families involved in this system - the ubiquitin-activating enzyme (E1), ubiquitin-conjugating enzyme (E2) and the ubiquitin ligases (E3) - were up-regulated. Amongst components of the 26S proteasome system, 19 genes were down-regulated after 1 h and 17 genes were up-regulated after 24 h (Figure 3.2; Table S3.2, Supporting information). These observations suggest a change from disruption of protein homeostasis after the initial salinity shock, to a state of increased protein breakdown after 24 h of stress.

3.3.3. Unfolded protein response (UPR) system

Transcriptomic data imply increased activity of the UPR system after 1 and 24 h of hypo-saline stress (Figure 3.2; Table S3.2, Supporting information) (Darling & Cook 2014). The UPR system, which is activated by the accumulation of misfolded proteins within the ER, relies on three major transmembrane proteins involved in sensing stress: the serine/threonine-protein kinase/endoribonuclease IRE1 (IRE1), the eukaryotic translation initiation factor 2-alpha kinase (PERK), and the activating transcription factor 6 (ATF6). Coral homologues to IRE1 (0.30 $\log_2$FC), its interacting pro-apoptotic effector BAX (BAX; 0.41 $\log_2$FC), and their down-stream members were up-regulated after 1 h. Different from PERK (0.60 $\log_2$FC) and ATF6 (0.41 $\log_2$FC) that were up-regulated after 24 h (Figure 3.2) of stress.

Figure 3.2 Differential expression of *A. millepora* homologues of components of the ER protein processing machinery (pathway 04141) after exposure of adult corals to 1 and 24 h of hypo-saline conditions. Colours represent genes (FDR< 0.05) that are up (red) or down-regulated (blue). The systems involved in ER protein processing and ER stress are indicated: glycosylation, ER associated degradation (ERAD), ubiquitin-proteasome system (UPS), and the unfolded protein response (UPR). A complete list of the genes involved in this pathway and $\log_2$FC values is provided as Table S3.2, Supporting information. Figure adapted from KEGG pathway database.

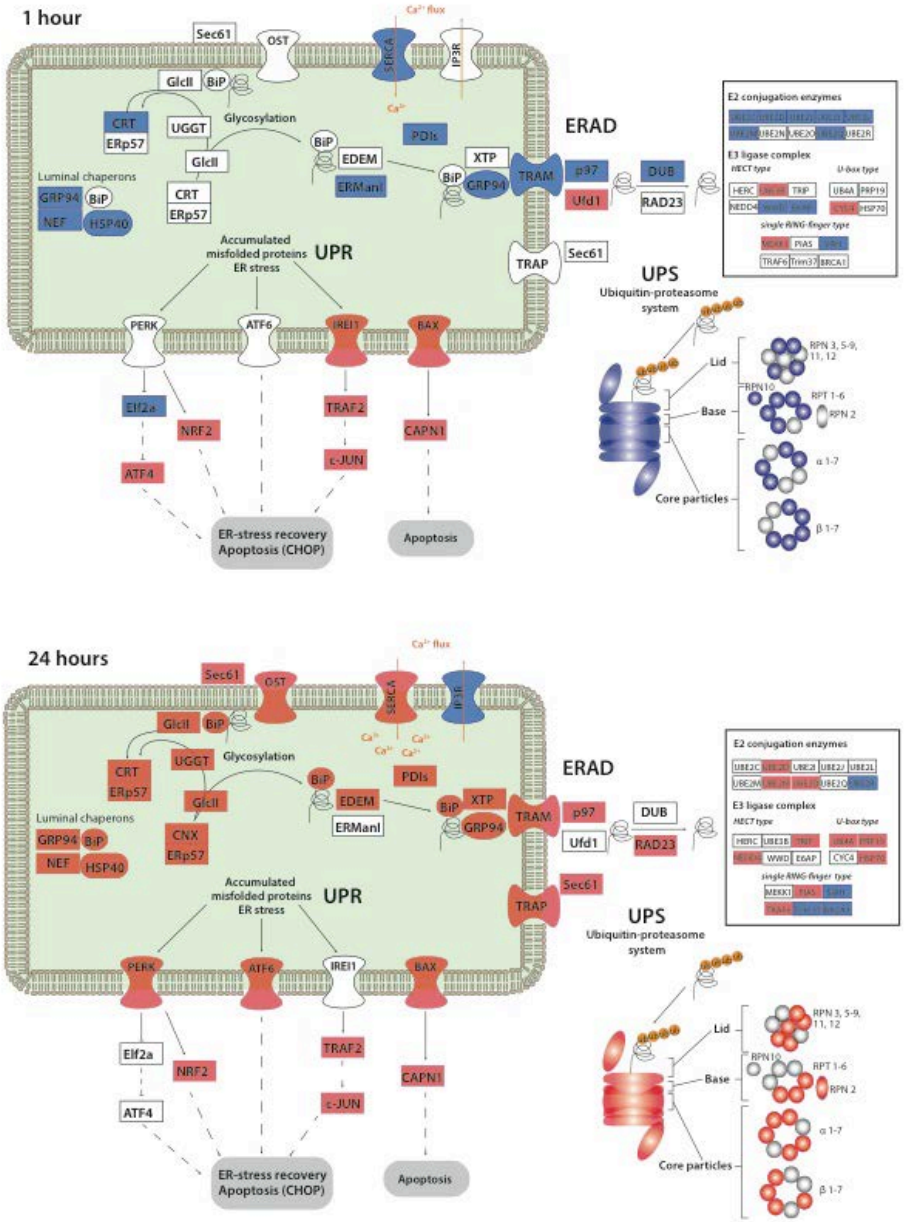

3.3.4. The response of genes involved in oxidative stress and osmoregulation

Hypo-saline stress induces expression of antioxidant defences that are protective against the reactive oxygen species (ROS) generated by different environmental stressors in

corals and other organisms (Lesser 2006). Genes involved in the peroxisomal antioxidant system that showed increased expression after 24 h of hypo-saline stress include: two superoxide dismutases (SOD, by 0.41 and 0.43 log_2FC), two catalases (CAT, by 0.49 and 1.44 log_2FC), and seven glutathione S-transferases (GST, EC:2.5.1.18) (Table S3.3, Supporting information). The glutathione (GSH) redox system, comprising the enzymes glutathione peroxidase (GPx, EC 1.11.1.9) that oxidizes GSH to glutathione disulphide (GSSG), and glutathione reductase (GSR) that reduces GSSG back to glutathione, also plays an important role in protection against oxidative damage. During hypo-saline stress, the coral GSR homologue was up-regulated after 24 h, while the GPx a homologue was down-regulated after 1 and 24 h of stress by -0.37 and -1.08 log_2FC respectively (Figure 3.3; Table S3.4, Supporting information), indicating a balance towards GSH reduction.

Osmotic stress involves changes in the cellular concentrations of many inorganic and organic molecules, and this was corroborated by altered expression of many genes associated with transport of ions or organic molecules, including several solute carrier (SLC) families, ATPases, voltage-gated K^+ channels, and voltage-dependant Ca^{2+} channels (VDCC). After 1 h of salinity stress, three of the nine $Na^+/(Ca^{2+}–K^+)$ exchangers (SLC24) identified were up-regulated, while four Na^+ and Cl^- dependent transporters (SLC6) were down-regulated (Table S3.5, Supporting information). After 24 h of hypo-saline stress, eight SLC6 genes and three SLC24 genes were down-regulated. In the case of ATPases, five genes were down-regulated at the 1 h time point, whereas five were up-regulated after 24 h of stress. Amongst the ATPases, the relative expression of the sarco/endoplasmic reticulum Ca^{2+} ATPase (SERCA; an ER-associated Ca^{2+} influx channel) changed from -1.40 log_2FC at 1 h to 1.63 log_2FC after 24 h. Conversely, expression of inositol 1,4,5-trisphosphate receptors (IP3Rs), which are Ca^{2+} efflux channel components, was down-regulated after 24 h (Figure 3.2, Table S3.2, Supporting information). In addition, three voltage-dependant Ca^{2+} channels were not differentially expressed after 1 h, but down-regulated after 24 h.

3.3.5. Glycine betaine and glutamate catabolism by hypo-saline stress

GO analysis revealed an over-representation of terms associated with AA metabolism, with a strong response of genes implicated in glycine betaine catabolism following osmotic stress (Figure 3.3, Table S3.4 Supporting information). Glycine betaine catabolism starts with the action of betaine-homocysteine *S*-methyltransferase (BHMT), which transfers a methyl group from glycine to homocysteine to produce dimethylglycine (DMG) and methionine. Two betaine-homocysteine *S*-methyltransferase (BHMT) homologues were up-regulated (by 2.5 and 5.43 log2FC) after 24 h of stress. The DMG produced by the BHMT reaction can be converted to glycine by two enzymes (DMGDH and SADH, Figure 3.3), homologues of both of which were up-regulated after 1 and 24 h of hypo-saline stress.

Hypo-saline stress also caused changes in the expression of genes involved in ammonia assimilation. The coral NADH-dependant glutamate dehydrogenase (GDH1), which catalyses the release of ammonia from glutamate, was up-regulated after 1 and 24 h of stress (log_2FC of 0.47 and 2.54 respectively). Conversely, some other genes involved in ammonia assimilation - the NADPH-dependant GDH (GDH2), glutamine synthase (GS), and glutamate synthase (GOGAT) - were down-regulated (Figure 3.3; Table S3.4, Supporting information). This suggests that during hypo-osmotic stress, nitrogen is not stored as glutamine through GS, or as glutamate through GOGAT, but rather converted into ammonia through the action of GDH1. Genes involved in the L-arginine degradation pathway were also up-regulated in hypo osmotic stress, expression of both ornithine transaminase (OAT), and pyrroline-5-carboxylate dehydrogenase (ALDH4A1) increasing (by 0.52 and 1.51 log_2FC respectively) after 24 h (Figure 3.3; Table S3.4, Supporting Information).

Figure 3.3 Expression of *A. millepora* homologues of genes involved in amino acid metabolism during hypo-osmotic stress in adult and juvenile corals. Colours represent up (red) and down-regulated (blue) genes (FDR<0.05) after 1 h (triangle) in the adults (A1) and 24 h (squares) in the adults (A24) and juveniles (J24). Table S3.3.4, Supporting information provides the complete list of genes involved in this pathway and details of expression levels.

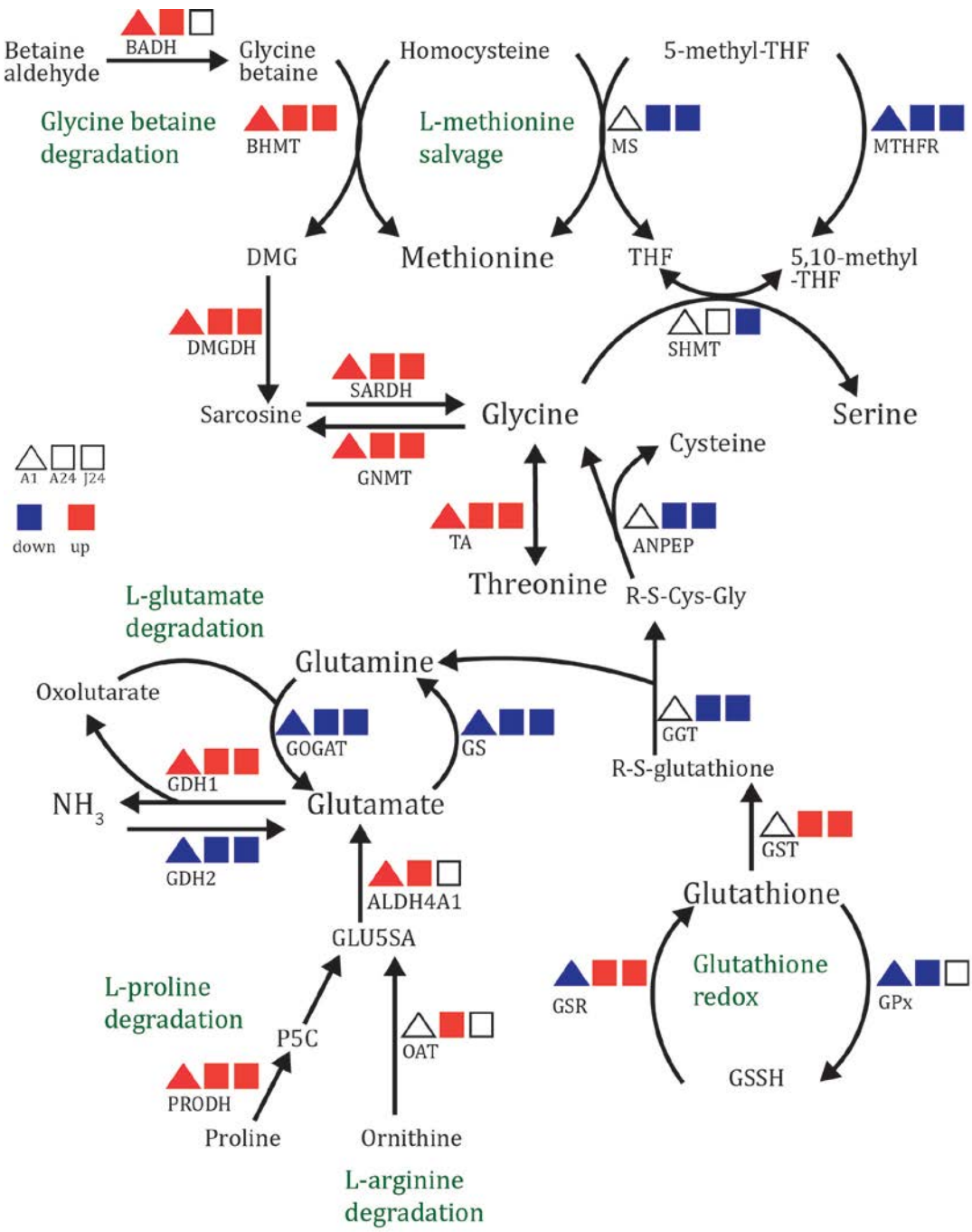

Abbreviations: ANPEP, aminopeptidase; BADH, betaine-aldehyde dehydrogenase; BHMT, betaine-homocysteine methyltransferase; DMGDH, dimethylglycine dehydrogenase; GGT, gamma-glutamyltranspeptidase; GDH1, glutamate dehydrogenase (NADH); GDH2, glutamate dehydrogenase (NADPH); GNMT, glycine N-methyltransferase; GOGAT, glutamate synthase;

GPx, glutathione peroxidase; GS, glutamine synthetase; GSR, glutathione reductase; GST, glutathione S-transferase; MS, methionine synthase; MTHFR, methylenetetrahydrofolate reductase; OAT, ornithine--oxo-acid transaminase; PRODH, proline dehydrogenase; SARDH, sarcosine dehydrogenase; SHMT, serine hydroxymethyltransferase; TA, threonine aldolase.

3.3.6. The responses of coral juveniles to hypo-saline stress

For a substantial number (1,191) of DEGs, the responses of adult and juvenile corals were similar after 24 h of stress (Figure S3.4, Supporting Information). For example, genes encoding proteasome subunits, components of the UPR system and involved in glycine betaine catabolism were up-regulated in both juveniles and adults at the 24 h time point (see above). Conversely, three important ER luminal chaperones (BiP, GRP94 and NEF) showed opposite expression trends in the two life stages, these being up-regulated in adults but down-regulated in juveniles (Table S3.2, Supplementary Information).

Of the four treatments studied, the prolonged (48 h) exposure of juveniles resulted in the lowest number (1,485, FDR<0.05) of differentially expressed genes. At the 48 h time point, expression levels of many of the genes that were differentially expressed at 24 h in juveniles had returned to control levels, suggesting that a degree of acclimation may have occurred. For example, at 48 h only two ubiquitin-proteasome system (UPS) subunits were differentially expressed, whereas the corresponding number at 24 h was ten (Table S3.2, Supporting information). A similar decrease was seen in the case of, E2 ubiquitin-conjugation enzymes - from 13 to three up-regulated members after 24 and 48 h respectively (Table S3.2, Supporting information). Whilst these results suggest the possibility of acclimation to hypo-saline stress after 48 h, experiments with longer exposure times are needed to understand if this response is maintained.

3.4. Discussion

Gene expression data revealed a strong response of the coral *A. millepora* to hypo-saline stress exposure, with clear differences between acute salinity shock (1 h) and more prolonged (24 h) exposure in adult corals. Here we describe a group of genes that are part of a general response to stress in corals, and a second group that are known to response to osmotic stress in other organisms but were not previously described in corals. The first group includes antioxidant genes, and genes involved in protein homeostasis, comprising molecular chaperones, and components of the ER associated protein degradation (ERAD) and unfolded protein response (UPR) systems. The second group comprises genes involved in osmoregulation, including molecular transporters and enzymes of amino acid (AA) metabolism, particularly glycine betaine catabolism. Together, changes in the expression of these two groups of genes provide insights into the molecular basis of hypo-osmotic stress in corals and the changes involved in adjusting to this stress over time.

3.4.1. The common response to stress in corals

Despite a lack of uniformity in experimental design and species used, comparisons between the responses of corals to different stressors are providing insights into the classes of genes, and sometimes the specific members of those classes, that are involved in adapting to different environmental stressors. For example, some components of the coral antioxidant repertoire (catalases, superoxide dismutases) respond not only to hypo-saline stress, but also to thermal and to elevated CO_2 stress, (Barshis *et al.* 2013; Downs *et al.* 2009; Moya *et al.* 2015) (Table 3.1). In contrast, thioredoxin and thioredoxin-reductase homologues, which are also part of the antioxidant repertoire, were differentially expressed in corals only under hypo-saline stress, as they also were in mussels (Table 3.1) (Lockwood *et al.* 2010).

A second group of genes involved in general stress responses are the HSP family. For some time, HSPs have been investigated in the context of responses of corals to thermal

stress (Leggat *et al.* 2011; Rodriguez Lanetty *et al.* 2009; Seveso *et al.* 2014), but the HSP repertoire has only recently been properly described in *A. millepora*, allowing comprehensive analyses of the response of this complex gene family to stress (Moya *et al.* 2015). Whereas multiple HSP90 and HSP70 variants are present in corals, and respond to a range of stressors (Barshis *et al.* 2013; Chow *et al.* 2009; Downs *et al.* 2009; Leggat *et al.* 2011), specific variants appear to respond to most or all types of stress. For example, Moya *et al*. (2015) identified a specific *A. millepora* HSP70 that also responded to high CO_2 and whose *A. hyacinthus* orthologue was involved in thermal tolerance (Barshis *et al.* 2013). Consistent with a role in he general stress response, this same HSP70 responded to hypo-saline conditions in the present study (1.2.19257.m1, 5.8 $\log_2$FC at 24 h, Table 3.1).

Of the HSPs associated with ER processes, the luminal chaperones glucose regulated protein 94 (GRP94; Figure 3.2, Table S3.2, Supporting information, 1.2.15211.m1), is of particular interest, as in other systems this calcium-binding protein plays a key role in facilitating recovery from ER stress by blocking apoptosis (Eletto *et al.* 2010). GRP94 expression was elevated after 24 h of salinity stress, and also responded to acute CO_2, (Moya *et al.* 2015) and thermal stress in corals (Rodriguez Lanetty *et al.* 2009); note that the mussel (*M. galloprovinciales)* orthologue also responded to hypo-saline stress (Tomanek *et al.* 2012) (Table 3.1). In the present study, the ER-lumenal HSP70 BiP, which is involved in protein folding and is a component of the ERAD system (Araki & Nagata 2011) was up-regulated under hypo-saline conditions, and is also induced by challenge with bacteria (Brown *et al.* 2013) or lipopolysaccharide (LPS; Chapter 2). However, BiP was not differentially expressed under high CO_2 stress (Moya *et al.* 2015), suggesting that it has a broad, but not universal, role in the coral stress response (Table 3.1). Although several studies have described the response of coral HSPs to stressors, differential expression of BiP co-chaperones under stress has only been documented in one previous study (Maor-Landaw *et al.* 2014). BiP has a range of functions, which are largely determined by its interaction of with different DnaJ/Hsp40 co-

chaperones, that modify its activity (Araki & Nagata 2011). In the present study, the BiP co-chaperones ERdj1, ERdj3 and ERdj6 were all up-regulated in adult corals after 24 h under hypo-saline conditions (Table 3.1, Table S3.2, Supporting information). ERdj3 and ERdj6 are involved in the ERAD system, which also responds to thermal stress in the coral *S. pistillata*, and to hypo-saline stress in the mussel *M. galloprovinciales* (Downs *et al.* 2009; Maor-Landaw *et al.* 2014; Tomanek & Zuzow 2010; Tomanek *et al.* 2012).

Whereas down-regulation of components of the ERAD system was observed after the acute salinity treatment (1 h), components of the unfolded protein response (UPR) system were up-regulated at both the 1 and 24 h time points, suggesting that misfolded proteins accumulated as early as 1 h after the onset of osmotic stress. The activation of the UPR system can have two opposite outcomes: it can promote survival and resistance to ER stress and/or it can activate a cell death response (Darling & Cook 2014). For example, in mammals the endoribonuclease inositol-requiring enzyme–1 (IRE1) signalling protein can interact with the pro-apoptotic protein BAX, or it can activate c-JUN to promote cell survival (Darling & Cook 2014). Like its mammalian orthologue, coral BAX promotes cell death (Moya *et al.* 2016), but the extent of up-regulation of BAX under hypo-osmotic stress was small compared to that of the pro-survival protein, c-JUN, suggesting that the latter outcome might predominate during hypo-saline stress. Previous studies by Maor-Landaw *et al*. (2014) in *S. pistillata* found that PERK increased during temperature stress, and expression of c-JUN and MAPK7 homologues increased under hypo-saline stress in the mussel (Lockwood & Somero 2011). However, the present study is the first to document differential expression of the three main transmembrane proteins that regulate the UPR (BAX, IREI1, and PERK), and components of the corresponding downstream signalling pathways (Figure 3.2; Table S3.2 Supporting information).

Table 3.1. Comparison between data presented here on the transcriptomic response of the coral *A millipora* to hypo-saline conditions and published gene expression and proteomic studies in marine invertebrates.

Table 1. Comparison between genes that are differentially express (FDR< 0.05) in *A. millepora adults* under hypo-saline conditions and other published gene expression or proteomics data

Osmotic stress signalling

2999

3.4.2. The specific response to hypo-saline stress in coral —osmoregulation and transporters

As adjustments to hypo-saline conditions require cell volume regulation, transport of ions through membranes plays an important role in adjusting this osmotic potential, and is mediated by H^+ translocating ATPases, Ca^{2+}-ATPases, secondary active transporters, and

channels (Hasegawa *et al.* 2000). While ion transport proteins have been extensively characterized in higher animals, fungi and plants (Jan & Jan 1997; Wang & Wu 2013), little is known about these genes families in cnidarians (but see Zoccola *et al.* (2015) and (2004)). When the results of the present study were compared with those of mussels under hypo-saline stress, the expression of several specific transporters (MCT, Nacra5, and ATP1A1) showed similar trends, whereas for others (SLC6A5, SLC17A5, and KCNA, Table 3.1) the opposite response was observed. However, some of these apparent differences may be a consequence of the difficulty in identifying true orthologues across the deep evolutionary divide between molluscs and cnidarians (Table 3.1 and Table S3.5, Supporting information). In general, and as mentioned by Lockwoodand Somero (2011), the responses of these transporters reflect two opposite adaptive mechanisms to stress: first, moving ions across the membrane to stop cell swelling, and second, arresting the transport activities when solute concentrations inside the cell exceed requirements (Hochachka & Somero 2002; Pierce 1982). Some of the results presented here might be explained in terms of the operation of some opposing activities, but also highlight the complexity of the genes families involved.

Marine invertebrates adjust their osmotic concentration not only by inorganic ion fluxes, but also via organic osmolytes such as taurine or betaines. Glycine betaine is thought to be an important osmolyte in corals, constituting >90% of the organic solutes measured in *Fungia, Pocillopora, Montipora* and *Tubastrea* (Yancey *et al.* 2010). Increased transcription of genes involved in glycine betaine catabolism was observed in the present study, implying that degradation of glycine betaine occurred during hypo-osmotic stress (Figure 3.3, Table S3.4 Supporting information). Previous experiments on the effects of hypo-saline stress in the Pacific oyster *Crassostrea gigas* also found an increase in transcription of betaine-homocysteine S-methyltransferase (BHMT), a key enzyme of glycine betaine catabolism (Zhang *et al.* 2015). Glycine betaine concentrations have been shown to decrease under hypo-saline stress in the marine alga *Platymonas subcordiformis* (Dickson & Kirst 1986), consistent

with this compound acting as an osmoticum. In a range of marine invertebrates that includes the sea anemone *Metridium senile* and the bivalve *Noetia ponderosa* (Deaton & Hoffman 1988; Pierce & Warren 2001), free amino acid (FAA) levels also decrease in response to hypo-osmotic stress. However, the limited body of work on FAA metabolism in corals is not consistent with this paradigm; the FAA pool in the coral *A. aspera* increased during hypo-saline stress (Cowlin 2012). The data presented here suggest that AA catabolism increased under hypo-saline stress, leading to increased ammonia production (GDH up-regulated, Figure 3.3), but measurements of AA levels are needed to better understand osmolyte responses under hypo-saline stress.

3.4.3. The response of adult coral vs. juveniles to hypo-saline stress

Whereas previous work on salinity stress has focused on adult corals, this is the first investigation to focus on both adult and juvenile corals; since these latter are aposymbiotic, the potential complication of the symbiotic dinoflagellate is removed. After 24 h of osmotic stress many aspects of the response were common between the adults and juveniles - for example, genes involved in adjusting cell volume (e.g., transporters, betaine catabolism). By contrast, the antioxidant system that was up-regulated in adults and largely unaffected by hypo-osmotic stress in juveniles (Table S3.5, Supporting information). This result could be explained by the need for symbiotic hosts to protect themselves against ROS produced by the symbiont leaking into the animal host (Tchernov *et al.* 2004).

In the present experiment, the expression of glutamate dehydrogenase (GDH1) was higher in adults compared to juveniles (2.54 compared to 0.24 $\log_2$FC), implying a higher rate of AA catabolism in the former. This could be explained by the complex nitrogen fluxes in the coral-dinoflagellate symbiosis, which is known to involve exchange of both ammonia and FAA between the two organisms (Davy *et al.* 2012). Consistent with this, under hypo-osmotic

stress, a greater number of genes involved in proteolysis (e.g. proteasome subunits) were expressed in adult corals than in juveniles.

As noted above, in the case of juveniles, by the later time point (48 h), significantly fewer genes were differentially expressed than after 24 h of exposure to hypo-saline conditions. In particular, the return after 48 h to baseline levels of many of the genes implicated in proteolysis and osmoregulation suggests that a degree of acclimation had occurred. A precedent for this is provided by the work of Moya *et al*. (2015) on the response of *A. millepora* juveniles to elevated CO_2, where acute (3 d) exposure to elevated CO_2 caused changes in the expression of many genes, after 9 d exposure, expression of most of those same genes had returned to baseline levels. It will be important to determine how corals respond to more prolonged exposure to hypo-saline conditions than those used here, and the physiological impacts of such treatments. Our results imply that juvenile corals may be able to cope with decreases in salinity during prolonged exposure to heavy rainfall, but experiments involving prolonged exposure, combined with physiological data, will be necessary to enable a better understanding of the response to hypo-saline stress.

3.5. Conclusions

Increases in the frequency and severity of heavy rainfall events are predicted for the next century, leading to corresponding increases in the exposure of adult and juvenile corals to hypo-saline conditions. The data presented here represent a starting point for understanding the molecular response of corals to hypo-saline conditions and highlight specific pathways as components of that response. As hypothesized, increases were observed in the expression of genes involved in proteolysis and oxidative stress, which are common responses to environmental stress. By contrast, the increased expression of a group of transporters appears to be a specific response to osmotic stress. To better understand the coral response, proteomics should be a focus of future work, and it is important that transcriptomic data are at some stage supplemented by physiological information.

3.6. Supporting information
Tables

Table S3.1. Differentially expressed genes and their GO as in the heat map Figure 3.1.

Genome ID	Protein ID	Adults		Juveniles		GO number	GO definition
		1 h log_2FC	24 h log_2FC	24 h log_2FC	48 h log_2FC		
1.2.21241.m1	Oligosaccharyltransferase	-0.22	0.64	0.31	0.06	5783	ER
1.2.3165.m1	Translocon	-0.20	0.54	0.16	0.01	5783	ER
1.2.3250.m1	Ribosome-binding protein	-0.16	0.48	0.08	0.25	5783	ER
1.2.14249.m1	Synaptobrevin	0.13	0.81	0.19	-0.04	5783	ER
1.2.3114.m1	EDEM1	0.03	0.74	0.21	-0.06	5783	ER
1.2.21359.m1	ER lectin 1	0.02	0.70	-0.04	-0.03	5783	ER
1.2.13517.m1	bax-mediated apoptosis inhibitor	0.06	0.70	-0.11	-0.05	5783	ER
1.2.13846.m1	Alpha 1,3-glucosidase	-0.17	0.66	0.06	0.20	5783	ER
1.2.20980.m1	Translocon-associated	-0.18	0.56	0.00	0.10	5783	ER
1.2.12601.m1	ER-Golgi intermediate compartment1	-0.24	0.89	-0.01	0.08	5783	ER
1.2.12868.m1	Sec13	-0.31	0.89	0.13	-0.15	5783	ER
1.2.6181.m1	Sec31b	-0.27	0.62	0.25	0.25	5783	ER
1.2.21656.m1	ERdj6	-0.53	0.58	0.01	0.08	5783	ER
1.2.8202.m1	Calcium-transporting ATPase sarcoplasmic ER	-0.49	0.71	0.14	0.48	5783	ER
1.2.1122.m1	Cathepsin X	-0.53	0.68	0.01	-0.06	5783	ER
1.2.517.m1	Rhomboid-related	-0.63	0.76	-0.11	-0.16	5783	ER
1.2.4275.m1	Surfeit locus protein 4 homolog	-0.01	0.56	0.05	-0.09	5783	ER
1.2.11284.m1	Sec61	-0.17	0.42	-0.06	-0.02	5783	ER
1.2.16315.m1	Calnexin	-0.16	0.53	-0.19	-0.04	5783	ER
1.2.11239.m1	Dolichyl diphosphooligosaccharide	-0.18	0.40	-0.19	-0.11	5783	ER
1.2.5524.m1	SARAF	0.14	0.92	-0.22	-0.18	5783	ER
1.2.10115.m1	SIL1 Nucleotide Exchange Factor	0.15	0.85	-0.34	-0.18	5783	ER
1.2.23785.m1	Sulfatase 2	-0.14	0.73	0.60	0.62	5783	ER
1.2.2683.m1	Calreticulin precursor	-0.46	1.14	-0.04	0.14	5783	ER
1.2.2424.m1	Hypoxia up-regulated protein 1	-0.64	0.90	-0.23	0.14	5783	ER
1.2.2535.m1	SAC1	-0.45	0.09	0.05	0.12	5783	ER
1.2.6185.m1	Coatomer subunit beta	-0.32	0.49	0.03	0.02	5783	ER
1.2.9574.m1	EIF5A	-0.26	0.38	0.07	-0.09	5783	ER
1.2.5585.m1	Sec23	-0.34	0.37	0.03	0.12	5783	ER
1.2.22852.m1	Ras-related protein Rab-1A	-0.32	0.22	0.02	0.01	5783	ER
1.2.9475.m1	Transmembrane emp24	-0.58	0.15	-0.09	-0.10	5783	ER
1.2.13624.m1	ER lumen protein retaining	-0.55	0.27	-0.12	-0.22	5783	ER
1.2.1974.m1	Calumenin	-0.25	0.48	0.01	0.08	5788	ER lumen
1.2.8532.m1	PPIB1	-0.29	0.64	0.03	0.00	5788	ER lumen
1.2.25530.m1	ERdj3	-0.30	1.04	0.44	0.29	5788	ER lumen
1.2.18585.m1	UGGT	-0.11	0.59	0.20	0.34	5788	ER lumen
1.2.1831.m1	Calumenin	-0.38	1.06	-0.15	-0.03	5788	ER lumen
1.2.4351.m1	BiP	-0.12	1.30	-0.20	0.11	5788	ER lumen
1.2.9956.m1	Alpha7	-0.43	0.20	-0.02	-0.16	502	proteasome complex
1.2.2830.m1	Alpha6	-0.12	0.56	0.08	-0.01	502	proteasome complex
1.2.7785.m1	Alpha3	-0.35	0.67	0.12	0.05	502	proteasome complex
1.2.9821.m1	Alpha5	-0.28	0.73	0.14	-0.03	6807	nitrogen metabolic
1.2.17385.m1	Alpha1	-0.28	1.06	0.32	0.17	6807	nitrogen metabolic
1.2.16235.m1	Rpn8	-0.25	0.91	0.28	0.24	10498	proteasomal catabolic
1.2.3354.m1	Rpn7	-0.54	0.45	0.11	0.03	502	proteasome complex
1.2.7613.m1	Rpn5	-0.57	0.20	-0.04	-0.15	502	proteasome complex
1.2.11418.m1	Rpn3	-0.46	0.30	-0.05	-0.15	502	proteasome complex
1.2.2366.m1	Rpn2	-0.19	0.68	0.01	0.02	6807	nitrogen metabolic
1.2.461.m1	Rpt4	-0.36	0.48	0.12	-0.01	5524	proteasome complex
1.2.2519.m1	Beta5	-0.50	0.48	0.09	-0.20	502	proteasome complex
1.2.1010.m1	Rpn10	-0.38	0.17	-0.05	-0.10	502	proteasome complex
1.2.14902.m1	E3 ubiquitin-protein ligase RNF146	-0.67	0.25	0.08	-0.25	44265	proteolysis
1.2.3007.m1	Ubiquitin-conjugating enzyme E2 L3	-0.32	0.10	0.22	0.05	44265	Cell macro catabolism
1.2.10753.m1	TCEB1	-0.41	0.02	0.18	0.04	44265	Cell macro catabolism
1.2.1434.m1	Ubiquitin-protein ligase E3A	-0.44	0.04	0.08	0.03	44265	Cell macro catabolism
1.2.2837.m1	Adenosine deaminase-like	-0.01	1.15	0.03	0.15	44282	small molecule catabo

1.2.8981.m1	Medium-chain specific acyl-CoA	-0.06	0.70	0.16	0.11	16491	oxidoreductase activity
1.2.5411.m1	Malate dehydrogenase	-0.06	0.45	0.16	0.01	16491	oxidoreductase activity
1.2.4737.m1	Dihydroorotate dehydrogenase	0.12	0.76	0.13	-0.01	16491	oxidoreductase activity
1.2.16944.m1	Glyceraldehyde 3-phosphate dehydrogenase	-0.24	0.66	0.17	0.01	16491	oxidoreductase activity
1.2.5704.m1	Protein disulfide isomerae	-0.16	0.77	-0.22	0.04	16491	oxidoreductase activity
1.2.2152.m1	ALDH3A2	-0.55	0.48	0.15	0.19	16491	oxidoreductase activity
1.2.1905.m1	6-phosphogluconate dehydrogenase	-0.27	0.57	-0.04	-0.07	16491	oxidoreductase activity
1.2.16373.m1	Glutamate dehydrogenase	0.07	0.95	0.01	-0.07	16491	oxidoreductase activity
1.2.10096.m1	Dehydrogenase/reductase SDR	-0.12	1.00	0.02	-0.14	16491	oxidoreductase activity
1.2.9018.m1	Protein disulfide isomerae	-0.36	0.87	-0.26	-0.05	16491	oxidoreductase activity
1.2.1667.m1	ERp57	-0.23	0.98	-0.40	-0.18	16491	oxidoreductase activity
1.2.9677.m1	Glutathione s-transferase	-0.19	0.85	0.49	0.14	16491	oxidoreductase activity
1.2.23763.m1	Cytochrome P450 reductase	-0.15	0.72	0.43	0.27	16491	oxidoreductase activity
1.2.3068.m1	Thioredoxin reductase 3	-0.23	0.43	0.52	0.37	16491	oxidoreductase activity
1.2.24842.m1	Succinate dehydrogenase	-0.40	0.72	0.72	0.36	16491	oxidoreductase activity
1.2.18297.m1	Alcohol dehydrogenase class-3	0.15	1.71	0.23	-0.10	16491	oxidoreductase activity
1.2.4919.m1	DBH-like monooxygenase 1	-0.22	1.96	-0.06	-0.16	16491	oxidoreductase activity
1.2.6992.m1	Catalase	-0.70	1.44	-0.49	-0.29	16491	oxidoreductase activity
1.2.4848.m1	Ceruloplasmin	0.35	1.05	-0.21	-0.46	16491	oxidoreductase activity
1.2.34.m1	Homogentisate dioxygenase	0.40	0.89	-0.09	-0.53	16491	oxidoreductase activity
1.2.20338.m1	Methylmalonate-semialdehyde dehydrogenase	0.40	0.88	-0.52	-0.41	5524	oxidoreductase activity
1.2.1180.m1	Phenylalanine hydroxlase	0.67	1.58	-0.35	-0.35	16491	oxidoreductase activity
1.2.21750.m1	Cytochrome heme	-0.41	0.46	0.25	0.16	55114	redox
1.2.10098.m1	GDP-L-fucose synthase	-0.32	0.40	0.17	0.13	55114	redox
1.2.725.m1	Cytochrome P450	-1.51	0.14	0.01	0.20	55114	redox
1.2.18589.m1	Glutathione peroxidase	-0.37	0.09	0.19	-0.06	55114	redox
1.2.21616.m1	NADH dehydrogenase	-0.42	0.03	0.16	0.13	55114	redox
1.2.22719.m1	Cytochrome b-c1 complex	-0.39	0.26	0.13	0.01	55114	redox
1.2.5445.m1	Glycogen phosphorylase	-0.24	0.71	0.15	0.13	6066	alcohol metabolic process
1.2.1093.m1	Transaldolase-like	-0.15	1.00	0.28	0.07	6066	alcohol metabolic process
1.2.877.m1	NUDT1	0.55	1.06	-0.71	-0.58	6066	alcohol metabolic process
1.2.12136.m1	Asparagine synthetase	-0.18	0.75	-0.14	0.02	6519	cellular AA derivative metabolic
1.2.7670.m1	Asparagine--tRNA cytoplasmic	-0.37	0.55	0.23	0.29	6519	cellular AA derivative metabolic
1.2.1587.m1	Aspartyl-tRNA synthetase	-0.06	0.48	-0.09	-0.12	6519	cellular AA derivative metabolic
1.2.25616.m1	Ornithine aminotransferase	-0.17	0.52	-0.10	0.09	6519	cellular AA derivative metabolic
1.2.1862.m1	BCAT	0.01	0.97	-0.10	-0.38	6519	cellular AA derivative metabolic
1.2.3574.m1	Threonine--tRNA cytoplasmic	-0.28	0.54	0.11	-0.02	6519	cellular AA derivative metabolic
1.2.5281.m1	Mago-nashi homolog	-0.09	0.69	0.30	0.12	6807	nitrogen metabolic
1.2.8113.m1	Nuclease-sensitive element-binding	-0.02	0.60	0.30	0.08	6807	nitrogen metabolic
1.2.14950.m1	Small nuclear ribonucleoprotein-associated	-0.16	0.68	0.21	0.17	6807	nitrogen metabolic
1.2.10806.m1	60S ribosomal protein L23	-0.10	0.46	0.24	-0.06	6807	nitrogen metabolic
1.2.11195.m1	Cyclin k	0.00	0.78	0.22	-0.03	6807	nitrogen metabolic
1.2.4175.m1	Cyclin-L2	-0.10	0.78	0.12	0.22	6807	nitrogen metabolic
1.2.21220.m1	Periodic tryptophan	-0.08	0.59	-0.07	-0.08	6807	nitrogen metabolic
1.2.988.m1	Nucleolar protein 14	0.06	0.54	-0.05	0.05	6807	nitrogen metabolic
1.2.17803.m1	Proteasome activator complex	-0.22	0.47	-0.10	0.07	6807	nitrogen metabolic
1.2.10902.m1	Transcription factor BTF3	-0.16	0.88	0.33	0.13	6807	nitrogen metabolic
1.2.12052.m1	Transcription factor 7-like	-0.22	1.10	0.45	0.08	6807	nitrogen metabolic
1.2.2133.m1	Cytochrome c	-0.58	1.17	0.38	0.51	6807	nitrogen metabolic
1.2.15517.m1	Prolyl endopeptidase	-0.68	0.47	0.31	0.28	8236	Serine peptidase
1.2.8959.m1	Casein kinase II	-0.57	0.03	0.16	0.13	8236	Serine peptidase
1.2.2531.m1	Lon proteas homolog	0.09	0.62	0.09	0.02	16921	ATPase activity
1.2.12141.m1	ATP-binding cassette sub-family B	-0.23	0.79	0.51	0.51	16903	ATPase activity

Table S3.2 *A. millepora* homologues to the ER protein processing system. (A) Results of the KEGG protein processing in the ER (nve04141) pathway searched in the *A. millepora* protein predictions. (B) Log_2FC values of significantly expressed (FDR <0.05) genes in response to the treatment (hypo-saline) over the control (35 PSU). Log_2FC colour indicate up (red) and down (blue) regulated genes.

(A)

Function	Gene name	Orthology	Blast Info				
			Coral ID	Entry	% ID	Length	e-value
Glycosylation	Sec61	protein transport SEC61 subunit beta	1.22267.m1	NEMVE_v1g158265	71.43	98	6.00E-41
	GlcII	alpha 1,3-glucosidase [EC:3.2.1.84]	1.213846.m1	NEMVE_v1g238696	60.35	744	0
	OSTc	dolichyl-diphosphooligosaccharide--protein glycosyltransferase [EC:2.4.99.18]	1.211239.m1	NEMVE_v1g180767	69.93	705	0
	OSTc	dolichyl-diphosphooligosaccharide--protein glycosyltransferase [EC:2.4.99.18]	1.212013.m1	NEMVE_v1g180767	57.08	727	0
	CNX	calnexin	1.216315.m1	NEMVE_v1g80092	78.19	431	0
	CRT	calreticulin	1.22683.m1	NEMVE_v1g61368	76.08	347	0
	UGGT	UDP-glucose:glycoprotein glucosyltransferase	1.218585.m1	NEMVE_v1g135950	51.97	660	0
Luminal chaperones	GRP94	heat shock protein 90kDa beta	1.215211.m1	NEMVE_v1g181671	85.06	261	2.00E-158
	MEF	hypoxia up-regulated 1	1.22424.m1	NEMVE_v1g172038	69.3	570	0
	BiP, GRP70	heat shock 70kDa protein 5	1.24351.m1	NEMVE_v1g216823	87.57	531	0
BiP cochaperons-HSP40, DnaJ-Like	ERdj1	DnaJ homolog subfamily C member 1	1.27940.m1	gi|21361912	41.77	541	2.00E-111
	ERdj3, DnaJB11	DnaJ homolog subfamily B member 11	1.225530.m1	gi|18203497	60.34	358	2.00E-150
	ERdj4	DnaJ homolog subfamily B member 9	1.220851.m1	gi|18203496	55.65	115	4.00E-32
	ERdj5	DnaJ homolog subfamily C member 10	1.222277.m1	NEMVE_v1g163820	61.75	779	0
	ERdj6, DnaJC3	DnaJ homolog subfamily C member 3	1.221656.m1	gi|73620807	53.81	472	7.00E-175
	SEC63	translocation protein SEC63 homolog isoform X1	1.2.143.m1	gi|767941799	46.7	349	2.00E-95
ERAD related proteins							
Processing and targeting	EDEM	ER degradation enhancer, mannosidase alpha-like 1	1.23114.m1	NEMVE_v1g199864	63.76	516	0
	XTP3B	endoplasmic reticulum lectin 1	1.221359.m1	NEMVE_v1g99617	29.73	111	1.00E-05
	ER-Man1	mannosyl-oligosaccharide alpha-1,2-mannosidase	1.24008.m1	NEMVE_v1g112545	72.44	479	0
	TRAP	translocon-associated protein subunit delta	1.23165.m1	NEMVE_v1g237405	61.03	136	7.00E-58
	TRAM	translocating chain-associated membrane protein 1	1.211248.m1	NEMVE_v1g186830	60.89	327	2.00E-131
	DERLIN	Derlin-2/3	1.2.918.m1	NEMVE_v1g179634	82.74	168	2.00E-93
Ligase complex							
E1 activating enzyme	UBE1	ubiquitin-activating enzyme E1 [EC:6.3.2.19]	1.214992.m1	nve:NEMVE_v1g:129964	74.47	1038	0
E2 conjugating enzyme	UBE2C	ubiquitin-conjugating enzyme E2 C [EC:6.3.2.19]	1.225429.m1	nve:NEMVE_v1g:237281	57.75	142	3.00E-44
	UBE2D/E	ubiquitin-conjugating enzyme E2 D/E [EC:6.3.2.19]	1.221247.m1	nve:NEMVE_v1g:236730	92.52	147	3.00E-100
	UBE2D/E	ubiquitin-conjugating enzyme E2 D/E [EC:6.3.2.19]	1.221685.m1	NEMVE_v1g127871	78.7	169	2.00E-98
	UBE2D/E	ubiquitin-conjugating enzyme E2 D/E [EC:6.3.2.19]	1.221689.m1	NEMVE_v1g127871	73.22	183	2.00E-94
	UBE2D/E	ubiquitin-conjugating enzyme E2 D/E [EC:6.3.2.19]	1.221680.m1	NEMVE_v1g127871	64.71	136	4.00E-51
	UBE1G1	ubiquitin-conjugating enzyme E2 G1 [EC:6.3.2.19]	1.2.802.m1	nve:NEMVE_v1g:167818	70.66	167	9.00E-90
	UBE2G2	ubiquitin-conjugating enzyme E2 G2 [EC:6.3.2.19]	1.222895.m1	nve:NEMVE_v1g:178088	90.3	165	4.00E-111
	UBE2I	ubiquitin-conjugating enzyme E2 I [EC:6.3.2.19]	1.26436.m1	nve:NEMVE_v1g:159579	75.95	158	7.00E-85
	UBE2J1	ubiquitin-conjugating enzyme E2 J1 [EC:6.3.2.19]	1.2.138.m1	nve:NEMVE_v1g:112619	86.72	128	5.00E-82
	UBE2L3	ubiquitin-conjugating enzyme E2 L3 [EC:6.3.2.19]	1.23007.m1	nve:NEMVE_v1g:235862	71.11	180	7.00E-87
	UBE2M	ubiquitin-conjugating enzyme E2 M [EC:6.3.2.19]	1.21863.m1	nve:NEMVE_v1g:171977	88.81	134	2.00E-86
	UBE2N	ubiquitin-conjugating enzyme E2 N [EC:6.3.2.19]	1.223020.m1	nve:NEMVE_v1g:236976	84.77	151	3.00E-92
	UBE2O	ubiquitin-conjugating enzyme E2 O [EC:6.3.2.19]	1.27586.m1	nve:NEMVE_v1g:198482	47.94	1114	0
	UBE2Q	ubiquitin-conjugating enzyme E2 Q [EC:6.3.2.19]	1.214941.m1	nve:NEMVE_v1g:230272	84.91	159	2.00E-98
	UBE2R	ubiquitin-conjugating enzyme E2 R [EC:6.3.2.19]	1.23573.m1	nve:NEMVE_v1g:194815	85.65	237	5.00E-138
HECT type E3	HERC1	E3 ubiquitin-protein ligase HERC1 [EC:6.3.2.19]	1.217650.m1	nve:NEMVE_v1g:240406	61.67	1320	0
	TRIP12	E3 ubiquitin-protein ligase TRIP12 [EC:6.3.2.19]	1.23515.m1	nve:NEMVE_v1g:191358	55.41	1617	0
	NEDD4	E3 ubiquitin-protein ligase NEDD4 [EC:6.3.2.19]	1.24310.m1	nve:NEMVE_v1g:161803	82.99	488	0
	UBE3B	ubiquitin-protein ligase E3 B [EC:6.3.2.19]	1.26288.m1	nve:NEMVE_v1g:160280	62.86	972	0
	WWP1	atrophin-1 interacting protein 5 [EC:6.3.2.19]	1.213267.m1	nve:NEMVE_v1g:158690	73.67	676	0
	E6AP	ubiquitin-protein ligase E3 A [EC:6.3.2.19]	1.21434.m1	nve:NEMVE_v1g:243312	66.33	796	0
U-box type E3	UBE4A	ubiquitin conjugation factor E4 A [EC:6.3.2.19]	1.214462.m1	nve:NEMVE_v1g:240861	50.14	718	0
	PRP19	pre-mRNA-processing factor 19 [EC:6.3.2.19]	1.2.883.m1	nve:NEMVE_v1g:199033	80.86	512	0
	CYC4	peptidyl-prolyl cis-trans isomerase like 2 [EC:5.2.1.8]	1.214889.m1	nve:NEMVE_v1g:248427	70.92	533	0
	Hsp70	heat shock 70kDa protein 1/8	1.28575.m1	NEMVE_v1g189485	80.83	652	0
single RING-finger type E3	MEKK1	mitogen-activated protein kinase kinase kinase 1	1.25530.m1	nve:NEMVE_v1g:120549	61.59	867	0
	TRAF6	TNF receptor-associated factor6	1.22897.m1	nve:NEMVE_v1g:178259	51.09	458	2.00E-158
	PIAS	E3 SUMO-protein ligase PIAS2 [EC:6.3.2.-]	1.211953.m1	nve:NEMVE_v1g:134544	69.87	385	0
	SIAH-1	E3 ubiquitin-protein ligase SIAH1 [EC:6.3.2.19]	1.220985.m1	nve:NEMVE_v1g93606	31.78	129	3.00E-10
	Trim37	tripartite motif-containing protein 37 [EC:6.3.2.19]	1.22625.m1	nve:NEMVE_v1g95966	90.64	267	2.00E-173
	BRCA1	breast cancer type 1 susceptibility protein	1.24545.m1	nve:NEMVE_v1g238046	41.41	227	4.00E-38
	SYVN, Hrd1	E3 ubiquitin-protein ligase synoviolin [EC:6.3.2.19]	1.210197.m1	nve:NEMVE_v1g32018	88.34	326	0
RING-finger type E3	RBX1	RING-box protein 1	1.215842.m1	nve:NEMVE_v1g:169697	90.18	112	2.00E-72
	RBX2	RING-box protein 2	1.2.598.m1	nve:NEMVE_v1g:181003	87.88	99	4.00E-61
	Cul3	cullin 3	1.2.480.m1	nve:NEMVE_v1g:191273	86.17	694	0
	Cul4	cullin 4	1.23461.m1	nve:NEMVE_v1g:171734	82.59	580	0
	DDB1	DNA damage-binding protein 1	1.213230.m1	nve:NEMVE_v1g:241997	75.81	1174	0
	F-box	F-box and WD-40 domain protein 7	1.220605.m1	nve:NEMVE_v1g:242260	68.55	671	0
Substrate extraction and recruiting	Ufd1	ubiquitin fusion degradation protein 1	1.2.679.m1	NEMVE_v1g189007	69.26	309	7.00E-142
	p97	transitional endoplasmic reticulum ATPase	1.219057.m1	NEMVE_v1g190325	90.14	771	0
Shuttle protein	DUB	Ataxin-3 [EC:3.4.22.-]	1.2.9216.m1	NEMVE_v1g34645	70	210	2.00E-99
	RAD23	UV excision repair protein RAD23	1.2.2686.m1	NEMVE_v1g246958	52.02	371	2.00E-109

Proteasome	Rpn2	26S proteasome regulatory subunit N2	1.2.2366.m1	nve:NEMVE_v1g193603	77.13	1019	0
	Rpn3	26S proteasome regulatory subunit N3	1.2.11418.m1	nve:NEMVE_v1g233482	73.31	502	0
	Rpn5	26S proteasome regulatory subunit N5	1.2.7613.m1	nve:NEMVE_v1g113443	73.54	446	0
	Rpn6	26S proteasome regulatory subunit N6	1.2.4538.m1	nve:NEMVE_v1g219029	75.72	416	0
	Rpn7	26S proteasome regulatory subunit N7	1.2.3354.m1	nve:NEMVE_v1g195005	76.53	277	7.00E-159
	Rpn8	26S proteasome regulatory subunit N8	1.2.16235.m1	nve:NEMVE_v1g161920	71.84	348	5.00E-166
	Rpn9	26S proteasome regulatory subunit N9	1.2.8883.m1	nve:NEMVE_v1g79078	70.48	376	0
	Rpn10	26S proteasome regulatory subunit N10	1.2.1010.m1	nve:NEMVE_v1g236108	65.13	413	4.00E-166
	Rpn11	26S proteasome regulatory subunit N11	1.2.12964.m1	nve:NEMVE_v1g239961	83.55	310	1.00E-178
	Rpn12	26S proteasome regulatory subunit N12	1.2.13351.m1	nve:NEMVE_v1g190193	79.85	263	4.00E-144
	Rpt1	26S proteasome regulatory subunit T1	1.2.16618.m1	nve:NEMVE_v1g189255	86.18	434	0
	Rpt2	26S proteasome regulatory subunit T2	1.2.5719.m1	nve:NEMVE_v1g176351	96.45	197	8.00E-134
	Rpt3	26S proteasome regulatory subunit T3	1.2.2345.m1	nve:NEMVE_v1g236753	90.67	418	0
	Rpt4	26S proteasome regulatory subunit T4	1.2.461.m1	nve:NEMVE_v1g215693	94.36	390	0
	Rpt5	26S proteasome regulatory subunit T5	1.2.3961.m1	nve:NEMVE_v1g244951	88.03	426	0
	Rpt6	26S proteasome regulatory subunit T6	1.2.12658.m1	nve:NEMVE_v1g196829	84.71	412	0
	alpha1	20S proteasome subunit alpha 1	1.2.17385.m1	nve:NEMVE_v1g238636	88.21	246	4.00E-169
	alpha2	20S proteasome subunit alpha 2	1.2.1573.m1	nve:NEMVE_v1g165493	91.45	234	1.00E-163
	alpha3	20S proteasome subunit alpha 3	1.2.7785.m1	nve:NEMVE_v1g148426	77.63	152	4.00E-85
	alpha4	20S proteasome subunit alpha 4	1.2.3696.m1	nve:NEMVE_v1g179894	88.54	253	1.00E-158
	alpha5	20S proteasome subunit alpha 5	1.2.9821.m1	nve:NEMVE_v1g168163	88.84	242	2.00E-161
	alpha6	20S proteasome subunit alpha 6	1.2.2830.m1	nve:NEMVE_v1g10968	85.36	239	3.00E-152
	alpha7	20S proteasome subunit alpha 7	1.2.9956.m1	nve:NEMVE_v1g235516	82.08	240	2.00E-148
	beta1	20S proteasome subunit beta 1	1.2.9584.m1	nve:NEMVE_v1g101124	82.23	197	5.00E-121
	beta2	20S proteasome subunit beta 2	1.2.10862.m1	nve:NEMVE_v1g127396	57.14	231	2.00E-77
	beta3	20S proteasome subunit beta 3	1.2.5977.m1	nve:NEMVE_v1g99390	88.78	205	7.00E-139
	beta4	20S proteasome subunit beta 4	1.2.22654.m1	nve:NEMVE_v1g193516	70.56	197	4.00E-104
	beta5	20S proteasome subunit beta 5	1.2.2519.m1	nve:NEMVE_v1g173323	83.39	277	7.00E-174
	beta6	20S proteasome subunit beta 6	1.2.8961.m1	nve:NEMVE_v1g191787	80.09	226	9.00E-136
	beta7	20S proteasome subunit beta 7	1.2.17366.m1	nve:NEMVE_v1g167347	76.79	56	3.00E-26
UPR: unfolded protein response							
IRE1 c	ERN1	endoribonuclease inositol-requiring enzyme 1	1.2.5693.m1	NEMVE_v1g93936	69.68	409	0
	TRAF2	TNF receptor-associated factor 2	1.2.2752.m1	NEMVE_v1g112390	44.7	528	3.00E-149
	TRAF2	TNF receptor-associated factor 2	1.2.1949.m1	NEMVE_v1g112390	40.49	568	2.00E-129
	TNF-R	tumor necrosis factor receptor	1.2.18805.m1	hsa:7132	35.14	148	1.00E-18
MAPK	TRAF2	TNF receptor-associated factor 2	1.2.3871.m1	hsa:7186	35.74	554	5.00E-94
	TRAF2	TNF receptor-associated factor 2	1.2.5426.m1	hsa:7186	32.48	545	6.00E-94
	TRAF2	TNF receptor-associated factor 2	1.2.10762.m1	hsa:7186	35.14	552	2.00E-99
	MEK7	mitogen-activated protein kinase kinase 7	1.2.2135.m1	NEMVE_v1g229025	70.03	317	4.00E-167
	c-Jun, JUN	transcription factor AP-1	1.2.21516.m1	hsa:3725	36.1	349	5.00E-45
BAX	BAX	apoptosis regulator BAX	1.2.7024.m1	NEMVE_v1g100129	71.57	102	9.00E-53
	XBP	X box-binding protein 1	1.2.15171.m1	NEMVE_v1g211292	61.42	127	6.00E-51
	CAPN1	calpain-1 [EC:3.4.22.52]	1.2.13821.m1	hsa:823	40.73	712	2.00E-166
	CASP12	caspase 12 [EC:3.4.22.-]	1.2.9586.m1	hsa:100506742	28.46	260	5.00E-20
PERK	PERK	eukaryotic translation initiation factor 2 alpha kinase 1	1.2.9243.m1	NEMVE_v1g200396	49.86	716	0
	eIF2a	translation initiation factor 2 subunit 1	1.2.8366.m1	NEMVE_v1g185797	82.8	314	0
	ATF4	cyclic AMP-dependent transcription factor ATF-4	1.2.2941.m1	hsa:468	50	90	4.00E-14
	NRF2	nuclear factor erythroid 2-related factor 2	1.2.25358.m1	hsa:4780	42.62	122	1.00E-22
ATF6	ATF6	cyclic AMP-dependent transcription factor ATF-6	1.2.4295.m1	NEMVE_v1g245260	38.32	689	5.00E-131
	S1P	membrane-bound transcription factor site-1	1.2.9725.m1	hsa:8720	57.36	1006	0
	S2P	S2P endopeptidase [EC:3.4.24.85]	1.2.21967.m1	NEMVE_v1g185856	68.96	480	0
ER homeostasis							
ER REDOX	ERO1	ERO1-like protein beta [EC:1.8.4.-]	1.2.10186.m1	NEMVE_v1g83316	59.34	391	0
	PDIs	protein disulfide-isomerase A6 [EC:5.3.4.1]	1.2.9018.m1	NEMVE_v1g117546	69.42	412	0
	PDIs	protein disulfide isomerase	1.2.5704.m1	NEMVE_v1g118540	70.43	443	0
	PDIs, ERp57	protein disulfide isomerase family A, member 3	1.2.1667.m1	NEMVE_v1g218982	43.72	462	3.00E-124
	PDIs, ERp57	protein disulfide isomerase family A, member 4	1.2.7144.m1	NEMVE_v1g218982	55.34	524	0
	GSR	glutathione reductase (NADPH) [EC:1.8.1.7]	1.2.3068.m1	hsa:2936	37.45	486	5.00E-87
Ca influx	SERCA2b	Ca2+-transporting ATPase, sarcoplasmic/endoplasmic reticulum [EC:3.6.3.8]	1.2.8202.m1	gi|24638454	68.93	1030	0
Ca efflux	ERp44	Endoplasmic reticulum resident protein 44	1.2.14444.m1	gi|31077035	51.71	381	3.00E-130
	CaMKII	calcium/calmodulin-dependent protein kinase type II	1.2.6981.m1	gi|26667203	53.92	549	0
	CaMKII	calcium/calmodulin-dependent protein kinase type II	1.2.8061.m1	gi|26667203	60.26	546	0
	IP3R1	inositol 1,4,5-trisphosphate receptor type 1 isoform	1.2.8787.m1	gi|269954694	59.19	2806	0
	STIM	stromal interaction molecule 2 isoform 1 precursor	1.2.4574.m1	gi|281182842	38.22	450	3.00E-102
	CaVL2	voltage-dependent L-type calcium channel	1.2.3113.m1	gi|600971714	57.24	877	0
	CaVL2	voltage-dependent L-type calcium channel	1.2.20611.m1	gi|600971714	44.97	1641	0

(B)

Coral ID	Gene name	Adults				Juveniles			
		1 h		24 h		24 h		48 h	
		log_2FC	FDR	log_2FC	FDR	log_2FC	FDR	log_2FC	FDR
1.2.22267.m1	Sec61	–	–	0.42	1.24E-02	–	–	–	–
1.2.13846.m1	GLcII	–	–	0.66	8.95E-06	–	–	–	–
1.2.11239.m1	OSTs	–	–	0.40	7.36E-03	-0.19	2.37E-02	–	–
1.2.12013.m1	OSTs	–	–	0.65	2.13E-06			–	–
1.2.16315.m1	CNX	–	–	0.53	1.60E-04	-0.19	1.49E-02	–	–
1.2.2683.m1	CRT	-0.46	2.15E-10	1.14	8.82E-22	–	–	–	–
1.2.18585.m1	UGGT	–	–	0.59	8.82E-04	–	–	0.34	3.65E-02
1.2.15211.m1	GRP94	-0.23	2.23E-02	1.21	7.26E-25	-0.16	4.66E-02	–	–
1.2.2424.m1	NEF	-0.64	3.86E-11	0.90	1.87E-07	-0.23	6.15E-03	–	–
1.2.4351.m1	BiP, GRP70	–	–	1.30	8.64E-19	-0.20	1.67E-02	–	–
1.2.7940.m1	ERdj1	–	–	1.76	1.52E-02	–	–	–	–
1.2.25530.m1	ERdj3, DnaJB11	–	–	1.04	1.03E-07	0.44	3.48E-08	0.29	5.71E-02
1.2.20851.m1	ERdj4	-0.27	3.51E-02	–	–	–	–	–	–
1.2.22277.m1	ERdj5	–	–	–	–	0.19	3.52E-02	–	–
1.2.21656.m1	ERdj6, DnaJC3	-0.53	1.64E-03	0.58	5.20E-03	–	–	–	–
1.2.143.m1	SEC63	-0.35	8.28E-03	–	–	–	–	–	–
1.2.3114.m1	EDEM	–	–	0.74	8.06E-04	–	–	–	–
1.2.21359.m1	XTP3B	–	–	0.70	1.63E-07	–	–	–	–
1.2.4008.m1	ERManI	-0.29	6.29E-02	–	–	–	–	–	–
1.2.3165.m1	TRAP	–	–	0.54	1.52E-03	–	–	–	–
1.2.11248.m1	TRAM	-0.24	3.16E-02	0.53	6.53E-04	-0.14	4.39E-02	–	–
1.2.918.m1	DERLIN	–	–	–	–	–	–	–	–
1.2.14992.m1	UBE1	–	–	0.34	1.94E-02	0.15	5.19E-04	–	–
1.2.25429.m1	UBE2C	-0.72	5.00E-02	–	–	–	–	–	–
1.2.21247.m1	UBE2D/E	-0.32	3.76E-04	0.43	2.65E-03	0.35	2.60E-07	–	–
1.2.21685.m1	UBE2D/E	–	–	–	–	0.39	5.71E-02	–	–
1.2.21689.m1	UBE2D/E	–	–	–	–	0.32	1.67E-02	–	–
1.2.21680.m1	UBE2D/E	–	–	0.57	2.90E-02	0.41	1.19E-04	0.25	9.01E-02
1.2.802.m1	UBE1G1	–	–	–	–	-0.25	4.34E-02	–	–
1.2.22895.m1	UBE2G2	–	–	–	–	0.37	1.16E-04	–	–
1.2.6436.m1	UBE2I	-0.45	1.69E-04	–	–	-0.17	3.15E-02	–	–
1.2.138.m1	UBE2J1	-0.49	7.95E-03	–	–	-0.21	2.22E-02	-1.27	2.08E-02
1.2.3007.m1	UBE2L3	-0.32	2.54E-03	–	–	0.22	1.26E-02	–	–
1.2.1863.m1	UBE2M	-0.59	7.38E-03	–	–	–	–	1.29	3.77E-02
1.2.23020.m1	UBE2N	–	–	0.38	4.96E-02	0.23	2.24E-03	–	–
1.2.7586.m1	UBE2O	–	–	0.63	1.20E-04	–	–	–	–
1.2.14941.m1	UBE2Q	-0.95	7.42E-05	–	–	–	–	–	–
1.2.3573.m1	UBE2R	–	–	-0.58	9.48E-03	-0.15	3.45E-02	–	–
1.2.17650.m1	HERC1	–	–	–	–	–	–	1.22	5.07E-02
1.2.3515.m1	TRIP12	–	–	1.25	5.20E-02	–	–	–	–
1.2.4310.m1	NEDD4	–	–	1.33	1.39E-02	–	–	1.16	3.24E-02
1.2.6288.m1	UBE3B	1.28	5.99E-02	–	–	-1.35	1.04E-05	–	–
1.2.13267.m1	WWP1	-1.12	5.79E-02	–	–	-1.08	5.76E-03	–	–
1.2.1434.m1	E6AP	-1.35	2.23E-03	–	–	–	–	–	–
1.2.14462.m1	UBE4A	–	–	1.49	9.56E-04	–	–	–	–
1.2.883.m1	PRP19	–	–	1.28	4.92E-02	–	–	–	–
1.2.14889.m1	CYC4	1.26	3.05E-02	–	–	–	–	–	–
1.2.8575.m1	Hsp70	–	–	1.07	6.37E-14	0.49	2.20E-13	0.30	1.94E-02
1.2.5530.m1	MEKK1	1.47	2.84E-04	–	–	–	–	–	–
1.2.2897.m1	TRAF6	–	–	4.20	4.96E-10	–	–	1.44	5.97E-03
1.2.11953.m1	PIAS	–	–	1.77	8.03E-05	1.13	9.92E-03	1.19	1.63E-02
1.2.20985.m1	SIAH-1	-1.96	1.08E-05	-1.88	6.90E-04	1.35	1.13E-09	1.44	1.77E-05
1.2.2625.m1	Trim37	–	–	-1.64	5.31E-04	-1.32	9.03E-07	–	–
1.2.4545.m1	BRCA1	–	–	-1.47	2.83E-02	-1.20	6.53E-03	–	–
1.2.10197.m1	SYVN, Hrd1	–	–	–	–	-1.25	4.92E-06	-1.16	2.03E-02
1.2.15842.m1	RBX1	–	–	1.62	2.64E-04	1.31	1.64E-07	–	–
1.2.598.m1	RBX2	–	–	–	–	1.35	2.07E-02	–	–
1.2.480.m1	Cul3	-1.16	5.18E-02	–	–	-1.13	8.19E-03	–	–
1.2.3461.m1	Cul4	–	–	–	–	-1.14	3.63E-03	-1.16	1.63E-02
1.2.13230.m1	DDB1	–	–	–	–	1.09	4.48E-02	1.19	7.15E-04
1.2.20605.m1	F-box	-1.22	5.39E-02	–	–	-1.30	2.27E-07	-1.21	5.73E-03
1.2.679.m1	Ubi1	0.35	2.53E-02	–	–	–	–	–	–
1.2.19057.m1	p97	-0.24	1.01E-02	0.84	1.82E-11	–	–	–	–
1.2.9216.m1	DUB	-0.37	4.62E-02	–	–	–	–	–	–
1.2.2686.m1	RAD23	–	–	0.41	1.57E-02	–	–	–	–

1.2.2366.m1	Rpn2	–	–	1.61	3.28E-07	–	–	–	–
1.2.11418.m1	Rpn3	-0.46	7.95E-05	–	–	–	–	–	–
1.2.7613.m1	Rpn5	-0.57	1.71E-04	–	–	–	–	–	–
1.2.4538.m1	Rpn6	–	–	0.43	4.29E-02	0.16	2.49E-02	–	–
1.2.3354.m1	Rpn7	-0.54	2.17E-03	0.45	4.64E-02	–	–	–	–
1.2.16235.m1	Rpn8	–	–	0.91	1.16E-07	0.28	7.83E-06	–	–
1.2.8083.m1	Rpn9	-0.29	3.47E-02	0.46	2.34E-02	–	–	–	–
1.2.1010.m1	Rpn10	-0.38	4.63E-03	–	–	–	–	–	–
1.2.12964.m1	Rpn11	–	–	0.37	8.31E-02	–	–	–	–
1.2.13351.m1	Rpn12	–	–	–	–	0.22	2.98E-02	–	–
1.2.16618.m1	Rpt1	-0.36	4.11E-03	–	–	–	–	–	–
1.2.5719.m1	Rpt2	-0.47	5.46E-04	–	–	–	–	–	–
1.2.2345.m1	Rpt3	-0.95	1.09E-07	–	–	–	–	–	–
1.2.461.m1	Rpt4	-0.36	2.77E-03	0.48	8.38E-03	–	–	–	–
1.2.3961.m1	Rpt5			0.54	1.08E-03	0.18	8.36E-03	–	–
1.2.12658.m1	Rpt6	-0.28	7.19E-03	0.45	2.47E-03	–	–	–	–
1.2.17385.m1	alpha1	-0.28	3.85E-02	1.06	3.17E-11	0.32	2.54E-05	–	–
1.2.1573.m1	alpha2	–	–	0.43	1.49E-02	–	–	–	–
1.2.7785.m1	alpha3	-0.35	7.68E-02	0.67	6.53E-04	–	–	–	–
1.2.3696.m1	alpha4	-0.45	1.09E-02	–	–	-0.23	4.19E-03	-0.35	1.88E-02
1.2.9821.m1	alpha5	–	–	0.73	5.32E-05	0.14	5.78E-02	–	–
1.2.2830.m1	alpha6	–	–	0.56	5.64E-03	–	–	–	–
1.2.9956.m1	alpha7	-0.43	6.50E-04	–	–	–	–	–	–
1.2.9584.m1	beta1	–	–	0.45	4.15E-02	0.22	3.88E-02	–	–
1.2.10862.m1	beta2	–	–	0.43	7.63E-02	–	–	–	–
1.2.5977.m1	beta3	-0.46	2.70E-03	–	–	-0.16	5.86E-02	-0.30	7.27E-02
1.2.22654.m1	beta4	-0.33	6.04E-02	–	–	–	–	–	–
1.2.2519.m1	beta5	-0.50	6.64E-04	0.48	2.54E-02	–	–	–	–
1.2.8961.m1	beta6	-0.59	2.01E-04	–	–	-0.26	5.16E-04	–	–
1.2.17366.m1	beta7	-0.35	8.78E-02	0.57	2.70E-02	–	–	–	–
1.2.5693.m1	ERN1	0.30	2.59E-02	–	–	–	–	–	–
1.2.2752.m1	TRAF2	0.86	2.68E-03	2.64	1.30E-27	–	–	–	–
1.2.1949.m1	TRAF2	0.39	4.24E-03	–	–	0.20	4.19E-02	–	–
1.2.18805.m1	TNF-R	–	–	–	–	0.26	3.65E-04	–	–
1.2.3871.m1	TRAF2	0.51	1.07E-04	0.97	1.05E-08	0.41	9.82E-09	–	–
1.2.5426.m1	TRAF2	3.67	8.42E-78	2.42	1.79E-26	–	–	–	–
1.2.10762.m1	TRAF2	–	–	-1.53	2.22E-06	-0.34	9.62E-02	–	–
1.2.2135.m1	MKK7	–	–	–	–	0.21	7.60E-03	–	–
1.2.21516.m1	c-Jun, JUN	3.11	2.59E-16	1.60	7.06E-13	0.38	8.01E-02	–	–
1.2.7024.m1	BAX	0.41	2.78E-02	0.68	1.10E-03	0.34	5.56E-05	–	–
1.2.15171.m1	XBP	–	–	–	–	-0.23	3.68E-09	-0.17	2.74E-02
1.2.13821.m1	CAPN1	0.17	2.50E-02	0.40	2.47E-03	–	–	–	–
1.2.9586.m1	CASP12	–	–	–	–	–	–	-1.16	3.09E-02
1.2.9243.m1	PERK	–	–	0.60	6.25E-03	0.32	1.94E-03	0.25	5.44E-02
1.2.8366.m1	eIF2a	-0.52	1.13E-04	–	–	–	–	–	–
1.2.2941.m1	ATF4	0.26	5.25E-02	–	–	-0.17	5.31E-02	–	–
1.2.25358.m1	NRF2	1.32	2.93E-16	0.52	1.68E-02	–	–	–	–
1.2.4295.m1	ATF6	–	–	0.42	1.89E-02	–	–	–	–
1.2.9725.m1	S1P	–	–	–	–	-0.28	8.80E-05		
1.2.21967.m1	S2P	–	–	–	–	-0.39	4.28E-05	-0.27	4.41E-02
1.2.10186.m1	ERO1	–	–	–	–	–	–	-0.29	7.78E-03
1.2.9018.m1	PDIs	-0.36	8.88E-04	0.87	6.24E-10	-0.26	2.13E-04	–	–
1.2.5704.m1	PDIs	–	–	0.77	2.42E-08	-0.22	1.25E-04	–	–
1.2.1667.m1	PDIs, ERp57	–	–	0.98	1.09E-13	-0.40	5.74E-06	–	–
1.2.7144.m1	PDIs, ERp57	–	–	1.24	1.74E-27	–	–	–	–
1.2.3068.m1	GSR	-0.23	4.01E-02	0.43	7.29E-03	0.52	1.30E-50	–	–
1.2.8202.m1	SERCA2b	-1.40	1.15E-09	1.63	3.59E-05	–	–	1.39	2.28E-04
1.2.14444.m1	ERp44	-1.30	3.60E-05	–	–	-1.26	4.74E-08	-1.32	3.11E-04
1.2.6981.m1	CaMKII	-1.37	6.23E-03	–	–	–	–	–	–
1.2.8061.m1	CaMKII	–	–	-1.41	1.53E-02	–	–	–	–
1.2.8787.m1	IP3R1	–	–	-1.35	4.05E-03	-1.12	5.78E-02	–	–
1.2.4574.m1	STIM	–	–	-1.32	4.95E-02	-1.16	2.46E-02	–	–
1.2.3113.m1	CaV1.2	–	–	-1.85	2.60E-08	–	–	–	–
1.2.20611.m1	CaV1.2	–	–	–	–	-1.16	3.83E-02	–	–

Table S3.3 *A. millepora* homologues to the peroxisome and lysosome systems. (A) Results of the KEGG peroxisome and lysosome pathways (nve04146 and nve04142) searched in the *A. millepora* protein predictions. (B) Log_2FC values of significantly expressed (FDR <0.05) genes in response to the treatment (hypo-saline) over the control (35 PSU). Log_2FC colour indicate up (red) and down (blue) regulated genes.

(A)

Function	Gene name	Orthology	Blast details				
			Coral ID	Entry	% ID	Length	e-value
Lysosome	TAPL	K05656 ATP-binding cassette	1.2.21081.m1	hsa:23457	32.15	790	2.00E-96
	NPC1	K12385 Niemann-Pick C1 protein	1.2.15804.m1	hsa:4864	48.38	1269	0
	NPC2	K13443 Niemann-Pick C2 protein	1.2.6509.m1	hsa:10577	54.26	129	4.00E-44
	SCARB2	K12384 lysosome membrane protein 2	1.2.12925.m1	hsa:950	36.36	231	2.00E-47
	CTSD	K01379 cathepsin D	1.2.7013.m1	hsa:1509	53.55	409	2.00E-151
	CTSX	K08568 cathepsin X	1.2.1122.m1	hsa:1522	64.18	282	1.00E-133
	CTSB	K01363 cathepsin B	1.2.16027.m1	hsa:1508	53.16	316	4.00E-110
	CTSB	K01363 cathepsin B	1.2.14228.m1	hsa:1508	38.44	333	2.00E-63
	CTSL	K01365 cathepsin L	1.2.5972.m1	hsa:1514	53.43	335	3.00E-114
	CTSH	K01366 cathepsin H	1.2.6471.m1	hsa:1512	42.39	309	9.00E-78
	CTSO	K01374 cathepsin O	1.2.12092.m1	hsa:1519	43.15	292	5.00E-71
	CTSO	K01374 cathepsin O	1.2.20750.m1	hsa:1519	36.81	288	3.00E-49
	CTSH	K01366 cathepsin H	1.2.6471.m1	hsa:1512	42.39	309	9.00E-78
	ATP6V0C	K02155 V-type H+-transporting ATPase 16kDa proteolipid subunit	1.2.9085.m1	hsa:527	34	150	2.00E-18
	SMPD1	K12350 sphingomyelin phosphodiesterase	1.2.21066.m1	hsa:6609	46.35	561	1.00E-169
	GAA	K12316 lysosomal alpha-glucosidase	1.2.6192.m1	hsa:2548	39.85	916	0
	LIPA	K01052 lysosomal acid lipase/cholesteryl ester hydrolase	1.2.21260.m1	hsa:3988	53.85	364	7.00E-140
	PSAP	K12382 saposin	1.2.6187.m1	hsa:5660	30.99	342	2.00E-45
	ACP5	K14379 tartrate-resistant acid phosphatase	1.2.22359.m1	hsa:54	45.19	312	2.00E-95
	GNPTG	K10087 N-acetylglucosamine-1-phosphate transferase	1.2.21359.m1	hsa:84572	33.33	105	8.00E-15
	LAMP1	K06528 lysosomal-associated membrane protein 1/2	1.2.451.m1	hsa:3916	29.77	262	5.00E-13
	FUCA1	K01206 alpha-L-fucosidase	1.2.6843.m1	hsa:2517	57.71	454	0
	CD63	K06497 CD63 antigen	1.2.18482.m1	hsa:967	36.25	240	8.00E-43
	CD164	K06546 CD164 antigen	1.2.269.m1	hsa:8763	34.15	41	2.00E-04
	SORT1	K12388 sortilin	1.2.3853.m1	hsa:6272	27.74	620	2.00E-54
	HGSNAT	K10532 heparan-alpha-glucosaminide N-acetyltransferase	1.2.2064.m1	hsa:138050	42.06	592	3.00E-122
	ABCA2	K05642 ATP-binding cassette, subfamily A (ABC1)	1.2.11936.m1	hsa:20	52.22	1038	0
	LGMN	K01369 legumain	1.2.9976.m1	hsa:5641	43.42	479	6.00E-123
	PLA2G15	K06129 lysophospholipase III	1.2.1415.m1	hsa:23659	42.27	388	5.00E-108
	PLA2G15	K06129 lysophospholipase III	1.2.1406.m1	hsa:23659	38.54	410	2.00E-105
	GNS	K01137 N-acetylglucosamine-6-sulfatase	1.2.23786.m1	hsa:2799	44.26	122	5.00E-16
	ACP2	K14410 lysosomal acid phosphatase	1.2.14329.m1	hsa:53	52.5	120	1.00E-32
	ASAH1	K12348 acid ceramidase	1.2.22081.m1	hsa:427	35.88	340	3.00E-59
	MAN2B1	K12311 lysosomal alpha-mannosidase	1.2.6127.m1	hsa:4125	48.35	1001	0
	LAMP1	K06528 lysosomal-associated membrane protein 1/2	1.2.458.m1	hsa:3916	29.01	262	8.00E-13
	GGA2	K12404 ADP-ribosylation factor-binding protein GGA	1.2.6430.m1	hsa:23062	26.28	293	5.00E-18
	CLTA	K04644 clathrin light chain A	1.2.2306.m1	hsa:1211	42.65	211	6.00E-40
	CLTC	K04646 clathrin heavy chain	1.2.15185.m1	hsa:1213	75.09	1132	0
	M6PR	K10089 cation-dependent mannose-6-phosphate receptor	1.2.14030.m1	hsa:4074	26.58	79	3.00E-05
	AP1G1	K12391 AP-1 complex subunit gamma-1	1.2.11304.m1	hsa:164	61.94	854	0
Peroxisome							
Peroxin	PEX1	K13338 peroxin-1	1.2.5735.m1	hsa:5189	35.75	565	1.00E-81
	PEX1	K13338 peroxin-1	1.2.3540.m1	hsa:5189	37.93	1147	0
	PEX5	K13342 peroxin-5	1.2.25613.m1	hsa:5830	46.27	657	9.00E-176
	PEX6	K13339 peroxin-6	1.2.19057.m1	hsa:5190	34.47	499	5.00E-73
	PEX7	K13341 peroxin-7	1.2.16331.m1	hsa:5191	32.68	205	3.00E-24
	PEX10	K13346 peroxin-10	1.2.1507.m1	hsa:5192	42.33	326	2.00E-77
	PEX13	K13344 peroxin-13	1.2.8365.m1	hsa:5194	46.99	266	4.00E-76
Antioxidant system	CAT	K03781 catalase	1.2.6992.m1	hsa:847	67.2	497	0
	CAT	K03781 catalase	1.2.12339.m1	hsa:847	64.05	509	0
	SOD1	K04565 superoxide dismutase, Cu-Zn family	1.2.240.m1	hsa:6647	65.07	146	3.00E-60
	SOD1	K04565 superoxide dismutase, Cu-Zn family	1.2.22720.m1	NEMVE_v1g234825	42.53	87	7.00E-15
	SOD1	K04565 superoxide dismutase, Cu-Zn family	1.2.1159.m1	NEMVE_v1g3582	34.38	96	2.00E-05
	NOS2	K13241 nitric oxide synthase, inducible	1.2.1319.m1	hsa:4843	44.73	1120	0
	NOS2	K13241 nitric oxide synthase, inducible	1.2.890.m1	hsa:4843	43.78	1222	0
	PRDX1	K13279 peroxiredoxin 1	1.2.5154.m1	hsa:5052	68.39	193	6.00E-91
	PRDX1	K13279 peroxiredoxin 1	1.2.66.m1	hsa:5052	69.95	193	7.00E-99
	PRDX1	K13279 peroxiredoxin 1	1.2.16198.m1	Cluster030963	96.74	92	2.00E-61
	EPHX2	K08726 soluble epoxide hydrolase / lipid-phosphate phosphatase	1.2.5185.m1	hsa:2053	30.94	320	4.00E-35
	DHRS4	K11147 dehydrogenase/reductase SDR family member 4	1.2.16310.m1	hsa:10901	31.82	110	3.00E-09

(B)

Coral ID	Gene name	Adults				Juveniles			
		1 h		24 h		24 h		48 h	
		log_2FC	FDR	log_2FC	FDR	log_2FC	FDR	log_2FC	FDR
1.2.21081.m1	TAPL	1.35	1.02E-82	1.96	2.63E-59	1.23	1.04E-128	1.02	3.97E-26
1.2.15804.m1	NPC1	–	–	1.40	3.45E-22	0.76	2.85E-16	0.85	1.75E-07
1.2.6509.m1	NPC2	–	–	1.22	8.11E-16	1.09	4.61E-33	0.80	1.52E-10
1.2.12925.m1	SCARB2	–	–	1.57	2.25E-18	–	–	–	–
1.2.7013.m1	CTSD	–	–	1.01	1.13E-15	-0.22	8.18E-04	–	–
1.2.1122.m1	CTSX	-0.53	2.27E-07	0.68	2.11E-06	–	–	–	–
1.2.16027.m1	CTSB	–	–	0.61	4.90E-06	–	–	–	–
1.2.14228.m1	CTSB	–	–	0.37	4.58E-02	0.63	4.74E-04	–	–
1.2.5972.m1	CTSL	-0.28	8.16E-03	0.60	8.05E-06	-0.13	2.97E-04	–	–
1.2.6471.m1	CTSH	–	–	0.79	3.52E-05	0.36	5.18E-07	–	–
1.2.12092.m1	CTSO	–	–	0.43	3.23E-02	–	–	–	–
1.2.20750.m1	CTSO	–	–	-0.27	4.35E-02	-0.21	7.58E-04	–	–
1.2.6471.m1	CTSH	–	–	0.79	3.52E-05	0.36	5.18E-07	–	–
1.2.9085.m1	ATP6V0C	–	–	0.64	5.63E-05	–	–	–	–
1.2.21066.m1	SMPD1	0.98	1.67E-07	1.47	1.22E-11	0.66	7.88E-14	0.38	1.06E-02
1.2.6192.m1	GAA	0.30	7.12E-02	-1.55	1.55E-09	-0.65	4.14E-08	–	–
1.2.21260.m1	LIPA	–	–	0.95	1.89E-09	–	–	–	–
1.2.6187.m1	PSAP	–	–	0.68	2.02E-09	–	–	–	–
1.2.22359.m1	ACP5	–	–	-1.13	2.67E-08	0.31	9.73E-03	–	–
1.2.21359.m1	GNPTG	–	–	0.70	1.63E-07	–	–	–	–
1.2.451.m1	LAMP1	–	–	0.57	2.72E-07	–	–	–	–
1.2.6843.m1	FUCA1	–	–	0.58	2.74E-06	–	–	–	–
1.2.18482.m1	CD63	-0.27	1.47E-02	0.61	6.75E-06	0.24	1.08E-02	–	–
1.2.269.m1	CD164	–	–	0.67	3.28E-05	–	–	–	–
1.2.3853.m1	SORT1	–	–	0.44	1.25E-04	–	–	–	–
1.2.2064.m1	HGSNAT	–	–	-0.83	1.62E-04	–	–	–	–
1.2.11936.m1	ABCA2	–	–	-0.53	1.68E-03	–	–	0.33	2.08E-02
1.2.9976.m1	LGMN	–	–	0.43	2.28E-03	–	–	–	–
1.2.1415.m1	PLA2G15	–	–	0.58	9.19E-02	0.97	2.51E-24	0.66	1.30E-03
1.2.1406.m1	PLA2G15	–	–	-1.45	4.57E-03	–	–	–	–
1.2.23786.m1	GNS	–	–	0.79	4.65E-03	–	–	0.87	3.79E-03
1.2.14329.m1	ACP2	–	–	0.48	7.44E-03	0.19	4.24E-02	–	–
1.2.22081.m1	ASAH1	–	–	0.57	1.16E-02	–	–	-0.26	2.40E-02
1.2.6127.m1	MAN2B1	0.17	4.77E-02	0.35	1.95E-02	–	–	–	–
1.2.458.m1	LAMP1	–	–	0.30	3.09E-02	-0.30	1.15E-11	-0.30	2.03E-05
1.2.6430.m1	GGA2	–	–	0.41	3.63E-02	-0.23	5.27E-03	–	–
1.2.2306.m1	CLTA	–	–	0.32	3.74E-02	–	–	–	–
1.2.15185.m1	CLTC	-0.20	4.42E-02	0.28	3.92E-02	–	–	–	–
1.2.14030.m1	M6PR	–	–	0.39	4.62E-02	0.16	4.27E-02	–	–
1.2.11304.m1	AP1G1	–	–	0.31	4.62E-02	–	–	–	–
		–	–	–	–	–	–	–	–
1.2.5735.m1	PEX1	-0.60	1.47E-04	–	–	-0.21	2.77E-02	-0.47	4.82E-02
1.2.3540.m1	PEX1	0.39	3.51E-03	–	–	–	–	–	–
1.2.25613.m1	PEX5	–	–	–	–	-0.26	4.99E-03	-0.47	3.78E-07
1.2.19057.m1	PEX6	-0.24	1.01E-02	0.84	1.82E-11	–	–	–	–
1.2.16331.m1	PEX7	–	–	–	–	0.17	3.36E-02	–	–
1.2.1507.m1	PEX10	–	–	0.55	2.41E-02	–	–	–	–
1.2.8365.m1	PEX13	-0.46	7.67E-03			–	–	–	–
1.2.6992.m1	CAT	-0.70	1.00E-08	1.44	1.93E-31	-0.49	1.26E-09	–	–
1.2.12339.m1	CAT	–	–	0.50	1.96E-02	-0.42	8.83E-06	-0.41	9.84E-06
1.2.240.m1	SOD1	–	–	0.42	1.07E-02	–	–	–	–
1.2.22720.m1	SOD1	–	–	0.44	4.68E-02	–	–	–	–
1.2.1159.m1	SOD1	-0.80	8.98E-06	-1.90	2.96E-07	–	–	–	–
1.2.1319.m1	NOS2	-2.27	5.38E-06	-2.99	3.43E-06	–	–	–	–
1.2.890.m1	NOS2	–	–	-0.70	5.51E-03	–	–	–	–
1.2.5154.m1	PRDX1	-0.30	6.59E-03	–	–	–	–	-0.19	2.17E-02
1.2.66.m1	PRDX1	-0.40	1.44E-02	–	–	-0.32	7.15E-06	–	–
1.2.16198.m1	PRDX1	–	–	–	–	–	–	-0.35	3.38E-03
1.2.5185.m1	EPHX2	-0.29	3.22E-02	0.56	6.49E-04	-0.28	8.21E-07	-0.21	5.84E-02
1.2.16310.m1	DHRS4	–	–	1.40	1.09E-31	1.60	3.39E-187	1.63	3.48E-66

Table S3.4 *A. millepora* homologues to amino acids metabolism. (A) Results of the KEGG amino acids pathways (00260 glycine, serine and threonine metabolism, 00270 cysteine and methionine metabolism, 00330 arginine and proline metabolism, and 00480 glutathione metabolism) searched in the *A. millepora* protein predictions. (B) Log_2FC values of significantly expressed (FDR <0.05) genes in response to the treatment (hypo-saline) over the control (35 PSU). Log_2FC colour indicate up (red) and down (blue) regulated genes.

Function	Gene name	Orthology	EC number	Blast details				
				Coral ID	Entry	% ID	Length	e-value
Glycine betaine degradation	CDH	K00108 choline dehydrogenase	1.1.99.1	1.2.6999.m1	nve:NEMVE_v1g112198	66.02	359	0
	ALDH7A1	K14085 aldehyde dehydrogenase family 7 member A1	1.2.1.31 1.2.1.8 1.2.1.3	1.2.25403.m1	nve:NEMVE_v1g175287	67.77	546	0
	BHMT	K00544 betaine-homocysteine S-methyltransferase	2.1.1.5	1.2.8566.m1	nve:NEMVE_v1g236455	71.97	396	0
	BHMT	K00544 betaine-homocysteine S-methyltransferase	2.1.1.5	1.2.19413.m1	NP_001012498.1	99	58	2E-142
	DMGDH	K00315 dimethylglycine dehydrogenase	1.5.8.4	1.2.3404.m1	nve:NEMVE_v1g243380	69.42	618	0
	GNMT	K00552 glycine N-methyltransferase	2.1.1.20	1.2.13833.m1	nve:NEMVE_v1g173936	66.56	311	4.00E-149
	SARDH	K00314 sarcosine dehydrogenase	1.5.8.3	1.2.1981.m1	nve:NEMVE_v1g174872	72.37	894	0
	MS	Methionine synthase	2.1.1.13	1.2.20586.m1	NP_932338.1	97	70	0
	SHMT	Serine hydroxymethyltransferase	2.1.2.1	1.2.6795.m1	XP_001625575.1	96	79	0
	MTHFR	Methylenetetrahydrofolate reductase	1.5.1.20	1.2.1458.m1	XP_001633891.1	93	70	0
Glycine synthesis	AGT	K00830 alanine-glyoxylate transaminase	2.6.1.44	1.2.7885.m1	nve:NEMVE_v1g112567	61.37	409	0
	AGT	K00827 alanine-glyoxylate transaminase	2.6.1.44	1.2.4389.m1	nve:NEMVE_v1g214753	40.18	453	1.00E-104
	TA	K01620 threonine aldolase	4.1.2.5	1.2.6387.m1	nve:NEMVE_v1g192932	66.12	245	8.00E-118
Glycine cleavage system	GLDC	K00281 glycine dehydrogenase	1.4.4.2	1.2.12004.m1	nve:NEMVE_v1g173380	75.13	571	0
	AMT	K00605 aminomethyltransferase	2.1.2.10	1.2.3288.m1	nve:NEMVE_v1g137645	71.57	313	1.00E-157
	DLD	K00382 dihydrolipoamide dehydrogenase	1.8.1.4	1.2.23266.m1	nve:NEMVE_v1g177276	75.15	511	0
Serine Biosynthesis	GLXR	K00049 glyoxylate/hydroxypyruvate reductase	1.1.1.79 1.1.1.81	1.2.4394.m1	nve:NEMVE_v1g159915	69.14	324	3.00E-160
	GPML	K15633 2,3-bisphosphoglycerate-independent phosphoglycerate mutase	5.4.2.12	1.2.1726.m1	nve:NEMVE_v1g183697	73.98	515	0
	3PGDH	K00058 D-3-phosphoglycerate dehydrogenase	1.1.1.95	1.2.6168.m1	nve:NEMVE_v1g170150	63.58	464	0
	PSAT1	K00831 phosphoserine aminotransferase	2.6.1.52	1.2.14345.m1	nve:NEMVE_v1g206542	65.48	336	4.00E-161
	PSPH	K01079 phosphoserine phosphatase	3.1.3.3	1.2.20067.m1	nve:NEMVE_v1g151322	65.91	44	9.00E-16
	SDS	K17989 L-serine/L-threonine deaminase	4.3.1.17 4.3.1.19	1.2.876.m1	nve:NEMVE_v1g241178	60.25	317	2.00E-129
Arginine metabolism	NOS1	K13240 nitric-oxide synthase, brain	1.14.13.39	1.2.890.m1	hsa:4842	45.66	1474	0
	NOS1	K13240 nitric-oxide synthase, brain	1.14.13.39	1.2.1319.m1	hsa:4842	45.3	1139	0
	ARG1	K01476 arginase	3.5.3.1	1.2.5621.m1	hsa:383	44.3	316	9.00E-92
	OAT	K00819 ornithine—oxo-acid transaminase	2.6.1.13	1.2.25616.m1	hsa:4942	62.2	455	0
	ALDH4A1	K00294 1-pyrroline-5-carboxylate dehydrogenase	1.2.1.88	1.2.12494.m1	hsa:8659	51.37	255	3.00E-85
Proline metabolism	PRODH	K00318 proline dehydrogenase	1.5.-.-	1.2.665.m1	hsa:102724788	48.79	248	5.00E-74
	PRODH	K00318 proline dehydrogenase	1.5.-.-	1.2.6653.m1	hsa:102724788	46.2	619	0
Glutamate metabolism	ALDH18A1	K12657 delta-1-pyrroline-5-carboxylate synthetase	2.7.2.11	1.2.21795.m1	hsa:5832	51.9	289	4.00E-80
L-glutamate degradation	GDH1	K00261 glutamate dehydrogenase (NADH)	1.4.1.3	1.2.12363.m1	nve:NEMVE_v1g243194	78.42	505	0
	NAGS	K11067 /N-acetylglutamate synthase	2.3.1.1	1.2.1353.m1	nve:NEMVE_v1g235893	50.15	327	1.00E-102
L-glutamate biosynthesis	GDH2	K00261 glutamate dehydrogenase (NADPH)	1.4.1.4	1.2.5656.m1	nve:NEMVE_v1g169502	75.73	445	0
	GOGAT	K00264 glutamate synthase (NADPH/NADH)	1.4.1.13	1.2.4000.m1	nve:NEMVE_v1g168875	67.42	1237	0
	GS	K01915 glutamine synthetase	6.3.1.2	1.2.21495.m1	hsa:2752	58.86	350	1.00E-151
	OPLAH	K01469 5-oxoprolinase (ATP-hydrolysing)	3.5.2.9	1.2.3712.m1	hsa:26873	57.98	1285	0
	CPS1	K01948 carbamoyl-phosphate synthase (ammonia)	6.3.4.16	1.2.23421.m1	hsa:1373	50.71	1477	0
	CPS1	K01948 carbamoyl-phosphate synthase (ammonia)	6.3.4.16	1.2.1352.m1	hsa:1373	65.46	1077	0
Glutathione REDOX	GSR	K00383 glutathione reductase (NADPH)	1.8.1.7	1.2.3068.m1	hsa:2936	37.45	486	5.00E-87
	GPx	K00432 glutathione peroxidase	1.11.1.9	1.2.3638.m1	hsa:2876	51.08	186	5.00E-63
	GPx	K00432 glutathione peroxidase	1.11.1.9	1.2.18589.m1	nve:NEMVE_v1g55851	42.11	114	2.00E-20
	GPx	K00432 glutathione peroxidase	1.11.1.9	1.2.11017.m1	nve:NEMVE_v1g81388	51.15	131	1.00E-41
	IDH1	K00031 isocitrate dehydrogenase	1.1.1.42	1.2.17652.m1	hsa:3417	67.57	404	0
	G6PD	K00036 glucose-6-phosphate 1-dehydrogenase	1.1.1.49	1.2.25769.m1	hsa:2539	67.02	470	0
	6PGD	K00033 6-phosphogluconate dehydrogenase	1.1.1.44	1.2.1905.m1	hsa:5226	69.65	481	0
	GSTO2	K00799 glutathione S-transferase	2.5.1.18	1.2.7742.m1	Cluster027041	99.58	236	6.00E-177
	GSTK1	K13299 glutathione S-transferase kappa 1	2.5.1.18	1.2.9677.m1	hsa:373156	42.65	272	5.00E-67
	GSTA4	K00799 glutathione S-transferase	2.5.1.18	1.2.22579.m1	hsa:2941	28.57	203	2.00E-14
	GSTO1	K00799 glutathione S-transferase	2.5.1.18	1.2.7897.m1	hsa:9446	43.78	217	2.00E-49
	GST	K00799 glutathione S-transferase	2.5.1.18	1.2.25046.m1	Cluster005175	99.26	136	2.00E-96
	GST	K00799 glutathione S-transferase	2.5.1.18	1.2.24505.m1	Cluster040146	96.3	135	1.00E-90
	GST	K00799 glutathione S-transferase	2.5.1.18	1.2.10776.m1	Cluster006475	99.42	344	0
	GGT	K18592 gamma-glutamyltranspeptidase	2.3.2.2	1.2.5072.m1	hsa:2678	43.03	588	4.00E-154
	ANPEP	K11140 aminopeptidase N	3.4.11.2	1.2.20802.m1	hsa:290	37.43	927	0
	ANPEP	K11140 aminopeptidase N	3.4.11.2	1.2.3061.m1	hsa:290	35.86	937	0

(B)

Coral ID	Gene name	Adults				Juveniles			
		1 h		24 h		24 h		48 h	
		log_2FC	FDR	log_2FC	FDR	log_2FC	FDR	log_2FC	FDR
1.2.6999.m1	CDH	–	–	–	–	–	–	–	–
1.2.25403.m1	ALDH7A1	0.42	1.68E-03	0.95	4.93E-10	–	–	–	–
1.2.8566.m1	BHMT	2.09	3.89E-139	2.52	6.39E-70	3.86	0.00E+00	4.02	0.00E+00
1.2.19413.m1	BHMT	–	–	5.43	2.38E-69	1.19	5.15E-12	1.07	3.85E-03
1.2.3404.m1	DMGDH	1.13	8.99E-22	2.19	1.06E-42	2.75	0.00E+00	2.68	2.54E-128
1.2.13833.m1	GNMT	1.56	2.39E-14	2.07	7.39E-41	2.70	6.16E-155	2.76	5.02E-249
1.2.1981.m1	SARDH	0.79	1.82E-13	1.61	5.25E-29	1.73	6.65E-176	1.72	9.41E-121
1.2.20586.m1	MS	–	–	-0.62	1.54E-04	-0.82	3.80E-74	-0.73	5.35E-11
1.2.6795.m1	SHMT	–	–	–	–	-0.40	5.28E-05	-0.38	1.86E-04
1.2.1458.m1	MTHFR	-1.02	6.56E-22	-1.72	6.65E-10	-2.63	5.00E-239	-2.61	3.13E-88
1.2.7885.m1	AGT	–	–	0.99	2.38E-12	0.29	9.44E-07	–	–
1.2.4389.m1	AGT	0.53	3.04E-03	1.16	6.64E-11	0.80	6.73E-34	0.72	2.20E-12
1.2.6387.m1	TA	–	–	0.86	1.57E-02	–	–	–	–
1.2.12004.m1	GLDC	–	–	–	–	-0.19	1.27E-02	–	–
1.2.3218.m1	AMT	–	–	–	–	-0.43	4.99E-03	–	–
1.2.23266.m1	DLD	–	–	–	–	–	–	–	–
1.2.4394.m1	GLXR	–	–	–	–	0.20	2.08E-02	–	–
1.2.1726.m1	GPML	-0.45	1.92E-03	–	–	0.14	2.62E-02	–	–
1.2.6168.m1	3PGDH	-0.60	1.04E-06	-0.77	5.04E-03	-0.57	9.34E-12	-0.53	3.87E-04
1.2.14345.m1	PSAT1	-0.40	7.99E-03	–	–	0.17	5.34E-02	–	–
1.2.20067.m1	PSPH	-1.13	3.67E-02	–	–	0.29	5.68E-02	0.61	8.90E-04
1.2.876.m1	SDS	–	–	–	–	-0.32	2.26E-02	-0.66	7.68E-03
1.2.890.m1	NOS1	–	–	-0.70	5.51E-03	–	–	–	–
1.2.1319.m1	NOS1	-2.27	5.38E-06	-2.99	3.43E-06	–	–	–	–
1.2.5621.m1	ARG1								
1.2.25616.m1	OAT	–	–	0.52	2.16E-05	–	–	–	–
1.2.12494.m1	ALDH4A1	0.79	2.17E-04	1.51	1.10E-11	–	–	–	–
1.2.665.m1	PRODH	–	–	1.10	5.41E-10	1.23	3.27E-70	0.76	1.80E-06
1.2.6653.m1	PRODH	0.93	1.04E-09	1.06	1.25E-06	1.31	5.45E-51	0.89	1.28E-02
1.2.21795.m1	ALDH18A1	–	–	–	–	–	–	0.31	5.97E-03
1.2.12363.m1	GDH1	0.47	1.21E-02	2.54	4.28E-55	0.24	4.59E-03	–	–
1.2.1353.m1	NAGS	0.56	1.87E-06	0.50	2.15E-02	–	–	–	–
1.2.5656.m1	GDH2	-0.80	1.46E-06	-2.40	1.74E-21	-0.17	4.59E-02	–	–
1.2.4000.m1	GOGAT	-0.24	1.49E-02	-0.70	1.43E-07	-0.38	2.31E-05	–	–
1.2.21495.m1	GS	-0.92	4.10E-15	-1.54	7.72E-21	-0.29	8.93E-06	–	–
1.2.3712.m1	OPLAH	–	–	-0.39	1.97E-02	-0.29	1.28E-07	–	–
1.2.23421.m1	CPS1	–	–	0.86	4.22E-07	–	–	–	–
1.2.1352.m1	CPS1	–	–	–	–	-0.35	6.31E-07	–	–
1.2.3068.m1	GSR	-0.23	4.01E-02	0.43	7.29E-03	0.52	1.30E-50		
1.2.3638.m1	GPx	-0.38	1.30E-03	-1.08	7.61E-10	–	–	–	–
1.2.18589.m1	GPx	-0.37	9.84E-03	–	–	–	–	–	–
1.2.11017.m1	GPx	–	–	-1.12	3.49E-03	-0.44	5.96E-05	-0.45	3.36E-04
1.2.17652.m1	IDH1	–	–	-0.64	4.73E-06	–	–	–	–
1.2.25769.m1	G6PD	–	–	-0.36	4.22E-02	–	–	–	–
1.2.1905.m1	6PGD	-0.27	5.60E-02	0.57	5.54E-05	–	–	–	–
1.2.7742.m1	GSTO2	-1.40	2.25E-02	-1.59	1.78E-02	-1.60	3.24E-10	–	–
1.2.9677.m1	GSTK1	–	–	0.85	1.27E-03	0.49	9.63E-15	–	–
1.2.22579.m1	GSTA4	-0.38	5.35E-03	0.80	3.38E-05	0.33	2.30E-10	–	–
1.2.7897.m1	GSTO1	–	–	0.61	2.15E-05	-0.13	5.87E-02	–	–
1.2.25046.m1	GST	–	–	0.82	1.92E-04	–	–	–	–
1.2.24505.m1	GST	–	–	1.56	1.43E-08	–	–	–	–
1.2.10776.m1	GST	–	–	–	–	0.55	9.03E-15	–	–
1.2.5072.m1	GGT	–	–	-1.52	1.15E-08	-0.29	1.14E-03	–	–
1.2.20802.m1	ANPEP	–	–	-0.58	1.96E-05	–	–	0.22	2.35E-02
1.2.3061.m1	ANPEP	–	–	–	–	-0.55	1.43E-02	–	–

Table S3.5 *A. millepora* homologues to membrane transporter. (A) Results of the KEGG transporters searched in the *A. millepora* protein predictions. (B) Log_2FC values of significantly expressed (FDR <0.05) genes in response to the treatment (hypo-saline) over the control (35 PSU). Log_2FC colour indicates up (red) and down (blue) regulated genes.

(A)

Function	Gene name	Gene ID	Blast details				
			Coral ID	Entry	% ID	Length	e-value
Solute carriers							
Bicarbonate transporters	SLC4A2	Anion exchange protein 2	1.2.16219.m1	Cluster000158m	96.25	960	0.00E+00
	SLC4A2	Anion exchange protein 2	1.2.16234.m1	Cluster000158m	57.83	1086	0.00E+00
	SLC4A3	Solute carrier family 4, member 3	1.2.10500.m1	Cluster000926	36.84	912	0.00E+00
	SLC4A10	Solute carrier family 4, member 10	1.2.18778.m1	Cluster000926	100	1188	0.00E+00
	SLC4A11	Solute carrier family 4, member 11	1.2.10134.m1	Cluster001846	93.96	861	0.00E+00
Na^+ and CL^- dependent transporters	SLC6A1	Solute carrier family 6, member 1	1.2.2642.m1	gi|128609|sp|P23978.1	65%	591	0.00E+00
	SLC6A1	Solute carrier family 6, member 1	1.2.7193.m1	gi|229462780|sp|P30531.2	62.20%	583	2.90E-141
	SLC6A5	Solute carrier family 6, member 5	1.2.764.m1	gi|145885602|gb|ES391184.1	44.27	192	2.00E-48
	SLC6A5	Solute carrier family 6, member 5	1.2.6220.m1	gi|52783378|sp|Q761V0.1	58%	564	2.10E-157
	SLC6A5	Solute carrier family 6, member 5	1.2.25412.m1	gi|52783378|sp|Q761V0.1	61.80%	660	2.60E-170
	SLC6A5	Solute carrier family 6, member 5	1.2.6219.m1	gi|52783378|sp|Q761V0.1	62.60%	605	1.30E-178
	SLC6A11	Solute carrier family 6, member 11	1.2.21883.m1	gi|400626|sp|P31647.1	65.20%	534	2.10E-165
	SLC6A11	Solute carrier family 6, member 11	1.2.11757.m1	gi|341942004|sp|P31650.2	68.40%	560	0.00E+00
	SLC6A13	Solute carrier family 6, member 13	1.2.21427.m1	gi|209573786|sp|A5PJX7.1	57.60%	690	3.10E-104
	SLC6A13	Solute carrier family 6, member 13	1.2.14967.m1	gi|400624|sp|P31646.1	63.80%	674	0.00E+00
	SLC6A13	Solute carrier family 6, member 13	1.2.21418.m1	gi|400624|sp|P31646.1	60.20%	643	2.60E-121
	SLC6A18	Solute carrier family 6, member 18	1.2.2523.m1	gi|48429099|sp|Q62687.1	60.60%	754	2.00E-156
	SLC6A18	Solute carrier family 6, member 18	1.2.4717.m1	gi|48429108|sp|O88576.1	63.40%	663	1.20E-170
	SLC6A19	Solute carrier family 6, member 19	1.2.7241.m1	gi|73919285|sp|Q695T7.1	63.80%	657	7.80E-147
	SLC6A19	Solute carrier family 6, member 19	1.2.2521.m1	gi|73919287|sp|Q5R6J1.1	52%	767	1.70E-90
	SLC6A19	Solute carrier family 6, member 19	1.2.20969.m1	gi|73919287|sp|Q5R6J1.1	52.60%	433	4.20E-68
Na^+/Ca^{2+} exchanger	NAC3	Solute carrier family 8, member 3	1.2.14821.m1	gi|2498054|sp|P70549.1	53%	804	1.10E-125
	NAC2	Solute carrier family 8, member 2	1.2.14679.m1	gi|10720116|sp|Q9UPR5.2	44.80%	886	1.90E-102
Na^+/H^+ exchanger	SLC9	Solute carrier family 9	1.2.622.m1	Cluster004770	83.23	662	0.00E+00
	SLC9A2	Solute carrier family 9, member 2	1.2.2250.m1	Cluster005704	99.6	755	0.00E+00
	SLC9A8	Solute carrier family 9, member 8	1.2.16650.m1	Cluster007852	99.83	594	0.00E+00
	SLC9A9	Solute carrier family 9, member 9	1.2.2407.m1	Cluster006121	90.94	629	0.00E+00
	SLC9A9	Solute carrier family 9, member 9	1.2.20148.m1	Cluster006121	53.95	569	0.00E+00
	SLC9B2	Solute carrier family 9 subfamily b member 2	1.2.4134.m1	gi|341941171|sp|Q5BKR2.2	63%	531	2.00E-111
	SLC9C1	Solute carrier family 9, member C1	1.2.1836.m1	gi|158563886|sp|Q4G0N8.2	50.80%	881	6.60E-83
Monocarboxylate transporter	SLC16A3	Monocarboxylate transporter 3	1.2.16615.m1	gi|149383394|gb|ES738463.1	34.85	132	4.00E-19
Vesicular glutamate transporter	SLC17A5	Solute carrier family 17, member 5	1.2.21296.m1	gi|145883711|gb|ES389293.1	35.96	178	5.00E-31
	SLC17A5	Solute carrier family 17, member 5	1.2.312.m1	hsa:26503	41.06	453	1.00E-103
$Na^+/(Ca^{2+}-K^+)$ exchanger	SLC24A1	Solute carrier family 24	1.2.457.m1	Cluster033035	100	141	1.00E-97
	SLC24A2	Solute carrier family 24 member 2	1.2.7150.m1	gi|17865498|sp|O54701.1	56.60%	659	5.20E-132
	SLC24A4	Solute carrier family 24, member 4	1.2.13525.m1	Cluster006401	99.28	553	0.00E+00
	SLC24A4	Solute carrier family 24, member 4	1.2.4324.m1	Cluster011028	20.2	510	4.00E-24
	SLC24A5	Solute carrier family 24, member 5	1.2.17180.m1	Cluster009582	51.58	444	4.00E-152
	SLC24A5	Solute carrier family 24, member 5	1.2.20341.m1	Cluster008099	93.65	567	0.00E+00
	SLC24A5	Solute carrier family 24, member 5	1.2.17183.m1	Cluster009582	98.66	449	0.00E+00
	SLC24A5	Solute carrier family 24, member 5	1.2.6851.m1	Cluster054035	57.45	94	8.00E-29
	SLC24A6	Solute carrier family 24, member 6	1.2.6296.m1	Cluster011028	98.21	336	0.00E+00
Mitochondrial carrier	SLC25A17	Solute carrier family 25, member 17	1.2.22387.m1	hsa:10478	53.51	271	3.00E-89
	SLC25A17	Solute carrier family 25, member 17	1.2.22651.m1	hsa:10478	31.43	245	2.00E-31
Multifunctional anion exchanger	SLC26A1	Solute carrier family 26	1.2.10089.m1	Cluster004291	62.45	719	0.00E+00
	SLC26A1	Solute carrier family 26	1.2.22559.m1	Cluster004291	93.23	739	0.00E+00
	SLC26A1	Solute carrier family 26	1.2.18457.m1	Cluster004248	92.53	790	0.00E+00
	SLC26A1	Solute carrier family 26	1.2.13625.m1	Cluster004980	76.83	574	0.00E+00
	SLC26A1	Solute carrier family 26	1.2.13627.m1	Cluster004980	72.92	288	4.00E-136

ATPases							
Na^+/K^+ transporting	ATP1A1	Na+/K+-ATPase alpha subunit	12.17116.m1	gi|149381259|gb|ES736328.1	61.17	188	2.00E-62
	ATP1A1	Na+/K+-ATPase alpha subunit	12.17104.m1	gi|149381259|gb|ES736328.1	63.33	150	5.00E-52
Ca++ transporting	ATP2C1	Calcium-transporting ATPase type 2C member 1	12.15136.m1	Cluster000652.m	100	919	0.00E+00
H^+ transporting, lysosomal	VAS1	V-type H+ transporting ATPase subunit S1	12.17585.m1	Cluster011030	100	462	0.00E+00
	ATP6B	V-type H+-transporting ATPase subunit B	12.1144.m1	nve.NEMVE_v1g99968	94.8	481	0
	VATD	V-type proton ATPase subunit D	12.15346.m1	Cluster017889	93.9	246	9.00E-162
	ATP6H	V-type H+-transporting ATPase subunit e	12.964.m1	nve.NEMVE_v1g192225	63.46	52	3.00E-17
	ATPeV1H	V-type H+-transporting ATPase subunit H	12.9026.m1	nve.NEMVE_v1g164874	60.04	468	0
	ATPeV1G	V-type H+-transporting ATPase subunit G	12.2284.m1	nve.NEMVE_v1g191954	70.43	115	5.00E-51
	ATPeV1E	V-type H+-transporting ATPase subunit E	12.14605.m1	nve.NEMVE_v1g237075	76.55	226	3.00E-121
	VA0D1	V-H+ATPase subunit a1-IV	12.15120.m1	Cluster009028	99.72	357	0.00E+00
	VPP1	V-H+ATPase subunit a1-IV	12.8634.m1	Cluster005272	99.53	856	0.00E+00
	VATF	V-type proton ATPase	12.11894.m1	Cluster028816	100	126	4.00E-89
	VATL	V-type proton ATPase	12.22335.m1	Cluster018458p	91.6	131	1.00E-75
ER	VCP	Transitional endoplasmic reticulum ATPase	12.19057.m1	nve.NEMVE_v1g190325	87.86	807	0
Potassium channels	KCTD3	Potassium voltage-gated shaker-related	12.15258.m1	gi|112823993|sp|Q9Y597.2	73.80%	654	0.00E+00
	KCNAW	Potassium voltage-gated shaker-related	12.22013.m1	gi|116444|sp|P17972.1	57%	1486	2.10E-105
	KCNQ	Potassium voltage-gated channel KQT-like subfamily	12.11257.m1	nve.NEMVE_v1g99775	68.23	277	2.00E-113
	KCNA1	Potassium voltage-gated shaker-related	12.25102.m1	gi|116420|sp|P16388.1	66.20%	509	1.10E-127
	KCNC1	Potassium voltage-gated channel Shaw-related subfamily C member 1	12.7045.m1	nve.NEMVE_v1g21646	79.9	403	0
	KCD20	Potassium voltage-gated shaker-related	12.21228.m1	gi|74750149|sp|Q7Z5Y7.1	82.20%	397	4.30E-131
	KCNA2	Potassium voltage-gated shaker-related member 10	12.5849.m1	gi|74575576|sp|Q09081.2	74%	565	2.10E-148
	KCNA2	Potassium voltage-gated shaker-related	12.15380.m1	gi|74575576|sp|Q09081.2	56.20%	488	8.40E-72
	BACD3	Potassium voltage-gated shaker-related	12.857.m1	gi|74733570|sp|Q9H3F6.1	81.80%	286	2.60E-130
	KCNA5	Potassium voltage-gated shaker-related member 10	12.8080.m1	gi|145882999|gb|ES388581.1	43.44	244	9.00E-53
	KCND2	Potassium voltage-gated channel Shal-related subfamily D	12.7519.m1	nve.NEMVE_v1g135889	84.71	484	0
	KCNH6	Potassium voltage-gated channel Eag-related subfamily H member 6	12.6126.m1	nve.NEMVE_v1g236199	73.87	532	0
	KCNA2	Potassium voltage-gated shaker-related	12.14042.m1	gi|82221700|sp|Q91830.1	57.20%	477	3.80E-76
Calcium channels	CAC1M	Voltage-dependent calcium channel alpha-1	12.23113.m1	nve.NEMVE_v1g88037	69.55	1051	0
	CACB4	Voltage-dependent L-type calcium channel beta-4	12.13199.m1	Cluster013385	100	336	0.00E+00
	CAC1H	Voltage-dependent T-type calcium channel alpha-1 subunit	12.13780.m1	Cluster046091	60.63	127	3.00E-48
	CAC1A	Voltage-dependent calcium channel alpha-1	12.10389.m1	Cluster000649	99.73	1477	0.00E+00
	CAC1A	Voltage-dependent calcium channel alpha-1	12.20611.m1	Cluster000601	44.61	1652	0.00E+00
	CA2D3	Voltage-dependent calcium channel alpha-2-3	12.718.m1	Cluster001718	99.82	551	0.00E+00
	CAC1A	Voltage-dependent P/Q-type calcium channel subunit alpha-1A	12.8465.m1	Cluster000649	47.55	1123	0.00E+00
	CACB2	Voltage-dependent L-type calcium channel beta	12.16220.m1	Cluster013385	46.25	240	2.00E-68
	CA2D3	Voltage-dependent calcium channel alpha-2	12.11288.m1	Cluster003383	29.26	1063	2.00E-113
	CA2D3	Voltage-dependent calcium channel alpha-2	12.15641.m1	Cluster003383	95.21	1085	0.00E+00
	CAC1H	Voltage-dependent T-type calcium channel alpha-1 subunit	12.26803.m1	Cluster046091	100	127	9.00E-82
Calcium Transporters	XCAT2	Calcium Transporter 3	12.21155.m1	Cluster001782	99.67	918	0.00E+00
	XCAT2	Calcium Transporter 4	12.21164.m1	Cluster007604	93.27	550	0.00E+00
	XCAT2	Calcium Transporter 2	12.21162.m1	Cluster001782	53.49	787	0.00E+00
Aquaporin	AQP	Aquaporin-3	12.11520.m1	gi|1351966|sp|P47862.1	48.06	283	1.00E-80
	AQP	Aquaporin-3	12.11518.m1	gi|1351966|sp|P47862.1	47.72	285	8.00E-87
	AQP	Aquaporin-3	12.11517.m1	gi|1351966|sp|P47862.1	51.68	238	8.00E-75
Receptors	NacrA5	Nicotinic acetylcholine receptor subunit a5	12.13318.m1	gi|145890050|gb|ES395632.1	28.47	295	1.00E-30

(B)

Coral ID	Gene name	Adults				Juveniles			
		1h		24h		24h		48h	
		$\log_2$FC	FDR	$\log_2$FC	FDR	$\log_2$FC	FDR	$\log_2$FC	FDR
1.2.16219.m1	SLC4A2	0.50	8.35E-08	–	–	–	–	–	–
1.2.16234.m1	SLC4A2	-0.48	3.87E-03	–	–	–	–	–	–
1.2.10500.m1	SLC4A3	–	–	1.66	3.16E-04	–	–	–	–
1.2.18778.m1	SLC4A10	-0.49	5.91E-07	-0.81	2.84E-11	–	–	–	–
1.2.10134.m1	SLC4A11	–	–	–	–	–	–	–	–
1.2.2642.m1	SLC6A1	–	–	–	–	–	–	–	–
1.2.7193.m1	SLC6A1	–	–	–	–	–	–	–	–
1.2.764.m1	SLC6A5	0.62	1.48E-04	0.93	2.85E-08	-0.20	1.89E-02	–	–
1.2.6220.m1	SLC6A5	-0.40	3.09E-02	-1.25	2.64E-22	-0.75	7.65E-13	–	–
1.2.25412.m1	SLC6A5	–	–	–	–	-0.44	3.23E-06	-0.34	1.12E-02
1.2.6219.m1	SLC6A5	-0.52	1.43E-06	-0.75	7.36E-07	–	–	–	–
1.2.21883.m1	SLC6A11	-0.67	9.27E-06	-1.24	2.65E-10	-0.38	2.58E-08	-0.50	3.85E-10
1.2.11757.m1	SLC6A11	–	–	-1.21	2.34E-02	–	–	–	–
1.2.21427.m1	SLC6A13	-0.27	7.48E-03	–	–	–	–	0.34	4.22E-02
1.2.14967.m1	SLC6A13	–	–	-1.20	3.06E-09	–	–	–	–
1.2.21418.m1	SLC6A13	–	–	–	–	–	–	–	–
1.2.2523.m1	SLC6A18	–	–	-0.77	2.76E-02	–	–	–	–
1.2.4717.m1	SLC6A18	–	–	–	–	0.25	2.69E-02	0.51	1.35E-07
1.2.7241.m1	SLC6A19	–	–	-0.81	2.17E-05	0.23	7.11E-03	0.44	2.35E-04
1.2.2521.m1	SLC6A19	–	–	–	–	–	–	–	–
1.2.20969.m1	SLC6A19	–	–	–	–	–	–	–	–
1.2.14821.m1	NAC3	0.60	1.32E-06	–	–	–	–	–	–
1.2.14679.m1	NAC2	–	–	–	–	–	–	–	–
1.2.622.m1	SLC9	–	–	-0.53	1.72E-02	-0.29	2.17E-04	–	–
1.2.2250.m1	SLC9A2	–	–	–	–	–	–	–	–
1.2.16650.m1	SLC9A8	-0.36	1.17E-02	–	–	–	–	–	–
1.2.2407.m1	SLC9A9	–	–	–	–	–	–	–	–
1.2.20148.m1	SLC9A9	–	–	–	–	–	–	–	–
1.2.4134.m1	SLC9B2	–	–	–	–	–	–	–	–
1.2.1836.m1	SLC9C1	–	–	–	–	–	–	–	–
1.2.16615.m1	SLC16A3	–	–	-2.43	2.71E-04	-0.59	7.07E-04	–	–
1.2.21296.m1	SLC17A5	–	–	–	–	-0.61	1.22E-02	–	–
1.2.312.m1	SLC17A5	–	–	0.63	7.74E-04	–	–	–	–
1.2.457.m1	SLC24A1	–	–	–	–	–	–	–	–
1.2.7150.m1	SLC24A2	–	–	–	–	–	–	–	–
1.2.13525.m1	SLC24A4	0.58	1.26E-04	-1.50	1.31E-12	-0.54	1.32E-03	–	–
1.2.4324.m1	SLC24A4	–	–	–	–	-0.37	4.53E-02	–	–
1.2.17180.m1	SLC24A5	–	–	-0.90	7.76E-03	-0.52	1.27E-04	–	–
1.2.20341.m1	SLC24A5	–	–	-1.45	2.39E-03	0.62	3.32E-04	–	–
1.2.17183.m1	SLC24A5	–	–	–	–	-0.20	4.58E-02	–	–
1.2.6851.m1	SLC24A5	–	–	–	–	–	–	–	–
1.2.6296.m1	SLC24A6	0.36	7.87E-04	–	–	–	–	–	–
1.2.22387.m1	SLC25A17	–	–	–	–	0.22	6.43E-04	–	–
1.2.22651.m1	SLC25A17	–	–	0.61	6.06E-03	0.32	3.57E-06	–	–
1.2.10089.m1	SLC26A1	-1.81	3.18E-34	-2.61	7.14E-105	1.00	4.44E-11	–	–
1.2.22559.m1	SLC26A1	-0.69	4.20E-03	-2.64	1.05E-23	–	–	–	–
1.2.18457.m1	SLC26A1	–	–	–	–	0.23	7.08E-04	0.28	1.38E-02
1.2.13625.m1	SLC26A1	–	–	–	–	–	–	0.40	1.35E-02
1.2.13627.m1	SLC26A1	–	–	–	–	–	–	–	–

1.2.17116.m1	ATP1A1	-0.73	9.23E-23	-1.00	7.73E-13	-0.14	2.57E-03	0.29	3.91E-03
1.2.17104.m1	ATP1A1	–	–	–	–	0.34	2.81E-02	0.58	1.59E-03
1.2.15136.m1	ATP2C1	–	–	-0.52	4.25E-03	-0.27	4.33E-03	–	–
1.2.17585.m1	VAS1	–	–	–	–	–	–	–	–
1.2.1144.m1	ATP6B	–	–	0.63	2.98E-06	0.20	2.72E-03	–	–
1.2.15346.m1	VATD	-0.33	1.77E-02	–	–	–	–	–	–
1.2.964.m1	ATP6H	–	–	0.64	6.94E-03	0.20	2.33E-02	–	–
1.2.9026.m1	ATPeV1H	–	–	0.76	3.78E-06	0.18	9.54E-04	–	–
1.2.2284.m1	ATPeV1G	-0.39	2.80E-03	–	–	–	–	–	–
1.2.14605.m1	ATPeV1E	-0.32	2.29E-02	0.46	1.94E-02	–	–	–	–
1.2.15120.m1	VA0D1	-0.26	4.74E-02	–	–	–	–	–	–
1.2.8634.m1	VPP1	–	–	0.41	7.85E-03	–	–	–	–
1.2.11894.m1	VATF	–	–	–	–	–	–	–	–
1.2.22335.m1	VATL	–	–	–	–	–	–	–	–
1.2.19057.m1	VCP	-0.24	1.01E-02	0.84	1.82E-11	–	–	–	–
1.2.15258.m1	KCTD3	0.52	4.02E-04	–	–	–	–	–	–
1.2.22013.m1	KCNAW	0.53	2.47E-02	–	–	–	–	–	–
1.2.11257.m1	KCNQ	0.44	2.03E-03	–	–	-0.30	4.99E-04	–	–
1.2.5102.m1	KCNA1	–	–	1.12	1.90E-02	–	–	–	–
1.2.7045.m1	KCNC1	–	–	0.85	2.31E-03	–	–	–	–
1.2.21228.m1	KCD20	–	–	0.42	3.79E-02	–	–	–	–
1.2.5849.m1	KCNA2	-0.85	2.00E-04	-0.80	9.42E-03	–	–	–	–
1.2.15380.m1	KCNA2	-0.88	3.98E-02	-1.75	1.01E-03	–	–	–	–
1.2.857.m1	BACD3	-0.31	3.05E-02	–	–	–	–	–	–
1.2.8080.m1	KCNAS	–	–	-1.04	1.63E-05	-0.21	5.79E-02	-0.32	4.60E-03
1.2.7519.m1	KCND2	–	–	–	–	-0.27	3.09E-02	–	–
1.2.6126.m1	KCNH6	–	–	-0.75	2.54E-03	–	–	–	–
1.2.14042.m1	KCNA2	–	–	-1.90	5.70E-04	–	–	–	–
1.2.3113.m1	CAC1M	–	–	-0.89	2.60E-08	–	–	–	–
1.2.13199.m1	CACB4	–	–	-0.89	3.89E-02	–	–	–	–
1.2.13780.m1	CAC1H	–	–	-0.80	1.32E-08	–	–	–	–
1.2.10389.m1	CAC1A	–	–	–	–	-0.22	2.61E-02	–	–
1.2.20611.m1	CAC1A	–	–	–	–	-0.21	3.83E-02	–	–
1.2.718.m1	CA2D3	–	–	–	–	–	–	–	–
1.2.8465.m1	CAC1A	–	–	–	–	–	–	–	–
1.2.16220.m1	CACB2	–	–	–	–	–	–	–	–
1.2.11288.m1	CA2D3	–	–	–	–	–	–	–	–
1.2.15641.m1	CA2D3	–	–	–	–	–	–	–	–
1.2.6803.m1	CAC1H	–	–	–	–	–	–	–	–
1.2.1155.m1	XCAT2	1.02	4.81E-02	–	–	–	–	–	–
1.2.1164.m1	XCAT2	–	–	-1.49	2.55E-02	–	–	–	–
1.2.1162.m1	XCAT2	–	–	–	–	–	–	–	–
1.2.11520.m1	AQP	–	–	-3.39	5.51E-11	-0.36	1.41E-03	–	–
1.2.11518.m1	AQP	–	–	-0.66	1.35E-05	-0.19	7.93E-03	-0.24	2.86E-02
1.2.11517.m1	AQP	–	–	–	–	–	–	–	–
1.2.13318.m1	Nacra5	–	–	-1.70	6.49E-17	-0.44	5.74E-04	–	–

Table S3.6 Comparison between data presented here on the transcriptomic response of the coral *A millipora* to hypo-saline conditions and published gene expression and proteomic studies in marine invertebrates.

Gene name	Species	Type of treatment
uperoxide dismutase		
GRP94		

A. millepora	Hypo-saline	Adults	↑	24 h	RNAseq	1.2.21656.m1	Aguilar, Chapter 3

Figures

Figure S3.1 Principal component analysis (PCA) from the normalized expression values of 26,622 genes in coral adults and juveniles. (A) Adults, each colour represents a colony (C1-C5, n=4 per colony). (B) Juveniles, each colour represents a salinity treatment (n=11 per treatment). Samples encircled by dashed represent 24 h (orange) and 48 h (grey) after the salinity treatment. PCA was generated by "arrayQualityMetrics" (Kauffmann *et al.* 2009).

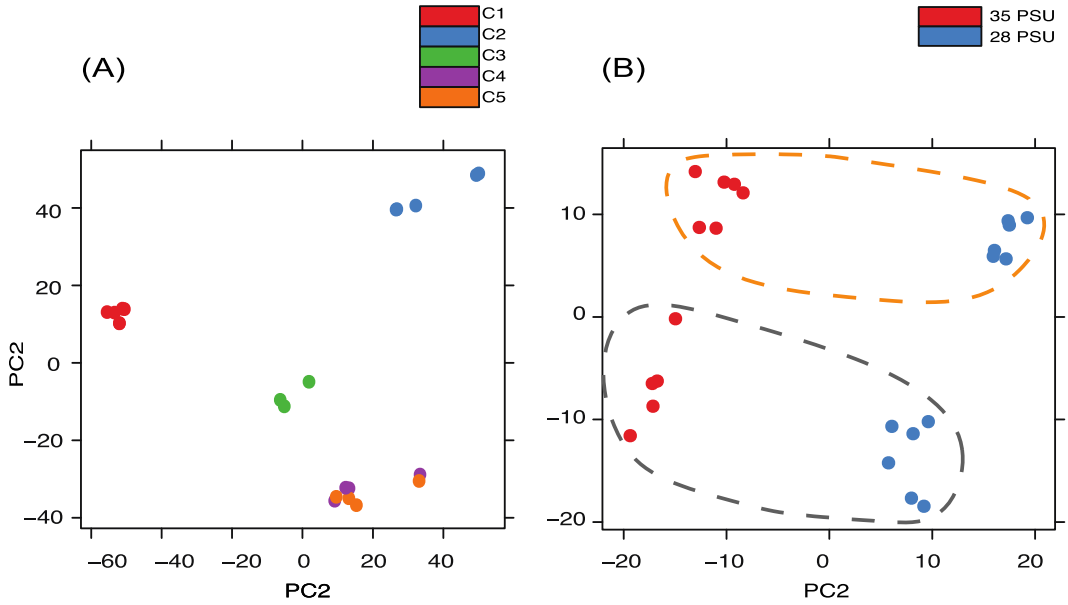

Figure S3.2 Total number of differentially expressed genes (DEGs) (FDR< 0.05) for each dataset. With the corresponding number of up-regulated (red) and down-regulated (blue) genes.

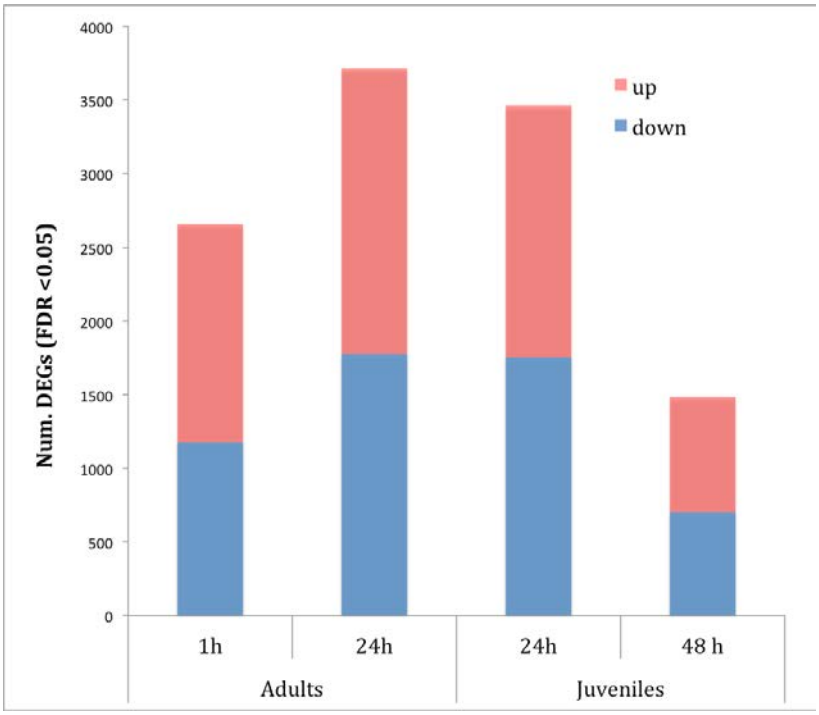

Figure S3.3 Venn diagrams of the differentially expressed genes (FDR< 0.05) after 24 h hypo-saline stress that were up- (red) and down- (blue) regulated in the adults and juveniles *A. millepora* corals. Indicating the subset of shared genes between each set of expression.

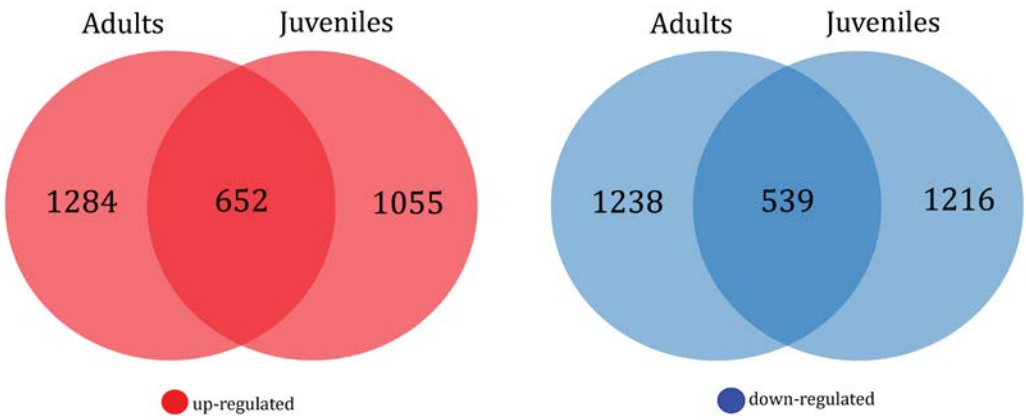

Chapter 4

Transcriptomic analysis of the response of *Acropora millepora* to hypo-osmotic stress provides insights into DMSP biosynthesis by corals

4.1. Introduction

Dimethylsulphoniopropionate (DMSP) and its volatile breakdown product dimethylsulphide (DMS) are key intermediates in the global sulphur cycle; the conversion of DMSP to DMS delivers biogenically-derived sulphate aerosols into the marine boundary layer, thereby transferring sulphur from the oceans to the atmosphere (Andreae & Crutzen 1997). DMS can subsequently be oxidized into sulphate particles and when combined with ultrafine sea salt and other marine organic aerosols, contributes to the formation of clouds, increasing their reflectance, thereby acting in local climate regulation (Ayers & Gras 1991). While DMSP is produced by several classes of algae and a few higher plants (Caruana 2010; Stefels 2000), coral reefs are hotspots of DMSP production due primarily to the high densities of the dinoflagellate *Symbiodinium* present in coral tissues (Broadbent *et al.* 2002; Jones *et al.* 2008). In addition, it has recently been demonstrated that the coral animal itself can produce DMSP (Raina *et al.* 2013). However, the molecular mechanisms underlying the production of DMSP by corals are unknown and are only partially understood in other organisms.

DMSP biosynthesis is thought to have evolved independently at least three times; two different pathways have been described in higher plants (Hanson *et al.* 1994; Kocsis *et al.* 1998), and a third, demonstrated in the marine macroalga *Ulva intestinales* (Gage *et al.* 1997), is also likely to operate in several phytoplankton species (Figure 4.1). The common denominator in these three pathways is the use of the sulphur-containing amino acid, methionine as a precursor. The chemical identities of the intermediates in the pathways have largely been established, providing insights into the classes of enzyme likely to be involved. However, at this time, the identities of the genes involved are unknown. Candidates for roles in the algal pathway have emerged from proteomic and gene expression analyses under conditions that lead to increased DMSP production. Proteomic analyses of DMSP-producing diatoms implicated particular aminotransferases, reductases, methyltransferases and decarboxylases in the algal DMSP biosynthesis pathway (Kettles *et al.* 2014; Lyon *et al.* 2011)

on the basis of their increased abundance under hypersaline conditions, though their involvement in DMSP synthesis remains to be confirmed.

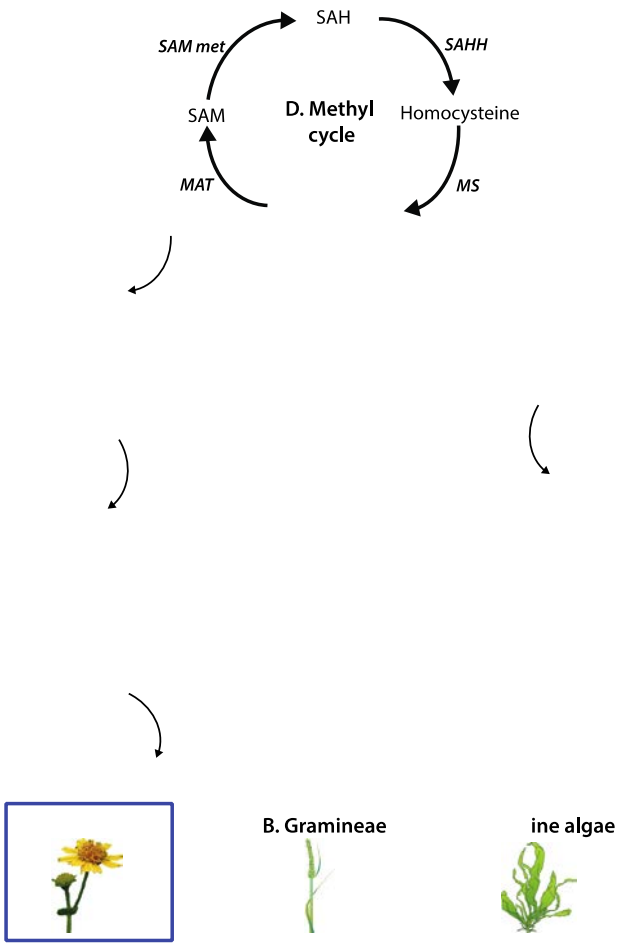

Figure 4.1 Pathways of DMSP biosynthesis in higher plants and marine algae (adapted from (Stefels 2000). (A) Compositae pathway (described in *Wollastonia biflora)*. (B) Gramineae pathway (described in *Spartina alterniflora*). (C) Pathway in marine algae (described in *Ulva intestinales*). (D) Methyl cycle and the enzymes involved in methionine biosynthesis. Dimethylsulphonio-2-hydroxybutyrate (DMSHB); dimethylsulphoniopropionate (DMSP); DMSP-aldehyde (DMSP-ald); 4-methylthio-2-hydroxybutyrate (MTHB); 2-oxo-4-mehtylthiobutanoate (MTOB); S-adenosylhomocysteine (SAH); S-adenosylmethione (SAM); S-methylmethionine (SMM). Enzyme types and associated cofactors are shown in italics (refer to Table 4.1 for the enzyme names).

A range of biological functions have been attributed to DMSP; it can act as an osmolyte (Dickson *et al.* 1980) or cryoprotectant (Karsten *et al.* 1996; Nishiguchi & Somero 1992). DMSP and its breakdown products acrylate, DMS and dimethylsulfoxide (DMSO) also

possess antioxidant capabilities, and are capable of scavenging hydroxyl radicals and reactive oxygen species (ROS), suggesting potential functions in the stress responses of organisms such as corals (Deschaseaux *et al.* 2014). Whilst the potential involvement of DMSP in ROS-scavenging in corals has been raised (Raina *et al.* 2013), osmoregulatory roles remain an additional possibility. Although corals have traditionally been thought of as stenohaline osmo-conformers, shallow water corals can experience major fluctuations in salinity and must therefore have mechanisms to tolerate these environmental conditions. Currently limited data are available on the effects of hyperosmotic stress on corals, but there is evidence that corals can tolerate acute exposure to hypersaline (40 PSU) conditions (Porter *et al.* 1999). Moreover, coral reefs occur in the Arabian Gulf and Gulf of Oman at 40-42 PSU, and appear to be adapted to these conditions (Coles 2002). On the Great Barrier Reef (GBR), rain associated with tropical cyclones can lower the salinity of surface waters significantly (up to 7-10 PSU) (Van Woesik *et al.* 1995), with these hyposaline conditions prevailing for weeks (Devlin *et al.* 1998). Hyposaline conditions can lead to coral mortality and changes in coral community composition; however, the response seems to vary among species and through time (Berkelmans *et al.* 2012). Heavy rainfall, induced by the increased occurrence and intensity of tropical storms and cyclones (Xie *et al.* 2010), is likely to expose coral reefs to more extreme and sudden salinity variations.

The genome of the reef-building coral *Acropora millepora* encodes orthologs of the reductase and methyltransferase (Fig 4.1C, steps 2 and 3) implicated in DMSP biosynthesis in algae, suggesting that corals also use an algal-like pathway to produce DMSP from methionine (Raina *et al.* 2013). To better understand the role and route of DMSP production in corals, the transcriptomic response of *A. millepora* to salinity stress was investigated, the rationale being that DMSP might serve as an osmolyte in corals and that genes involved in the synthesis of this compound might be up-regulated under conditions that lead to its increased production. Adult colonies (harboring DMSP-producing photosynthetic symbionts), as well as

aposymbiotic juveniles (devoid of any photo-symbionts) of *A. millepora* were exposed to hyposaline conditions reflecting those experienced in extreme weather events (25 PSU for the adults and 28 PSU for the juveniles) in parallel experiments and hypersaline (40 PSU) conditions for the adults. The analyses presented here focused on genes that are candidates for involvement in the known pathways of DMSP synthesis in algae (including those previously identified as candidates; Raina *et al.* 2013) and plants. Whilst the expression data reported here are consistent with corals being equipped with the necessary enzymatic machinery for DMSP biosynthesis and being able to rapidly change the expression of the corresponding genes, the production of DMSP by corals under hyposaline stress maybe an inevitable consequence of osmolyte catabolism rather than an adaptive stress response.

Table 4.1. List enzymes abbreviations and their EC number.

Abbrev.	Enzyme name	EC number
BADH	Betaine-aldehyde dehydrogenase	1.2.1.8
BHMT	Betaine-homocysteine methyltransferase	2.1.1.5
CDH	Choline dehydrogenase	1.1.99.1
DMGDH	Dimethylglycine dehydrogenase	1.5.8.4
GNMT	Glycine N-methyltransferase	2.1.1.20
MAT	Methionine adenosyltransferase	2.5.1.6
MS	Methionine synthase	2.1.1.13
MTHFR	Methylenetetrahydrofolate reductase	1.5.1.20
SAHH	S-adenosylhomocysteinase	3.3.1.1
SAM met	S-adenosylmethione methyltransferase	2.1.1.37
SARDH	Sarcosine dehydrogenase	1.5.8.3
SHMT	Serine hydroxymethyltransferase	2.1.2.1

4.2. Materials and Methods

4.2.1. Adult and juveniles sampling

The methods for the salinity stress experiments in both adults and juveniles, are described in Chapter 3 (3.2.1 Coral salinity stress experiment). Post the salinity changes coral nubbins for quantitative nuclear magnetic resonance (qNMR) were sampled as described below.

4.2.1.1. Adults sampling

Coral nubbins (n = 2 per colony) were sampled at three time points qNMR analysis: prior to the salinity change, and after 1 and 24 h post the salinity change. Nubbins were immediately extracted in 5 ml of HPLC-grade methanol (details provided below). Another set of nubbins (n = 1 per colony) were collected, incorporating another time point (12h post salinity change), for the determination of zooxanthellae density.

4.2.1.2. Juveniles sampling

Samples were collected at 24, and 48 h post salinity changes and processed as below (4.2.3). The size of each settled juvenile in the sampled well was measured using a motorized stereomicroscope (Leica Microsystems MZ16A) operating with the Application Suite Version 3.8 software. The average juvenile size at 48 h was 1.27 mm^2 (±0.06).

4.2.2. Symbiodinium efficiency, density estimation and genotyping

A diving pulse amplitude modulated (PAM) (Walz Gmbh, Germany) fluorometer was used to measure the photosystem II (PSII) photochemical efficiency of *Symbiodinium* associated with the adult coral nubbins. Measurements were taken one day before, and 8, 16, 28 h after changing the salinity, by taking 3 replicates per 23 nubbins in each condition. *Symbiodinium* density estimation was conducted as described in Raina *et al.* (2013); for each homogeneous extract, 6 replicate measurements were recorded at 600 nm on a DSM-Micro densitometer (Laxco). For genotyping, DNA was extracted from the crushed coral (see RNA extraction) using SNET buffer (20mM Tris-HCl pH 8.0, 5 mM EDTA, 1% SDS (w/v), 400mM NaCl, 400 µg ml^{-1} Proteinase K) and incubated overnight at 55 °C. The supernatant was transferred to an equal volume of phenol-chloroform mixture (1:1) and precipitated with isopropanol. The DNA pellet was solubilized in ~50µl of sterile water and stored at -20 °C. The *Symbiodinium* type was determined by ITS sequencing using the primers "ITSintfor2"

(5'GAATTGCAGAACTCCGTG-3') and "ITS2CLAMP" (5'GGGATCCATATGCTTAAGTTCAGCGGGT-3') (LaJeunesse 2002). All *A. millepora* colonies harboured *Symbiodinium* clade C1.

4.2.3. DMSP quantification by qNMR analysis

DMSP and acrylate in adult nubbins and settled juveniles were quantified according to Raina *et al.* (2013) with minor modifications. Briefly, coral nubbins were extracted in methanol for 30 min with sonication followed by a second extraction with an additional 2 ml of methanol for 10 min, after which the extracts were pooled and analysed via ^{1}H NMR as in Raina *et al.* (2013) using the ERETIC method (Tapiolas *et al.* 2013). The surface area of each individual adult nubbin was used to normalise the corresponding qNMR and *Symbiodinium* density data. Nubbins were bleached (10% bleach) and then lyophilized (Dynavac Freeze Drier FD12) with the surface area determined using the wax dipping technique originally described by Veal *et al.* (2010).

For juveniles, seawater was decanted from individual wells and residual seawater gently absorbed using a sterile cotton tip, taking care not to disturb the animal. CD_3OD (300 □l) and D_2O (200 □l) were added to each well. Plates were gently shaken for 30 s and a 200 □l aliquot transferred into a 3 mm Bruker MATCH NMR tube for immediate analysis. In addition, negative control wells containing no larvae or settled juveniles, but which did contain the CCA-derived settlement cue, were extracted following the same procedure. The concentrations of DMSP and acrylate were normalized initially to the number of settled coral juveniles in the respective well. They were then normalized to the averaged surface area of the juveniles as in Raina *et al.* (2013).

DMSP concentration data were analysed using the open source software R Version 3.1.0 (R Core team, 2014) using the "car" (Fox & Weisberg 2011) and "doBy" (Højsgaard *et al.* 2014) libraries. Multivariate analyses of variance MANOVA were used to test for changes in

DMSP concentration over the course of the experiment. Repeated measures ANOVA were used to test for difference in DMSP concentration at each time point and over time (Table S4.1, Supporting information).

4.2.4. Identification of candidate genes

The methods for transcriptomics analysis including RNA extractions, sequencing, reads mapping, and gene expression analysis of the salinity stress experiments are detailed in Chapter 3 (3.2.3. RNA extraction sequencing and gene expression analyses).

To identify homologs of the known algal and plant DMSP biosynthesis enzymes in the coral genome, protein sequences from the diatom *Fragilariopsis cylindrus* v1.0 (algal pathway) (Kettles *et al.* 2014; Lyon *et al.* 2011) in addition to sequences from the two known enzymes involved in the plant pathway (Enzyme Commission (EC) 2.1.1.12 and 1.2.1.3, downloaded from http://www.uniprot.org) were used to retrieve protein family (Pfam) domain and gene ontology (GO) annotation. In addition to complete sequences, protein domains were used to search the *A. millepora* genome for homologs of the algal and plant enzymes. Additionally, sequences with characteristic GO domains of the enzymes involved in DMSP biosynthesis from four algae and two plant genomes were retrieved and blasted against the *A. millepora* genome (E-value ranged from 0.003-0.1, retrieving at least five sequences). Sequences were retrieved from: the marine microalga *Emiliania huxleyi (Read et al. 2013), the green alga Chlamydomonas reinhardtii* v5.5 (Merchant *et al.* 2007), the diatom *Thalassiosira pseudonana* v3.0 (Kettles *et al.* 2014), the dinoflagellate *Symbiodinium minutum* Clade B1 v.1.0 (Shoguchi *et al.* 2013) (dataset downloaded from *http://marinegenomics.oist.jp/genomes/downloads?project_id=21,* last accessed October 27, 2014*), and the* flowering plants *Arabidopsis thaliania TAIR10* (Lamesch *et al.* 2012) (Lamesch 2012) and *Brachypodium distachyon v2.1* (The International Brachypodium Initiative 2010). *All the* databases (except for the *S. minutum*) were downloaded from the U.S. Department of

Energy Joint Genome Institute (JGI; http://genome.jgi-psf.org, last accessed October 15, 2014). The nomenclature of *A. millepora* proteins used here is based on BlastP searches of non-redundant protein sequences at NCBI or by hidden Markov models in HMMER (http://hmmer.janelia.org; Finn *et al.* 2011) assignments (results are listed in Table 4.2 and Table S4.4, Supporting information). KEGG orthology (KO) identifiers were used to retrieve EC numbers and search for characteristics in the enzyme information system BRaunschweig ENzyme DAtabase (BRENDA; http://www.brenda-enzymes.org/index.php) and the metabolic pathways database (MetaCyc; http://metacyc.ai.sri.com). After obtaining the BlastP results based on the *A. millepora* gene predictions, differentially up-regulated genes (FDR < 0.05) in any of the datasets were used for subsequent analysis.

4.3. Results

4.3.1. Concentration of DMSP in coral tissues

Exposure of adult *A. millepora* colonies to a sudden decrease in salinity (25 PSU) resulted in a 2.6 fold increase in tissue DMSP concentration after 1 h (from 9.02 nmol mm^{-2} at 35 PSU to 23.76 nmol mm^{-2} in the treatment) compared to the controls. DMSP levels in these colonies continued to increase through time, reaching 31.46 nmol mm^{-2} after 24 h, representing a 3.5 fold increase in DMSP relative to the control (TukeyHSD, p adj <0.05; Figure 4.2A and Table S4.1, Supporting information). In aposymbiotic *A. millepora* juveniles, exposure to low salinity (28 PSU) triggered an increase of DMSP levels of 1.2 fold after 24h (from 2.66 nmol mm^{-2} at 35 PSU to 3.27 nmol mm^{-2} in the treatment) and of 1.4 fold after 48 h relative to control juveniles maintained at 35 PSU (ANOVA, p<0.0005; Figure 4.2B and Table S4.3).

In contrast, adult *A. millepora* nubbins exposed to hypersaline conditions (40 PSU) exhibited no significant change in tissue DMSP concentrations compared to the controls (TukeyHSD, p adj >0.05; Figure 4.2 and Table S4.1, Supporting information). At both time

points the concentration of the DMSP breakdown product acrylate did not differ significantly from controls in either treatment (Figure S4.1, Supporting information). Furthermore, no clear physiological changes were observed in the corals during the 24 h period of both hypo- and hyper-salinity stress experiments, as assessed by PAM fluorometry (MANOVA, H-F Pr > 0.05; Figure S4.2, Table S4.2, Supporting information) and *Symbiodinium* cell density (Figure S4.2, Supporting information).

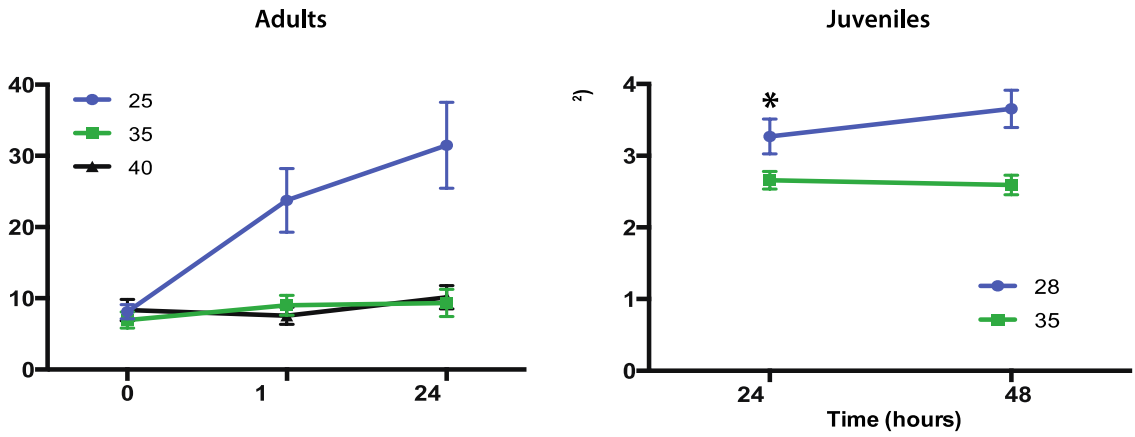

Figure. 4.2. Changes in DMSP concentration (mean ± s.e.) in adult corals (*n=5*) and settled juveniles (*n=6*) of the coral *A. millepora*. Adults (A) were exposed to ambient/control (35 PSU, green) and two salinity stress conditions (25 and 40 PSU in blue and black respectively). DMSP concentrations increased significantly under hyposaline stress (25 PSU; *H-F Pr<0.005) and through time compared to both the control and hypersaline stress conditions (40 PSU; *p adj<0.05). No significant changes in DMSP levels were observed between the control and 40 PSU treatments. Juveniles (B) were exposed to ambient/control (35 PSU, green) or hyposaline (28 PSU, blue) conditions. In this case, DMSP levels differed significantly between treatments and controls (F = 17.70, *p<0.0005), but did not differ significantly with time.

4.3.2. Candidate DMSP biosynthesis genes

Differential gene expression analysis of the hyposaline stress in adults and juveniles are described in Chapter 3 (3.3.1. Differential gene expression analyses).

BlastP analysis of the *A. millepora* gene predictions led to the identification of coral members of gene families implicated in DMSP biosynthesis in other organisms (Table 4.2 and

Table S4.4, Supporting information), some of which were differentially expressed in response to hyposaline stress and on this basis are considered to be candidates for roles in DMSP biosynthesis in corals. Amongst the genes up-regulated under hyposaline conditions were members of each class of enzyme in the DMSP biosynthesis pathway previously described in the alga *Ulva intestinalis* (Gage *et al.* 1997), whereas there was no evidence for up-regulation of genes specifically associated with DMSP-synthesis in higher plants (DMSP-amine oxidase and *S*-methylmethionine (SMM) transaminase-decarboxylase; Table 4.2 and Fig 4.1A and B, step 3).

Six transaminase family members (Table 4.2, AT1- AT6) were identified as candidates for the initial aminotransferase step in the algal biosynthetic pathway (conversion of L-methionine to 2-oxo-4-methylthiobutanoate; MTOB), on the basis of elevated levels of expression in adults and/or juveniles during hypo-osmotic stress. One of these candidate genes, AT1 was expressed at higher levels at both time points in both juveniles and adults, and is therefore of particular interest. Although BlastP NR database comparisons classified the AT1 predicted protein as most similar to ethanolamine-phosphate phospholyases (EC2.6.1.88), its overall sequence similarity ($5E^{-35}$) to the aminotransferase candidate (269005) from the diatom *Fragilariopsis cylindricus* (Lyon *et al.* 2011) is consistent with the hypothesis that the two proteins play analogous roles in DMSP metabolism. While the expression levels of five other aminotransferases (AT2 – AT6) were less consistent across the treatments, BlastP NR comparisons imply that their transamination reactions are likely to be 2-oxoglutarate dependant and hence cannot be excluded as candidates for roles in DMSP biosynthesis.

The second step in the algal DMSP biosynthesis pathway involves the reversible reduction of MTOB to 4-methylthio-2-hydroxybutyrate (MTHB), but this reaction is not restricted to DMSP-producing organisms (Summers *et al.* 1998). Table 4.2 lists the

differentially expressed genes (REDOX1-REDOX10) that encode NAD- or NADP-dependant dehydrogenases. Due to their redox capacities, the dehydrogenases corresponding to EC1.2.1.3 (Table 4.2, REDOX2, REDOX3, REDOX5 and REDOX8) could equally well correspond to the enzyme carrying out the terminal step (oxidation of DMSP-aldehyde; DMS-ald) in the plant DMSP biosynthetic pathway or that which converts MTOB to MTHB in the algal pathway. REDOX1 was consistently up-regulated in adult and juvenile corals with database comparisons indicating that it is a 10-tetrahydrofolate reductase since the N-terminal part of the protein contains a hydrolase domain highly specific for this class of enzyme ($5.79E^{-144}$ similarity with cd08647). Moreover, TargetP (http://www.cbs.dtu.dk/services/TargetP/) predicts that REDOX1 is mitochondrial, which is consistent with the location of the best NR database matches and therefore of relevance to its ability to function in DMSP synthesis. REDOX2 and REDOX3 were differentially up-regulated in the adults when excluding time as a factor (Table S4.5, Supporting information), and significantly up-regulated in juveniles (at 24 h in the case of REDOX3; at both time points for REDOX2). REDOX2 may be the best candidate for enzymatic reduction of MTOB, as it matches ($9.31E^{-12}$) to a dehydrogenase (177646) that is highly up-regulated in the diatom *F. cylindricus* under conditions that lead to DMSP biosynthesis via the algal pathway (Lyon *et al.* 2011).

Both the plant and algal DMSP biosynthesis pathways feature SAM-dependent methylation steps; in the algal pathway, conversion of MTHB to dimethysulphonio-2-hydroxybutyrate (DMSHB) involves a SAM-dependant methyltransferase, as does the conversion of methionine to SMM in the plant pathway (Figure 4.1). Two methyltransferases (METHYL1 and METHYL2) were up-regulated during salinity stress (Table 4.2), although database comparisons suggest other primary roles for both METHYL1 and METHYL2 due to their methyltransferase domains (cd02440) being class I type, as is also the case for the methionine *S*-methyltransferase Q9LTB2 (which functions in the plant DMSP pathway), and the algal methyltransferase (212856) identified by Lyon *et al.* (2011). Of the candidates,

METHYL1 was the most consistently up-regulated in the hyposaline treatments. A third SAM-dependant methyltransferase METHYL3 (Table 4.2), was initially identified as the most likely candidate for the conversion of MTHB to DMSHB (Raina *et al.* 2013) based on its similarity to the primary candidate for this role in the alga *F. cylindrus* (Lyon *et al.* 2011). Note however that METHYL3 was not differentially expressed as a result of exposure to altered salinity conditions.

The final step in the algal DMSP biosynthesis pathway, the transformation of DMSHB to DMSP, is the least well understood. The enzyme involved is thought to be an oxygen dependant decarboxylase (Summers *et al.* 1998), but has not been characterised. Four candidate enzymes (DECARB1-DECARB4) were identified in the coral on the basis of similarity with the diatom decarboxylases implicated in DMSP biosynthesis (Lyon *et al.* 2011), but neither these nor the candidates from the diatom are likely to be oxygen-dependent. All of the four *Acropora* candidates encode pyridoxal phosphate (PP) dependent decarboxylases; like the diatom candidate 263016 (Lyon *et al.* 2011), DECARB1 encodes a group IV PP-dependent decarboxylase (Pfam02784). The remaining three coral candidate decarboxylases are of the group II PP-dependent type (Pfam00282). None of these coral candidate decarboxylases showed consistent up-regulation across the hyposaline manipulation experiments (Table 4.2).

Table 4.2. Changes in expression levels of candidate genes involve in DMSP biosynthesis in *A. millepora* under hyposaline stress.

1 h							
log2FC	FDR	log2FC	FDR	log2FC	FDR	log2FC	FDR
				2.63	5.00E-239	-2.61	3.13E-88

For each candidate gene, the table provides $\log_2$ fold change ($\log_2$FC) and false discovery rate (FDR) data for the hyposaline treatment relative to the control. Red shading indicates genes that were up-regulated; blue shading indicates genes that were down-regulated (FDR <0.05).
* Candidates previously identified by Raina *et al.,* (2013).
** Genes differentially up-regulated in the adult treatments when time was excluded as a factor (Table S4.5, Supporting information).

4.3.3. Differential expression of genes involved in methionine metabolism

Although methionine adenosyltransferases (MAT1 and MAT2), which convert methionine to its activated form (*S*-adenosyl methionine), were up-regulated under

hyposaline conditions (Table 4.2, Figure 4.3), other coral genes implicated in methionine salvage and the methyl cycle (Table 4.2) were down-regulated. Methionine synthase (MS), which methylates homocysteine to regenerate methionine, was down regulated in both adults and juveniles, as were the other methyl cycle enzymes, methylenetetrahydrofolate reductase (MTHFR) and serine hydroxymethyltransferase (SHMT; Table 4.2). Although methionine synthase was down-regulated under hyposaline conditions, methionine can also be generated by methylation of homocysteine by the action of betaine-homocysteine methyltransferase (BHMT; Figure 4.3), two coral homologs of which (BHMT1 and BHMT2) were up-regulated in both adults and juveniles (Table S4.4, Supporting information). In addition to generating methionine, the action of BHMT converts betaine to dimethylglycine (DMG), which can be converted to glycine by a series of enzymes (Figure 4.3; DMGDH (EC1.5.8.4), SARDH (EC1.5.8.3) and GNMT (EC2.1.1.20), all of which were up-regulated in under hyposaline conditions (Table S4.4, Supporting information). It is also interesting to note that, of a list of genes potentially involved in methionine salvage from SAM (Figure 4.3, EC 4.1.1.50, 2.5.1.16, 2.4.1.28, 4.2.1.109 and 3.1.3.77), the only gene differentially expressed under hyposaline conditions was that enabling the final conversion to 3-methylthiopropionate of this pathway (Figure 4.3, EC1.13.11.53) and this was down-regulated (Table S4.4, Supporting information) in both adults and juveniles. Finally, the coral homolog to the enzyme involved in the methionine trans-sulphuration pathway (cystathionine γ-lyase (CGL), EC4.4.1.1; Table S4.4, Supporting information) was not differentially expressed, providing further evidence that methionine is not shunted into either the methyl cycle or the methionine salvage pathways, but rather being driven into DMSP biosynthesis.

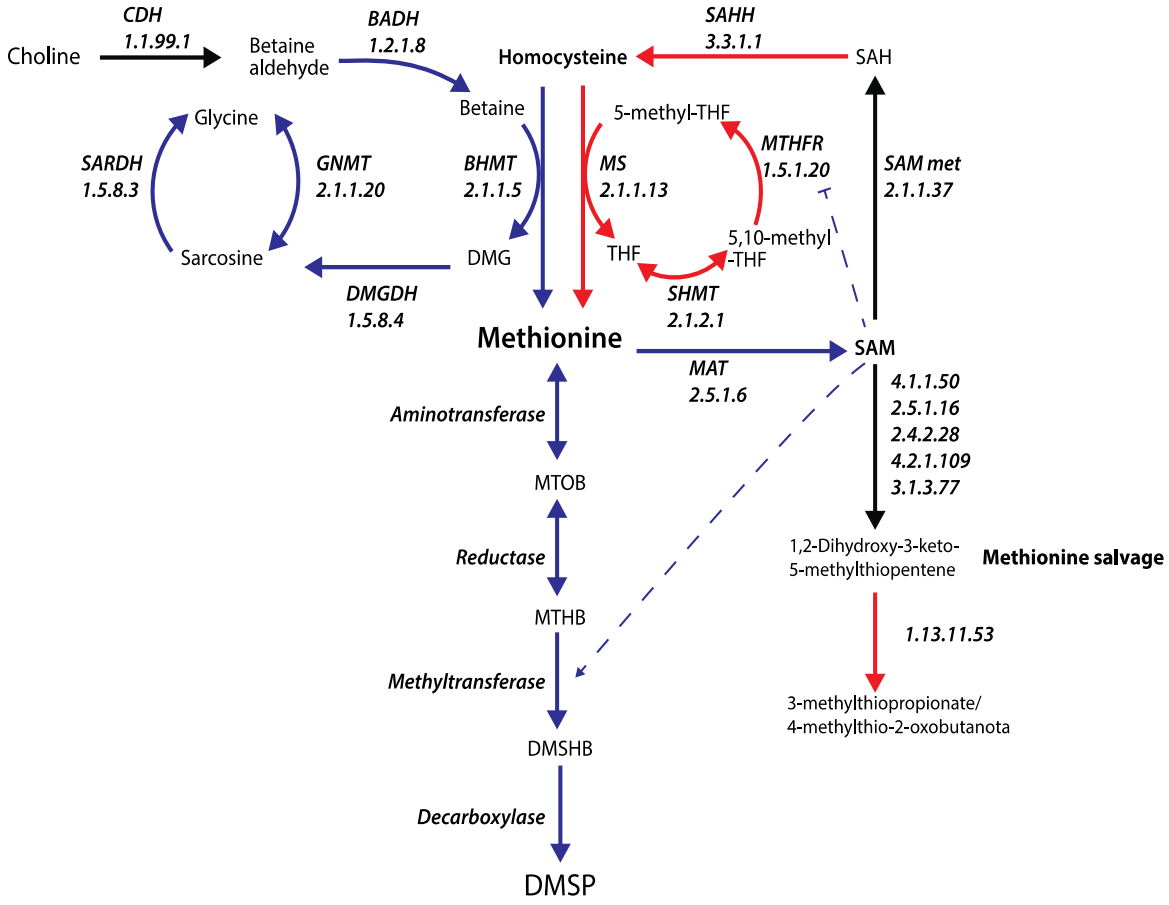

Figure. 4.3. Changes in expression levels of genes involved in methionine metabolism during hyposaline stress in the coral *A. millepora*. Enzyme names and EC numbers are shown in italics (names as in Table 1). Blue, red or black arrows represent steps where genes are up-regulated, down-regulated or do not change significantly, respectively, during hyposaline stress in adult and/or juvenile corals. Dashed arrows indicate other roles of SAM (FDR <0.05, see Table S4.4, Supporting information for values). Dimethylglycine (DMG); tetrahydrofolate (THF). Abbreviations for compounds are as in the legend to Figure 4.1.

4.4. Discussion

4.4.1. Corals increase production of DMSP under hyposaline stress

DMSP concentrations in adult corals increased 3.5 fold after 24 h exposure to 25 PSU with similar trends observed for aposymbiotic coral juveniles. This is the first report of DMSP production under hyposaline conditions by a coral. Increased DMSP production under hyposaline conditions argues against a role for this compound in osmoregulation in corals and contrasts with the situation in a number of other organisms (Trossat *et al.* 1998;

Vairavamurthy *et al.* 1985) where DMSP biosynthesis increases under hypersaline conditions. Importantly, in the case of *A.millepora*, DMSP concentrations did not change significantly under hypersaline conditions (40 PSU), indicating that corals use different mechanisms to adjust to changes in osmotic conditions. Increased levels of DMSP have also been observed in adult and aposymbiotic juvenile *A. millepora* exposed to heat stress (Raina *et al.* 2013). Taken together, these results suggest that increases in DMSP concentration in the coral (animal and *Symbiodinium*) might be a more general response to stress, although DMSP levels did not increase when *Montastraea franksi* was exposed to copper stress (Yost *et al.* 2010). DMSP has been shown to function in scavenging hydroxyl radicals and reactive oxygen species (ROS) generated under high light and UV stress in some organisms (Darroch *et al.* 2015; Sunda *et al.* 2002). Although it is not yet clear whether ROS are generated in corals during salinity stress, the observed increase in DMSP levels under hyposaline conditions are consistent with possible functions as an antioxidant.

The response of corals to decreased salinity is not well understood. In *A. aspera,* free amino acid (FAA) concentrations have been shown to increase 2.6-fold after 1 h of exposure to hyposaline (28 PSU) conditions (Cowlin 2012) but remained unchanged under hypersaline (42 PSU) conditions. Thus, under hyposaline stress, the concentration of free methionine, the precursor of DMSP, is likely to increase in coral tissue.

4.4.2. Putative coral enzymes involved in the DMSP algal-like pathway

RNA sequencing results presented here are consistent with the hypothesis that corals produce DMSP via an alga-like pathway (Raina *et al.* 2013), but that the identities of genes and enzymes involved needs to be revisited in the light of the transcriptomic responses reported here. Clear differences were observed between adults and juveniles with respect to the responses of genes that are considered candidates for roles in DMSP synthesis by corals

(Figure 4.4), presumably as consequences of the presence of the dinoflagellate symbionts in the former but not the latter.

In the proposed algal-like pathway of DMSP synthesis, the transamination of methionine and subsequent reduction/oxidation step are both known to be reversible and, while not specific to DMSP producers, exhibit high activity in DMSP accumulating organisms (Summers *et al.* 1998). The gene referred to here as AT1 is considered the best candidate for involvement in the initial transamination step, as it was up-regulated in both adults and juveniles at all time points. In the case of the reduction step, three candidate genes (REDOX1-REDOX3) were up-regulated in all the datasets, whereas the expression data for REDOX8, previously identified as a candidate on the basis of similarity with the diatom reductase (Raina *et al.* 2013) were less consistent. Although REDOX1 showed the most consistent up-regulation of expression across the datasets, its likely mitochondrial localisation may limit its involvement in the proposed pathway, hence REDOX2/3 are also considered to be candidates for roles in DMSP production.

The last two steps in the proposed DMSP biosynthesis pathway involve methylation followed by decarboxylation and, unlike the transamination and oxidation/reduction steps, are not reversible. The enzyme referred to here as METHYL3 was initially identified as a candidate for the methylation step (Raina *et al.* 2013) on the basis of similarity to a candidate for the same step from a diatom (Lyon *et al.* 2011) but the corresponding gene was not up-regulated in the present study (Table 4.2). However, one other putative SAM-dependant methyltransferase (METHYL1) was highly up-regulated across the hyposaline treatment datasets and is thus a candidate for involvement in DMSP biosynthesis.

The identities of genes or enzymes associated with the decarboxylation step of DMSP synthesis are unknown. Two candidates for this role in diatoms have been put forward (Lyon

et al. 2011), but neither of these enzymes is likely to be oxygen-dependent, which is inconsistent with earlier metabolic data for this step (Gage *et al.* 1997). No clear candidates for this role emerged from the hyposaline treatment experiments described here.

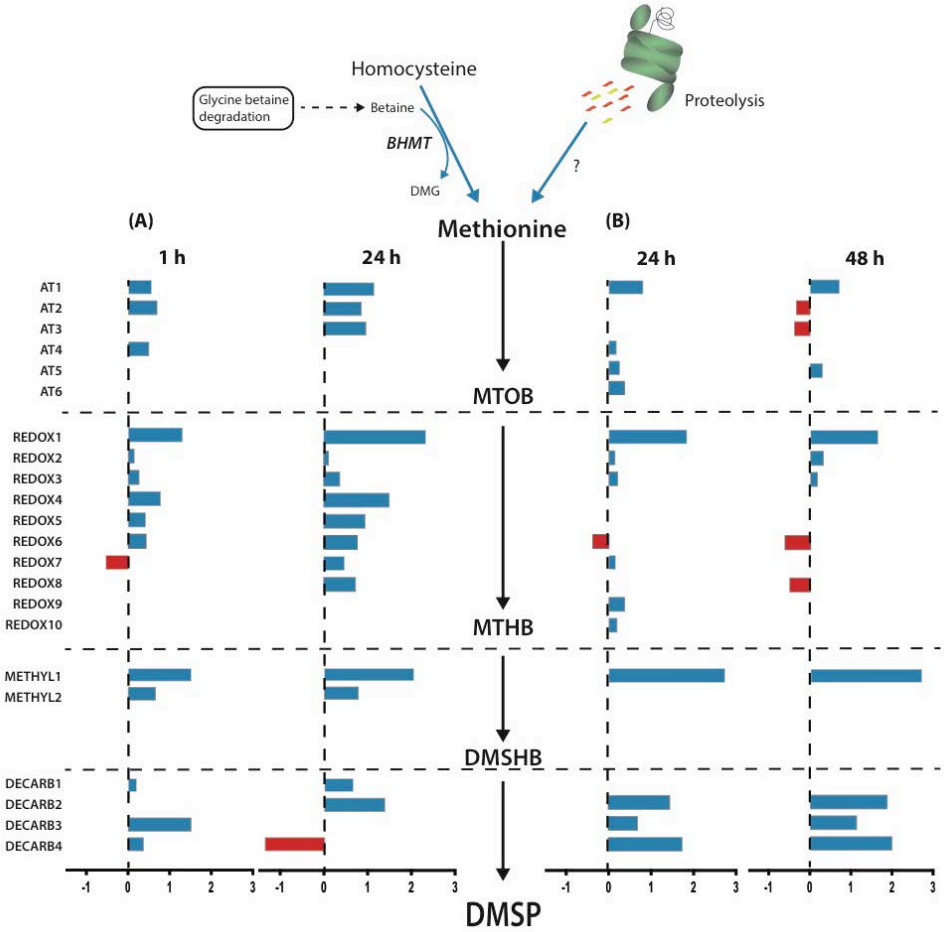

Figure 4.4. Summary of changes in expression levels of coral genes that are candidates for involvement in an algal-like pathway of DMSP synthesis. For each candidate gene, transcripts levels are indicated as a bar, the length of which indicates $\log_2$-fold change (as in the *x* axis) relative to control in (A) adult and (B) juvenile corals. Blue bars and red bars represent the expression levels of up-regulated and down-regulated genes, respectively. Values of candidate gene expression are in Table 4.2, and abbreviations are as in Figure 4.1 and Table 4.1.

4.4.3. Corals do not use a plant-like pathway for DMSP synthesis

Some steps in the algal and higher plant DMSP pathways are biochemically similar, but it is unlikely that the production of DMSP by corals occurs through a plant-like pathway. Possible coral equivalents of S-methyl-L-methionine decarboxylase (SDC) (Table 4.2, DECARB1), and two DMSP-amine oxidases (Table 4.2, DOX1 and DOX2) (Figure 4.1B, step 3)

are present, but the two DOX homologs were down-regulated in both the adults and juveniles in response to hyposaline stress, making their involvement in DMSP production by coral unlikely. The oxidation of DMSP-aldehyde to DMSP (Figure 1A and B, step 4) in the plant pathway is biochemically similar to the reductase step of the algal pathway (Figure 1C, step 2 and Figure 4.4), hence the observed up-regulation of REDOX candidate genes is the only evidence that the corals could use a plant-like DMSP pathway.

4.4.4. DMSP production in corals in response to hypo-osmotic stress

The increased production of DMSP in corals under hyposaline stress precludes an osmoregulatory function, but is consistent with a role in conferring protection against ROS generated under these conditions. However, DMSP is produced in some systems (e.g. the alga *Tetraselmis subcordiformis*) simply in response to the availability of excess methionine (Gröne & Kirst 1992; Vierstra 1993), and this situation may occur in corals in response to hyposaline conditions.

Osmoregulation has not been extensively studied in corals, but betaines have emerged as likely to have major roles as osmolytes. Early evidence for this was based on HPLC data where Yancey *et al.* (2010) surveyed a range of osmolyte candidates in seven corals and some other cnidarians, identifying glycine betaine (also known as *N,N,N*-trimethyl glycine) as the dominant osmoregulatory molecule in all of the corals studied except *Porites* species. Similarly, glycine betaine was also implicated as the primary osmolyte in developing larvae of the mushroom coral *Fungia scutaria* (Hagedorn *et al.* 2010). The presence of high concentrations of betaines, particularly glycine betaine and taurine betaine, in *Madracis* spp. corals has been confirmed by coupled HPLC/mass spectrometry (Hill *et al.* 2010). Increasing levels of betaine correlated with higher light exposure in *Madracis*, suggesting roles in ROS scavenging (Hill *et al.* 2010).

Although, to our knowledge, osmolyte concentrations in *Acropora* have not been documented, on the basis of the precedents above, betaines are likely candidates, and the responses of *Acropora* to hypo-osmotic stress should be viewed in the context of the requirement to decrease internal osmolarity by reducing betaine levels. Betaines are catabolised via methionine and in the present study, betaine aldehyde dehydrogenase (EC1.2.1.8; BADH) and betaine homocysteine methyltransferase (EC2.1.1.5; BHCMT) were up-regulated in response to hyposaline conditions, which is consistent with betaine breakdown. The action of BHCMT generates methionine and dimethylglycine, the latter of which is metabolised to glycine (and hence to central metabolism) via sarcosine by the sequential actions of dimethylglycine dehydrogenase (EC1.5.8.4; DMGDH) and either glycine-*N*-methyltransferase (EC2.1.1.20; GNMT) or sarcosine dehydrogenase (EC1.5.8.3), all of which were up-regulated under hyposaline conditions in the present study. Because of the flux of homocysteine to methionine driven by betaine catabolism, methionine synthase activity is redundant, which can account for the observed down-regulation of this enzyme (EC2.1.1.13) and the others of the methyl cycle. Some methionine is rescued by conversion to the activated form *S*-adenosyl methionine (note that methionine adenosyltransferase is up-regulated under hyposaline conditions), while the excess is converted to DMSP via the pathways discussed above. Excess DMSP itself can be metabolised by coral-associated bacteria to the volatile compound DMS (Raina *et al.* 2010), effectively removing it from the system. Note that some homocysteine can be directed into cysteine biosynthesis in other animals (and possibly other corals), however, *Acropora* spp. lack the enzyme cystathionine synthase (EC4.2.1.22; Shinzato *et al.,* 2011), and so are unable to achieve this.

In addition to being produced as a consequence of betaine catabolism, methionine (and cysteine) will arise in corals as a consequence of proteolysis, which is clearly implied by the up-regulation of many genes encoding proteasome components observed during hypo-osmotic stress (Chapter 3, Table S3.2, Supporting information). Increases in levels of free

amino acids, including methionine, have previously been observed when the coral *Acropora aspera* was exposed to hyposaline conditions (Cowlin 2012).

4.5. Conclusions

Hyposaline stress increased DMSP production in both adults and aposymbiotic juvenile corals, and transcriptomic analyses highlight the potential involvement of specific candidate genes in the production of DMSP via an alga-like pathway. The DMSP produced is likely to provide protection against ROS arising as a consequence of stress, but may also constitute a molecular sink for methionine arising as a consequence of osmolyte catabolism as well as proteolysis. The biochemistry of DMSP production is not well established for any eukaryotic system and, as the first animals in which it has been demonstrated, this is particularly true in the case of corals. The transcriptomic data presented here have enabled the identification of candidates for roles in DMSP biosynthesis in corals but, given its critical roles in diverse biological processes, a thorough investigation of the molecular mechanisms leading to its production by corals is required.

4.6. Supporting information

Tables

Table S4.1. Statistical tests for DMSP concentration under salinity stress on the adult *Acropora millepora* corals significance levels for: (A) MANOVA, and (B) Tukey post-hoc test. Asterisk (*) represents significant differences (p adj< 0.05).

(A)

Effect	DF	H-F Pr
Intercept	1	0.00001
Salinity	2	0.00459*
Colony	1	0.71576
Salinity:Colony	2	0.86481
Residuals	9	

(B)

Salinity (PSU)	Time (hours)	Diff	lwr	upr	p adj
35-40	1	1.476597	-9.09894	12.05213	0.926825
25-40	1	16.21631	5.640781	26.79185	0.0039486*
25-35	1	14.73972	4.164184	25.31525	0.0076419*
35-40	24	0.787524	-13.4579	15.03293	0.988091
25-40	24	22.11324	7.867837	36.35865	0.0036137*
25-35	24	21.32572	7.080313	35.57112	0.0046846*

Table S4.2. Statistical tests for PAM data under salinity stress on the adult *Acropora millepora* corals significance levels for MANOVA.

Effect	DF	H-F Pr
Intercept	1	0
Salinity	2	0.08826
Colony	1	0.12466
Salinity:Colony	2	0.92476
Residuals	5	

Table S4.3. Sums of squares (SS), mean squares (MS) and significance levels for ANOVA of DMSP concentration under salinity stress on juveniles of *Acropora millepora* corals. Asterisk (*) represents significant differences (p< 0.05).

Effect	SS	df	MS	F	p
Salinity	6.373	1	6.373	17.703	0.00024 *
Time	0.192	1	0.192	0.534	0.47081
Salinity:Time	0.379	1	0.379	1.053	0.31357
Residuals	10.079	28			

Table S4.4. *A. millepora* candidate genes to the DMSP biosynthesis pathway, glycine betaine catabolism, and methionine salvage pathway. (A) Differentially expressed genes in response to hyposaline stress, log2 fold change (log2FC) and false discovery rate (FDR) are reported for each of the experiment datasets of the treatment (hyposalinic) relative to the control, including EC pathway details. Red shading indicates genes that are differentially up-regulated; blue shading indicates genes that are differentially down-regulated (FDR <0.05). (B) Best blast hit, HMMER, and KOGG annotation listed for each enzyme.

(A)

Pathways	Step Abbrev.	Genome ID	abbrev.	Protein ID	Adults				Juveniles				EC pathways		
					1 h		24 h		24 h		48 h		EC number	Reaction Type	Cofactors
					log2FC	FDR	log2FC	FDR	log2FC	FDR	log2FC	FDR			
DMSP biosynthesis	AT1	1.2.4389.m1	ETNPPL	Ethanolamine-phosphate phospho-lyase	0.54	1.35E-03	1.17	1.23E-13	0.80	6.73E-34	0.72	2.20E-12	4.2.3.2	Elimination	pyridoxal 5'-phosphate
Transamination	AT2	1.2.3643.m1	TAT	Tyrosine aminotransferase	0.66	1.69E-03	0.87	3.01E-03	0	0	-0.34	4.46E-02	2.6.1.5	amino group transfer	pyridoxal 5'-phosphate
	AT3	1.2.1862.m1	ilvE	Amino acid aminotransferase	0	0	0.97	2.85E-04	0	0	-0.38	3.59E-05	2.6.1.42	amino group transfer	pyridoxal 5'-phosphate
	AT4	1.2.6453.m1	ALT	Alanine aminotransferase	0.47	6.58E-02	0	0	0.17	4.65E-02	0	0	2.6.1.2	amino group transfer	pyridoxal 5'-phosphate
	AT5	1.2.6452.m1	ALT	Alanine aminotransferase	0	0	0	0	0.24	3.75E-04	0.30	2.89E-03	2.6.1.2	amino group transfer	pyridoxal 5'-phosphate
	AT6	1.2.6454.m1	ALT	Alanine aminotransferase	0	0	0	0	0.36	1.26E-03	0	0	2.6.1.2	amino group transfer	pyridoxal 5'-phosphate
Reduction/ Oxidation	REDOX1	1.2.9800.m1	ALDH	Formyltetrahydrofolate dehydrogenase	1.33	1.27E-16	2.35	5.22E-68	1.82	4.50E-171	1.63	2.26E-138	1.5.1.6	redox reaction	10-formyltetrahydrofolate
	REDOX2	1.2.22357.m1	ALDH	Aldehyde dehydrogenase (NAD+)	0	0	0	0	0.14	1.42E-03	0.31	6.18E-04	1.2.1.3	redox reaction	NAD+
	REDOX3	1.2.21229.m1	ALDH	Aldehyde dehydrogenase	0	0	0	0	0.20	7.18E-02	0	0	1.2.1.3	redox reaction	NAD+
	REDOX4	1.2.12494.m1	putA	L-glutamate gamma-semi-aldehyde dehydrogenase	0.79	2.17E-04	1.51	1.10E-11	0	0	0	0	1.2.1.88	redox reaction	NAD+
	REDOX5	1.2.25403.m1	ALDH; BADH	Aldehyde dehydrogenase	0.42	1.68E-03	0.95	4.93E-10	0	0	0	0	1.2.1.3 1.2.1.8	redox reaction	NAD+
	REDOX6	1.2.20338.m1	ALDH	Aldehyde dehydrogenase	0.44	7.94E-03	0.78	1.03E-04	-0.38	1.99E-07	-0.62	4.33E-09	1.2.1.18 1.2.1.27	redox reaction	NAD+, CoA,
	REDOX7	1.2.2152.m1	ALDH	Aldehyde dehydrogenase	-0.55	3.83E-12	0.48	4.30E-03	0.15	1.49E-04	0	0	1.2.1.5	redox reaction	NAD+
	REDOX8	1.2.11968.m1	_	NADPH-dependent FMN reductase*	0	0	0.73	8.24E-05			-0.51	3.00E-02	1.2.1.3	redox reaction	NAD+
	REDOX9	1.2.57.m1	AKR1A1	Alcohol dehydrogenase (NADP+)	0	0	0	0	0.37	1.75E-04	0	0	1.1.1.2	redox reaction	NADP+, NADPH
	REDOX10	1.2.25591.m1	CBR	NADH-cytochrome b5 reductase	0	0	0	0	0.19	9.73E-03	0	0	1.6.2.2	redox reaction	NADPH
Methylation	METHYL1	1.2.13833.m1	GNMT	Glycine N-methyltransferase	1.56	2.39E-14	2.07	7.39E-41	2.70	6.16E-155	2.76	5.02E-249	2.1.1.20	methyl group transfer	–
	METHYL2	1.2.12191.m1	PRMT	Arginine N-methyltransferase	0.67	1.02E-03	0.78	5.72E-03	0	0	0	0	2.1.1.-	–	–
	METHYL3	1.2.14921.m1	_	SAM-dependent methyltransferase*	0	0	0	0	0	0	0	0		–	–
Decarboxylation	DECARB1	1.2.3018.m1	ODC1	Ornithine decarboxylase	0.21	5.60E-02	0.66	3.85E-06	0	0	0	0	4.1.1.17	decarboxylation	pyridoxal 5'-phosphate
	DECARB2	1.2.4120.m1	_	PLP dependant decarboxylase	0	0	1.39	7.15E-13	1.46	8.22E-28	1.85	2.48E-24	–	–	–
	DECARB3	1.2.4118.m1	_	Decarboxylase	1.54	1.42E-03	0	0	0.69	2.38E-05	1.11	5.85E-12	–	–	–
	DECARB4	1.2.4119.m1	_	Decarboxylase	0.38	4.31E-02	-1.38	1.77E-09	1.75	1.53E-14	1.97	1.62E-29	–	–	–
Oxidative deamination	DOX1	1.2.174.m1	AOC1	Diamine oxidase	0	0	-1.20	1.58E-07	-0.47	5.61E-05	0	0	1.4.3.22	oxidation	2,4,5-trihydroxyphenylalanine quinone
	DOX2	1.2.8765.m1	AOC1	Diamine oxidase	0	0	-0.99	1.02E-03	0	0	0	0	1.4.3.22	oxidation	2,4,5-trihydroxyphenylalanine quinone
Methyl Cycle	–	1.2.8442.m1	MAT	Methionine adenosyltransferase	0.51	8.67E-05	1.41	1.21E-04	0.22	9.12E-05	0.51	3.96E-06	2.5.1.6	adenosyl group transfer	ATP
	–	1.2.9082.m1	MAT	Methionine adenosyltransferase	0.41	3.51E-03	3.40	3.71E-238	0.59	3.66E-06	0.64	4.04E-03	2.5.1.6	adenosyl group transfer	ATP
	–	1.2.10409.m1	SAM-met	SAM methyltransferase	0	0	0	0	0	0	0	0	2.1.1.37	cysteine and methionine metabolism	S-adenosyl-L-methionine
	–	1.2.2524.m1	SAHH	S-adenosylhomocysteine hydrolase	0	0	-0.39	9.36E-02	-0.55	6.40E-20	-0.82	4.09E-13	3.3.1.1	hydrolysis of thioether	NAD+
	–	1.2.20586.m1	MS	Methionine synthase	0	0	-0.62	1.54E-04	-0.82	3.80E-74	-0.73	5.35E-11	2.1.1.13	methyl group transfer	S-adenosyl-L-methionine
	–	1.2.6795.m1	SHMT	Serine hydroxymethyltransferase	0	0	0	0	-0.40	5.28E-05	-0.38	1.86E-04	2.1.2.1	hydroxymethyl group transfer	pyridoxal 5'-phosphate
	–	1.2.1458.m1	MTHFR	Methylenetetrahydrofolate reductase	-1.02	6.56E-22	-1.72	6.65E-10	-2.63	5.00E-239	-2.61	3.13E-88	1.5.1.20	redox reaction	
Methionine trans-sulphuration	–	1.2.10238.m1	CGL	Cystathionine gamma-lyase	0	0	0	0	0	0	0	0	4.4.1.1	alpha,gamma-elimination	
Glycine betaine degradation	–	1.2.6999.m1	CDH	Choline dehydrogenase	0	0	0	0	0	0	0	0	1.1.99.1	redox reaction	FAD
	–	1.2.8566.m1	BHMT	Betaine—homocysteine S-methyltransferase	2.09	3.89E-139	2.52	6.39E-70	3.86	0.00E+00	4.02	0.00E+00	2.1.1.5	methyl group transfer	–
	–	1.2.19413.m1	BHMT	Betaine—homocysteine S-methyltransferase	0	0	5.43	2.38E-69	1.19	5.15E-12	1.07	3.85E-03	2.1.1.5	methyl group transfer	–
	–	1.2.3404.m1	DMGDH	Dimethylglycine dehydrogenase	1.13	8.99E-22	2.19	1.06E-42	2.75	0.00E+00	2.68	2.54E-128	1.5.8.4	redox reaction, oxidative deamination	FAD
	–	1.2.1981.m1	SARDH	Sarcosine dehydrogenase	0.79	1.82E-13	1.61	5.25E-29	1.73	6.65E-176	1.72	9.41E-121	1.5.8.3	redox reaction	FAD, tetrahydrofolate
	–	1.2.13833.m1	GNMT	Glycine N-methyltransferase	1.56	2.39E-14	2.07	7.39E-41	2.70	6.16E-155	2.76	5.02E-249	2.1.1.20		
Methionine SALVAGE	–	1.2.4059.m1	AMD1	Adenosylmethionine decarboxylase	0	0	0	0	0	0	0	0	4.1.1.50	decarboxylation	pyridoxal 5'-phosphate
	–	1.2.4123.m1	SRM	Spermidine synthase	0	0	0	0	0	0	0	0	2.5.1.16	aminopropyl group transfer	Ca2+, K+, Na+
	–	1.2.11993.m1	mtaP	Methylthioadenosine phosphorylase	0	0	0	0	0	0	0	0	2.4.2.28	pentosyl group transfer	–
	–	1.2.8464.m1	mtnA	Methylthioribose-1-phosphate	0	0	0	0	0	0	0	0	5.3.1.23	intramolecular oxidoreduction	–
	–	1.2.7046.m1	mtnB	Methylthioribulose-1-phosphate dehydratase	0	0	0	0	0	0	0	0	4.2.1.109	dehydration	–
	–	1.2.8848.m1	ENOPH1	Enolase-phosphatase	0	0	0	0	0	0	0	0	3.1.3.77	acireductone synthase	–
	–	1.2.21614.m1	ADI1	1,2-dihydroxy-3-keto-5-methylthiopentene dioxygenase	-0.28	8.51E-02	0	0	-0.22	5.07E-02	0	0	1.13.11.5 1.13.11.53	oxidation	–
	–	1.2.7815.m1	IL4I1	L-amino-acid oxidase	0	0	0	0	0	0	0	0	1.4.3.2	redox reaction	FAD

(B)

Pathways	Genome ID	Best blast hit	Query cover (%)	E value	Identity (%)	Domain ID	E-value	HMMER ID	HMMER Name	KEGG	KEGG ORTHOLOGY
DMSP biosynthesis	1.2.4389.m1	XP_001633045.1 | predicted protein [Nematostella vectensis]	99	0	63	cd00610	2.59E-153	PF00202.16	Aminotransferase class-III	K14286	ethanolamine phosphate phospho-lyase
Transamination	1.2.3643.m1	XP_001632576.1 | predicted protein [Nematostella vectensis]	97	0	61	cd00609	3.79E-70	PF00155.16	Aminotransferase class I and II	KD0815	tyrosine aminotransferase
	1.2.1862.m1	XP_001627427.1 | predicted protein [Nematostella vectensis]	94	0	66	cd01557	1.22E-131	PF01063.14	Aminotransferase class IV	KD0826	branched-chain amino acid aminotransferase
	1.2.6453.m1	XP_001627535.1 | predicted protein [Nematostella vectensis]	93	0	54	cd00609	5.76E-48	PF00155.16	Aminotransferase class I and II	KD0814	alanine transaminase
	1.2.6452.m1	XP_001622550.1 | hypothetical protein [Nematostella vectensis]	98	0	73	cd00609	1.20E-49	PF00155.16	Aminotransferase class I and II	KD0814	alanine transaminase
	1.2.6454.m1	XP_001627535.1 | predicted protein [Nematostella vectensis]	96	9.00E-150	44	cd00609	2.25E-47	PF00155.16	Aminotransferase class I and II	KD0814	alanine transaminase
Reduction/ Oxidation	1.2.9800.m1	XP_002734670.1.1 | mitochondrial 10-formyltetrahydrofolate dehydrogenase-like [Saccoglossus kowalevskii]	99	0	71	cd08647+	7.01E-144	PF00171.17+	Aldehyde dehydrogenase family	KD0289	formyltetrahydrofolate dehydrogenase
	1.2.22357.m1	XP_001639716.1 | predicted protein [Nematostella vectensis]	95	0	74	cd07141	0	PF00171.17	Aldehyde dehydrogenase family	KD0128	aldehyde dehydrogenase (NAD+)
	1.2.21229.m1	XP_001630371.1 | predicted protein [Nematostella vectensis]	97	0	80	cd07111 +	0.00E+00	PF00171.17	Aldehyde dehydrogenase family	KD0128	aldehyde dehydrogenase (NAD+)
	1.2.12494.m1	NP_001096184.1 | delta-1-pyrroline-5-carboxylate dehydrogenase [Xenopus laevis]	99	9.00E-88	53	cd07123	2.11E-124	PF00171.17	Aldehyde dehydrogenase family	KD0294	1-pyrroline-5-carboxylate dehydrogenase
	1.2.25403.m1	XP_007252494.1 | alpha-aminoadipic semialdehyde dehydrogenase [Astyanax mexicanus]	94	0	70	cd07130	0	PF00171.17	Aldehyde dehydrogenase family	K14085	aldehyde dehydrogenase family 7 member A1
	1.2.20338.m1	XP_001641635.1 | predicted protein [Nematostella vectensis]	99	0	68	cd07085	0.00E+00	PF00171.17	Aldehyde dehydrogenase family	KD0140	methylmalonate-semialdehyde dehydrogenase
	1.2.2152.m1	XP_001629556.1 | predicted protein [Nematostella vectensis]	99	0	66	cl11961	0	PF00171.18	Aldehyde dehydrogenase family	KD0129	aldehyde dehydrogenase (NAD(P)+)
	1.2.11968.m1	XP_001632685.1 | predicted protein [Nematostella vectensis]	77	9.00E-77	68	cl00438	2.80E-07	PF03358.10	NADPH-dependent FMN reductase	KD0128	aldehyde dehydrogenase (NAD+)
	1.257.m1	XP_001628474.1 | predicted protein [Nematostella vectensis]	95	9.00E-122	59	cd06660	9.81E-84	PF00248.16	Aldo/keto reductase family	KD0002	alcohol dehydrogenase (NADP+)
	1.2.25591.m1	XP_001631871.1 | predicted protein [Nematostella vectensis]	97	9.00E-139	75	cd06183	1.41E-113	PF00970.19+	Oxidoreductase FAD-binding domain	KD0326	cytochrome-b5 reductase
Methylation	1.2.13833.m1	XP_001625366.1 | predicted protein [Nematostella vectensis]	86	1.00E-145	67	cd02440	6.39E-12	PF12847.2	Methyltransferase	KD0552	glycine N-methyltransferase
	1.2.12191.m1	XP_780353.2 | protein arginine N-methyltransferase 7 like [Strongylocentrotus purpuratus]	98	0	41	cd02440	1.40E-03	PF12847.2	Methyltransferase	K11438	protein arginine N-methyltransferase 7
	1.2.14921.m1	XP_002611771.1.1 | hypothetical protein [Branchiostoma floridae]	95	8.00E-171	63	cl04109	7.99E-23	PF03492.10	SAM dependent carboxyl methyltransferase	[]	[]
Decarboxylation	1.2.3018.m1	XP_001636251.1.1 | predicted protein [Nematostella vectensis]	88	0	69	cd00622	0.00E+00	PF02784.11	tyrosine aspartate decarboxylase, pyridoxal binding domain	KD1581	ornithine decarboxylase
	1.2.4120.m1	XP_001632404.1 | predicted protein [Nematostella vectensis]	72	0	46	cl18945	1.53E-73	PF00282.14	Pyridoxal-dependent decarboxylase conserved domain	[]	[]
	1.2.4118.m1	XP_001622382.1 | predicted protein [Nematostella vectensis]	95	0	40	cl18945	1.30E-75	PF00282.14	Pyridoxal-dependent decarboxylase conserved domain	–	–
	1.2.4119.m1	XP_001632404.1 | predicted protein [Nematostella vectensis]	73	0	46	cl18945	1.07E-72	PF00282.14	Pyridoxal-dependent decarboxylase conserved domain	–	–
Oxidative deamination	1.2.874.m1	XP_001632737.1 | predicted protein [Nematostella vectensis]	99	0	45	pfam01179	1.00E-130	PF01179.15	Copper amine oxidase, enzyme domain	K11182	diamine oxidase
	1.2.8765.m1	XP_001627145.1 | predicted protein [Nematostella vectensis]	90	0	43	cl08309	3.29E-113	PF01179.15	Copper amine oxidase, enzyme domain	K11182	diamine oxidase
Methyl Cycle	1.2.8442.m1	XP_001629913.1 | predicted protein [Nematostella vectensis]	93	0	81	pfam02772+	1.95E-69	PF02773.11 +	S-adenosylmethionine synthetase, C-terminal domain+	KD0789	S-adenosylmethionine synthetase
	1.2.9082.m1	XP_001637180.1 | predicted protein [Nematostella vectensis]	100	0	76	pfam02772+	5.90E-66	PF02773.11+	S-adenosylmethionine synthetase+	KD0789	S-adenosylmethionine synthetase
	1.2.10409.m1	XP_001626663.1 | predicted protein [Nematostella vectensis]	81	0	69	cl04760+	3.31E-45	PF00145.12+	C-5 cytosine-specific DNA methylase+	KD0558	DNA (cytosine-5)-methyltransferase 1
	1.2.2524.m1	XP_001639319.1 | predicted protein [Nematostella vectensis]	100	0	87	cd00401	0.00E+00	PF05221.12+	S-adenosyl-L-homocysteine hydrolase+	KD1251	adenosylhomocysteinase
	1.2.20486.m1	NP_932338.1 | methionine synthase [Danio rerio]	97	0	70	cd00740+	1.16E-130	PF02574.11+	Homocysteine S-methyltransferase+	KD0548	5-methyltetrahydrofolate--homocysteine methyltransferase
	1.2.6795.m1	XP_001625575.1 | predicted protein [Nematostella vectensis]	96	0	79	cd00378	0.00E+00	PF00464.14	Serine hydroxymethyltransferase	KD0600	glycine hydroxymethyltransferase
	1.2.1458.m1	XP_001633891.1 | predicted protein [Nematostella vectensis]	93	0	70	cd00537	4.02E-100	PF02219.12	Methylenetetrahydrofolate reductase	KD0297	methylenetetrahydrofolate reductase (NADPH)
Methionine trans-sulphuration	1.2.10238.m1	XP_001634593.1 | predicted protein [Nematostella vectensis]	99	0	71	cd00614	0.00E+00	PF01053.15	Cys/Met metabolism PLP-dependent enzyme	KD1758	cystathionine gamma-lyase
Glycine betaine degradation	1.2.6999.m1	[XP_002588882.1 | hypothetical protein BRAFLDRAFT_235936 [Branchiostoma floridae]	91	0	69	pfam00732+	4.63E-58	PF00732.14	GMC oxidoreductase	KD0108	choline dehydrogenase
	1.2.8566.m1	XP_001639806.1 | predicted protein [Nematostella vectensis]	97	0	72	cl21457	9.45E-58	PF02574.11	Homocysteine S-methyltransferase	KD0544	betaine-homocysteine S-methyltransferase
	1.2.19413.m1	NP_001012498.1 | betaine--homocysteine S-methyltransferase 1 [Danio rerio]	99	2.00E-142	58	cl21457	1.42E-51	PF02574.12	Homocysteine S-methyltransferase	KD0544	betaine-homocysteine S-methyltransferase
	1.2.3404.m1	XP_001632395.1 | predicted protein [Nematostella vectensis]	97	0	70	pfam01571+	4.14E-66	PF01266.19+	FAD dependent oxidoreductase+	KD0315	dimethylglycine dehydrogenase
	1.2.1981.m1	XP_001624293.1 | predicted protein [Nematostella vectensis]	96	0	72	pfam01571+	6.94E-61	PF01266.19+	FAD dependent oxidoreductase+	KD0314	sarcosine dehydrogenase
	1.2.13833.m1	XP_001625366.1 | predicted protein [Nematostella vectensis]	86	2.00E-145	67	cd02440	1.49E-12	PF13649.3	Methyltransferase domain	KD0552	glycine N-methyltransferase
Methionine SALVAGE	1.2.4059.m1	XP_001628454.1 | predicted protein [Nematostella vectensis]	96	2.00E-69	58	cl03253	6.16E-67	PF01536.11	Adenosylmethionine decarboxylase	KD1611	S-adenosylmethionine decarboxylase
	1.2.4123.m1	XP_001634423.1 | predicted protein [Nematostella vectensis]	85	2.00E-156	76	cd02440	7.46E-07	PF01564.12	Spermine/spermidine synthase	KD0797	spermidine synthase
	1.2.11993.m1	XP_001626994.1 | predicted protein [Nematostella vectensis]	97	1.00E-128	64	TIGR01694	3.96E-109	PF01048.15	Phosphorylase superfamily	KD0772	5'-methylthioadenosine phosphorylase
	1.2.8464.m1	XP_006003718.1 | methylthioribose-1-phosphate isomerase-like [Latimeria chalumnae]	98	4.00E-161	64	TIGR00512	6.66E-176	PF01008.12	Initiation factor 2 subunit family	KD1963	methylthioribose-1-phosphate isomerase
	1.2.7046.m1	XP_007239178.1 | methylthioribulose-1-phosphate dehydratase-like [Astyanax mexicanus]	92	3.00E-88	70	TIGR03328	6.80E-57	PF00596.16	Class II Aldolase and Adducin N-terminal domain	KD1964	methylthioribulose-1-phosphate dehydratase
	1.2.8848.m1	XP_006010154.1 | enolase-phosphatase E1 [Latimeria chalumnae]	86	2.00E-77	47	TIGR01691	5.82E-55	PF13419.1	Haloacid dehalogenase-like hydrolase	KD9880	enolase-phosphatase E1
	1.2.21614.m1	XP_002399605.1 | acireductone dioxygenase, putative [Ixodes scapularis]	95	2.00E-83	66	pfam03079	2.58E-65	PF03079.9	ARD/ARD' family	KD8967	1,2-dihydroxy-3-keto-5-methylthiopentene dioxygenase
	1.2.7815.m1	gb|ACZ88355.1|amine oxidase, flavin-containing [Streptosporangium roseum]	86	4.00E-63	30	pfam01593	4.42E-48	PF01593.19	Flavin containing amine oxidoreductase	KD3334	L-amino-acid oxidase

Table S5.5. Differentially expressed *A. millepora* aldehydes in response to hyposaline stress, independent of the time factor. Log2 fold change (log2FC) and false discovery rate (FDR) are reported for each of the experiment datasets of the treatment (hyposalinic) relative to the control when excluding time as a factor. Red shading indicates genes that are differentially up-regulated; blue shading indicates genes that are differentially down-regulated (FDR <0.05).

Step Abbrev.	Genome ID	Protein ID	Adults		Juveniles	
			log2FC	FDR	log2FC	FDR
REDOX1	1.2.9800.m1	Formyltetrahydrofolate dehydrogenase	1.77	9.08E-23	1.75	1.40E-277
REDOX2	1.2.22357.m1	Aldehyde dehydrogenase	0.15	1.91E-02	0.22	3.03E-06
REDOX3	1.2.21229.m1	Aldehyde dehydrogenase	0.30	1.54E-03	0.19	2.13E-02
REDOX4	1.2.12494.m1	L-glutamate gamma-semialdehyde dehydrogenase	1.12	1.90E-12		
REDOX5	1.2.25403.m1	Aldehyde dehydrogenase	0.63	1.55E-09	-0.10	4.40E-02
REDOX6	1.2.20338.m1	Aldehyde dehydrogenase	0.58	2.84E-07	-0.50	4.74E-14
REDOX7	1.2.2152.m1	Aldehyde dehydrogenase			0.17	3.96E-04
REDOX8	1.2.11968.m1	NADPH-dependent FMN reductase*	0.48	6.03E-04	-0.37	4.02E-03
REDOX9	1.2.57.m1	Alcohol dehydrogenase (NADP+)			0.30	1.79E-05

Figures

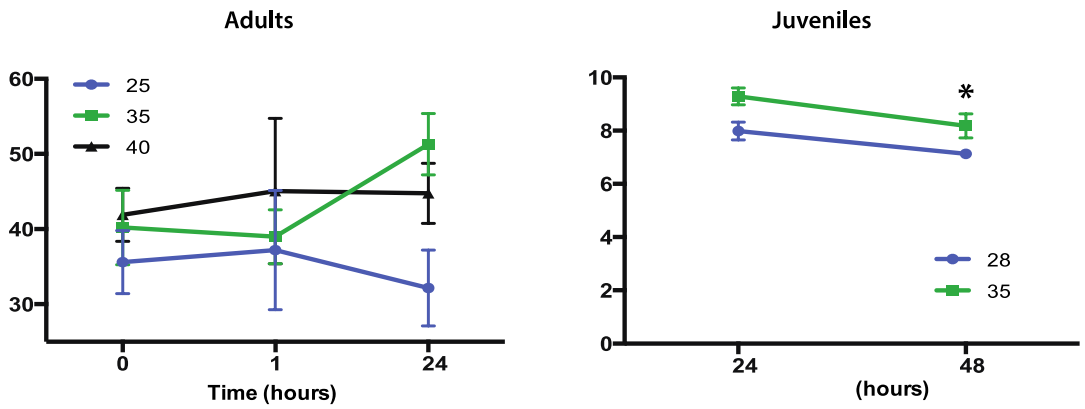

Figure S4.1. Changes acrylate concentrations (mean ± s.e.) in adult corals (*n=5*) and settled juveniles (*n=6*) of the coral *A. millepora*. Adults (A) were exposed to control (35 PSU, green) and two salinity stress conditions (25 PSU in blue and 40 PSU in black). Acrylate concentrations were not significant between the control and treatments (H-F Pr > 0.05). Juveniles (B) were exposed to control (35 PSU, green) and one salinity stress condition (28 PSU, blue). Acrylate concentrations were significantly different between the salinity treatment and control of the *A. millepora* juveniles (F=10.59, *p<0.005). Concentrations were not significant different through time.

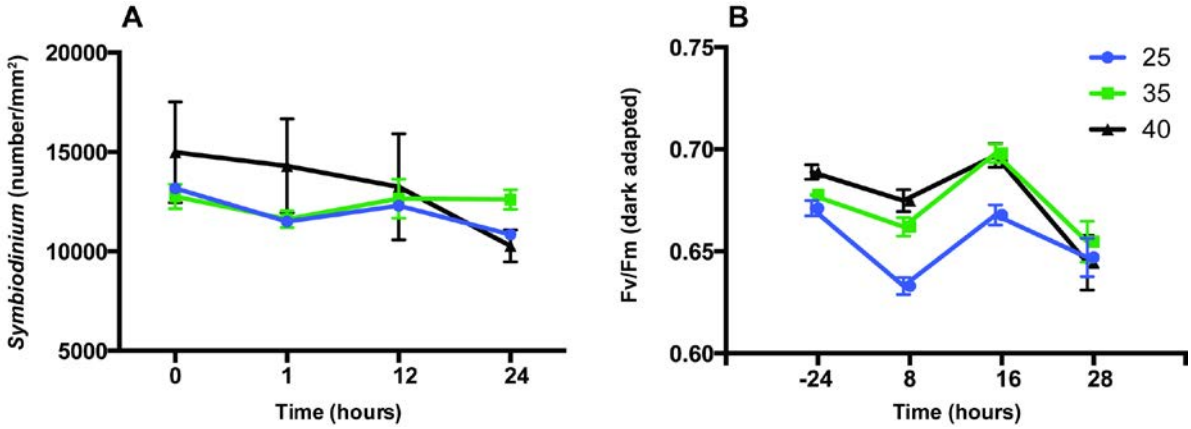

Figure S4.2. *Symbiodinium* cell density and photosynthetic efficiency (mean ± s.e.) within the adults of the coral *Acropora millepora* under control (35 PSU, green) and two salinity stress conditions (25 PSU in blue and 45 PSU in black). (A) Density of *Symbiodinium* cells in the coral nubbins through time (n=3). (B) Photosystem II photochemical efficiency (maximum quantum yields: Fv/Fm) through time (n=9 in all time points, but n=3 at 28 h) (MANOVA, H-F Pr > 0.05; Table S4.2, Supporting information).

Chapter 5: General discussion

The key molecular components involved in the coral response to environmental stress

General contribution

This thesis represents a substantial contribution towards understanding the molecular bases of the responses of the coral *A. millepora* to a number of stressors – osmotic stress, and an immune challenge both with and without the additional stress of high pCO_2 conditions. In this chapter, these results are discussed with a focus on identifying a core set of general stress response genes that are induced by temperature, salinity and high pCO_2 conditions. This chapter also focuses on the significance of this work in understanding the connection between the coral health and the changing environment.

5.1. Genes involved in the cellular stress response in corals

Previous studies have enabled the description of general cellular stress responses that are common across a wide range of organisms. These universal mechanisms represent cellular responses to macromolecular damage that are independent of the type of stress and conserved across a broad range of cellular organisms (Kultz 2005; Petrak *et al.* 2008). The general response was analysed by Wang *et al*. (2009); this meta analysis used 66 proteomic studies across 5 model species (worm, fly, human, mouse, rat), and samples taken from different tissues, organs and conditions, to generate a list of 44 proteins that were detected independent of the organism or stressor. These proteins grouped into five main functional classes: energy metabolism, cytoskeleton organization, cellular growth, cycle and death, and molecular chaperones. In the case of *A. millepora,* homologues of 26 of these 44 "universal" stress response proteins were up-regulated under hypo-saline stress in our study (Table 5.1, Chapter 3). An additional seven of these proteins were involved in the transcriptional responses to stress in other coral studies (Chapter 3 Table S3.6). The molecular function protein homeostasis is the most obvious component of the response of *Acropora* to hypo-saline stress, and was one of the general stress responses identified in the Wang *et al.* (2009) study.

At the top of the list of the most frequently detected proteins is the heat-shock protein 70kDa protein 5 (HspA5, also known as grp78 and binding immunoglobulin protein or BiP). This chaperone, has a central function in the endoplasmic reticulum (ER) (Araki & Nagata 2011) and its expression increased in the coral *A. millepora* under high temperature and under bacterial challenge (Brown *et al.* 2013; Rodriguez Lanetty *et al.* 2009). In the current thesis, the HspA5 (1.2.4351.m1; Table 5.1) also displayed increased expression when corals were exposed to hyposaline conditions or subjected to an immune challenge (Chapters 2 and 3, respectively). Two other Hsp70 genes (1.2.8575.m1 and 1.2.8573.m1; Table S3.6) were up-regulated in response to both high temperature (in *S. pistillata* and *A. aspera*), and to hypo-saline conditions in *A. millepora* (Chapter 3). Interestingly, in previous transcriptomic studies these two Hsp70 were not differentially expressed in *A. millepora* juveniles under high pCO_2 stress, whereas expression of other Hsps, including grp94 and other Hsp70s did increase under these conditions (Moya *et al.* 2015) (Table 5). In general, the response of specific Hsps constitutes a defined thermal stress indicator that is highly conserved across a wide range of taxa that includes marine invertebrates (Hofmann 1999). For example, Hsp70 expression levels were correlated to the intensity of temperature stress in mussels (Gracey *et al.* 2008). Several specific Hsps24 were also shown to increase in expression under heat stress in two *Mytilus* species, and it has been suggested that these may be general abiotic stress biomarkers (Lockwood *et al.* 2010).

Table 5.1. *A. millepora* homologues of the "universal" stress response proteins identified by Wang *et al*. (2009; Table 2). Salinity (24 h) data represent the differentially expressed values under hypo-saline stress in *A. millepora* (Chapter 3). Entries in the "Other studies" column refer to coral stress response studies that have identified orthologues of the *A. millepora* genes (for details see Table S3.6).

Protein Name	Coral Genome ID	Protein ID	Salinity 24 h		Other studies	
			log2FC	Padj	Type of stressor	Authors
BiP, HSP70 kDa protein 5 (glucose-regulated protein, 78 kDa)	1.2.4351.m1	sp|P11021|GRP78_HUMAN	1.30	8.64E-19	High temperature, bacteria and LPS challenge	Rodriguez-Lanetty (2009), Brown et al. (2013)
Heat shock 70 kDa protein 8	1.2.8573.m1	sp|P11142|HSP7C_HUMAN	1.07	6.37E-14	High temperature	Maor-Landaw et al. (2014), Leggat et al. (2011)
Heat shock 70 kDa protein 8	1.2.8575.m1	sp|P11142|HSP7C_HUMAN	1.77	6.54E-28	High temperature	Maor-Landaw et al. (2014), Leggat et al. (2011)
Heat shock 60 kDa protein 1 (chaperonin)	1.2.6096.m1	sp|P10809|CH60_HUMAN	1.29	1.21E-21	–	–
Heat shock 27 kDa protein 1	1.2.6070.m1	sp|P04792|HSPB1_HUMAN	2.96	1.36E-37	High temperature and LPS challenge	Palumbi et al. (2014)
Superoxide dismutase 1	1.2.240.m1	sp|P00441|SODC_HUMAN	0.42	1.07E-02	High temperature	Palumbi et al. (2014)
Calreticulin	1.2.2683.m1	sp|P27797|CALR_HUMAN	1.14	8.82E-22	High temperature	Maor-Landaw et al. (2014)
Protein disulfide isomerase family A	1.2.1667.m1	sp|P07237|PDIA1_HUMAN	0.98	1.09E-13	High temperature	Maor-Landaw et al. (2014)
Protein disulfide isomerase family A	1.2.7144.m1	sp|P07237|PDIA1_HUMAN	1.24	1.74E-27	–	–
Protein disulfide isomerase family A	1.2.5704.m1	sp|P07237|PDIA1_HUMAN	0.77	2.42E-08	–	–
Enolase 1, (alpha)	1.2.9573.m1	sp|P06733|ENOA_HUMAN	1.96	2.47E-42	–	–
Peroxiredoxin	1.2.10889.m1	sp|P30041|PRDX6_HUMAN	0.45	6.20E-04	–	–
Rho GDP dissociation inhibitor (GDI) alpha	1.2.5696.m1	sp|P52565|GDIR1_HUMAN	0.36	9.25E-03	–	–
Tubulin, beta	1.2.2538.m1	sp|P07437|TBB5_HUMAN	1.47	3.43E-36	–	–
Tubulin, beta	1.2.3539.m1	sp|P07437|TBB5_HUMAN	0.60	5.29E-03	–	–
Tubulin, beta	1.2.2537.m1	sp|P07437|TBB5_HUMAN	0.76	3.98E-07	–	–
Phosphoglycerate kinase 1	1.2.9109.m1	sp|P00558|PGK1_HUMAN	0.55	1.04E-02	–	–
Glyceraldehyde-3-phosphate dehydrogenase	1.2.16944.m1	sp|P04406|G3P_HUMAN	0.66	2.59E-05	–	–
Eukaryotic translation elongation factor 2	1.2.8169.m1	sp|P13639|EF2_HUMAN	1.10	5.41E-19	–	–
Eukaryotic translation initiation factor 5A	1.2.9574.m1	sp|P63241|IF5A1_HUMAN	0.38	7.13E-03	–	–
Tumour protein, translationally controlled	1.2.343.m1	sp|P13693|TCTP_HUMAN	1.14	1.38E-17	–	–
Aldolase A, fructose-bisphosphate	1.2.6905.m1	sp|P04075|ALDOA_HUMAN	0.51	1.08E-04	–	–
Aldehyde dehydrogenase 2 family	1.2.9800.m1	sp|P05091|ALDH2_HUMAN	2.35	5.22E-68	–	–
Cathepsin D	1.2.7013.m1	sp|P07339|CATD_HUMAN	1.01	1.13E-15	–	–
Prohibitin	1.2.18477.m1	sp|P35232|PHB_HUMAN	0.59	1.32E-03	–	–
Peptidylprolyl isomerase A (cyclophilin A)	1.2.18288.m1	sp|P62937|PPIA_HUMAN	0.49	4.43E-05	–	–
Peptidylprolyl isomerase A (cyclophilin A)	1.2.8532.m1	sp|P62937|PPIA_HUMAN	0.64	1.81E-04	–	–
Triosephosphate isomerase	1.2.14534.m1	sp|P60174|TPIS_HUMAN	0.52	7.57E-03	–	–
T-complex 1	1.2.11253.m1	sp|P17987|TCPA_HUMAN	0.69	3.69E-07	–	–
Nonmetastatic cells 2	1.2.6632.m1	sp|P22392|NDKB_HUMAN	0.41	1.83E-02	–	–
Nonmetastatic cells 2	1.2.6628.m1	sp|P22392|NDKB_HUMAN	1.34	1.73E-21	–	–
Tyrosine 3-monooxygenase	1.2.12060.m1	sp|P63104|1433Z_HUMAN	0.28	4.07E-02	–	–
Annexin A5	1.2.3250.m1	sp|P08758|ANXA5_HUMAN	0.48	4.50E-04	–	–

Other coral genes involved in the universal stress response include genes associated with the ER protein folding and stress apparatus, such as protein disulphide isomerase (PDI), calreticulin (CRT), and superoxide dismutase (SOD). These genes were consistently differentially expressed under hyposaline conditions in *A. millepora* (Chapter 3) and under

thermal stress in *S. pistillata* and *A. hyacinthus* (see Figure 5.1 identifying genes involved in different environmental stressors in corals) (Maor-Landaw *et al.* 2014; Palumbi *et al.* 2014). Note that the coral response to hypo-saline stress involved differential expression of a higher proportion of the general cellular stress response genes in *A. millepora*, than has been documented in any previously published study (Table 5.1).

Altogether, these results confirm that cellular responses to macromolecular damage are involved in responses to both hypo-saline and thermal stress in corals, and that the coral responses include homologues of proteins that respond to abiotic stressors in a wide range of animals (Figure 5.1). Previous studies have described the expression of some members of this core set of genes in stressed corals, but the work described here is the first to make a comprehensive comparison with the general stress response of higher organisms. With the application of transcriptomic and proteomic techniques, it should now be possible to identify biomarkers diagnostic of the health status of natural coral populations. However, important caveats that should be taken into account include the potential for spatial and temporal variation in levels of these markers, and the potential for lack of correspondence between the transcriptome and proteome levels (Somero 2012). For example, in both mussels and corals, the expression of genes encoding specific Hsps and proteolytic enzymes varies with the circadian cycle, in addition to there being temporal variation in the expression of groups of genes involved in a specific metabolic functions (Gracey *et al.* 2008; Levy *et al.* 2011). Also, as discussed by Feder & Walser (2005), the correlation between mRNA and protein abundance levels was less than 50% in several human and yeast studies, and there is evidence that the degree of correlation differs between classes of genes / proteins (Greenbaum *et al.* 2003). These limitations highlight important considerations for future work in corals such as investigating temporal variation, and complementing transcriptomic analyses with proteomic studies. As highlighted by Wang *et al*. (2009), there is also a need to identify biomarkers for specific stressors. From this perspective, it is important to investigate the functions of genes

that respond only to a specific stressor. For example, genes of specifically expressed under hypo-saline conditions in both corals and mussels (Chapter 3) (Lockwood & Somero 2011; Tomanek *et al.* 2012). This PhD work (Chapter 3 and 5) contributes by identifying repertoires of genes that could potentially indicate that corals had experienced specific environmental stressors.

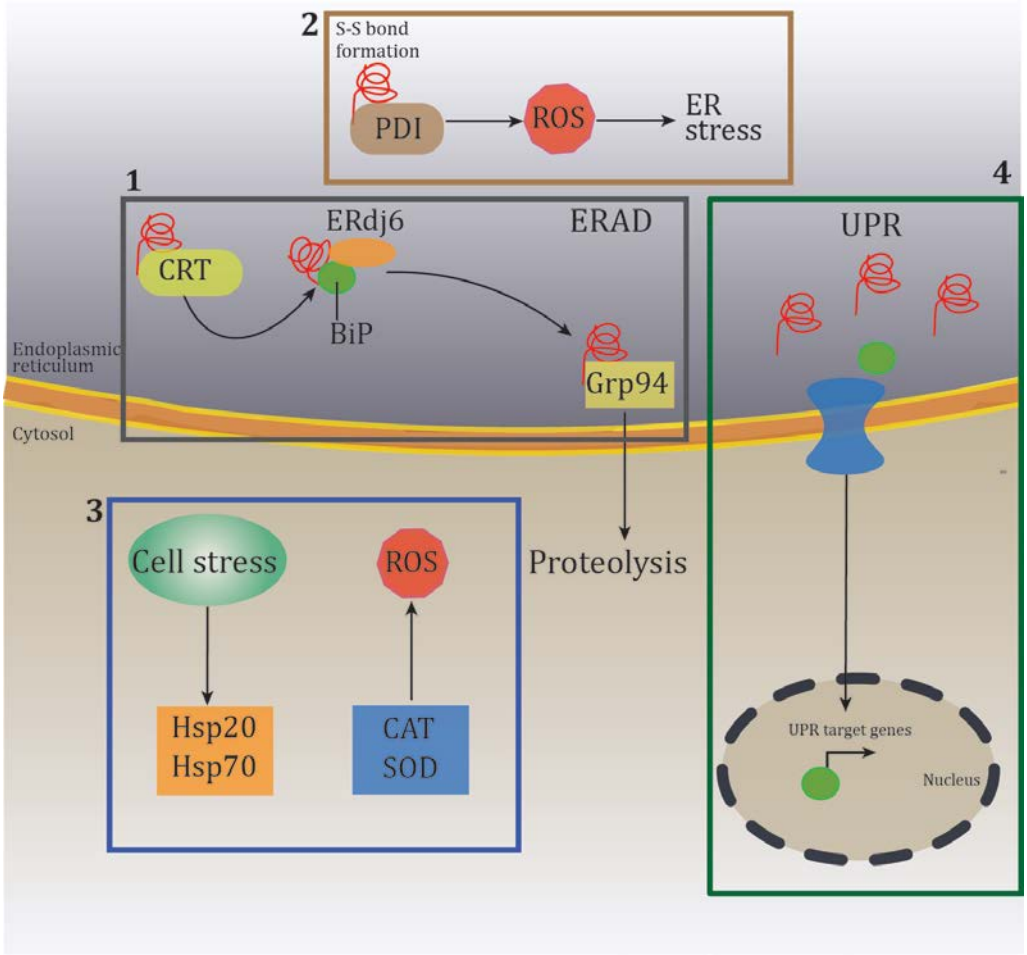

Figure 5.1. Schematic representation of general responses of *Acropora* to abiotic stress based on known mammalian responses (Araki & Nakata, 2011; Zhang & Kaufman 2008). The figure is based on data from a number of different stress response experiments, details of which are given in Table 5.1 and Table S3.6. Mechanisms potentially operating inside coral cells under stress include: 1) ER chaperone activity by calretiulin (CRT) and calnexin (not shown), promotes proper protein folding and prevents aggregation. CNX/CRT can also lead unfolded proteins to be targeted by BiP and its co-chaperones (ERdj6) into the ER-associated degradation pathway (ERAD). This pathway involves a ligase complex (which includes GRP94) and brings about protein translocation to the cytosol where they are finally degraded. 2) ER protein folding involving the oxidation of disulphide bonds by protein disulphide isomerase (PDI) generates reactive oxygen species (ROS) and therefore leads to ER stress. 3) Cellular stress can lead to increased levels of Hsps and generates ROS, leading to the activation of the antioxidant system, which includes superoxide dismutase (SOD) and

catalase (CAT) activities. 4) Accumulation of unfolded proteins in the ER can activate the unfolded protein response (UPR). This system is mediated by membrane proteins that are activated by the release of BiP. The activated signalling cascade results in translation of ER recovery genes.

5.2. Cellular stress response under an immune challenge

Previous studies have demonstrated crosstalk between cellular stress and immune responses in a number of animals. For example, BiP produced as an ER stress response can act as a cytokine and increase pro-inflammatory responses in man (Asea *et al.* 2000; Pinsino & Matranga 2015). The coral response to LPS challenge included the up-regulation of several Hsp20s (1.2.6070.m1, 1.2.6572.m1, 1.2.6574.m1; Table S3.6), an Hsp70 and BiP (1.2.4351.m1, 1.2.19257.m1; Table S3.6), as demonstrated in Chapter 3 of this thesis. These increases do not necessarily indicate stress, and could rather be considered part of the innate immune response (Pinsino & Matranga 2015), particularly in view of the fact that no other stress response genes were up-regulated (Table 5.1). Although we do not have further information on the function of these Hsps in corals, the transcriptomic response of specific Hsps in our salinity and immune challenge experiments (Chapters 2 and 3), in addition to other elevated temperature, high pCO_2 stress studies, suggests that these proteins are involved in a common stress response. In particular, the ubiquity of BiP expression noted here suggests that this gene may be suitable as a general biomarker of the stressed state in corals.

5.3. DMSP production under environmental stress

DMSP is a key intermediate in the sulphur cycle molecule and precursor of the volatile gas dimethylsuphide (DMS). DMSP is known to be generated by higher plants and algae, and has also recently been shown to be produced by the coral animal (Raina *et al.* 2013). This compound has several important roles in plants, which produce DMSP in response to a variety of environmental stressors (i.e. light, salinity, temperature and nitrogen limitation) (Stefels 2000). Several studies have focused on the plant response to hyper-saline conditions,

where DMSP increases with salinity and the molecule likely functions as an osmolyte (Trossat *et al.* 1998; Vairavamurthy *et al.* 1985). Although there have been relatively few studies on the influence of hypo-osmotic stress on DMSP biosynthesis in plants, loss of DMSP from algal cells under these conditions has been documented (Dickson & Kirst 1986; Niki *et al.* 2007). The results reported in Chapter 4 demonstrate that DMSP production by the coral animal increased under hypo-saline conditions but remained unchanged under hyper-saline conditions. These results indicate that DMSP does not act as an osmolyte in corals, but appears to have a more general role in the response to stress, as its production increases under both hypo-saline (Chapter 4) and high temperature conditions (Raina *et al.* 2013).

The data reported in this thesis, including the combination of qNMR and transcriptomics, represents a major advance in understanding DMSP biosynthesis in corals (Chapter 4). This thesis identified candidate genes for roles in DMSP biosynthesis in corals, based on the rationale that the genes involved are likely to be up-regulated under environmental conditions that resulted in increased production of DMSP. In addition, the trancriptomic approach identified the pathways involved in the biosynthesis of methionine, the precursor of DMSP. Increases in the expression of genes involved in methionine production, in addition to increases in the expression of genes involved in proteolysis and stress responses, supports the conclusion that DMSP serves as a scavenger of ROS and is produced in coral as a sink for excess methionine.

5.4. Ecological significance and concluding remarks

The genus *Acropora* is of particular ecological significance on the GBR and in the wider Indo-Pacific, because it is the dominant and most diverse genus in this region (Veron 2000). However, the high sensitivity of *Acropora* spp. to elevated temperatures makes them particularly vulnerable to bleaching (Loya *et al.* 2001), and understanding the impacts of not only of heat stress, but also other environmental stressors is key for predicting how well or

badly they are likely to fare in future. This PhD work contributed to a broader understanding of the molecular responses of *A. millepora* to environmental stress. By studying the response to osmotic conditions resembling those experienced during heavy rainfall events, this study determined that these conditions lead to up-regulation of the protein degradation and antioxidant systems in corals (Chapter 3). These results aid our understanding of the molecular processes that may drive coral mortality and declines following hypo-saline events on the GBR (Berkelmans *et al.* 2012; Butler *et al.* 2015; Downs *et al.* 2009). Interestingly, during low salinity events, the coral *A. millepora* increases DMSP production, potentially contributing higher flux of DMS to the atmosphere. This DMS can influence local climate as it reacts to form sulphate aerosols (sulphate and methane sulphonate) within the marine atmospheric boundary and can influence cloud albedo (Charlson *et al.* 1987). Likewise, quantifying DMS production on the reef will be important to understand the influence of low salinity events on the biogenic sulphur cycle (Broadbent & Jones 2004).

This PhD work also contributed to understanding the interactions between the environment, biotic stressors, and the coral holobiont (Figure 1.7), first by identifying genes involved in the immune response, and second by indicating the impact on the immune response of exposure to elevated pCO_2 conditions approximating to near future ocean acidification values (IPCC 2013) (Figure1.2). Further studies should investigate the extent to which the coral immune system can acclimate to prolonged elevated pCO_2. There are precedents for acclimation to stress. For example, Palumbi *et al*. (2014) described acclimation of a field population of *A. hyacinthus* to a more challenging temperature regime within one year.

The ability of corals to acclimate is unlikely to be uniform; more likely, some species will have a greater capacity to acclimate to environmental and immune stressors than others (Mydlarz *et al.* 2010). *Acropora* species appear to be more vulnerable than many other corals

to environmental stress. For example, acroporoid corals were reported to be declining in the Caribbean due to environmental stressors, whereas *Porites spp.* were found to be more tolerant (Green *et al.* 2008). However, the molecular bases of this observation are currently unknown. The results presented in this study (Chapter 2 and 4) provide candidates for a comparative analysis of stress response genes between species. It will be informative to compare both the stress response repertoire and the levels of expression of these genes across a range of species that represent a spectrum of stress sensitivity types.

Importantly, protein-coding genes and gene regulation are the primary determinants of the ability of species to cope with environmental change by regulating cellular stress while providing the species with phenotypic plasticity (Somero 2012). This PhD work has made a major contribution in identifying protein-coding genes that are central in the coral molecular response to present and future environmental conditions. In addition the study has provided new insights into the genes that have a key role in defending to coral against environmental stress and maintaining coral health. However, results presented in this thesis are only part of a larger picture with further research required to characterise the functions of these proteins, which will be a significant step to further understand the corals response to both abiotic and biotic stressors under climate change challenges.

References

Akira S, Takeda K (2004) Toll-like receptor signalling. *Nat Rev Immunol* **4**, 499-511.

Akira S, Uematsu S, Takeuchi O (2006) Pathogen Recognition and Innate Immunity. *Cell* **124**, 783-801.

Anders S, Pyl PT, Huber W (2015) HTSeq--a Python framework to work with high-throughput sequencing data. *Bioinformatics* **31**, 166-169.

Andreae MO (1990) Ocean-atmosphere interactions in the global biogeochemical sulfur cycle. *Marine Chemistry* **30**, 1-29.

Andreae MO, Crutzen PJ (1997) Atmospheric aerosols: biogeochemical sources and role in atmospheric chemistry. *Science* **276**, 1052-1058.

Araki K, Nagata K (2011) Protein folding and quality control in the ER. *Cold Spring Harb Perspect Biol* **3**, a007526.

Asea A, Kraeft S-K, Kurt-Jones EA*, et al.* (2000) HSP70 stimulates cytokine production through a CD14-dependant pathway, demonstrating its dual role as a chaperone and cytokine. *Nature medicine* **6**, 435-442.

Asplund ME, Baden SP, Russ S*, et al.* (2014) Ocean acidification and host-pathogen interactions: blue mussels, *Mytilus edulis*, encountering *Vibrio tubiashii*. *Environ Microbiol* **16**, 1029-1039.

Augustin R, Fraune S, Bosch TCG (2010) How Hydra senses and destroys microbes **22**, 54-58.

Ayers GP, Gras JL (1991) Seasonal relationship between cloud condensation nuclei and aerosol methanesulphonate in marine air. *Nature* **353**, 834 - 835.

Baker AC, Glynn PW, Riegl B (2008) Climate change and coral reef bleaching: An ecological assessment of long-term impacts, recovery trends and future outlook. *Estuarine, Coastal and Shelf Science* **80**, 435-471.

Barshis DJ, Ladner JT, Oliver TA*, et al.* (2013) Genomic basis for coral resilience to climate change. *PNAS* **110**, 1091-6490.

Bay LK, Ulstrup KE, Nielsen HB*, et al.* (2009) Microarray analysis reveals transcriptional plasticity in the reef building coral *Acropora millepora*. *Molecular ecology* **18**, 3062-3075.

Bellwood DR, Hughes TP, Folke C, Nystrom M (2004) Confronting the coral reef crisis. *Nature* **429**, 827- 833.

Ben-Haim Y, Zicherman-Keren M, Rosenberg E (2003) Temperature-regulated bleaching and lysis of the coral *Pocillopora damicornis* by the novel pathogen *Vibrio coralliilyticus*. *Applied Environ Microbiol* **69**, 4236-4242.

Benjamini Y, Hochberg Y (1995) Controlling the false discovery rate: A practical and powerful approach to multiple testing. *J R Stat Soc, B* **57**, 289–300.

Berkelmans R, Jones AM, Schaffelke B (2012) Salinity thresholds of *Acropora* spp. on the Great Barrier Reef. *Coral Reefs* **31**, 1103-1110.

Bosch TCG, Augustin R, Anton-Erxleben F*, et al.* (2009) Uncovering the evolutionary history of innate immunity: the simple metazoan Hydra uses epithelial cells for host defence. *Dev Comp Immunol* **33**, 559-569.

Bourne DG, Garren M, Work TM*, et al.* (2009) Microbial disease and the coral holobiont. *Trends in microbiology* **17**, 554-562.

Broadbent AD, Jones GB (2004) DMS and DMSP in mucus ropes, coral mucus, surface films and sediment pore waters from coral reefs in the Great Barrier Reef. *Mar Freshwater Res* **55**, 849-855.

Broadbent AD, Jones GB, Jones RJ (2002) DMSP in corals and benthic algae from the Great Barrier Reef. *Estuar Coast Shelf Sci* **55**, 547-555.
Brown T, Bourne D, Rodriguez-Lanetty M (2013) Transcriptional activation of c3 and hsp70 as part of the immune response of *Acropora millepora* to bacterial challenges. *PLoS One* **8**, e67246.
Butler IR, Sommer B, Zann M, Zhao JX, Pandolfi JM (2015) The cumulative impacts of repeated heavy rainfall, flooding and altered water quality on the high-latitude coral reefs of Hervey Bay, Queensland, Australia. *Mar Pollut Bull* **96**, 356-367.
Cantin NE, Cohen AL, Karnauskas KB, Tarrant AM, McCorkle DC (2010) Ocean warming slows coral growth in the central Red Sea. *Science* **329**, 322-325.
Caruana A (2010) *DMS and DMSP production by marine dinoflagellates* PhD thesis, University of East Anglia.
Cervino JM, Hayes RL, Polson SW*, et al.* (2004) Relationship of Vibrio species infection and elevated temperatures to yellow blotch/band disease in Caribbean corals. *Applied and environmental microbiology* **70**, 6855-6864.
Charlson RJ, Lovelock JE, Andreae MO, Warren SG (1987) Oceanic phytoplankton, atmospheric sulphur, cloud albedo and climate. *Nature* **326**, 655-661.
Chow AM, Ferrier-Pages C, Khalouei S, Reynaud S, Brown IR (2009) Increased light intensity induces heat shock protein Hsp60 in coral species. *Cell Stress Chaperones* **14**, 469-476.
Coles SL (2002) Coral species diversity and environmental factors in the Arabian Gulf and the Gulf of Oman: A comparison to the Indo-Pacific region. *Atoll Res. Bull* **507**, 1- 19.
Cowlin M (2012) *Osmoregulation and the anthozoan- dinoflagellate symbiosis* Msc Thesis, Victoria University of Wellington.
Cravatte S, Delcroix T, Zhang D, McPhaden M, Leloup J (2009) Observed freshening and warming of the western Pacific warm pool. *Climate Dynamics* **33**, 565-589.
Cummins EP, Oliver KM, Lenihan CR*, et al.* (2010) NF-kappaB links CO2 sensing to innate immunity and inflammation in mammalian cells. *J Immunol* **185**, 4439-4445.
Cummins EP, Selfridge AC, Sporn PH, Sznajder JI, Taylor CT (2014) Carbon dioxide-sensing in organisms and its implications for human disease. *Cell Mol Life Sci* **71**, 831-845.
Darling NJ, Cook SJ (2014) The role of MAPK signalling pathways in the response to endoplasmic reticulum stress. *Biochim Biophys Acta* **1843**, 2150-2163.
Darroch LJ, Lavoie M, Levasseur M*, et al.* (2015) Effect of short-term light- and UV-stress on DMSP, DMS, and DMSP lyase activity in *Emiliania huxleyi*. *Aquatic Microbial Ecology* **74**, 173-185.
Davy SK, Allemand D, Weis VM (2012) Cell biology of cnidarian-dinoflagellate symbiosis. *Microbiol Mol Biol Rev* **76**, 229-261.
De Zoysa M, Jung S, Lee J (2009) First molluscan TNF-α homologue of the TNF superfamily in disk abalone: Molecular characterization and expression analysis. *Fish Shellfish Immunol* **26**, 625-631.
De'ath G, Fabricius KE, Sweatman H, Puotinen M (2012) The 27-year decline of coral cover on the Great Barrier Reef and its causes. *PNAS* **109**, 17995-17999.
De'ath G, Lough JM, Fabricius KE (2009) Declining coral calcification on the Great Barrier Reef. *Science* **323**, 116-119.
Deaton LE, Hoffman RJ (1988) Hypoosmotic volume regulation in the sea anemone *Metridium senile*. *comp Biochem Physiol* **91**, 187-191.

Delanghe JR, Speeckaert R, Speeckaert MM (2014) Complement C3 and its polymorphism: biological and clinical consequences. *Pathology* **46**, 1-10.
DeSalvo MK, Sunagawa S, Voolstra CR, Medina M (2010) Transcriptomic responses to heat stress and bleaching in the elkhorn coral *Acropora palmata*. *Marine Ecology Progress Series* **402**, 97-113.
Deschaseaux ESM, Jones GB, Deseo MA*, et al.* (2014) Effects of environmental factors on dimethylated sulfur compounds and their potential role in the antioxidant system of the coral holobiont. *Limnology and Oceanography* **59**, 758-768.
Devlin M, Taylor J, Brodie J (1998) Flood plumes, extent, concentration and composition. *GBRMPA Reef Res* **8**, 1-9.
Devlin MJ, Brodie J (2005) Terrestrial discharge into the Great Barrier Reef Lagoon: nutrient behavior in coastal waters. *Mar Pollut Bull* **51**, 9-22.
Dickson A, Millero F (1987) A comparison of the equilibrium constants for the dissociation of carbonic acid in seawater media. *Deep Sea Research Part A. Oceanographic Research Papers* **34**, 1733-1743.
Dickson DM, Wyn Jones RG, Davenport J (1980) Steady state osmotic adaptation in *Ulva lactuca*. *Planta* **150**, 158-165.
Dickson DMJ, Kirst GO (1986) The role of beta-dimethylsulphoniopropionate, glycine betaine and homarine in the osmoacclimation of *Platymonas subcordiformis*. *Planta* **167**, 536-543.
Doney SC, Fabry VJ, Feely RA, Kleypas JA (2009) Ocean acidification: the other CO2 problem. *Ann Rev Mar Sci* **1**, 169-192.
Downs CA, Kramarsky-Winter E, Woodley CM*, et al.* (2009) Cellular pathology and histopathology of hypo-salinity exposure on the coral *Stylophora pistillata*. *Sci Total Environ* **407**, 4838-4851.
Durack PJ, Wijffels SE, Matear RJ (2012) Ocean salinities reveal strong global water cycle intensification during 1950 to 2000. *Science* **336**, 455-458.
Economics DA (2013) Economic Contribution of the Great Barrier Reef. *Great Barrier Reef Marine Park Authority, Townsville* **195**.
Eletto D, Dersh D, Argon Y (2010) GRP94 in ER quality control and stress responses. *Semin Cell Dev Biol* **21**, 479-485.
Fabricius K, De'ath G, McCook L, Turak E, Williams DM (2005) Changes in algal, coral and fish assemblages along water quality gradients on the inshore Great Barrier Reef. *Marine pollution bulletin* **51**, 384-398.
Fabricius KE (2005) Effects of terrestrial runoff on the ecology of corals and coral reefs: review and synthesis. *Marine pollution bulletin* **50**, 125-146.
Feder M, Walser JC (2005) The biological limitations of transcriptomics in elucidating stress and stress responses. *J Evol Biol* **18**, 901-910.
Finn RD, Clements J, Eddy SR (2011) HMMER web server: interactive sequence similarity searching. *Nucleic Acids Res* **39**, W29-37.
Fox J, Weisberg S (2011) *An R Companion to Applied Regression*, Thousand Oaks CA.
Fujita T, Matsushita M, Endo Y (2004) The lectin-complement pathway – its role in innate immunity and evolution. *Immunological Reviews* **198**, 185-202.
Gage DA, Rhodes D, Nolte KD*, et al.* (1997) A new route for synthesis of dimethylsulphoniopropionate in marine algae. *Nature* **387**.
Gardner TA, Côté IM, Gill JA, Grant A, Watkinson AR (2003) Long-term region-wide declines in Caribbean corals. *Science, New Series* **301**, 958-960.

Girardin SE, Boneca IG, Viala J*, et al.* (2003) Nod2 is a general sensor of peptidoglycan through muramyl dipeptide (MDP) detection. *Journal of Biological Chemistry* **278**, 8869-8872.
Gracey AY, Chaney ML, Boomhower JP*, et al.* (2008) Rhythms of gene expression in a fluctuating intertidal environment. *Curr Biol* **18**, 1501-1507.
Great Barrier Reef Marine Park A (2014) Great Barrier Reef Outlook Report 2014. Great Barrier Reef Marine Park Authority, Townsville.
Green DH, Edmunds PJ, Carpenter RC (2008) Increasing relative abundance of Porites astreoides on Caribbean reefs mediated by an overall decline in coral cover. *Marine Ecology Progress Series* **359**, 1-10.
Greenbaum D, Colangelo C, Williams K, Gerstein M (2003) Comparing protein abundance and mRNA expression levels on a genomic scale. *Genome Biol* **4**, 117.
Gröne T, Kirst GO (1992) The effect of nitrogen deficiency, methionine and inhibitors of methionine metabolism on the DMSP contents of *Tetraselmis subcordiformis* (Stein). *Marine Biology* **112**, 497-503.
Hagedorn M, Carter VL, Ly S*, et al.* (2010) Analysis of internal osmolality in developing coral larvae, Fungia scutaria. *Physiol Biochem Zool* **83**, 157-166.
Hamada M, Shoguchi E, Shinzato C*, et al.* (2012) The complex NOD-like receptor repertoire of the coral Acropora digitifera includes novel domain combinations. *Mol Biol Evol* **30**, 167-176.
Hanson AD, Rivoal J, Paquet L, Gage DA (1994) Biosynthesis of 3-dimethylsulfoniopropionate in *Wollastonia biflora* (L.) DC. *Plant Physiol.* **105** 103–110.
Harborne AR, Mumby PJ, Micheli F*, et al.* (2006) The functional value of Caribbean coral reef, seagrass and mangrove habitats to ecosystem processes. **50**, 57-189.
Harvell C, Kim K, Burkholder J*, et al.* (1999) Emerging marine diseases--climate links and anthropogenic factors. *Science* **285**, 1505.
Harvell D, Altizer S, Cattadori IM, Harrington L, Weil E (2009) Climate change and wildlife diseases: When does the host matter the most? *Ecology* **90**, 912--920.
Harvell D, Jord·n-Dahlgren E, Merkel S*, et al.* (2007) Coral disease, environmental drivers, and the balance between coral and microbial associates. *Oceanography* **20**, 172-195.
Hasegawa PM, Bressan RA, Zhu J-K, Bohnert HJ (2000) Plant cellular and molecular response to high salinity. *Annu. Rev. Plant Physiol. Plant Mol. Biol.* **51**, 463-499.
Helenius IT, Krupinski T, Turnbull DW*, et al.* (2009) Elevated CO2 suppresses specific Drosophila innate immune responses and resistance to bacterial infection. *Proc Natl Acad Sci U S A* **106**, 18710-18715.
Hemmrich G, Miller DJ, Bosch TCG (2007) The evolution of immunity: a low-life perspective. *Trends in Immunology* **28**, 449-454.
Hernroth B, Baden S, Thorndyke M, Dupont S (2011) Immune suppression of the echinoderm *Asterias rubens* (L.) following long-term ocean acidification. *Aquatic Toxicology* **103**, 222-224.
Hill RW, Li C, Jones AD, Gunn JP, Frade PR (2010) Abundant betaines in reef-building corals and ecological indicators of a photoprotective role. *Coral Reefs* **29**, 869-880.
Hochachka PW, Somero GN (2002) *Biochemical adaptations: mechanism and process in physiological evolution* Oxford University Press.

Hoegh-Guldberg O (1999) Climate change, coral bleaching and the future of the world's coral reefs. *Marine and freshwater research* **50**, 839-866.
Hoegh-Guldberg O, Mumby P, Hooten A*, et al.* (2007) Coral reefs under rapid climate change and ocean acidification. *Science* **318**, 1737.
Hofmann GE (1999) Ecologically relevant variation in induction and function of heat shock proteins in marine organisms. *American zoologist* **39**, 889-900.
Højsgaard S, Halekoh U, from wc*, et al.* (2014) doBy: doBy - Groupwise summary statistics, LS means, general linear contrasts, various utilities. *R package version 4.5-11*.
Hughes TP (1994) Catastrophes, phase shifts, and large-scale degradation of a Caribbean coral reef. *Science* **265**, 1547.
IPCC (2013) Climate Change 2013: The physical science basis: working group I contribution to the fifth assessment report of the Intergovernmental Panel on Climate Change. Cambridge University Press, New York.
Jackson J, Donovan M, Cramer K, Lam V (2014) Status and Trends of Caribbean Coral Reefs.
Jan LY, Jan YN (1997) Cloned potassium channels from eukaryotes and prokaryotes. *Annu Rev Neurosci* **20**, 91-123.
Jones AM, Berkelmans R, van Oppen MJ, Mieog JC, Sinclair W (2008) A community change in the algal endosymbionts of a scleractinian coral following a natural bleaching event: field evidence of acclimatization. *Proc Biol Sci* **275**, 1359-1365.
Kanneganti T-D, Lamkanfi M, Núñez G (2007) Intracellular NOD-like receptors in host defense and disease. *Immunity* **27**, 549-559.
Karsten U, Kück K, Vogt C, Kirst GO (1996) Dimethylsulfoniopropionate production in phototrophic organisms and its physiological functions as a cryoprotectant. In: *Biological and environmental chemistry of DMSP and related sulfonium compounds* (eds. Kiene R, Visscher P, Keller M, Kirst G), pp. 143-153. Springer US.
Kauffmann A, Gentleman R, Huber W (2009) arrayQualityMetrics - a Bioconductor package for quality assessment of microarray data. *Bioinformatics* **25**, 415-416.
Kerswell A, Jones RJ (2003) Effects of hypo-osmosis on the coral Stylophora pistillata nature and cause of low-salinity bleaching. *Marine Ecology Progress Series* **253**, 145-154.
Kettles NL, Kopriva S, Malin G (2014) Insights into the regulation of DMSP synthesis in the diatom *Thalassiosira pseudonana* through APR activity, proteomics and gene expression analyses on cells acclimating to changes in salinity, light and nitrogen. *PLOSone* **9**.
Kim D, Pertea G, Trapnell C*, et al.* (2013) TopHat2: accurate alignment of transcriptomes in the presence of insertions, deletions and gene fusions. *Genome Biol* **14**, R36.
Kimura A, Sakaguchi E, Nonaka M (2009) Multi-component complement system of Cnidaria: C3, Bf, and MASP genes expressed in the endodermal tissues of a sea anemone, *Nematostella vectensis*. *Immunobiology* **214**, 165-178.
Kirst GO (1990) Salinity tolerance of eukaryotic marine algae. *Annu Rev Plant Physiol Plant Mol Biol* **41**, 21-53.

Kleypas JA, Langdon C (2006) Coral reefs and changing seawater carbonate chemistry. *Coastal and Estuarine Studies: Coral Reefs and Climate Change Science and Management* **61**, 73-110.
Kocsis MG, Nolte KD, Rhodes D*, et al.* (1998) Dimethylsulfoniopropionate biosynthesis in *Spartina alterniflora*. *Plant Physiol* **117**, 273-281.
Kultz D (2005) Molecular and evolutionary basis of the cellular stress response. *Annu Rev Physiol* **67**, 225-257.
Kushmaro A, Banin E, Loya Y, Stackebrandt E, Rosenberg E (2001) *Vibrio shiloi* sp. nov., the causative agent of bleaching of the coral *Oculina patagonica*. *Int J Syst Evol Microbiol* **51**, 1383-1388.
Kvennefors EC, Leggat W, Hoegh-Guldberg O, Degnan BM, Barnes AC (2008) An ancient and variable mannose-binding lectin from the coral *Acropora millepora* binds both pathogens and symbionts. *Dev Comp Immunol* **32**, 1582-1592.
Kvennefors EC, Leggat W, Kerr CC*, et al.* (2010) Analysis of evolutionarily conserved innate immune components in coral links immunity and symbiosis. *Dev Comp Immunol* **34**, 1219-1229.
LaJeunesse TC (2002) Diversity and community structure of symbiotic dinoflagellates from Caribbean coral reefs. *Marine Biology* **141**, 387-400.
Lamesch P, Berardini TZ, Li D*, et al.* (2012) The Arabidopsis Information Resource (TAIR): improved gene annotation and new tools. *Nucleic Acids Res* **40**, D1202-1210.
Lange C, Hemmrich G, Klostermeier UC*, et al.* (2011) Defining the origins of the NOD-like receptor system at the base of animal evolution. *Mol Biol Evol* **28**, 1687-1702.
Leggat W, Seneca F, Wasmund K*, et al.* (2011) Differential responses of the coral host and their algal symbiont to thermal stress. *PLoS One* **6**, e26687.
Lesser MP (2006) Oxidative stress in marine environments: biochemistry and physiological ecology. *Annu Rev Physiol* **68**, 253-278.
Levy O, Kaniewska P, Alon S*, et al.* (2011) Complex diel cycles of gene expression in coral-algal symbiosis. *Science* **331**, 175-175.
Lewis E, Wallace D (1998) Program Developed for CO2 System Calculations (Carbon Dioxide Information Analysis Center, Oak Ridge National Laboratory, US Dept. of Energy, Oak Ridge, TN). *ORNL/CDIAC-105*.
Lockwood BL, Connor KM, Gracey AY (2015) The environmentally tuned transcriptomes of *Mytilus mussels*. *Journal of Experimental Biology* **218**, 1822-1833.
Lockwood BL, Sanders JG, Somero GN (2010) Transcriptomic responses to heat stress in invasive and native blue mussels (genus *Mytilus*): molecular correlates of invasive success. *J Exp Biol* **213**, 3548-3558.
Lockwood BL, Somero GN (2011) Transcriptomic responses to salinity stress in invasive and native blue mussels (genus *Mytilus*). *Mol Ecol* **20**, 517-529.
Love MI, Huber W, Anders S (2014) Moderated estimation of fold change and dispersion for RNA-seq data with DESeq2. *Genome biology* **15**, 1-21.
Loya Y, Sakai K, Yamazato K*, et al.* (2001) Coral bleaching: the winners and the losers. *Ecology letters* **4**, 122-131.
Lyon BR, Lee PA, Bennett JM, DiTullio GR, Janech MG (2011) Proteomic analysis of a sea-ice diatom: salinity acclimation provides new insight into the

dimethylsulfoniopropionate production pathway. *Plant Physiol* **157**, 1926-1941.
Maere S, Heymans K, Kuiper M (2005) BiNGO: a Cytoscape plugin to assess overrepresentation of gene ontology categories in biological networks. *Bioinformatics* **21**, 3448-3449.
Maor-Landaw K, Karako-Lampert S, Waldman Ben-Asher H*, et al.* (2014) Gene expression profiles during short-term heat stress in the red sea coral *Stylophora pistillata*. *Glob Chang Biol* **20**, 3026-3035.
Mehrbach C, Culberson C, Hawley J, Pytkowicx R (1973) Measurement of the apparent dissociation constants of carbonic acid in seawater at atmospheric pressure. *Limnol Oceanogr* **18**, 897-907.
Merchant SS, Prochnik Se Fau - Vallon O, Vallon O Fau - Harris EH*, et al.* (2007) The *Chlamydomonas* genome reveals the evolution of key animal and plant functions. *Science* **318**, 245-250.
Miller DJ, Hemmrich G, Ball EE*, et al.* (2007) The innate immune repertoire in Cnidaria-ancestral complexity and stochastic gene loss. *Genome Biol* **8**, R59.
Moberg F, Folke C (1999) Ecological goods and services of coral reef ecosystems. *Ecological economics* **29**, 215-233.
Moya A, Huisman L, Ball EE*, et al.* (2012) Whole transcriptome analysis of the coral *Acropora millepora* reveals complex responses to CO2-driven acidification during the initiation of calcification. *Mol Ecol* **21**, 2440-2454.
Moya A, Huisman L, Foret S*, et al.* (2015) Rapid acclimation of juvenile corals to CO2 - mediated acidification by upregulation of heat shock protein and Bcl-2 genes. *Mol Ecol* **24**, 438-452.
Moya A, Sakamaki K, Mason BM*, et al.* (2016) Functional conservation of the apoptotic machinery from coral to man: the diverse and complex Bcl-2 and caspase repertoires of *Acropora millepora*. *Bmc Genomics* **17**, 1.
Mydlarz LD, McGinty ES, Harvell CD (2010) What are the physiological and immunological responses of coral to climate warming and disease? *J Exp Biol* **213**, 934-945.
Nakano Y, Tsuchiya M, Rungsupa S, Yamazato K (2009) Influence of severe freshwater flooding during the rainy season on the coral community around Khang Khao Island in the inner Gulf of Tahiland. *Galaxea, Journal of Coral Reef Studies* **11**, 131-138.
Niki T, Shimizu M, Fujishiro A, Kinoshita J (2007) Effects of salinity downshock on dimethylsulfide production. *Journal of Oceanography* **63**, 873-877.
Nishiguchi MK, Somero GN (1992) Temperature – and concentration-dependence of compatibility of the organic osmolyte ß-dimethylsulfoniopropionate. *Cryobiology* **29**, 118–124.
Ocampo I, Zárate-Potes A, Pizarro V*, et al.* (2015) The immunotranscriptome of the Caribbean reef-building coral *Pseudodiploria strigosa*. *Immunogenetics* **67**, 515-530.
Ogawa D, Bobeszko T, Ainsworth T, Leggat W (2013) The combined effects of temperature and CO2 lead to altered gene expression in *Acropora aspera*. *Coral Reefs* **32**, 895-907.
Orr JC, Fabry VJ, Aumont O*, et al.* (2005) Anthropogenic ocean acidification over the twenty-first century and its impact on calcifying organisms. *Nature* **437**, 681-686.

Palmer CV, Bythell JC, Willis BL (2010) Levels of immunity parameters underpin bleaching and disease susceptibility of reef corals. *The FASEB Journal* **24**, 1935.
Palmer CV, Mydlarz LD, Willis BL (2008) Evidence of an inflammatory-like response in non-normally pigmented tissues of two scleractinian corals. *Proc R Soc Lond [Biol]* **275**, 2687.
Palumbi SR, Barshis DJ, Traylor-Knowles N, Bay RA (2014) Mechanisms of reef coral resistance to future climate change. *Science* **344**, 895-898.
Pandolfi JM, Bradbury RH, Sala E*, et al.* (2003) Global trajectories of the long-term decline of coral reef ecosystems. *Science* **301**, 955-958.
Petrak J, Ivanek R, Toman O*, et al.* (2008) Deja vu in proteomics. A hit parade of repeatedly identified differentially expressed proteins. *Proteomics* **8**, 1744-1749.
Pierce SK (1982) Invertebrate cell volume control mechanisms: a coordinated use of intracellular amino acids and inorganic ions as osmotic solute. *Biol. Bull* **163**, 405 - 419.
Pierce SK, Warren JW (2001) The taurine efflux portal used to regulate cell volume in response to hypoosmotic stress seems to be similar in many cell types: Lessons to be learned from molluscan red blood cells. *Amer Zool* **41**, 710-720.
Pinsino A, Matranga V (2015) Sea urchin immune cells as sentinels of environmental stress. *Dev Comp Immunol* **49**, 198-205.
Pinzón JH, Kamel B, Burge CA*, et al.* (2015) Whole transcriptome analysis reveals changes in expression of immune-related genes during and after bleaching in a reef-building coral. *Royal Society Open Science* **2**.
Plaisance L, Caley MJ, Brainard RE, Knowlton N (2011) The diversity of coral reefs: What are we missing? *PLoS One* **6**, e25026.
Poole AZ, Weis VM (2014) TIR-domain-containing protein repertoire of nine anthozoan species reveals coral-specific expansions and uncharacterized proteins. *Dev Comp Immunol* **46**, 480-488.
Porter JW, Lewis SK, Porter KG (1999) The effect of multiple stressors on the Florida Keys coral reef ecosystem: A landscape hypothesis and a physiological test. *Limnology and Oceanography* **44**, 941-949.
Quistad SD, Stotland A, Barott KL*, et al.* (2014) Evolution of TNF-induced apoptosis reveals 550 My of functional conservation. *PNAS* **111**.
Raina JB, Dinsdale EA, Willis BL, Bourne DG (2010) Do the organic sulfur compounds DMSP and DMS drive coral microbial associations? *Trends in microbiology* **18**, 101-108.
Raina JB, Tapiolas DM, Foret S*, et al.* (2013) DMSP biosynthesis by an animal and its role in coral thermal stress response. *Nature* **502**, 677-680.
Read BA, Kegel J Fau - Klute MJ, Klute Mj Fau - Kuo A*, et al.* (2013) Pan genome of the phytoplankton *Emiliania* underpins its global distribution. *Nature*.
Reed K, Muller E, Van Woesik R (2010) Coral immunology and resistance to disease. *Diseases of aquatic organisms* **90**, 85-92.
Ricaurte M, Schizas NV, Ciborowski P, Boukli NM (2016) Proteomic analysis of bleached and unbleached Acropora palmata, a threatened coral species of the Caribbean. *Marine pollution bulletin*.
Rodriguez Lanetty M, Harii S, Hoegh Gulberg O (2009) Early molecular responses of coral larvae to hyperthermal stress. *Molecular ecology* **18**, 5101-5114.
Rosenberg E, Falkovitz L (2004) The *Vibrio shiloi/Oculina patagonica* model system of coral bleaching. *Annu. Rev. Microbiol.* **58**, 143-159.

Rosenberg E, Koren O, Reshef L, Efrony R, Zilber-Rosenberg I (2007) The role of microorganisms in coral health, disease and evolution. *Nature Reviews Microbiology* **5**, 355-362.
Rosenberg E, Kushmaro A, Kramarsky-Winter E, Banin E, Yossi L (2008) The role of microorganisms in coral bleaching. *The ISME journal* **3**, 139-146.
Seveso D, Montano S, Strona G*, et al.* (2014) The susceptibility of corals to thermal stress by analyzing Hsp60 expression. *Mar Environ Res* **99**, 69-75.
Shinagawa A, Suzuki T, Konosu S (1992) The role of free amino acids and betaines in intracellular osmoregulation of marine sponges. *Nippon Suisan Gakkaishi* **58**, 1717-1722.
Shinzato C, Mungpakdee S, Satoh N, Shoguchi E (2014) A genomic approach to coral-dinoflagellate symbiosis: studies of *Acropora digitifera* and *Symbiodinium minutum*. *Front Microbiol* **5**, 336.
Shinzato C, Shoguchi E, Kawashima T*, et al.* (2011) Using the *Acropora digitifera* genome to understand coral responses to environmental change. *Nature* **476**, 320-323.
Shoguchi E, Shinzato C, Kawashima T*, et al.* (2013) Draft assembly of the Symbiodinium minutum nuclear genome reveals dinoflagellate gene structure. *Curr Biol* **23**, 1399-1408.
Siboni N, Abrego D, Motti CA, Tebben J, Harder T (2014) Gene expression patterns during the early stages of chemically induced larval metamorphosis and settlement of the coral *Acropora millepora*. *PLoS One* **9**, e91082.
Sievert SM, Kiene RP, Schultz-Vogt HN (2007) The sulfur cycle. *Oceanography* **20**, 117-123.
Smoot ME, Ono K, Ruscheinski J, Wang PL, Ideker T (2011) Cytoscape 2.8: new features for data integration and network visualization. *Bioinformatics* **27**, 431-432.
Somero GN (2012) The physiology of global change: linking patterns to mechanisms. *Ann Rev Mar Sci* **4**, 39-61.
Stefels J (2000) Physiological aspects of the production and conversion of DMSP in marine algae and higher plants *Journal of Sea Research* **43**, 183-197.
Summers PS, Kurt D. Nolte, Arthur J.L. Cooper*, et al.* (1998) Identification and stereospecificity of the first three enzymes of 3-dimethylsulfoniopropionate biosynthesis in a chlorophyte alga. *Plant Physiol.*
Sunda W, Kieber DJ, Kiene RP, Huntsman S (2002) An antioxidant function for DMSP and DMS in marine algae. *Nature* **418**, 317-320.
Sussman M, Willis BL, Victor S, Bourne DG (2008) Coral pathogens identified for White Syndrome (WS) epizootics in the Indo-Pacific. *PLoS One* **3**, e2393.
Takeda K, Akira S (2005) Toll-like receptors in innate immunity. *Int Immunol* **17**, 1-14.
Tapiolas DM, Raina J-B, Lutz A, Willis BL, Motti CA (2013) Direct measurement of dimethylsulfoniopropionate (DMSP) in reef-building corals using quantitative nuclear magnetic resonance (qNMR) spectroscopy. *J Exp Mar Biol Ecol* **443**, 85-89.
Taylor CT, Cummins EP (2011) Regulation of gene expression by carbon dioxide. *J Physiol* **589**, 797-803.
Tchernov D, Gorbunov MY, de Vargas C*, et al.* (2004) Membrane lipids of symbiotic algae are diagnostic of sensitivity to thermal bleaching in corals. *Proc Natl Acad Sci U S A* **101**, 13531-13535.

Tebben J, Tapiolas DM, Motti CA, *et al.* (2011) Induction of larval metamorphosis of the coral *Acropora millepora* by tetrabromopyrrole isolated from a *Pseudoalteromonas* bacterium. *PLoS One* **6**, e19082.
The International Brachypodium Initiative (2010) Genome sequencing and analysis of the model grass *Brachypodium distachyon*. *Nature* **463**, 763-768.
Tomanek L, Zuzow MJ (2010) The proteomic response of the mussel congeners *Mytilus galloprovincialis* and *M. trossulus* to acute heat stress: implications for thermal tolerance limits and metabolic costs of thermal stress. *J Exp Biol* **213**, 3559-3574.
Tomanek L, Zuzow MJ, Hitt L, Serafini L, Valenzuela JJ (2012) Proteomics of hyposaline stress in blue mussel congeners (genus *Mytilus*): implications for biogeographic range limits in response to climate change. *J Exp Biol* **215**, 3905-3916.
Trossat C, Rathinasabapathi B, Weretilnyk EA, *et al.* (1998) Salinity promotes accumulation of 3-dimethylsulfoniopropionate and its precursor S-methylmethionine in chloroplasts. *Plant Physiol.* **116**, 165-171.
Vairavamurthy A, Andreae MO, Iverson RL (1985) Biosynthesis of dimethylsulfide and dimethylpropiothetin by *Hymenomonas carterae* in relation to sulfur source and salinity variations. *Limmnol. Oceanogr.* **301**, 59-70.
Van Woesik R, De Vantier LM, Glazebrook JS (1995) Effects of Cyclone 'Joy' on nearshore coral communities of the Great Barrier Reef. *Mar Ecol Prog Ser* **128**, 261-270.
Veal CJ, Carmi M, Fine M, Hoegh-Guldberg O (2010) Increasing the accuracy of surface area estimation using single wax dipping of coral fragments. *Coral Reefs* **29**, 893-897.
Veron J (2000) *Corals of the World* Australian Institute of Marine Science, Townsville.
Vidal-Dupiol J, Dheilly NM, Rondon R, *et al.* (2014) Thermal stress triggers broad *Pocillopora damicornis* transcriptomic remodeling, while *Vibrio coralliilyticus* infection induces a more targeted immuno-suppression response. *PLoS One* **9**.
Vidal-Dupiol J, Ladriere O, Meistertzheim AL, *et al.* (2011) Physiological responses of the scleractinian coral *Pocillopora damicornis* to bacterial stress from *Vibrio coralliilyticus*. *J Exp Biol* **214**, 1533-1545.
Vierstra RD (1993) Protein degradation in plants. *Annu Rev Plant Physiol Plant Mol Bioi* **44**, 385-410.
Wang N, Gates KL, Trejo H, *et al.* (2010) Elevated CO2 selectively inhibits interleukin-6 and tumor necrosis factor expression and decreases phagocytosis in the macrophage. *The FASEB Journal* **24**, 2178-2190.
Wang Y, Wu WH (2013) Potassium transport and signaling in higher plants. *Annu Rev Plant Biol* **64**, 451-476.
Wang Z, Gerstein M, Snyder M (2009) RNA-Seq: a revolutionary tool for transcriptomics. *Nat Rev Genet* **10**, 57-63.
Weiss Y, Foret S, Hayward D, *et al.* (2013) The acute transcriptional response of the coral *Acropora millepora* to immune challenge: expression of GiMAP/IAN genes links the innate immune responses of corals with those of mammals and plants. *Bmc Genomics* **14**.
West MA, Hackam DJ, Baker J, *et al.* (1997) Mechanism of decreased in vitro murine macrophage cytokine release after exposure to carbon dioxide: relevance to laparoscopic surgery. *Annals of Surgery* **226**, 179-190.

Wiens GD, Glenney GW (2011) Origin and evolution of TNF and TNF receptor superfamilies. *Dev Comp Immunol* **35**, 1324-1335.
Wiens M, Korzhev M, Perovic-Ottstadt S*, et al.* (2007) Toll-like receptors are part of the innate immune defense system of sponges (demospongiae: Porifera). *Mol Biol Evol* **24**, 792-804.
Xie S-P, Deser C, Vecchi GA*, et al.* (2010) Global warming pattern formation: sea surface temperature and rainfall. *Journal of Climate* **23**, 966-986.
Yancey PH, Heppenstall M, Ly S*, et al.* (2010) Betaines and dimethylsulfoniopropionate as major osmolytes in cnidaria with endosymbiotic dinoflagellates. *Physiol Biochem Zool* **83**, 167-173.
Yost DM, Jones RJ, Mitchelmore CL (2010) Alterations in dimethylsulfoniopropionate (DMSP) levels in the coral *Montastraea franksi* in response to copper exposure. *Aquat Toxicol* **98**, 367-373.
Yu D, Huber W, Vitek O (2013) Shrinkage estimation of dispersion in Negative Binomial models for RNA-seq experiments with small sample size. *Bioinformatics* **29**, 1275-1282.
Yuen B, Bayes JM, Degnan SM (2014) The characterization of sponge NLRs provides insight into the origin and evolution of this innate immune gene family in animals. *Mol Biol Evol* **31**, 106-120.
Zhang Y, Sun J, Mu H*, et al.* (2015) Proteomic basis of stress responses in the gills of the Pacific oyster *Crassostrea gigas*. *J Proteome Res* **14**, 304-317.
Zoccola D, Ganot P, Bertucci A*, et al.* (2015) Bicarbonate transporters in corals point towards a key step in the evolution of cnidarian calcification. *Sci Rep* **5**, 9983.
Zoccola D, Tambutte E, Kulhanek E*, et al.* (2004) Molecular cloning and localization of a PMCA P-type calcium ATPase from the coral *Stylophora pistillata*. *Biochim Biophys Acta* **1663**, 117-126.